4-2017

Evaluating the Impacts of Grassland Conversions to Experimental Forest on Groundwater Recharge in the Nebraska Sand Hills

Zablon A. Adane
University of Nebraska-Lincoln, ZABLON@HUSKERS.UNL.EDU

EVALUATING THE IMPACTS OF GRASSLAND CONVERSIONS TO EXPERIMENTAL FOREST ON GROUNDWATER RECHARGE IN THE NEBRASKA SAND HILLS

by

Zablon A. Adane

A DISSERTATION

Presented to the Faculty of

The Graduate College at the University of Nebraska

In Partial Fulfillment of Requirements

For the Degree of Doctor of Philosophy

Major: Earth and Atmospheric Sciences

(Hydrogeology)

Under the Supervision of Professor Vitaly A. Zlotnik

Lincoln, Nebraska

April, 2017

EVALUATING THE IMPACTS OF GRASSLAND CONVERSIONS TO EXPERIMENTAL FOREST ON GROUNDWATER RECHARGE IN THE NEBRASKA SAND HILLS

Zablon A. Adane, Ph.D.

University of Nebraska, 2017

Adviser: Vitaly A. Zlotnik

The Nebraska Sand Hills grasslands provide the greatest groundwater recharge rates in the High Plains Aquifer. However, the grasslands and their ecological services have become vulnerable to land use change and degradation. Further, many grassland communities worldwide have been identified as suitable for future afforestation and reforestation programs. This study used a series of field data to investigate the effects of grassland conversion to forest on groundwater recharge rates in a century-old experimental forest containing grasses, ponderosa pine, and eastern red cedar in the Sand Hills. The results show that the impact of grassland conversion on recharge was dependent on the species and plantation density. Estimated recharge rates beneath the dense plantations represent reductions of 86–94% relative to the surrounding native grassland. Results of ^{1}H Nuclear Magnetic Resonance spectral analysis suggested that the surface soil organic carbon beneath pine plantations also contain up to 3 times the ratio of hydrophobic components relative to the native grasslands and may alter the soil hydraulic properties and cause declining soil infiltration capacity. This investigation also uncovered a previously overlooked feedback between the effect of soil organic carbon chemical shift

generated by the ponderosa pine needle litter decomposition and recharge; namely that the alteration may have a link to reduced groundwater recharge rates. Thus, a global optimizer algorithm was used to estimate the effective soil hydraulic parameters from observed monthly soil moisture contents, and recharge rates were then estimated through HYDRUS 1-D numerical modeling for soil profiles representing native grassland and dense pine forest conditions. The impact of grassland conversion to dense pine was an overall reduction of groundwater recharge by nearly 100%. These outcomes highlight the significance of the grassland ecology for water resources, particularly groundwater recharge, in the Sand Hills and the overall sustainability of the High Plains Aquifer and other similar aquifers worldwide.

Acknowledgements

This study is partially based upon work funded by the National Science Foundation (Award number: IIA-1415035), Edgren Fellowship, Yatkola-Edwards research grant from the Nebraska Geological Society, American Association of Petroleum Geologist research grant, and Department of Earth and Atmospheric Sciences Fellowship.

I would first like express my deepest gratitude to my advisor Dr. Vitaly Zlotnik who has inherited me as a student and yet held my work to the highest standard. I am forever grateful for his time, patience, guidance, expertise, intelligent critic, and honest assessment. Our conversations on world travel, politics, and literature have also been incredibly fascinating. The timely quotes and anecdotes in our conversation have also made me develop greater appreciation for Winston Churchill and Alexander Pushkin.

I am also deeply indebted to my mentor Dr. John Gates for his continuous help, time, patience, motivation, and most of all his guidance since the inception of the project. The soil profile coring field expeditions were undoubtedly my most favorite time of this program. While 12 hours a day of hand auguring dry sand to depths of 20 feet at minute increments were less pleasant, the intelligent, insightful, and interesting conversations ranging from the hydrogeology of the Sand Hills to our first jobs as teenagers are among my fondest memories in my time in Nebraska. I will be forever grateful for all his guidance in the field, laboratory, in the class room, and in life.

I would also like to thank the rest of my dissertation committee: Dr. David Wedin for providing access to the forest plots, resources such as a truck for my first trip to

Halsey, and a number of indispensable datasets including long term TDR soil moisture content, leaf area index, and litter deposition rates as well as root depth information. I cannot imagine completing this program without his continuous and ever-positive help and guidance; Dr. Dean Eisenhauer for access to his lab for the dry end of the soil water retention curves, van Genuchten parameter data for Valentine sand, and his guidance; and Dr. Sheri Fritz her effort and recommendation for a grant, support, and continuous encouragement throughout the program. My sincere thanks also goes out to Dr. Paolo Nasta for his help with field work, research, edits, and his friendship and guidance.

Earnest thanks are also due to Jeremy Hiller and Dr. Tala Awada for access to the Nebraska National Forest plots, data, and continuous support. I would also like to thank Dr. Martha Morton, Cathleen McFarland, and Dr. Dan Snow for access to the chemistry, ecology, and water science laboratories.

I am also extremely grateful to have supporting friends and colleagues at the Department of Earth and Atmospheric Sciences, namely Justin Gibson, Nathan Rossman, JP Traylor, Philip Paitz, and Doruk Ozturk and at the Nebraska Department of Natural Resources; Mahesh Pun, Jessie Winter, Amy Zoller, and Kari Burgert.

I am as always forever indebted to my father Dej. Afera Adane, mother Yeromnesh Belete, Seble Afera Adane, and all my family for their sacrifice, support, and unconditional love. Also, to the sister who has followed me everywhere but drew the line on moving to Nebraska, I cannot imagine a better sister or a better human being than you and I am forever thankful to have you.

Cheers and God bless!

Table of Contents

List of Figures

List of Tables

List of Appendices

CHAPTER 1

INTRODUCTION

Grassland communities have been under constant threat by land use and land cover changes throughout history. In the early part of the 18th century, grasslands and other natural vegetation covers were often converted to agricultural land in response to drastic human population growth. While conversions to cropland accommodated the drastic population growth, the environmental consequences following these conversions were also numerous and included deforestation, soil degradation, species and habitat loss, changes to the water regime, and even climate change. Effects of land use and land cover changes on groundwater recharge have been extensively documented across diverse environmental settings (Leduc et al. 2001; Scanlon et al. 2006; Owuor and Butterbach-Bahl 2016). The most documented land use change scenario with respect to groundwater recharge has been the conversion of natural vegetation to agriculture, which has been investigated in field studies from Australia (Allison et al. 1990), the African Sahel (Favareau et al. 2009), the United States (Scanlon et al. 2007), South America (Jayawickreme et al. 2011), and elsewhere (Wang et al. 2008). Land use shifts to agriculture have tended to result in a net increase in rates of deep drainage and groundwater recharge in most cases depending on local climatic and hydrological conditions. The impact of land use changes other than those related to agriculture have received relatively less attention.

In the past few decades, global climate change has been one of the main challenges facing the planet. In addition to reducing CO_2 emissions, preserving and

expanding forest coverage through extensive afforestation and reforestation programs worldwide have emerged as important tools to combat climate change. Such programs help in the effort to minimize climate change by providing a sink for CO_2 through carbon sequestration both in the trees and forest soils. Further, forests have lower albedo than other landscapes as less energy is reflected back into the atmosphere reducing localized warming and global climate change. However, the land needed for the afforestation programs have not been obtained mainly from conversions from agricultural lands but through alterations of other natural landscapes, particularly grasslands, which have many notable ecological contributions, especially to water resources.

In recent times, natural regeneration and afforestation programs of various land uses, including of grasslands have also increased forest area. The increase in forest area will likely continue mainly at the expense of grasslands, which have been identified as particularly suitable for forest coverage expansion programs by the World Resources Institute (WRI) tasked with finding appropriate locations for such efforts (Bond 2015). While forests provide a number of beneficial ecological services (reviewed in Nasi et al. 2010), many case studies have also shown situations in which land use conversions to forests have substantially reduced soil moisture (McVicar et al. 2007) and groundwater recharge rates (Scanlon et al. 2009). Several studies have also attributed soil moisture and groundwater recharge reductions primarily to the relatively higher transpiration rates of the planted woody vegetation (Zhang et al. 2001). Other studies (e.g. Owens et al. 2006) have also associated these reductions in soil moisture and recharge rates to greater rainfall interception of the introduced plantations, which can range up to 10% to 40% of annual rainfall.

In addition to evapotranspiration changes, forests have also been recognized to alter soil hydraulic properties (Lichner et al. 2010); however, subsequent impacts of these changes on the water cycle have received relatively little attention. Plantations can alter soil physical properties such as porosity (Roberts 2000), biological and microbial activity (Janssens et al. 2010) as well as chemical properties through the decomposition of litter, deposition of organic matter, and buildup of waxes and resins, which may cause soil hydrophobicity (water repellency) (Buckzo et al. 2010). The causes, presence, and impacts of soil hydrophobicity on the soil water balance have been characterized by several studies under different land uses and environmental settings (reviewed in Doerr et al. 2000). Hydrophobicity in soils results from either partial or complete coating of hydrophilic mineral particles with organic matters containing long aliphatic chains that have the tendency to be more hydrophobic (Kajiura et al. 2012). Known sources of hydrophobic substances include bacteria, fungi, algae, and many higher order plants, including eucalypts and several pine species (Doerr et al. 2000). Dry soil conditions also strongly affect the manifestation or the severity of soil hydrophobicity (Dekker and Ritsema 1994, de Jonge et al. 2007). The variability of soil hydrophobicity in its spatial and temporal distribution is also a major factor in the severity of its consequences on recharge (Rye and Smettem 2015). Soil hydrophobicity is common in sandy soils and is often exacerbated by the relatively low specific hydrophilic surface area of the particles resulting in organic matter coating (Wallis et al. 1991).

The soil hydrophobicity and other alterations related to land use change, such as reduction in soil porosity and decrease in soil organic carbon and retention capacity have to be accounted for in order to properly characterize site conditions and evaluate the

impact of land use change on groundwater recharge and the overall water budget. These characteristics are very important for water flux through the unsaturated zone. While they are very difficult to characterize individually, the soil hydraulic properties still govern the movement of water through the unsaturated zone profile. Once the effective soil hydraulic properties are optimized for both the native land use and the plantations, the upper boundary conditions can be applied to simulate recharge rates to evaluate the impact of the land use land cover changes in the Nebraska Sand Hills.

The objectives of this study are: 1) to characterize groundwater recharge rates beneath the native grassland profile and the forest plantations representing the land use change through solute mass balance analysis of field soil cores 2) to evaluate the extent of soil hydrophobicity resulting from grassland conversion to different plantation densities of ponderosa pine and eastern red cedar forests, 3) to assess the impact of surface soil hydrophobicity on annual recharge rates and to model how extreme assumptions of the hydrophobicity effect on the soil hydraulic properties impact the water balance 4) to obtain effective soil hydraulic properties for the grass and dense pine profiles through optimization and inverse modeling using monthly TDR soil moisture content measurements, and 5) to evaluate the impact of grassland conversions to forests on recharge and the overall water budget using the optimized effective soil hydraulic properties through numerical modeling using HYDRUS 1-D.

In chapter 2 of this dissertation, historical groundwater recharge rates beneath the grassland plot profile representing native vegetation conditions and nine different vegetation plots of various species types and planting densities representing the land use change scenarios were assessed using solute (chloride and sulfate) mass balance based on

vegetation type and planting density. The results have also been published in Adane and Gates (2015) in Hydrogeology Journal.

Chapter 3 further explores the previously overlooked feedback between ponderosa pine trees (the dominant land use change) induced surface soil hydrophobicity and reduction in groundwater recharge beneath the pine vegetation plots using field infiltration tests, laboratory water and ethanol drop tests, ^{1}H Nuclear Magnetic Resonance, and, HYDRUS 1-D numerical modeling. The results are published in Adane et al. 2017 in Forest Science.

Chapter 4 of this dissertation explores changes in soil hydraulic properties associated with land use changes. The DiffeRential Evolution Adaptive Metropolis ($DREAM_{ZS}$) global optimizer algorithm was coupled with Markov-Chain Monte-Carlo sampling scheme to estimate the effective soil hydraulic properties beneath the grassland and the dense pine profiles. The effective soil hydraulic properties were used to numerically model water flux through the unsaturated zone under the grassland and dense pine profiles to evaluate the impact of land use on recharge in the Nebraska Sand Hills. The results of this study have been submitted to Journal of Hydrology in Adane et al. 2017. This case study thoroughly describes the impact of grassland conversion to forests on groundwater recharge in the Nebraska Sand Hills and provides further evidence of the importance of grassland ecology to water resources, particularly to groundwater systems. This dissertation also makes the case for a detailed evaluation and proper considerations of the impacts of these plantation efforts on long term water sustainability, especially in semi-arid climates prior to any plantation efforts in the High Plains Aquifer and other similarly vulnerable aquifers worldwide.

References

Adane, Z.A., Nasta, P., and Gates, J.B., 2017. Links between soil hydrophobicity and groundwater recharge under plantations in a sandy grassland setting, Nebraska Sand Hills, USA. Forest Science. doi:10.5849/FS-2016-137

Adane, Z.A. and Gates, J.B., 2015. Determining the impacts of experimental forest plantation on groundwater recharge in the Nebraska Sand Hills (USA) using chloride and sulfate. Hydrogeology Journal 23, 81–94, doi: 10.1007/s10040-014-1181-6.

Allison, G.B, Cook, P.G, Barnett, S.R., Walker, G.R., Jolly, I.D, Hughes, M.W., 1990. Land clearance and river salinisation in the western Murray Basin, Australia. J Hydrol 119, 1–20.

Bond, W. J., 2016. Ancient grasslands at risk. Science. 351, 120–122.

Buczko, U., Bens, O., and. Huttl, R.F., 2005. Variability of soil water repellency in sandy forest soils with different stand structure under Scots pine (*Pinus sylvestris*) and beech (*Fagus sylvatica*). *Geoderma* 126, 317–336.

Calder, I.R., Prasanna, K.T., Hall, R.L., 1993. Hydrological impact of Eucalyptus plantation in India. J Hydrol 150, 635–648.

Dekker, L.W., and Ritsema, C.J., 1994. How water moves in a water repellent sandy soil: 1. Potential and actual water repellency. *Water Resour. Res.* 30, 2507–2517.

Doerr, S.H., Shakesby, R.A., and.Walsh, R.P.D., 2000. Soil water repellency: Its causes, characteristics and hydro-geomorphological significance. Earth Sci. Rev. 51, 33–65.

de Jonge, L.W., Moldrup, P., and Jacobsen, O.H., 2007. Soil-water content dependency of water repellency in soils. *Soil Sci.* 172, 577–588.

Favreau, G., Cappelaere, B., Massuel, S., Leblanc, M., Boucher, M., Boulain, N., Leduc, C., 2009. Land clearing, climate variability, and water resources increase in semiarid southwest Niger: A review. Water Resour Res. doi: 10.1029/2007WR006785

Issar, A., Nativ, R., Karnieli, K., Gat, J.R., 1984. Isotopic evidence of the origin of groundwater in arid zones. Proc Symp 85–105. IAEA, Vienna, 1984

Janssens, I.A., Dieleman, W., Luyssaert, S., Subke, J., Reichstein, M., Ceulemans, R. Ciais, P., et. al. 2010. Reduction of forest soil respiration in response to nitrogen deposition. *Nat. Geosci.* 5:315–322.

Jayawickreme, D.H., Santoni, C.S., Kim, J.H., Jobbagy, E.G., Jackson, R.B., 2011. Changes in hydrology and salinity accompanying a century of agricultural conversion in Argentina. Ecol Appl 21, 2367–2379. doi:10.1890/10-2086.1

Kajiura, M., Etori, Y., and, Tange, T., 2012. Water condition control of in situ soil water repellency: An observational study from a hillslope in a Japanese humid-temperate forest. *Hydrol. Process.* 26, 3070 –3078.

Leduc, C., Favreau, G., Schroeter, P., 2001. Long-term rise in a Sahelian water-table: the continental terminal in south-west Niger. J Hydrol 243:43–54. doi:10.1016/S0022-1694(00)00403-0

Lichner, L., Hallett, P.D., Orf´anus, T., Czachor, H., Rrajkai, K., S˘ ir, M., and Tesa˘r, M., 2010. Vegetation impact on the hydrology of an aeolian sandy soil in a continental climate. *Ecohydrology* 3, 413– 420.

Mcvicar, T.R., Li, L., Van Niel, T.G., Zhang, L., Li, R., Yang, Q., Zhang, X., et al. 2007. Developing a decision support tool for China's re-vegetation program: Simulating

regional impacts of afforestation on average annual streamflow in the Loess Plateau. *For. Ecol. Manage.* 251, 65– 81.

Nasi, R., Wunder, S., Campos, J.J.A., 2002. Forest ecosystem services: can they pay our way out of deforestation? Fondo Glob. para el Medio Ambient. 1–11.

Roberts, J., 2000. The influence of physical and physiological characteristics of vegetation on their hydrological response. *Hydrol. Process.* 14, 2885–2901.

Scanlon, B.R., Jolly, I., Sophocleous, M., Zhang, L., 2007. Global impacts of conversions from natural to agricultural ecosystems on water resources: Quantity versus quality, Water Resour Res 43, 1–18.

Rye, C.F., and K.R.J. Smettem. 2015. Seasonal and interannual variability of the effective flow cross-sectional area in a water-repellent soil. *Vadose Zone J.* 14 3. doi:10.2136/vzj2014.10.0141.

Scanlon, B.R., Keese, K.E., Flint, A.L., Flint, L.E., Gaye, C.B., Edmunds, W.M., and Simmers, I., 2006. Global synthesis of groundwater recharge in semiarid and arid regions. Hydrol Process 20, 3335–3370. doi: 10.1002/hyp.6335

Scanlon, B.R., Stonestrom, D.A., Reedy, R.C., Leaney, F.W., Gates, J.B., Cresswell, R.G., 2009. Inventories and mobilization of unsaturated zone sulfate, fluoride, and chloride related to land use change in semiarid regions, southwestern United States and Australia, Water Resour Res 45.W00A18. doi:10.1029/2008WR006963

Wallis, M., Scotter, D., and Horne. D., 1991. An evaluation of the intrinsic sorptivity water repellency index on a range of New Zealand soils. *Aust. J. Soil Res.* 29:353.

Wang, B., Jin, M., Nimmo, J.R., Yang, L., Wang, W., 2008. Estimating groundwater recharge in Hebei Plain, China under varying land use practices using tritium and bromide tracers. J Hydrol 356, 209–222. doi: 10.1016/j.jhydrol.2008.04.011

Zhang, L., Dawes, W.R., Walker, G.R., 2001. Response of mean annual evapotranspiration to vegetation changes at catchment scale. Water Resour Res 37, 701–708. doi:10.1029/2000WR900325

CHAPTER 2

IMPACTS OF EXPERIMENTAL FOREST PLANTATION ON GROUNDWATER RECHARGE IN THE NEBRASKA SAND HILLS USING CHLORIDE AND SULFATE

Zablon A. Adane · John B. Gates

Z. A. Adane · J. B. Gates

Department of Earth and Atmospheric Sciences University of Nebraska-Lincoln

Lincoln, NE 68588-0340, USA, Zablon@huskers.unl.edu; john.gates@climate.com

Citation: Adane, Z.A. and Gates, J.B., 2015. Determining the impacts of experimental forest plantation on groundwater recharge in the Nebraska Sand Hills (USA) using chloride and sulfate. Hydrogeology Journal 23, 81–94, doi: 10.1007/s10040-014-1181-6.

Abstract

Although impacts of land use changes on groundwater recharge have been widely demonstrated across diverse environmental settings, most previous research has focused on the role of agriculture. This study investigates recharge impacts of tree plantations in a century-old experimental forest surrounded by mixed-grass prairie in the US Northern High Plains (Nebraska National Forest). Recharge was estimated using solute mass balance methods from unsaturated zone cores beneath 10 experimental plots with different vegetation and planting densities. Pine and cedar plantation plots had uniformly lower moisture contents and higher solute inventories than grasslands within comparable textural and climatic conditions. Solute inventories were greatest beneath the plots with the highest planting densities (chloride inventories 225%-240% and sulfate inventories 175%-230% of the grassland plot). Estimated recharge rates beneath the dense plantations (4-10 mm yr^{-1}) represent reductions of 86-94% relative to the surrounding native grassland. Relationships between sulfate, chloride, and moisture content in the area's relatively homogenous sandy soils confirm that the unsaturated zone solute signals reflect partitioning between drainage and evapotranspiration in this setting. This study is among the first to explore afforestation impacts on recharge beneath sandy soils and sulfate as a tracer of deep drainage.

Key words: Groundwater recharge; Unsaturated zone; Environmental tracers; Nebraska Sand Hills; Grassland plantations

Introduction

Effects of land use and land cover changes on groundwater recharge have been extensively documented across diverse environmental settings (Issar 1984; Leduc et al. 2001; Scanlon et al. 2006). The most widely-documented land use change scenario with respect to groundwater recharge has been the conversion of natural vegetation to agriculture, which has been investigated in field studies from Australia (Allison et al. 1990; Barnett 1989; Kenneth-Smith et al. 1994; Cook et al. 2001), the African Sahel (Leduc et al. 2001; Favareau et al. 2002; and reviewed in Favareau et al. 2009), the United States (Scanlon et al. 2005; Scanlon et al. 2007; Zhang and Schilling 2006), South America (Jayawickreme et al. 2011; Oliviera et al. 2005), and elsewhere (Singh 2000; Wang et al. 2008). Land use shifts to agriculture have tended to result in a net increase in rates of deep drainage and groundwater recharge in most cases. Consequent environmental issues associated with increased recharge have varied widely depending on local climatic and hydrological conditions, and have included groundwater salinization (Jayawickreme et al. 2011), soil degradation (Salama et al. 1999), water table rise (Leduc et al. 2001), and nutrient and fertilizer leaching from agricultural soils (Zhang and Schilling 2006; Scanlon et al. 2005).

Studies on groundwater recharge impacts of other land use changes not associated with row crops have been less frequent; further attention to these scenarios are desirable in order to augment current scientific understanding of linkages between land use, plant water use, and recharge. In particular, effects of afforestation on groundwater recharge are in need of increased attention for a combination of scientific and societal reasons. For one, conversion to forests is known to often have profound impacts on surface water and

watershed hydrology overall (Bosch and Hewlett 1982; Brown et al. 2005), raising the question as to whether subsurface components of the water cycle may be similarly affected in some situations.

Although firm data on recharge rate changes before and after forest plantation are scarce, some studies have demonstrated cases where afforestation of grasslands has reduced recharge rates (examples include Calder et al. 1993; Gates et al. 2011; Huang and Gallichand 2006; Jobbagy and Jackson 2004; Lima et al. 1990; Scott and Lesch 1997).

This study focuses on impacts of tree plantations on groundwater recharge in an experimental forest in the Nebraska Sand Hills (NSH) region of the central United States. The NSH offers an excellent test case for assessing grassland afforestation impacts on recharge because regional recharge rates beneath the grassland are already well-constrained through previous studies (Billesbach and Arkebauer 2012; Szilagyi et al. 2003; Szilagyi et al. 2011). The current study makes use of unsaturated zone solute tracer methods in order to determine groundwater recharge impacts of grassland afforestation. Unsaturated zone tracer methods have had longstanding use in recharge studies, including land use change investigations. In addition to the widely-used chloride mass balance method, this work explores the use of an analogous sulfate mass balance. Although recharge estimation with sulfate has been uncommon to date (Lin et al. 2013; Scanlon et al. 2006), the present study suggests that the approach holds promise as an independent check on chloride-based estimates in settings where the soil sulfur cycle can be sufficiently well-constrained. Moreover, the study has high relevance to regional water resources. NSH has both the highest recharge rates and the highest recharge to rainfall

ratios in the High Plains Aquifer System (Scanlon et al. 2012), which is one of the largest aquifers in the world and a critical groundwater resource for irrigation, drinking water, and aquatic ecological habitats.

Materials and Methods

Site description

The field investigation was conducted at Nebraska National Forest (Bessey Ranger District) in the south-central part of the NSH (Fig. 1.1; 41°51'45'' N and 100°22'06'' W; near Halsey, Nebraska, USA). The NSH region is the largest vegetation-stabilized sand dune area in the Western hemisphere, spanning approximately 50,000 km^2 (Gosselin et al. 2006). The landscape and vadose zone of the NSH is comprised mainly of eolian sand dune deposits that were deposited as recently as 8,000 years ago (Bleed and Flowerday 1998). The soils are predominantly moderately well-sorted sand consisting (approximately 92% to 97% sand; Wang et al. 2009). The dominant natural vegetation of the NSH region consists of mixed-prairie grassland including little bluestem (*S. scoparium*), switchgrass (*P. virgatum*), sand dropseed (*Sporobolus cryptandrus*), and Kentucky bluegrass (*Poa pratensis*). The predominant land use is cattle grazing. Unconfined groundwater is present throughout the NSH region. Water table depths vary significantly within short distances from <1 m in some interdunal valleys (many of which host seasonal groundwater-fed lakes and marshes) up to >90 m beneath dune ridges. Climate is semi-arid continental with an average annual precipitation of approximately 575 mm and evapotranspiration of approximately 650 mm yr^{-1} (Szilagyi et al. 2011). Mean annual precipitation of the NSH ranges between ~ 400 and 700 mm yr^{-1} and

potential evapotranspiration ranges between ~300 to 1360 mm yr^{-1} (Szilagyi et al. 2011, Wang et al. 2009). The majority of the precipitation (77%) falls between April and September. Mean annual temperature is 8.4 °C while the mean minimum daily temperature in January (winter) is –13.8 and mean maximum daily temperature in July (summer) is 31.3 °C (Eggemeyer et al. 2008).

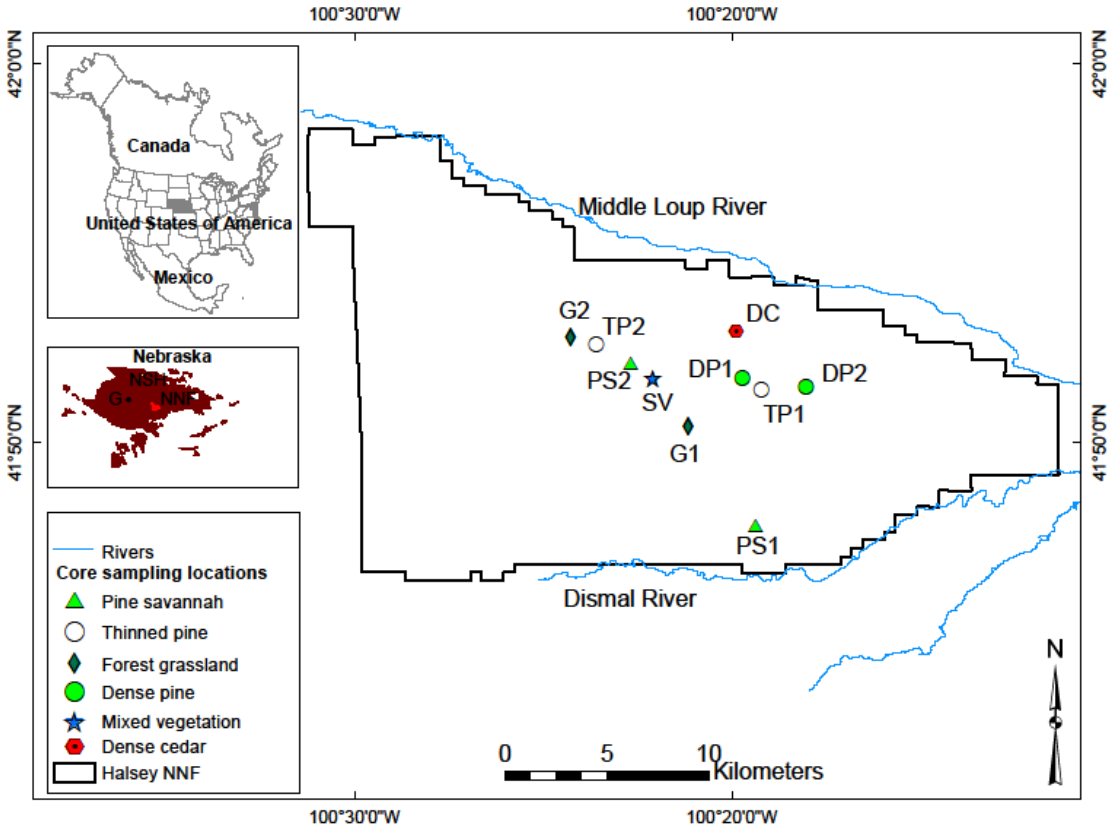

Fig. 2.1. Location of study area, core sampling, and rivers

The portion of Nebraska National Forest (NNF) investigated in this work was established in 1902 by botanist Charles Bessey as a field experiment and as a means of erosion control (Bessey 1913; Hunt 1965). It is currently the largest man-made forest in the United States, covering over 10,000 ha (Hellerich 2006). The forest was planted with

various coniferous tree species including jack pine (*P. banksiana*) and eastern red cedar *(J. virginiana*) but the majority of the forest consists of ponderosa pine (*P. ponderosa*) (Hunt 1965). The well-recorded site history, texturally-uniform soils, similar plantation ages, and differing densities of plantations, as well as the presence of native grasslands in the surrounding area, make NNF an attractive natural laboratory to investigate the effect of afforestation on groundwater recharge.

Ten experimental plots within the forest and one native grassland plot in the surrounding Sand Hills were selected for analysis (Table 2.1). Afforested plots include hand-planted forest vegetation dominated by Ponderosa pine (*P. Pondorosa*) and eastern red cedar (*J. virginiana*) (Eggemeyer et al. 2008). The plots were categorized according to vegetation type and planting density into the following five main categories: native and forest grassland (G1 and G2), sparse mixed vegetation (SV), thinned pine (TP1 and TP2), pine savannah (PS1 and PS2), dense pine (DP1 and DP2), and dense cedar (DC). The grassland plot G1 within NNF is considered to be the best approximation of the natural grassland conditions of the NSH. G2 is a plot that is currently under grassland vegetation but was forested up until 2005 and so does not provide a suitable baseline for natural conditions. The sparse vegetation plot contains mixed cedar and pine trees planted about 6 m apart. The thinned pine plots at TP1 and TP2 have been thinned as forest fire mitigation measures in the summer of 2008. The dense pines and dense cedar plots contain trees planted approximately 2.5 m apart.

Table 2.1 Cored profile plot locations, vegetation type, and profile depth summary

Profile	Plot	Vegetation Type	Longitude	Latitude	Elevation (m)	Core depth (m)	No. of Samples	Water Table depth (m)
1	G1	Native grassland	100°21’16’’	41°50’41’’	860	6	22	31
2	G2	Forest grassland	100°24’28’’	41°52’80’’	871	6	22	42
3	SV	Sparse vegetation	100°22’10’’	41°51’69’’	870	6	21	41
4	PS1	Pine savannah	100°19’37’’	41°47’81’’	839	6	22	10
5	PS2	Pine savannah	100°23’58’’	41°52’56’’	871	6	22	42
6	TP1	Thinned pine	100°19’22’’	41°51’39’’	848	6	22	19
7	TP2	Thinned pine	100°22’68’’	41°52’07’’	857	6	22	28
8	DP1	Dense pine	100°19’71’’	41°51’69’’	854	6	22	25
9	DP2	Dense pine	100°18’04’’	41°51’44’’	842	6	22	13
10	DC	Dense cedar	100°19’89’’	41°52’93’’	850	6	22	21

Experimental Methods

Field

Unsaturated zone sediment profiles were collected in May 2012 to a maximum depth of 6 meters for each of the 10 study plots using a 10 cm diameter hollow-stem hand auger (models SA5010C and SOS5010C, Dormer Engineering, Australia). Sediment samples were divided into 0.125 m intervals for the top 1 m of the profile, 0.25 m interval for depths between 1 m and 3 m, and every 0.50 m for depths from 3 m to 6 m (219 samples total). The samples from each interval were placed in a Whirl-Pak® 710 cm^3 sampling plastic bag, and then immediately sealed and refrigerated to prevent moisture

loss. Water samples for ion analysis were also collected from two rivers bordering the forest to the north and south (Loup River and Dismal River) and groundwater within the streambed of the Dismal River (Fig. 1.1). Streambed groundwater was extracted from a depth interval of 50-100 cm below the streambed surface using peristaltic pumping from a slotted drive point. Water samples were collected into 30 ml pre-washed HDPE screw-cap bottles and refrigerated until analysis.

Laboratory

In order to extract pore water from unsaturated zone sediments for analysis of chloride and sulfate, 15 g of deionized water was added to 25 g of a sediment sample in a 50 ml centrifuge tube. The slurry was then mixed in an orbital shaker for 4 hours and then centrifuged for approximately 15 minutes to separate out suspended sediments. Pore water extraction supernatant solutions and groundwater/river samples were filtered through 0.45 μm pore diameter nylon mesh filters and analyzed for chloride (Cl^-) and sulfate (SO_4^{2-}) using ion chromatography (Dionex IC2100, Thermo Scientific, Waltham, MA) (Gates et al. 2008a). Quality control procedures included field and laboratory blanks and regular repeats of analytical standards and unknowns. Analytical uncertainty was <10% of sample concentrations based on replicate analyses. Moisture contents at corresponding depths were determined gravimetrically by oven-drying at 105 ^oC for 24 hours.

Data Analysis

Environmental tracers are the most widely used recharge estimation techniques in the unsaturated zone (Scanlon et al. 2006); the use of unsaturated zone environmental

tracers for recharge was developed in the 1970s (e.g. Allison and Hughes 1978) and has been since used in many studies (e.g. Edmunds et al. 1988; Gates et al. 2008a; Huang and Pang 2012; Phillips et al. 1994; Scanlon 2000). A range of modeling approaches have been previously used to interpret ion concentrations in the unsaturated zone to develop recharge or deep drainage rate estimates, including steady-state (Allison et al. 1990; Scanlon 2002; Gates et al. 2008a) and transient mass balance expressions (Ginn and Murphy 1997; Cook et al. 2004; Scanlon et al. 2007) and solute front displacement methods (Cook et al. 1994; Kenneth-Smith et al. 1994). In this study, a simple steady-state conservative tracer mass balance approach was favored because of the short solute residence times in the profile (see Section 4.4). Using the steady-state approach, recharge is estimated as a function of profile solute concentrations, moisture contents, and atmospheric deposition rates. The approach has been discussed in detail previously and is briefly summarized here (Allison and Hughes 1978; Edmunds et al. 1988; Healy 2010).

The method is derived from a 1-dimensional soil water budget equation where input equals the sum of output and change in water storage.

$$I = O + \Delta S \tag{1}$$

where I is the input of water added, O is the water output, and ΔS is change in water storage. Considering common sources and sinks of soil moisture and assuming steady state, the water budget equation expands to the following:

$$P + Q_{on} = ET + Q_{off} + R \tag{2}$$

where P is precipitation, Q_{on} is surface flow in the form of run-on onto the plot, Q_{off} is surface flow out of the plot, ET is evapotranspiration and R is drainage beneath the root zone (i.e. potential recharge). A corresponding conservative tracer mass balance equation can be written:

$$P \cdot C_P + Q_{on} C_{on} + D = Q_{off} C_{off} + R \cdot C_s \quad (3)$$

where C_p is tracer concentration in precipitation, C_{on} and C_{off} are concentrations in surface run on and runoff, and C_s is tracer concentration in unsaturated zone porewater. D is the rate of tracer influx as atmospheric dry fallout and accounts for dry deposition from additional sources. This equation assumes no tracer mass loss in the subsurface (e.g. from mineral precipitation or adsorption) or through evapotranspiration. Due to the high hydraulic conductivity of the sandy soils in the study area (Wang et al. 2009), surface runoff rates are considered negligible (Szilagyi et al. 2011).

Setting runoff terms equal to zero and solving for R yields:

$$R = (P \cdot C_P + D) / C_S \quad (4)$$

C_s is specified using measured pore water solute concentrations below the base of the root zone to the base of the profile (depth-weighted total solute mass divided by total water content for samples collected between 0 m and 6 m below surface). In this study, the wet deposition rates for Cl^- and SO_4^{2-} were estimated using all available data from the nearest station of the National Atmospheric Deposition Program (North Platte Agricultural Experiment station; Site ID NE99; http://nadp.sws.uiuc.edu/nadpdata/annualReq.asp?site=NE99; 132 km from the study

area). The mean values for 1985–2012 were 0.34 kg/ha Cl^- and 3.97 kg/ha SO_4^{2-}, equal to 0.14 mg/L Cl^- and 1.62 mg/L SO_4^{2-} on a flux-weighted basis. No dry deposition data were available for the study area. Previous solute mass balance recharge studies in the U.S have mostly used either the model-based dry deposition estimates of the Clear Air Status and Trends Network (CASTNET) program (Liao et al. 2012; Nolan et al 2007; Sullivan et al. 2012), an assumption that wet deposition equals dry deposition (Scanlon and Goldsmith 1997; Szilagyi et al. 2011), or an assumption that dry deposition is negligible (McMahon et al. 2006). CASTNET dry deposition estimates from the two nearest CASTNET stations (Santee Sioux NE, Station 184 (340 km from study site), and Konza Prairie KS, Station 189; 565 km away from study site) indicate average dry deposition rates of 0.021 kg/ha of Cl^- and 1.080 kg/ha of SO_4^{2-} and 0.016 kg/ha of Cl^- and 0.710 kg/ha of SO_4^{2-}, respectively. These estimates represent less than 3.5% and 11.5% of the estimated wet deposition rates of Cl^- and SO_4^{2-}, respectively. For the purposes of this study, the dry deposition rate is assumed to be equal to the wet deposition rate because CASTNET dry deposition estimates for Cl^- and SO_4^{2-} have not been validated for the current study area, and in order to maintain consistency with previous work from the northern, central, and southern High Plains in the absence of more detailed data. Also, a previous groundwater chloride mass balance estimate for the Sand Hills region using this assumption compared favorably with independent regional recharge estimates from remote sensing (Szilagyi et al. 2011). Uncertainties associated with field sampling, moisture content determination, and analytical measurement of solute yield a cumulative error propagation of approximately ±13% in recharge estimates.

Sulfate mass balance considerations

Cl^- has been the most widely used ion in Eq. 4 given its very simple geochemical behavior in most non-saline low-temperature environments. In contrast, the use of sulfate (SO_4^{2-}) requires more scrutiny given its potential to participate in common chemical reactions in the subsurface. For one, reduction of SO_4^{2-} to hydrogen sulfide (H_2S) or bisulfide (HS^-) is a potential sink for SO_4^{2-} in reducing environments, for example in oxygen-poor carbon-rich soils (Connell and Patrick 1969; Massmann et al. 2003). However, sufficiently reducing conditions are unlikely to occur in the unsaturated zone of the current study area given its well-drained and organic-poor soils and subsoil sediments (Wang et al. 2009). Moisture contents in the present dataset do not exceed 0.18, which is not likely to be sufficiently high to promote anaerobic conditions in sandy soils (Davidson et al. 2000; Linn and Doran 1984).

Plant and microbial SO_4^{2-} uptake can potentially serve as another sulfate sink given that it can function as macronutrient for amino acid, protein, and vitamin formation (Freney and Williams 1983; Taiz and Zeiger 2010). However, the consumed SO_4^{2-} can also return to the soil system through plant litter and residue decomposition (Maynard et al. 1984) thus possibly maintaining a quasi-steady state in forest soils (Harrison et al. 1989). For example, Johnson et al. (1980) found that a forest sulfur pool was generally at steady state and thus SO_4^{2-} was acting as a conservative ion. Field (Strickland et al. 1985) and laboratory (Schindler et al. 1986) studies have shown that SO_4^{2-} can transform to organic sulfur within a few days of incubation period. However, field observations have shown that approximately 70% of the converted organic sulfur can transform back to SO_4^{2-} within one to two days (Houle et al. 2001).

Weathering of sulfur-bearing minerals (e.g. gypsum, pyrite, epsomite, jarosite) can be a source of SO_4^{2-} where these minerals are present and in contact with mobile pore water (Likens et al. 2002). In the current study area, available mineralogical information suggests that sulfur-bearing minerals are not present in the region's typical aeolian dune sediment matrix (Winspear and Pye 1996). Of a potentially greater concern in the NSH study area is ion adsorption. SO_4^{2-} has been found to adsorb to charged clay particles that are associated with non-silicate aluminum like hydrous aluminum and iron oxides (Alves and Lavorenti 2004; Johnson and Todd, 1983; Liu et al. 1999; Stevenson and Cole 1999). Although the NSH dune sediments contain only on the order of 1% clay-sized particles by weight (Wang et al. 2009), local clay mineralogy within the unsaturated zone includes smectite and illite-rich clays (e.g micaceous clays) (Winspear and Pye 1996), which have significant ion exchange capacities ranging between 80–150 meq/100g and 15–40 meq/100g, respectively (Reganold and Harsh 1985). The likelihood of adsorption onto clays as a significant sink of SO_4^{2-} in the unsaturated zone is further assessed using correlations with Cl^- in Section 4.3. However, laboratory adsorption dataset using field sediments is desirable to underpin these results and is recommended for future sulfate mass balance applications.

Results

Moisture content

Depth-weighted profile mean moisture contents varied by a factor of approximately 4 across the 10 profile sites. Grassland profiles (G1, G2) had the highest moisture contents overall (depth-weighted mean 9.7 % for G1 and G2; Fig. 1.2; Table 2.2). The

mixed vegetation plot with sparse vegetation (SV) had a moisture content of 8.3%, which was the second highest of the five land use categories.

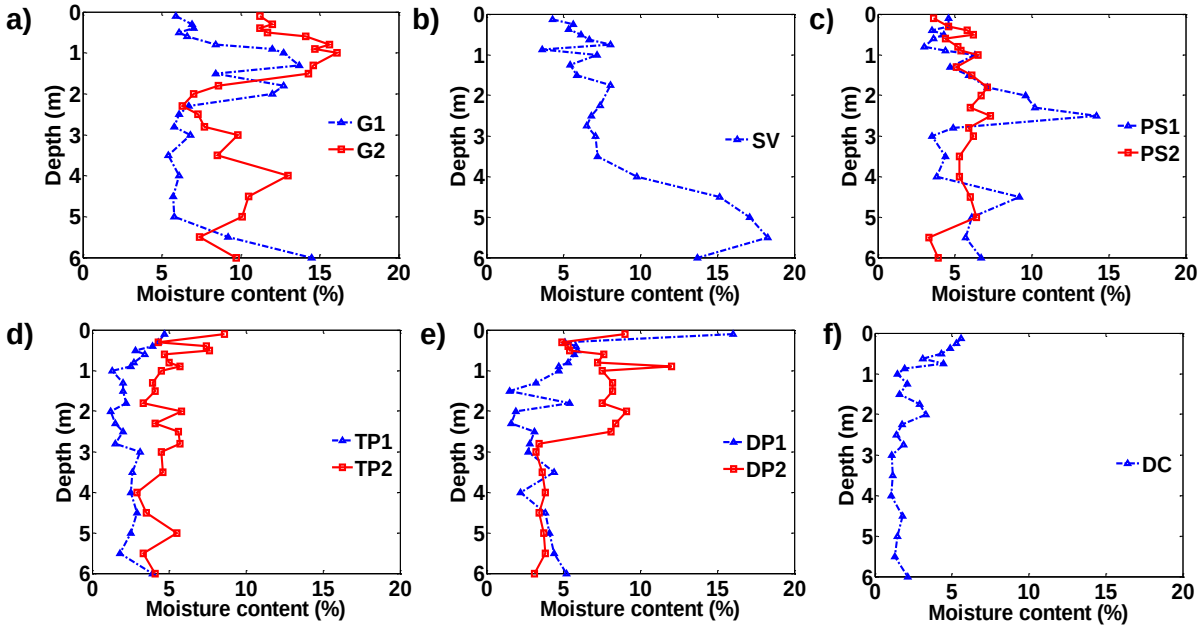

Fig. 2.2. Depth-weighted moisture content profiles for a) grasslands b) sparse vegetation c) pine savannah d) dense pine e) thinned pine and f) dense cedar plots, grouped in increasing planting density

The pine savannah profiles (PS1, PS2) together had a depth-weighted mean of 5.8%. The moisture contents beneath dense tree stands were the lowest, ranging from 2.5% to 5.3% for individual profiles. The driest profile overall was underlying the dense cedar plot (depth-weighed mean 2.5%). No significant vertical trends in moisture content were common across the profiles. Six of the 10 profiles had moisture content maxima in the root zone that were higher than moisture contents below the root zone, including both grassland profiles (Fig. 2.2a). Profiles SV and G1 both had elevated moisture contents near the base of their profiles. Based on topographic positions of the locations, it is not

likely that the increased moisture was associated with capillary rise from the regional water table. Rather, it may be associated with zones of locally fine-textured sediments interbedded in the dune sands, for example buried soils with reduced hydraulic conductivity.

Table 2.2. Summary of weighted profile moisture contents, weighted solute concentrations, and total solute concentrations

Profile	Moisture content (%)			Cl^- concentration (mg/L)			Total Cl^- storage (g/m^2)	SO_4^{2-} concentration (mg/L)			Total SO_4^{2-} storage (g/m^2)
	mean	min	max	mean	min	max		mean	min	max	
Grasslands	9.7	5.4	14.6	3.5	0.3	11.1	2.6	15.7	3.8	68.0	12.2
G1	8.4	5.4	14.5	2.9	0.7	11.1	1.4	12.4	3.8	68.0	6.1
G2	11.0	6.3	14.6	4.0	0.3	8.5	3.8	18.9	11.4	27.9	18.4
Sparse Veg.	8.3	3.6	18.3	3.4	0.7	15.8	1.9	35.0	3.4	135.4	18.5
Pine Savannah	5.8	3.3	7.3	4.7	0.8	30.3	2.0	31.8	12.1	80.6	12.3
PS1	5.9	3.5	7.1	4.6	2.1	10.2	1.8	29.9	14.3	79.4	10.7
PS2	5.6	3.3	7.3	4.8	0.8	30.3	2.2	33.6	12.1	80.6	14.0
Thinned pine	3.8	2.9	11.0	8.1	0.8	26.8	1.9	90.2	5.0	238.3	26.8
TP1	2.6	8.0	11.0	9.8	4.8	18.0	1.8	105.9	44.7	233.5	21.5
TP2	4.9	2.9	8.6	6.4	0.8	26.8	2.4	74.5	5.0	238.3	32.0
Dense Pine	5.4	1.6	16.0	8.5	1.7	20.5	3.4	41.1	5.4	150.2	13.5
DP1	4.5	1.6	16.0	9.9	1.8	20.5	3.4	42.7	14.0	150.2	14.1
DP2	6.2	3.1	12.0	7.0	1.7	16.0	3.3	39.5	5.4	89.7	12.9
Dense Cedar DC	2.5	1.0	5.6	16.6	4.9	46.7	3.1	62.3	17.0	231.1	10.7

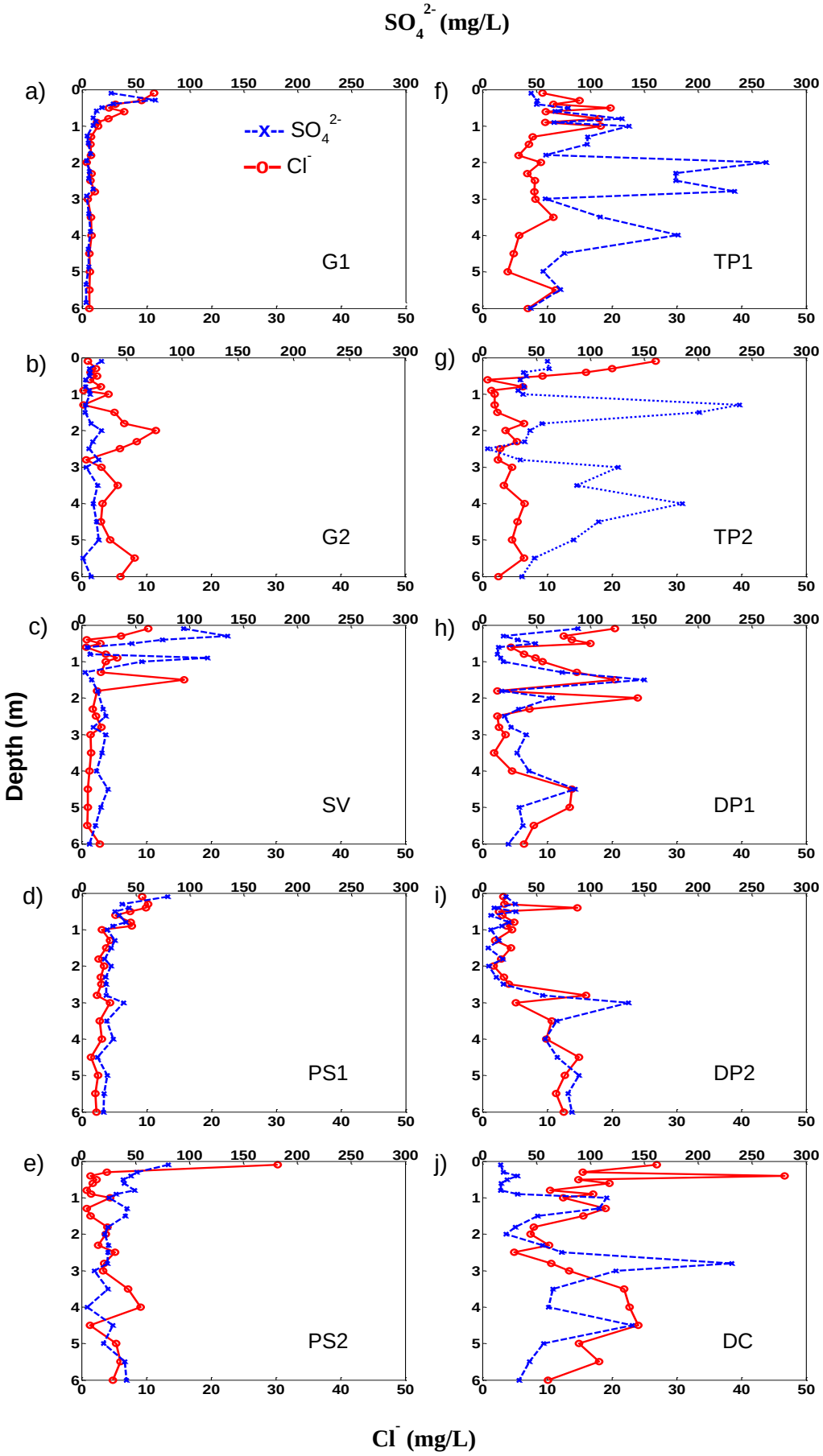
SO4 2- (mg/L)
a)
b)
c)
d)
e)
f)
g)
h)
i)
j)
--x-- SO4 2-
–o– Cl-
G1
G2
SV
PS1
PS2
TP1
TP2
DP1
DP2
DC
Depth (m)
Cl- (mg/L)

Fig. 2.3. Depth-weighted chloride and sulfate concentrations for grasslands (a and b), sparse vegetation (c), pine savannah (d and e), thinned pine (f and g), dense pine (i and h), and dense cedar (j), arranged in order of increasing planting density

Chloride and sulfate concentrations

Profile mean Cl^- concentrations were <20 mg/L in all cases and were generally lower in sparse vegetation plots than dense vegetation plots (Fig. 2.3; Table 2.2). The mean Cl^- concentration of the two grassland profiles was approximately ~3.5 mg/L, while a marginally higher average concentration (4.0 mg/L) was measured for the sparse mixed vegetation profile. The profile underlying the dense cedar plantation had the highest depth-weighted mean Cl^- concentration (~17 mg/L). Similarly to Cl^-, SO_4^{2-} concentrations were generally lower in grasslands and sparse vegetation profiles than dense vegetation plots (Fig. 2.3; Table 2.2). Unlike the Cl^- measurements, the thinned pine profiles had the highest SO_4^{2-} concentrations, (mean concentration 90.2 mg/L) followed by the dense cedar profile (mean concentration 62 mg/L of SO_4^{2-}). The depth-weighted mean SO_4^{2-} concentration below the grassland was lower than the dense cedar plantations by a factor of 8 (Fig. 2.3; Table 2.2). The cumulative profile storage values ranged from 13.8 to 38.9 kg ha^{-1} for Cl^- and 6.1 to 32.0 kg ha^{-1} for SO_4^{2-}. Vertical solute concentration trends were not consistent across plots (Fig. 2.3); however, grassland, sparse vegetation, and pine savanna plots generally contained maximum pore water solute concentrations in the top 2 m and uniformly lower concentrations beneath 3 m. The dense vegetation pine and cedar plots (Fig. 2.3 f–i) contained highly variable vertical solute concentrations.

Streambed groundwater and surface water samples had lower Cl^- and SO_4^{2-} concentrations than most unsaturated zone pore water samples (Table 2.3). The river samples both < 1 mg/L Cl^- and ~8 mg/L SO_4^{2-}. The riverbed sample had < 1 mg/L Cl^- and 6.4 mg/L of SO_4^{2-}. These ranges are consistent with previously reported groundwater ion concentrations in the region (Stanton and Qi 2007).

Table 2.3. Water sample solute concentrations for rivers and streambed groundwater

Sample	Concentration	
	Cl^- (mg/L)	SO_4^{2-} (mg/L)
Loup River	0.98	7.78
Dismal River	0.82	7.98
Dismal River streambed groundwater	0.68	6.40

Discussion

Relationships among land use, unsaturated zone moisture content, and unsaturated zone solute concentrations

Depth-weighted mean moisture contents varied substantially across vegetation types. The highest moisture contents were beneath the native grassland (G1) and sparse vegetation (SV) plots (Table 2.2). The pine savannah profiles, which contained thin and scattered pine plantations along with a grassland understory, also had relatively high moisture contents (depth-weighted average 8.3%; Table 2.2). In contrast, the dense pine and cedar plantations all contained relatively low depth-weighted moisture contents; the lowest depth-weighted profile moisture content was 2.5% for the dense cedar (DC) profile (Fig. 2.4). Although the moisture content distribution of the dense pine plots ranged from 2% to 20%, the majority of the samples were less than 6% (Fig. 2.4). The

moisture contents within the dense cedar profile were all less than 6% and a majority of them were in the 2% range.

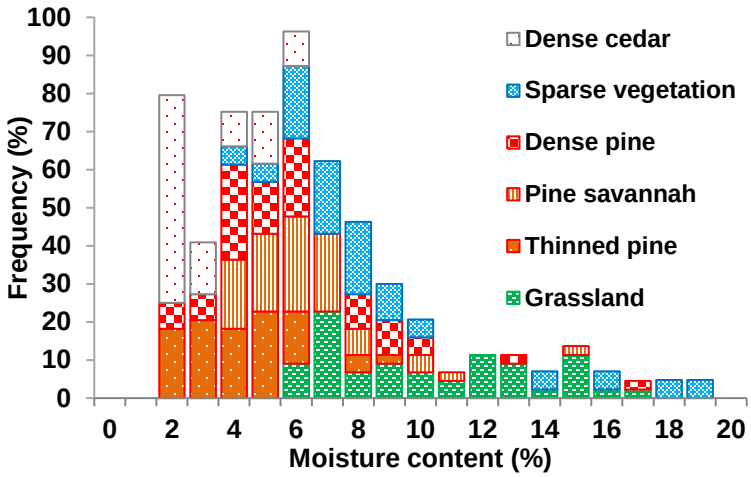

Fig. 2.4. Depth-weighted moisture content distribution frequency based on vegetation type

Overall, moisture content patterns point toward a general trend of decreasing moisture content with increasing planting density. Results for the thinned pine plots represented the only deviation from this trend. In particular, the depth-weighted profile moisture contents beneath the thinned pine plots (2.6% in TP1 and 4.9% in TP2; Table 2.2) were lower than those beneath the dense pine profiles (4.5% in DP1 and 6.2% in DP2; Table 2.2). Forestry records indicate that the thinned pine plots were thinned in summer of 2008 (4 years prior to sampling) in association with forest fire mitigation activities. Prior to thinning in 2008, tree density in TP1 and TP2 was approximately twice the 2012 density, which would have been comparable to tree densities in the dense pine plots (DP1 and DP2). Therefore, the low moisture contents in TP1 and TP2 may reflect

the effects of the prior and denser tree cover. Reasons why the profiles have not apparently increased in moisture content between 2008 and 2012 following a decline in tree density are not clear from the current dataset, but a working hypothesis may be the effect of secondary growth. Previous studies (Moore and Deiter 1992; Moore et al. 2006) have found greater throughfall precipitation and light intensity following thinning of ponderosa pine plots encourage the growth of herbaceous understory which can increase evapotranspiration from the unthinned plot and reduce soil moisture. Also, Simonin et al. (2007) found that compared to unthinned plots, thinned ponderosa pine plots have higher light penetration, which may increase soil temperature and result in higher soil evaporation. However, further exploration beyond the current dataset is required to explain the thinned pine plots moisture content difference from the dense pine plots and their deviation from the general trend. Wilcoxon-signed rank tests were also used to compare profile moisture medians on a pairwise basis; Table 2.4 shows *p*-values for the 95% confidence interval.

Table 2.4. Depth-weighted moisture content statistical analysis results (*p*-values) using Wilcoxon-signed rank test where $\alpha = 0.05$ significance level.

Land use Categories	Plot	Grasslands		Spars Vegetation	Pine savannah		Thinned pine		Dense pine	
		G1	**G2**	**SV**	**PS1**	**PS2**	**TP1**	**TP2**	**DP1**	**DP2**
Grass-lands	G1									
	G2	0.050								
Sparse Vegetation	SV	0.880	0.159							
Pine savannah	PS1	0.019	<0.001	0.002						
	PS2	0.002	<0.001	0.028	0.984					
Thinned pine	TP1	<0.001	<0.001	<0.001	<0.001	<0.001				
	TP2	0.002	<0.001	0.006	0.074	<0.001	<0.001			
Dense pine	DP1	<0.001	<0.001	0.002	0.023	<0.001	<0.001	0.150		
	DP2	0.002	<0.001	0.223	0.667	0.960	<0.001	0.124	0.089	
Dense cedar	DC	<0.001	<0.001	<0.001	<0.001	<0.001	0.313	<0.001	<0.001	<0.001

Results suggest that there is a significant effect of land use category in most cases, included for all pairings involving a pairing of a grassland profile with either a dense pine or dense cedar profile. Conversely, medians were not significant at $p = 0.05$ for paired profiles within a given land use category for five of the six land use categories (the exception was the thinned pine pair of TP1 and TP2 with $p < 0.001$).

Depth-weighted mean Cl^- concentrations varied by factors of ~ 1 to 6 between vegetation types. In general, depth-weighted mean Cl^- concentrations tend to increase with increasing plantation density. The lowest concentrations were observed beneath the native grassland (G1) and sparse mixed vegetation plot (SV), with approximately 2.9 mg/L and 3.4 mg/L of Cl^-, respectively. The pine savannah plantations contained marginally higher depth-weighted mean concentration of 4.7 mg/L. The Cl^- concentrations from thinned pine and dense pine plantations (8.1 and 8.5 mg/L, respectively) were more than twice the concentration of the native grassland. The dense cedar plantations had the highest profile depth-weighted Cl^-concentration (16.6 mg/L), which is approximately 6 times the concentration of the native grassland. The thinned pines contained marginally lower concentrations of Cl^- and total Cl^- storage (1.85×10^{-3} kg/m^2) compared to dense pine plots (3.35×10^{-3} kg/m^2; Table 2.2).

Similar to Cl^-, depth-weighted mean SO_4^{2-} concentrations were lower in the native grassland than the afforested plots. The lowest depth-weighted mean concentration was observed beneath the native grassland (G1; 16 mg/L of SO_4^{2-}); the sparse mixed vegetation plot and pine savannah plots had intermediate concentrations (32 mg/L and 35 mg/L of SO_4^{2-}, respectively.), and the dense cedar plot had 62 mg/L of SO_4^{2-}. Unlike the results for Cl^-, the thinned pine plot had a depth-weighted average concentration of 90

mg/L, which was more than twice the concentration of SO_4^{2-} observed in the dense pines (~41 mg/L). The total SO_4^{2-} storage of the thinned pine (2.7×10^{-2} kg/m^2) was approximately twice that of the dense pine profiles (1.4×10^{-2} kg/m^2).

The use of conservative solute mass balance for recharge rate estimation in the unsaturated zone requires that the increase in solute concentrations in porewater below the root zone relative to surface inputs is caused only by evapotranspiration. Comparison of profile-averaged solute concentrations and moisture contents between plot profiles, where relatively high solute concentrations are observed in low moisture content profiles, qualitatively supports this assumption for the study area. Similar inverse relationships between solute storage and moisture content have been found in other areas where landscape features or land uses result in strong spatial or temporal variability in recharge (Allison and Hughes 1983; Gates et al. 2011; Huang and Pang 2012; Scanlon et al. 2005).

Recharge rate estimates with chloride and sulfate mass balance

Recharge calculations based on the chloride mass balance indicate a mean recharge rate of 27 mm yr^{-1} (17 – 37 mm yr^{-1}; 3.4 to 7.5 % of annual precipitation) for the two profiles underlying the grasslands. The sparse mixed vegetation plot has a chloride-based recharge estimate of 32 mm yr^{-1} (6.6% of mean annual precipitation). Recharge beneath the pine savannah, thinned pine, and dense pine profiles were all less than 19 mm yr^{-1} (<4% of mean annual precipitation). The dense cedar profile had the lowest recharge rate of approximately 4 mm yr^{-1} (< 1% of mean annual precipitation).

Table 2.5 summarizes recharge rates as linear values (mm yr^{-1}), percentages of mean annual precipitation, and percentages of the estimated grassland (G1) recharge rate.

The G1 grassland plot was selected as the recharge baseline because it was hypothesized to be representative of the Sand Hills grassland ecology prior to the plantations. Expressing recharge rates relative to grassland recharge rates is an advantageous approach in order to eliminate the subjectivity introduced by the atmospheric deposition terms. Provided that atmospheric deposition rates are uniform across the experimental plots, the reported values of recharge rates relative to grassland rates will not be affected by errors in the estimated atmospheric deposition rate, and are thus independent of the largest source of uncertainty in the tracer mass balance method (Gates et al. 2008a; Healy et al. 2008). However, it should be noted that the possibility of plot-scale differences in atmospheric deposition cannot be definitively ruled out without site-specific deposition monitoring. The physical basis for local plot-scale variability in dry deposition rates is the fact that deposition is controlled by aerosol concentration and particle size, meteorological conditions such as wind speed and precipitation, vegetative cover, and surface roughness (Holsen and Noll 1992; Rogers et al. 2012). This linkage has not often been addressed in the literature on land use impacts on recharge. However, a recent study conducted in coastal South Australia found that chloride concentration was nearly 30% (under eucalyptus) and 90% (under pines) higher than the surrounding open areas because of differences in leaf area index and vegetation height (Deng et al. 2013). Although the impact of canopy enhancement is higher in coastal areas than inland (Ten Harkel 1997), mass balance approaches can underestimate groundwater recharge by up to 100% if canopy enhancement effect is not considered (Deng et al. 2013). Other potential solute input sources could include road salt and localized dust sources from industrial

activity, but these are considered unlikely to be meaningful contributors in this study area.

Chloride-based recharge estimates of the vegetated profiles relative to the native grassland plot indicate recharge reduction by up to ~90% (Table 2.5). The sparse mixed vegetation profile (SV) had nearly 87% of the recharge rate observed under the native grassland plot. Recharge rates beneath the pine savannah and dense pine plots were approximately 25% and 23% relative to the native grassland profile, respectively.

Table 2.5. Chloride and sulfate-based recharge estimates. Values are expressed using both linear rate estimates (mm yr^{-1}) and as percentages of the recharge rate estimate beneath native grassland.

Profile	CMB recharge estimate			SMB recharge estimate		
	Recharge (mm yr^{-1})	% of native grassland	% of precipitation	Recharge (mm yr^{-1})	% of native grassland	% of Precipitation
Grassland	27	72.2	3.4 – 7.5	69	71.1	8.5 – 20.0
G1	37	100.0	7.5	98	100	20.0
G2	17	43.0	3.4	41	42.2	8.5
Sparse Veget.	32	86.6	6.6	37	37.7	7.6
Pine savannah	18	24.7	3.2 – 4.4	29	29.2	5.5 – 6.2
PS1	21	57.3	4.4	30	31.0	6.2
PS2	16	42.2	3.2	27	27.9	5.5
Thinned pine	10	26.1	1.7 – 2.4	10	9.9	1.6 – 2.1
TP1	8	22.6	1.7	8	8.2	1.6
TP2	12	29.6	2.4	10	10.6	2.1
Dense pine	9	22.8	1.5 – 2.1	20	20.4	3.5 – 4.7
DP1	7	18.8	1.5	17	17.3	3.5
DP2	10	27.2	2.1	23	23.5	4.7
Dense Cedar	4	11.6	0.01	14	14.0	2.8

The lowest relative recharge estimates were for the thinned pine and dense cedar plots, with approximately 13% and 12% of the native grassland plot, respectively. The grassland profile under G2 resulted in a recharge rate estimate that is less than the grassland at G1 by approximately 57% (tree stumps present in the sampling vicinity of this location suggest that solute conditions at this site may have been affected by previous

tree plantings, which is the reason that G1 is treated as the indicator of the baseline grassland case rather than G2). In summary, all profile moisture content values are lower than the G1 value and all solute concentrations are greater than the G1 value, suggesting that recharge rates at all plantation sites are lower than the grassland recharge rate, consistent with the conclusion that grassland conversion to plantations locally reduces groundwater recharge rates.

Similar to the chloride-based estimates, sulfate-based relative recharge estimates for the afforested plots indicate decreases in recharge compared to native grassland (Table 2.5). The sparse mixed vegetation profile (SV) was ~38% of the recharge rate observed under the native grassland plot. Recharge estimates for the pine savannah and dense pine plots were approximately 30% and 20% of the native grassland profile, respectively. The lowest recharge estimates were found for the thinned pine and dense cedar plots, with approximately 10% and 14% of the native grassland, respectively.

Solute mass balance recharge rate estimates from samples obtained from streams and streambed groundwater in the study area yielded 100 mm yr^{1} for chloride and 99 mm yr^{-1} for sulfate. These recharge rate estimates are in good agreement with one another but are higher than any of the unsaturated zone-based estimates in this study, including the grassland plots G1 and G2. However, these higher rates compare favorably with regional recharge rates estimated by previous studies in the Sand Hills grasslands. Szilagyi et al. (2011) reported a regional median value of 73 mm yr^{-1} using remote sensing. Billesbach and Arkebauer (2012) reported 115 ±20 for a grazed grassland site (no trees present) ~110 km from the present study site. Previous work on recharge estimation using saturated zone groundwater Cl^{-} has suggested that groundwater-based estimates provide

greater spatial integration than unsaturated zone-based estimates because of lateral flow and mixing (Edmunds et al. 2002; Erickson and Khunakasem 1969; Wood and Sanford 1995). Therefore, it may be that the groundwater-based estimates of recharge in this case are reflecting regional Sand Hills values rather than local plantation-affected values. However, the contrast between the groundwater-based estimate of ~100 mm yr^{-1} and the G1 unsaturated zone-based estimate of 37 mm yr^{-1} raises the question as to whether the grassland plots in NNF may be unrepresentative of conditions prior to plantation establishment. In particular, forest management activities of the plots are not fully documented prior to the 1980s, and the G1 site could have included prior plantation species that are no longer present. Use of regional estimates of ~100 mm yr^{-1} as indicated by saturated groundwater solute mass balance and previous studies (Billesback and Arkebauer 2012) in place of the G1 estimate would suggest that the percent recharge rate reductions beneath the plantation plots reported in Table 2.5 underestimate the magnitude of actual reductions (by a factor of approximately 2.7).

Chloride and sulfate mass balance recharge estimate evaluation and assessment

The sulfate mass balance approach resulted in higher recharge rate estimates than chloride mass balance for all of the plot profiles. The sulfate-based recharge rates were higher than the chloride-based estimates by a factor of 2 to 3 in the grassland, dense pine, and dense cedar profiles (Table 2.5). However, SO_4^{2-} recharge rates were nearly equivalent to the Cl^- based estimates in the thinned pines and only marginally higher in the sparse vegetation and pine savannah profiles. The fact that SO_4^{2-} produced on average higher recharge rates than Cl^- may be consistent either with a SO_4^{2-} sink or with a bias in atmospheric deposition rate estimates. However, the apparent grouping of both chloride-

based and sulfate-based estimates by vegetation types would suggest that the SO_4^{2-} sink possibility is the more likely source of the discrepancy. Moreover, the similarity between chloride-based estimates and sulfate-based estimates under some vegetation types suggests that the sink is not functioning uniformly across vegetation conditions, and that the effect is not a simple function of vegetation density or species. In one of the few previous sulfate mass balance applications in the unsaturated zone, Lin et al. (2013) also observed that in some profiles sulfate mass balance overestimated weighted mean recharge by up to 2.3 times compared to chloride mass balance, and concluded that plant-specific sources and sinks of tracers should be considered.

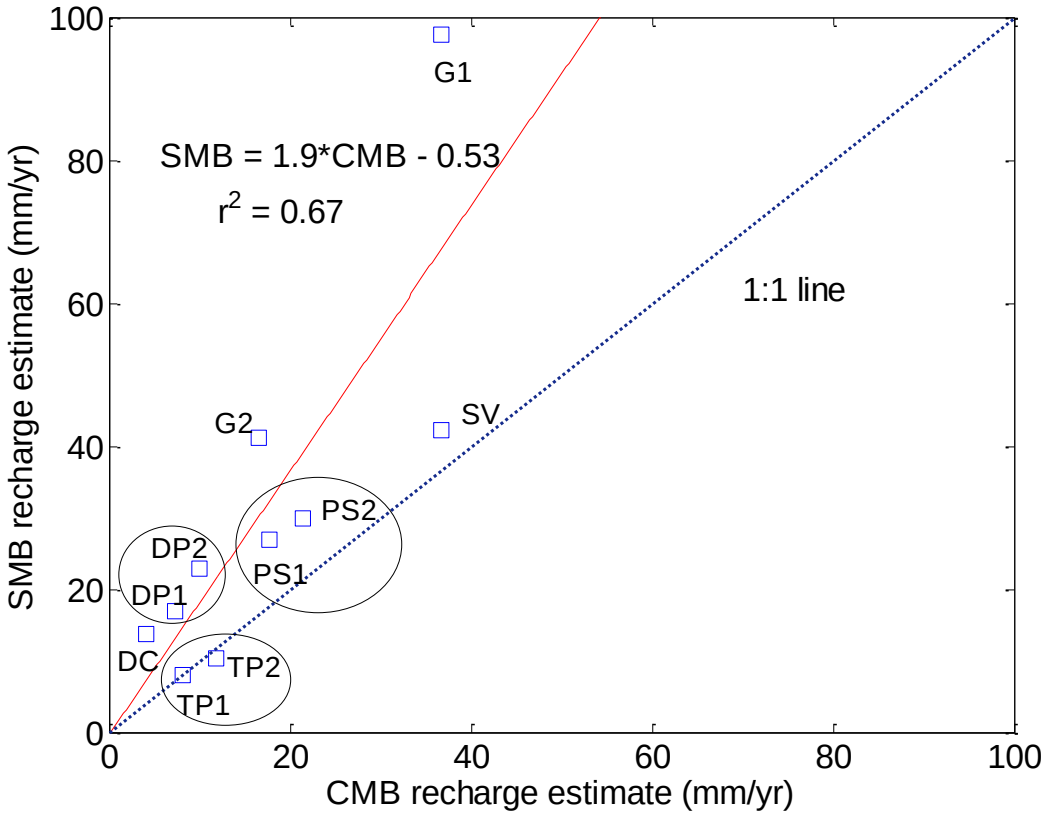

Fig. 2.5. Relationship between chloride-based and sulfate-based mass balance recharge rate estimates

The current results support that finding. Nevertheless, an overall reasonable linear correlation (R^2=0.67 is observed between chloride and sulfate-based recharge estimates (R^2=0.85 when the outlier sparse vegetation profile is omitted from consideration; Fig. 2.5).

Therefore, SO_4^{2-} inventories may be a tractable approach to constrain groundwater recharge in some (aerobic) unsaturated zones. However, more attention to constraining biogeochemical processes affecting sulfur in the root zone is needed.

Unsaturated zone evidence of temporal variability in deep drainage

Temporal changes in drainage rates can impart vertical gradients in solute concentrations and soil water contents in the unsaturated zone, and in some studies these archives of temporal changes have been apparent from cumulative tracer plots and interpreted in the context of environmental changes (Lin et al. 2013; Scanlon 1991; McMahon et al. 2003; Gates et al 2008b,). Unlike Eq. 4, this approach assumes uniform piston flow as the dominant solute transport mechanism. Using chloride mass storage in the profile divided by input rate, tracer ages at the bottoms of the 6 m profiles ranged from a minimum of 26 years (PS1) to a maximum of 56 years (G2; ages at the bottom of the dense vegetation profiles are up to 30 years older than the native grassland and sparse vegetation). In Figure 2.6, several plots show some apparent inflections in drainage rates; the most pronounced is an apparent increase in drainage rates in approximately 1996 in Profile DP2. However, there is no temporally-consistent pattern across the profiles. Available meteorological data for the Sand Hills region (http://www.hprcc.unl.edu/) does

not indicate any obvious climatic events around 1996 that would lead to a pronounced change in drainage rates, and only a single profile reflects this apparent change.

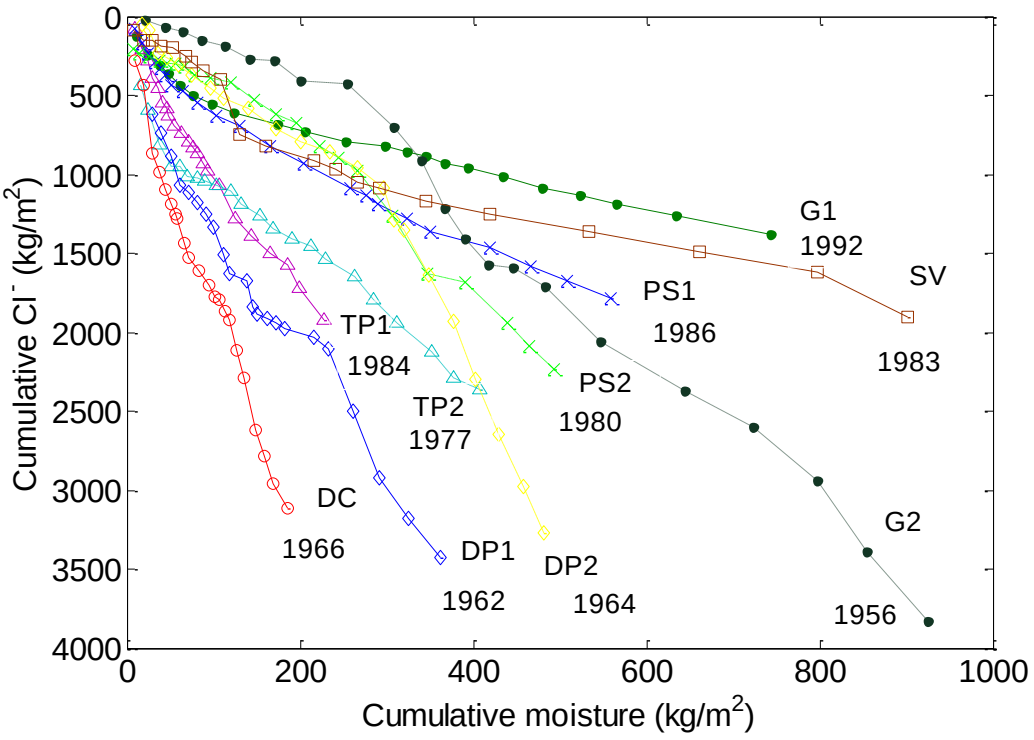

Fig. 2.6. Cumulative chloride (Cl–) concentration plotted against cumulative water flux in all profiles

The inferred change may therefore potentially be related to forest management activities. Unfortunately, the currently available profiles do not archive a solute record of the initial effects of tree planting, which took place primarily over the period of 1902-1930. Based on extrapolating age/depths curves, water that infiltrated around 1902-1930 would be located between 8 and 35 m below surface, depending on the profile/vegetation cover. For comparison, extrapolated unsaturated zone thicknesses in the study area are approximately 10-42 m (Table 2.1).

Conclusion

The results of this study suggest that conversion of grasslands to forest plantations has generated substantial reductions in recharge rates in the study area (sandy soils, semi-arid climate). The decrease in moisture content, increase in solute concentration, and reduction in recharge from plantations vary amongst different types of vegetation and plantation density. Estimates indicate that recharge was reduced by 77% and 88% in the ponderosa pine and eastern red cedar plots relative to grassland. Sulfate mass balance recharge estimates were generally higher than chloride mass balance recharge estimates, possibly associated with sulfur adsorption or assimilation in the soil zone. The results of this study underscore the importance of the currently-dominant mixed-grass prairie land cover for groundwater recharge in the Nebraska Sand Hills.

Acknowledgements

The authors would like to acknowledge the financial support of the Nebraska Geological Society and American Association of Petroleum Geologists. Thanks are due to Dave Wedin, Jeremy Hiller, and the staff of Nebraska National Forest – Bessey Ranger District for providing site access and logistical support, and to Paolo Nasta for field assistance.

References

Allison GB, Cook PG, Barnett SR, Walker GR, Jolly ID, Hughes MW (1990) Land clearance and river salinisation in the western Murray Basin, Australia. J Hydrol 119:1–20.

Allison GB, Hughes MW (1978) The use of environmental tritium and chloride to estimate total recharge to an unconfined aquifer. Aust J Soil Sci 16:181–195.

Allison GB, Hughes MW (1983) The use of natural tracers as indicators of soil-water movement in a temperate semi-arid region. J Hydrol 60:157–173. doi: 10.1016/0022-1694(83)90019-7

Alves ME, Lavorenti A (2004) Sulfate desorption from representative soils of the São Paulo State, Brazil. Geoderma 118:89–99.

Barnett SR (1989) The effect of land clearance in the Malle Region on River Murray salinity and land salinization. BMR Journ of Aust Geol and Geophysics 11:205–208.

Bessey C (1913) Some of the next steps in botanical science. Science 37:1–13. doi: 10.1126/science.37.940.1

Billesbach DP, Arkebauer TJ (2012) First long-term, direct measurements of evapotranspiration and surface water balance in the Nebraska SandHills. Agric For Meteorol 156:104–110. doi: 10.1016/j.agrformet.2012.01.001

Bleed AS, Flowerday CA (1998) An Atlas of the Sand Hills. Nebraska: Conservation and Survey Division, University of Nebraska, 1–17.

Bosch JM, Hewlett JD (1982) A review of catchment experiments to determine the effect of vegetation changes on water yield and evapotranspiration. J Hydrol 55:3–23.

Brown AE, Zhang L, McMahon TA, Western AW, Vertessy RA (2005) A review of paired catchment studies for determining changes in water yield resulting from alterations in vegetation. J Hydrol 310:28–61.

Calder IR, Prasanna KT, Hall RL (1993) Hydrological impact of Eucalyptus plantation in India. J Hydrol 150:635–648.

Connell WE, Patrick WH (1968) Sulfate reduction in soil: effects of redox potential and pH. Science 159:86–87.

Cook PG, Leaney FW, Jolly ID (2001) Groundwater recharge in the Mallee region, and salinity implications for the Murray River. CSIRO Land and Water, Tech. Rep. 45/01.

Cook PG, Leaney FW, Miles M (2004) Groundwater recharge in the North-East Mallee region, South Australia. CSIRO Land and Water Tech. Rep 25/04.

Davidson EA, Verchot L V, Cattanio JH, Ackerman IL, Carvalho JEM (2000) Effects of soil water content on soil respiration in forests and cattle pastures of eastern Amazonia. Biogeochemistry 48:53–69. doi: 10.1023/A:1006204113917

Deng Z, Priestley SC, Guan H, Love AJ, Simmons CT (2013) Canopy enhanced chloride deposition in coastal South Australia and its application for the chloride mass balance method. J Hydrol 497:62–70.

Edmunds WM, Darling WG, Kinniburgh DG (1988) Solute profile techniques for recharge estimation in semi-arid areas and arid terrain. In: Simmers I (ed)

Estimation of natural groundwater recharge. Kluwer, Dordrecht, The Netherlands, pp 13–157.

Edmunds WM, Fellman E, Goni IB, Prudhomme C (2002) Spatial and temporal distribution of groundwater recharge in northern Nigeria. Hydrogeol J 10:205–215. doi: 10.1007/s10040-001-0179-z

Eggemeyer KD, Awada T, Harvey FE, Wedin DA, Zhou X, Zanner CW (2009) Seasonal changes in depth of water uptake for encroaching trees Juniperus virginiana and Pinus ponderosa and two dominant C4 grasses in a semiarid grassland. Tree Physiol 29:157–169.

Eriksson E, Khunakasem V (1969) Chloride concentration in groundwater, recharge rate and rate of deposition of chloride in the Israel Coastal Plain. J Hydrol 7:178–197.

Favreau G, Cappelaere B, Massuel S, Leblanc M, Boucher M, Boulain N, Leduc C (2009) Land clearing, climate variability, and water resources increase in semiarid southwest Niger: A review. Water Resour Res. doi: 10.1029/2007WR006785

Favreau G, Leduc C, Marlin C, Dray M, Taupin JD, Massault M, Le Gal La Salle C, Babic M (2002). Estimate of recharge of a rising water-table in semi-arid Niger from ^{3}H and ^{14}C modeling. Ground Water 40:144–151.

Freney JR, Williams CH (1983). The sulphur cycle in soil. In the global biogeochemical sulphur cycle. Scientific committee on the problems of the environment (SCOPE)

No. 19 (ed. M. V. Ivanov and J.R. Freney), pp. 129–201. John Wiley & Sons, New York.

Gates JB, Edmunds WM, Ma J, Scanlon BR (2008a). Estimating groundwater recharge in a cold desert environment in northern China using chloride. Hydrogeol J 16:893–910.

Gates, JB, Edmunds WM, Ma J, and Sheppard PR (2008b). A 700-year history of groundwater recharge in the drylands of NW China. The Holocene 18(7): 1045-1054.

Gates JB, Scanlon BR, Mu X, Zhang L (2011) Impacts of soil conservation on groundwater recharge in the semi-arid Loess Plateau, China. Hydrogeol J 19:865–875.

Ginn TR, Murphy EM (1997) A transientflux model for convective infiltration: forward and inverse solution for chloride mass balance studies. Water Resour Res 33:2065–2079.

Gosselin DC, Sridhar V, Harvey FE, Goeke JW (2006) Hydrological Effects and Groundwater Fluctuations in Interdunal Environments in the Nebraska Sandhills. Gt Plains Res 16:17–28.

Guswa AJ and Spence CM (2012) Effect of throughfall variability on recharge: application to hemlock and deciduous forests in western Massachusetts. Ecohydrol. 5:563–574. doi: 10.1002/eco.281

Harrison RB, Johnson DW, Todd DE (1989) Sulfate Adsorption and Desorption Reversibility in a Variety of Forest Soils. J. Environ Qual.18:419–426.

Healy RW (2010) Estimating groundwater recharge, Cambridge University Press, Cambridge UK

Healy RW, Rice CA, Bartos TT, and McKinley MP (2008) Infiltration from an impoundment for coal-bed natural gas, Powder River Basin, Wyoming: Evolution of water and sediment chemistry, Water Resour. Res., 44, W06424, doi: 10.1029/2007WR006396

Hellerich JA (2006) Influence of afforestation and hillslope position on soil carbon dynamics in the Nebraska Sand Hills, Master's thesis, Univ of Nebraska-Lincoln

Holsen TM, Noll KE (1992) Dry deposition of atmospheric particles - application of current models to ambient data. Environmental Science and Technology, 26:1807–1815.

Houle D, Carignan R, Ouimet R (2001) Soil organic sulfur dynamics in a coniferous forest. Biogeochemistry 53:105–124.

Huang M, Gallichand J (2006) Use of the SHAW model to assess soil water recovery after apple trees in the gully region of the Loess Plateau, China. Agric Water Manage 85:67–76.

Huang T, Pang Z (2011) Estimating groundwater recharge following land-use change using chloride mass balance of soil profiles: a case study at Guyuan and Xifeng in the Loess Plateau of China. Hydrogeol J 19:177–186.

Hunt JC (1965) The Forest that Men Made. American Forests. OCLC Number 8515325. 13p.

Issar A, Nativ R, Karnieli K, Gat JR (1984) Isotopic Evidence of the origin of groundwater in arid zones. Proc Symp 85–105. IAEA, Vienna.

Jackson RB, Schenk HJ (2005) Mapping the global distribution of deep roots in relation to climate and soil characteristics. Geoderma 126:129–140.

Jayawickreme DH, Santoni CS, Kim JH, Jobbagy EG, Jackson RB (2011) Changes in hydrology and salinity accompanying a century of agricultural conversion in Argentina. Ecol Appl 21:2367–2379. doi: 10.1890/10-2086.1

Jobbágy EG, Jackson RB (2004) Groundwater use and salinization with grassland afforestation. Glob Chang Biol 10:1299–1312.

Johnson DW, Todd DB. (1983) Relationship among iron, aluminum, carbon and sulfate in a variety of forest soils. Soil Sci Soc Am J 47:792–800.

Johnson DW, Hornbeck JM, Kelly JM, Swank WT, Todd DE (1980) Regional patterns of soil sulfate accumulation: relevance to ecosystem sulfur budgets. In: Shriner S (ed), Atmospheric sulfur deposition: environmental impact and health effects. Ann Arbor Science Publishers Inc, Ann Arbor, MI.

Kennett-Smith A, Cook PG, Walker GR (1994) Factors affecting groundwater recharge following clearing in the south western Murray Basin. J Hydrol 154:85–105. doi: 10.1016/0022-1694(94)90213-5

Leduc C, Favreau G, Schroeter P (2001) Long-term rise in a Sahelian water-table: the continental terminal in south-west Niger. J Hydrol 243:43–54. doi: 10.1016/S0022-1694(00)00403-0

Liao L, Green CT, Bekins BA, Böhlke JK (2012) Factors controlling nitrate fluxes in groundwater in agricultural areas. Water Resour Res. 48:1–18. doi: 10.1029/2011WR011008

Likens GE, Driscoll CT, Buso DC, Mitchell MJ, Lovett GT, Bailey SW, Siccama TG, Reiners WA, Alewell C (2002) The biogeochemistry of sulfur at Hubbard Brook. Biogeochemistry 60:235–316.

Lin D, Jin M, Liang X, Zhan H (2013) Estimating groundwater recharge beneath irrigated farmland using environmental tracers fluoride, chloride and sulfate. Hydrogeol J 21:1469–1480.

Linn DM, Doran JW (1984) Effect of Water-Filled Pore Space on Carbon Dioxide and Nitrous Oxide Production in Tilled and Nontilled Soils1. Soil Sci Soc Am J 48:1267. doi: 10.2136/sssaj1984.03615995004800060013x

Lima W de P, Zakia MJB, Libardi PL, Filho AP de S (1990) Comparative evapotranspiration of Eucalyptus, Pine and natural "Cerrado" vegetation measure by the soil water balance method. IPEF Int 1:5–11.

Liu F, He J, Colombo C, Violante A (1999) Competitive adsoption of sulfate and oxalate on goethite in the absence or presence of phosphate. Soil Sci 164:180–189.

Massmann G, Tichomirowa M, Merz C, Pekdeger A (2003) Sulfide oxidation and sulfate reduction in a shallow groundwater system (Oderbruch Aquifer, Germany). J Hydrol 278:231–243. doi: 10.1016/S0022-1694(03)00153-7

Maynard DG, Stewart JWB, Bettany JR (1984) Sulfur cycling in grassland and parkland soils. Biogeochemistry 1:97–111.

McCulloch JSG, Robinson M (1993) History of forest hydrology. J Hydrol 150:189–216.

McMahon PB, Dennehy KF, Bruce BW, Böhlke JK, Michel RL, Gurdak JJ, Hurlbut DB (2006) Storage and transit time of chemicals in thick unsaturated zones under rangeland and irrigated cropland, High Plains, United States. Water Resour Res. doi: 10.1029/2005WR004417

McMahon PB, Dennehy KF, Michel RL, Sophocleous MA, Ellett KM, Hurlbut DB (2003) Water Movement Through Thick Unsaturated Zones Overlying the Central High Planes Aquifer, Southwestern Kansas, 2000-2001. Water-Resources Investig Rep 03-4171 32.

Moore MM, Casey CA, Bakker JD, Springer JD, Fule PZ, Covington WW, Laughlin DD (2006) Herbaceous vegetation responses (1992–2004) to restoration treatments in a ponderosa pine forest. Rangeland Ecol Manage 59:135–144.

Moore M, Deiter DA (1992) Stand density index as a predictor of forage production in northern Arizona pine forests. J Range Manag 45:267–271. doi: 10.2307/4002976

Nolan BT, Healy RW, Taber PE, Perkins K, Hitt KJ, Wolock DM (2007) Factors influencing groundwater recharge in the eastern United States. J Hydrol 332:187–205.

Oliveira RS, Bezerra L, Davidson EA, Pinto F, Klink CA, Nepstad DC, and Moreira A (2005) Deep root function in soil water dynamics in cerrado savannas of central Brazil. Funct Ecol 19:574–581. doi: 10.1111/j.1365-2435.2005.01003.x

Phillips FM (1994) Environmental tracers for water movement in desert soils of the American Southwest. Soil Sci Soc Am J 58:14–24

Prasanna KT, Calder IR, Rosier PTW, Parameswarappa S (1997) Eucalyptus water use greater than rainfall input - possible explanation from southern India. Hydrol Earth Syst Sci 1:249–256. doi: 10.5194/hess-1-249-1997

Reganold JP, Harsh JB (1985) Expressing cation exchange capacity in milliequivalents per 100 grams and in SI units. J of Agronomic Ed 14:84–90.

Rogers C, Lavery T, Mishoe K, and Baumgardner R (2012) Evaluation of data replacement strategies for CASTNET dry deposition. Modeling J Env Sci and Eng 1:789–799.

Salama RB, Otto CJ, Fitzpatrick RW (1999) Contributions of groundwater conditions to soil and water salinization. Hydrogeol J 7:46–64. doi: 10.1007/s100400050179

Scanlon BR (1991) Evaluation of moisture flux from chloride data in desert soils. J Hydrol 128:137–156. doi: 10.1016/0022-1694(91)90135-5

Scanlon BR (2000) Uncertainties in estimating water fluxes and residence times using environmental tracers in an arid unsaturated zone. Water Resour Res 36:395–409.

Scanlon BR, Faunt CC, Longuevergne L, Reedy RC, Alley WM, McGuire VL, McMahon PB (2012) Groundwater depletion and sustainability of irrigation in the US High Plains and Central Valley. Proc Natl Acad Sci 109:9320–9325. doi: 10.1073/pnas.1200311109

Scanlon BR, Goldsmith RS (1997) Field study of spatial variability in unsaturated flow beneath and adjacent to playas. Water Resour Res 33:2239. doi: 10.1029/97WR01332

Scanlon BR, Keese KE, Flint AL, Flint LE, Gaye CB, Edmunds WM, Simmers I (2006) Global synthesis of groundwater recharge in semiarid and arid regions. Hydrol Process 20:3335–3370. doi: 10.1002/hyp.6335

Scanlon BR, Jolly I, Sophocleous M, Zhang L (2007), Global impacts of conversions from natural to agricultural ecosystems on water resources: Quantity versus quality, Water Resour Res 43:1–18.

Scanlon BR, Reedy RC, Stonestrom DA, Prudic DE, Dennehy KF (2005) Impact of land use and land cover change on groundwater recharge and quality in the southwestern US. Glob Chang Biol 11:1577–1593.

Scanlon BR, Stonestrom DA, Reedy RC, Leaney FW, Gates JB, Cresswell RG (2009) Inventories and mobilization of unsaturated zone sulfate, fluoride, and chloride related to land use change in semiarid regions, southwestern United States and Australia, Water Resour Res 45:W00A18. doi:10.1029/2008WR006963

Schindler SC, Mitchell MJ, Scott TJ, Fuller RD, Driscoll CT (1986) Incorporation of Sulfur-35 Sulfate into Inorganic and Organic Constituents of Two Forest Soils. Soil Sci Soc Am J 50:457–462.

Scott DF, Lesch W (1997) Streamflow responses to afforestation with Eucalyptus grandis and Pinus patula and to felling in the Mokobulaan experimental catchments, Mpumalanga Province, South Africa. J Hydrol. 199:360–377.

Simonin K, Kolb TE, Montes-Helu M, Koch GW (2007) The influence of thinning on components of stand water balance in a ponderosa pine forest stand during and after extreme drought. Agric For Meteorol 143:266–276. doi: 10.1016/j.agrformet.2007.01.003

Singh (2000) Environmental consequences of agricultural development: a case study from the Green Revolution state of Haryana, India. Agric Ecosyst Environ 82:97–103. doi: 10.1016/S0167-8809(00)00219-X

Stanton JS and Qi SL (2007) Ground-water quality of the northern High Plains aquifer, 1997, 2002–04: U.S. Geological Survey Scientific Investigations Report 2006–5138 1–60.

Stevenson FJ, Cole MA (1999) Cycles of soil: carbon, nitrogen, sulfur, micronutrients. John Wiley & Sons, Inc., New York.

Strickland TC, Fitzgerald JW, Swank WT (1985) In situ measurements of sulfate incorporation into forest floor and soil organic matter. Can J For Res 16:549–553.

Sullivan PL, Price RM, Miralles-Wilhelm F, Ross MS, Scinto LJ, Dreschel TW, Sklar FH, Cline E (2012) The role of recharge and evapotranspiration as hydraulic drivers of ion concentrations in shallow groundwater on Everglades tree islands, Florida (USA) Hydrol Process. 10:75–95. doi: 10.1002/hyp

Szilagyi J, Harvey EF, Ayers JF (2003) Regional estimation of base recharge to groundwater using water balance and a base-flow index. Ground Water 41:504–513.

Szilagyi J, Zlotnik VA, Gates JB, Jozsa J (2011) Mapping mean annual groundwater recharge in the Nebraska Sand Hills, USA. Hydrogeol J 19:1503–1513.

Taiz L, Zeiger E (2010) Plant physiology, 5th edn. Sinauer Associates, Inc., Sunderland, MA.

Ten Harkel MJ (1997) The effects of particle-size distribution and chloride depletion of sea-salt aerosols on estimating atmospheric deposition at a coastal site. Atmos Environ. 31:417–427.

Wang B, Jin M, Nimmo JR, Yang L, Wang W (2008) Estimating groundwater recharge in Hebei Plain, China under varying land use practices using tritium and bromide tracers. J Hydrol 356:209–222. doi: 10.1016/j.jhydrol.2008.04.011

Wang T, Zlotnik VA, Šimunek J, Schaap M (2009) Using process-based models and pedotransfer functions for soil hydraulic characteristics to estimate groundwater recharge in semi-arid regions. Water Resour Res 45:W04412. doi: 10.1029/2008WR006903

Winspear NR, Pye K (1995) Textural, geochemical and mineralogical evidence for the origin of peoria loess in Central and Southern Nebraska, USA. Earth Surf Process Landforms 20:735–745. doi: 10.1002/esp.3290200805

Wood WW, Sanford WE (1995) Chemical and isotopic methods for quantifying ground-water recharge in a regional, semiarid environment. Ground Water 33:458–468.

Zhang YK, Schilling KE (2006) Increasing streamflow and baseflow in Mississippi River since the 1940s: Effect of land use change. J Hydrol 324:412–422. doi: 10.1016/j.jhydrol.2005.09.033

CHAPTER 3

LINKS BETWEEN SOIL HYDROPHOBICITY AND GROUNDWATER RECHARGE UNDER PLANTATIONS IN THE A SANDY GRASSLAND SETTING, NEBRASKA SAND HILLS, USA

Zablon A. Adane · Paolo Nasta · John B. Gates

Z. A. Adane

Department of Earth and Atmospheric Sciences, University of Nebraska–Lincoln, Lincoln, NE, 68588, USA, zablon@huskers.unl.edu

P. Nasta

University of Naples Federico II. Via Università, n. 100 – 80055 Portici (Napoli), Italy, paolo.nasta@unina.it

J. B. Gates

The Climate Corporation, 201 Third Street, Suite 1100 San Francisco, CA 94103, USA, john.gates@climate.com

Citation: Adane, Z.A., Nasta, P., and Gates, J.B., 2017. Links between soil hydrophobicity and groundwater recharge under plantations in a sandy grassland setting, Nebraska Sand Hills, USA. Forest Science (x): xxx–xxx doi:10.5849/FS-2016-137

Abstract

This study addresses relationships between soil hydrophobicity and groundwater recharge through the unsaturated zone in semi-arid sandy grasslands containing mature tree plantations. Field and laboratory investigations of soil properties and recharge rates were undertaken at ten experimental plots within the Nebraska Sand Hills. Plots included a range of plantation species and planting densities in addition to grasslands. Hydrophobicity was characterized using a combination of methods including water and ethanol drop penetration tests, Nuclear Magnetic Resonance spectral analysis, and field infiltration tests. Water and ethanol drop tests indicate that surface soils beneath pine plots were moderately to strongly hydrophobic and that plantations are 3 to 13 times more hydrophobic than the grasslands. The spectral analysis suggested that the surface soil organic carbon beneath pine plantations contains up to 3 times the ratio of hydrophobic components than the grasslands. Mini-infiltrometer tests demonstrate that changing grassland into tree plantations leads to declining soil infiltration capacity and lowering down sorptivity and hydraulic conductivity (at -2 cm pressure head) by an order of magnitude. Previously published chloride-based annual recharge estimates beneath these plantations represent reductions of up to 90% relative to the grassland, and showed strong relationship (R^2 = 0.94) with unsaturated hydraulic conductivity retrieved from the field infiltration experiments. HYDRUS 1-D synthetic numerical modeling was also performed to corroborate decreasing recharge rates (25 to 31.4 %) under land-use change dynamics.

Keywords: soil water repellency, groundwater recharge, grassland plantation, numerical modeling, infiltration test, Halsey Forest

Introduction

During the period between 1750 and 1900, the forest cover in the United States was reduced from 450 million to 300 million hectares resulting from conversion to farm land (FAO 2012). Such drastic deforestation has many negative effects on the environment including change in hydrological regimes (Coe et al. 2009), land degradation (Bruun et al. 2015, Ozalp et al. 2015), loss of habitat and wild life (Brooks et al. 2002), and even exacerbating climate change (Malhi et al. 2008). In the last 100 years however, natural regeneration on converted farm lands and afforestation programs of various land uses has increased forest area (McCleery 1992). While forests provide beneficial ecological services, many case studies have also shown situations in which land use conversions to forested land have substantially reduced soil moisture (Huang and Pang 2011, McVicar et al. 2007) and groundwater recharge rates (Calder et al. 1993, Lima et al. 1990, Scanlon et al. 2009, Jobbágy and Jackson 2004, Lesch and Scott 1997). Several of these studies have also attributed soil moisture and groundwater recharge reductions primarily to the relatively higher transpiration rates of the planted woody vegetation (Gates et al. 2011, Huang and Gallichand 2006, Huang and Pang 2011). Other studies (e.g. Owens et al. 2006) have also associated these reductions in soil moisture and recharge rates to greater rainfall interception of the introduced plantations, which can range up to 10% to 40% of annual rainfall, twice that of adjacent grasslands (Bosch and Hewlett 1982).

Forests have also been recognized to alter soil hydraulic properties of the soil (Wahl et al. 2003, Wine et al. 2011, Kajiura et al. 2012); however, subsequent impacts of these changes on the water cycle have received relatively little attention. Plantations can alter soil physical properties such as porosity (Roberts 2000), biological and microbial activity (Janssens et al. 2010) as well as chemical properties through the decomposition of litter,

deposition of organic matter, and buildup of waxes and resins, which may cause soil hydrophobicity (water repellency) (Doerr et al. 2000). The causes, presence, and impacts of soil hydrophobicity on the soil water balance have been characterized by several studies under different land uses (Buczko et al. 2002, Dekker and Ritsema 1994, Urbanek et al. 2007), climate (Buczko et al. 2005, Jaramillo et al. 2003), soils (Bachmann and Van Der Ploeg 2002), forest fire (Robichaud and Hungerford 2000, Keesstra et al. 2016), grassland fire (Pereira et al. 2014), and other scenarios (Nadav et al. 2011, York and Canaway 2003, Bodi et al. 2013) and have been thoroughly summarized (Doerr 1998, Doerr et al. 2000, King 1981; Letey et al. 2000). Hydrophobicity in soils results from either partial or complete coating of hydrophilic mineral particles with organic matters containing long aliphatic chains that have the tendency to be more hydrophobic (Kajiura et al. 2012). Known sources of hydrophobic substances include bacteria, fungi, algae, and many higher order plants including grasses, eucalypts, and several pine species (Horn et al. 1964, Doerr et al. 2000). Dry soil conditions also strongly affect the manifestation or the severity of soil hydrophobicity (Dekker and Ritsema 1994, de Jonge et al. 2007). The variability of soil hydrophobicity in spatial and temporal distribution is also a major factor in the severity of its consequences (Dekker and Ritsema 1994, Rye and Smettem 2015). Soil hydrophobicity is common in sandy soils and is often exacerbated due to the relatively low specific hydrophilic surface area of the particles resulting in organic matter coating (Wallis et al. 1991).

The objectives of this study are threefold: 1) to evaluate the extent of soil hydrophobicity resulting from grassland conversion to different plantation densities of ponderosa pine and eastern red cedar forests, 2) to assess the impact of hydrophobicity on

annual groundwater recharge rates, and 3) to perform a synthetic numerical modeling exercise to observe how extreme assumptions of hydrophobicity effect on the soil hydraulic properties impact the water balance. Although several studies have documented the impact of vegetation on soil hydrophobicity and infiltration rates (Clothier et al. 2000, Doerr and Thomas 2000, Ritsema et al. 1998, Wang et al. 2003) none have used multiple measurements to assess hydrophobicity and its subsequent indirect implications on groundwater recharge rates. This investigation aims to fill a gap in this literature by providing a case study where both hydrophobicity and groundwater recharge were characterized.

Materials and Methods

Site description

The field experiment was conducted at Nebraska National Forest (NNF) (Bessey Ranger District) in the south-central part of the Nebraska Sand Hills (NSH) (Fig. 3.1; 41°51'45" N and 100°22'06" W; near Halsey, Nebraska, USA). The NSH landscape is comprised mainly of eolian sand dunes that were deposited as recently as 8,000 years ago (Gosselin et al. 2006). The Sand Hills soils are moderately well sorted sand consisting of approximately 96% sand (Wang et al. 2009). Similarly, the grassland, pine, and dense cedar plots at the NNF consist of mainly Valentine sands (Hellerich 2006), which are described as 95% sand, 4% silt, and 1% clay (Kettler et al. 2001). The natural vegetation of the NSH region consists of mixed-prairie grassland. The climate is semi-arid continental with mean annual precipitation ranging between approximately 400 and 700 mm yr^{-1} and potential evapotranspiration ranging between 300 to 1360 mm yr^{-1} (Szilagyi et al. 2011). Mean

annual temperature is 8.4 ^{o}C while the mean minimum daily temperature in January is -13.8 °C and mean maximum daily temperature in July is 31.3 ^{o}C (Eggemeyer et al. 2009).

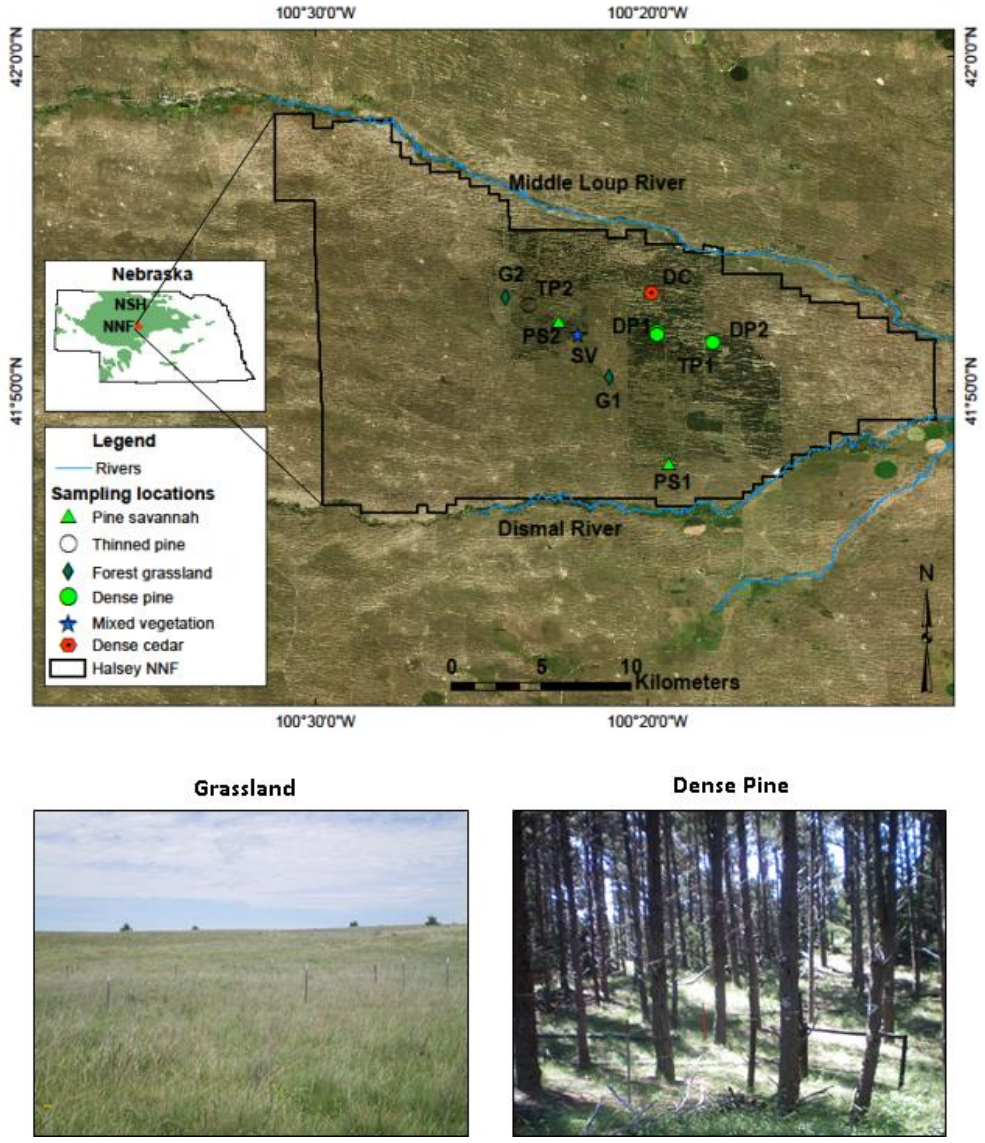

Fig. 3.1. Locations of sampling plots, the Nebraska Sand Hills (NSH), Nebraska National Forest (NNF) in Halsey, NE, and grassland and dense pine pictures of the forest.

Nebraska National Forest is the largest man-made forest in the United States covering 10,000 ha and contains various coniferous tree species with differing planting

densities, many of which were planted as early as the 1930s (Hellerich 2006). Ten plots with 10 m x 10 m dimensions were selected based on vegetation type and planting density into the six main categories (Table 3.1) as well as the availability of existing plot level groundwater recharge rate estimates.

Table 3.1. Plot locations, vegetation type, elevations, tree density, and average Leaf Area Index (LAI)

Profile	Plot	Vegetation type	Longitude	Latitude	Elevation (m)	Tree density (trees ha^{-1})	Average LAI (-)
1	G1	Native grassland	100°21’16’’	41°50’41’’	860	-	-
2	G2	Forest grassland	100°24’28’’	41°52’80’’	871	-	-
3	SV	Sparse vegetation	100°22’10’’	41°51’69’’	870	-	0.31
4	PS1	Pine savannah	100°19’37’’	41°47’81’’	839	100-300	1.68
5	PS2	Pine savannah	100°23’58’’	41°52’56’’	871	100-300	1.68
6	TP1	Thinned pine	100°19’22’’	41°51’39’’	848	300-700	1.87
7	TP2	Thinned pine	100°22’68’’	41°52’07’’	857	300-700	1.87
8	DP1	Dense pine	100°19’71’’	41°51’69’’	854	700-1000	2.20
9	DP2	Dense pine	100°18’04’’	41°51’44’’	842	700-1000	2.20
10	DC	Dense cedar	100°19’89’’	41°52’93’’	850	1800-2000	1.87

The native grassland (G1 only) plot is considered the best approximation of the natural grassland conditions of the NSH (Fig.3.1). The grassland plots and understory vegetation within the forest include perennial species dominated by little bluestem (*S. scoparium*), switchgrass (*P. virgatum*), sand dropseed (*S. cryptandrus*), Kentucky bluegrass (*Poa pratensis* L.), and white sage (*Artemesia ludoviciana* Nutt.) (Eggemeyer et al. 2009). The sparse vegetation (SV) plot contains mixed cedar and pine trees planted

about 6 m apart. The pine savannah (PS1 and PS2) plots contain grasslands with pine plantations at a density of 100 to 300 trees ha^{-1}. The thinned pine plots (TP1 and TP2) have been thinned as forest-fire-mitigation measures in the summer of 2008 and contain 300 to 700 trees ha^{-1} on average. The dense pines (DP1 and DP2) and dense cedar (DC) plots contain trees at approximately 700 to 1000 and 1800 to 2000 trees ha^{-1}, respectively (Hellerich 2006, Table 3.1). The study locations correspond to those displayed in Fig.3.1.

Experimental methods to assess soil hydrophobicity

Soil samples were collected in May 2012 from 10 experimental plots using a 10-cm diameter hollow-stem hand auger (model SA5010C and SOS5010C, Dormer Engineering, Australia). Samples were cored and collected to a depth of 50 cm at 12.5 cm intervals and were placed in a Whirl-Pak 710 cm^3 sampling plastic bag, immediately sealed, and refrigerated to prevent moisture loss and maintain soil field condition. Each soil core interval from each plot was then subsampled to perform the laboratory analyses discussed below so that the results are readily comparable.

Methods used to assess soil hydrophobicity in this study are summarized below and have been previously presented in detail (Letey et al. 2000, Buczko et al. 2005, Doerr et al. 2000).

Field moisture content and organic carbon

Moisture contents were determined gravimetrically by oven-drying at 105 °C for 24 h at the end of the experiments.

The presence of soil organic material is common to all hydrophobic soils (Nadav et al. 2011) and plays a significant role in soil hydrophobicity. Soil samples were analyzed for soil organic carbon content by dry combustion GC analysis on a Costech ECS 4010 (Costech Analytical Technologies, Inc., Valencia, CA USA).

The Water Drop Penetration Test (WDPT) and the Ethanol Percentage Test (EPT)

Field-moist and oven-dried (72 hours at 45 ^{o}C) soil samples were placed in weighing dishes with 6 cm diameter and 1 cm depth. In the WDPT and EPT (oven-dried samples only) tests, 3 drops of water or ethanol were repeatedly applied onto a smoothed soil sample surface using a 5 ml pipette, and the time required for the drop to penetrate the soil was recorded. The drop penetration time of 5 replicates was taken as representative of each sample and reported in Table 3.2.

Table 3.2. Results summary of median WDPT (s) and EPT (% ethanol in drops needed for penetration of soil surface to occur in less than 5 s)

	WDPT (s)								EPT (% ethanol)			
	Depth intervals (cm)											
	Field condition				Oven-dried				Oven-dried			
Plot	0-12	12 - 25	25 - 37	37 - 50	0 - 12	12 - 25	25 - 37	37 - 50	0 - 12	12 - 25	25 - 37	37 - 50
G1	3	3	3	3	3	3	3	3	0	0	0	0
G2	3	3	3	3	3	3	3	3	0	0	0	0
SV	13	3	3	3	184	3	3	3	0	0	0	0
PS1	18	3	3	3	657	3	3	3	3	0	0	0
PS2	612	10	3	3	638	190	3	3	5	0	0	0
TP1	3	6	3	3	618	120	9	5	3	3	0	0
TP2	607	69	3	3	612	15	3	3	5	0	0	0
DP1	3	3	3	3	617	3	3	3	5	0	0	0
DP2	5	3	3	3	662	3	3	3	3	0	0	0
DC	3	3	3	3	3	3	3	3	0	0	0	0

The soil hydrophobicity classification based on the median drop penetration time of 5 replicates has been adopted from Doerr (1998) to be consistent with the effort to standardize soil hydrophobicity reporting (Table 3.3).

Table 3.3. WDPT and EPT soil hydrophobicity classes

Class	Description	WDPT (s)	Volume of ethanol (%)
7	Extremely hydrophobic	>18000	36
6	Severely hydrophobic	3600 - 18000	24
5	Strongly hydrophobic	600 - 3600	13
4	Moderately hydrophobic	180 - 600	8.5
3	Slightly hydrophobic	60 - 180	5
2	Hydrophilic	5 - 60	3
1	Very hydrophilic	<5	0

^{1}H NMR analysis

Hydrophobic characteristics are closely related to the properties of the organic material rather than just the quantity (Flores-Mangual et al. 2013). Nuclear Magnetic Resonance (^{1}H NMR) spectroscopy to identify chemical components can be used for soil organic carbon characterization (Ivanova and Randall 2003). The ^{1}H NMR experiments were conducted using Bruker AVANCE DRX 500 MHz NMR (Bruker Corporations, MA USA). ^{1}H NMR spectra of each of the soil samples were obtained for a chemical shift range of 0 to 11 ppm. The solution for each sediment samples were obtained by dissolving and extracting 200 mg of the soil samples with 25 ml of CH_2Cl_2. The samples solutions were stirred occasionally overnight to insure complete extraction prior to filtration. The extracts were dried at 37 ^{o}C over 24 h then partially dissolved in $CDCl_3$ to extract hydrophobic constituents within the fulvic material of the soil organic matter. An aliquot (500 µL) of

these extracts was placed in an NMR tube and 50 µL of D_2O was added to each sample to ensure proper extraction of the humic materials not dissolved by $CDCl_3$.

The integrated area under the curve of specific chemical shift ranges of the magnetic field spectrum (in ppm) was used for ^{1}NMR spectral analysis of each sample. The spectral range signals the type of proton of the chemical compound there by enabling the identification of the hydrophobic compounds such as aliphatic groups. The spectral range signals identified include aliphatic (3.2 – 0.5 ppm) and aromatic (8.5 – 6.5 ppm) as well as non-hydrophobic halogens, alcohols, and esters (6.5 – 3.2 ppm) (Silverstein et al. 2014). The ratios of integrated areas of non-hydrophobic to hydrophobic spectral signals are used to represent a quantitative indication of hydrophobicity (Tarchitzky et al. 2007). Samples with a higher ratio of aromatic and aliphatic structures may show higher tendency towards soil hydrophobicity (Nadav et al. 2011).

Field infiltration method

In-situ field infiltration measurements were used to observe water movement under natural conditions. Field infiltration tests were performed once for water and ethanol beneath the vegetation of each plot by using mini-disk infiltrometer devices (Madsen and Chandler 2007, Dohnal et al. 2010) (Decagon Devices, Pullman, WA USA) approximately 1.5 meters from the trunk of the trees and within the canopy extents and boundaries of each plot. The infiltrometer was set to pressure head of h_o = -2 cm (Lichner et al. 2010) based on the capillarity and higher pore radius of coarse sandy soils (Hallett 2008).

The cumulative infiltration I is described by the Philip infiltration equation (Philip 1957; Moody et al. 2009, Robichaud et al. 2009, Lichner et al. 2010).

$$I = C_1(h_0)t^{1/2} + C_2(h_0)t \quad (1)$$

where t is time, C_1, and C_2 are coefficients obtained from the slope and optimization of a cumulative infiltration versus square root of time plot (Lichner et al. 2007).

The sorptivity $S(h_o)$ and unsaturated hydraulic conductivity $K(h_o)$ at negative pressure head ($h_o < 0$) can be estimated using infiltration times less than 180 s (Hallett 2008).

$$S(h_0) = \frac{C_1(h_0)}{A} \quad (2)$$

and

$$K(h_0) = \frac{C_2(h_0)}{A} \quad (3)$$

where $A = 1.73$ for sandy soils and suction head $h_0 = -2$ cm (Lichner et al. 2007). The $K(h_o = -2$ cm) will be referred hereinafter as K_u.

Water and ethanol infiltration measurements were also used to estimate soil hydrophobicity factor H in the field, calculated as follows:

$$H = 1.95\frac{S_e(h_0)}{S_w(h_0)} \quad (4)$$

where hydrophobicity index H is a ratio of sorptivities of ethanol (S_e) and water (S_w) at suction $h_0 =$ -2 cm (Hallett et al. 2001).

HYDRUS 1-D Numerical modeling to evaluate groundwater recharge

Numerical hydrological processes have been simulated using the HYDRUS 1-D software package (Šimůnek et al. 2008, Wang et al. 2015) that numerically solves the following one-dimensional Richards equation for variably-saturated soil water flow:

$$\varphi(h)\,\frac{\partial h(z,t)}{\partial t} \;=\; \frac{\partial}{\partial z}\left\{ K(h)\left[\frac{\partial h(z,t)}{\partial z}+1\right]\right\} - \zeta(h) \qquad (5)$$

where t is time, z is the vertical coordinate (positive upward), h is pressure head, θ is the soil volumetric water content, $\varphi(h)=\delta\theta/\delta h$ signifies the differential soil-water capacity function, and $\zeta(h)$ is the volumetric sink term function that describes macroscopic root water uptake. The soil water retention, $\Theta(h)$, and hydraulic conductivity, $K\Theta$), functions are described by the van Genuchten (1980) analytical relationships:

$$\Theta(h) \;=\; \frac{\theta(h)-\theta_r}{\theta_s-\theta_r} \;=\; \left[1+\left(\alpha|h|\right)^n\right]^{-m} \qquad (6a)$$

$$K(\Theta) \;=\; K_s\,\Theta^l\left[1-\left[1-\Theta^{1/m}\right]^m\right]^2 \qquad (6b)$$

where θ_s ($cm^3 \cdot cm^{-3}$) and θ_r ($cm^3 \cdot cm^{-3}$) are the saturated and residual volumetric soil water contents, respectively, α (cm^{-1}), n (-) and m = (1–1/n) are the shape parameters of water retention function, K_s ($cm \cdot d^{-1}$) is the saturated hydraulic conductivity, whereas l (-) is the pore connectivity parameter of hydraulic conductivity function. The degree of saturation,Θ (-) varies between 0 (when $\theta = \theta_r$) and 1 (when $\theta = \theta_s$). The shape parameter α is inversely related to the air-entry value (van Genuchten, 1980). A twelve-year time record (2003-2014) of weather data (namely precipitation, relative humidity, air temperature, wind speed

and solar radiation) were retrieved from High Plains Regional Climate Center (HPRCC) for the Halsey, NE station (41°47'0" N and 100°32'6"W).

The potential evapotranspiration, ET_p (cm·d^{-1}), is computed by the Penman–Monteith equation from the meteorological data (Allen et al. 1998). ET_p is partitioned into potential evaporation E_p (cm·d^{-1}) and potential transpiration T_p according to the following empirical equation:

$$E_p = ET_p e^{-\kappa LAI} \tag{7}$$

where κ (-) is the dimensionless extinction coefficient for global solar radiation inside the canopy and is assumed to be equal to 0.463 (Ritchie 1972). The residual fraction of the potential evapotranspiration is assumed equal to the potential transpiration, T_p (cm·d^{-1}). Precipitation, P, and potential evaporation, E_p, represent the system-dependent upper boundary condition, whereas T_p determines the potential root water uptake [$\zeta(h)$] that is reduced through the Feddes' condition (Nasta and Gates 2013). The root density distribution is assumed to decrease linearly with increasing root depth, z_r. Free drainage is set as the lower boundary condition for the soil profile (z = 600 cm), enabling drainage to occur in a unit hydraulic gradient. The simulation of the first year (2003) is considered as the provisional year in order to provide 'pseudo-realistic' initial conditions for the subsequent 11 years (2004–2014) in the water budget simulation.

Synthetic numerical simulations were run with three scenarios in order to observe the impact of a severe hydrophobic layer. The first scenario was a baseline simulation representing the native grassland conditions of the study area. This baseline scenario is a uniform (single-layer) simulation with "standard" non-hydrophobic sandy soil condition

with a maximum rooting depth of 0.50 meters. The second and third scenarios represent a soil profile with pine plantation with maximum root depth of 2 meters. The second scenario comprises also a uniform (single-layer) soil profile with the same standard sandy soil conditions but with an extended maximum rooting depth of 2 meters to account for the longer root depth distribution of pine trees. The third scenario represents soil hydrophobic soils conditions beneath the pine plantations characterized by a heterogeneous (two-layered) soil profile, where the top layer (depth of 10 cm) comprises an air entry value (α) reduced by 25% (Dimantopoulos et al. 2013, Van Dam et al. 1990) and soil hydraulic conductivity (K_s) value reduced by 70% (Novak et al. 2009; Sheridan et al. 2007) intended to mimic the most severe water repellent conditions (Robinson et al. 2009). The summary of numerical modeling input soil hydraulic parameters and rooting depth for each scenario are included in Table 3.4.

Table 3.4. Summary of numerical modeling input soil hydraulic parameters and root depths (R_d) used in the three recharge rate simulations

Simulation	Layer	Soil hydraulic parameters						
		θ_r ($cm^3\ cm^{-3}$)	θ_s ($cm^3 cm^{-3}$)	α (cm^{-1})	n (-)	K_s ($cm\ d^{-1}$)	l (-)	R_d (cm)
Scenario 1	1	0.04	0.43	0.147	2.67	700	0.5	50
Scenario 2	1	0.04	0.43	0.147	2.67	700	0.5	200
Scenario 3	1	0.04	0.43	0.110	2.67	210	0.5	10
	2	0.04	0.43	0.147	2.67	700	0.5	190

These artificial reduction values do not consider the spatial and temporal variability of soil hydrophobicity and are designed to observe the impact of maximum surface soil hydrophobicity on the water budget. The remaining 590 cm of the profile (bottom layer) contains similar soil hydraulic properties of the standard sandy soils reported in the first

two scenarios. The soil hydraulic properties used for the simulations are values obtained from Rosetta for sandy soils (Schaap et al. 2001). The simulations were run for 12 years and recharge outputs for the 6 meters soil profile are generated on daily time steps, which were aggregated into monthly and yearly values.

Groundwater recharge rate estimates

The chloride mass balance approach was used to estimate groundwater recharge rates for the profiles beneath each vegetation plot in a previous study. The evaluation of groundwater recharge rates and the results of each vegetation plot profiles have been summarized and thoroughly discussed in Adane and Gates (2015). The recharge results pertinent to this soil hydrophobicity study are presented here.

Statistical Analyses of soil hydrophobicity measurements

Simple linear regression analyses were performed to observe the relationships between soil hydrophobicity and soil moisture contents (WDPT vs soil moisture content) as well as soil organic carbon content (^{1}H NMR hydrophobic ratios vs soil organic carbon content) for the surface soil sediment samples. A multivariate linear regression analysis was done to examine the combined effect of soil moisture content and soil organic carbon content on hydrophobicity as represented by water drop penetration times. The relationship between unsaturated hydraulic conductivity (K_u), which is known to be impacted by soil hydrophobicity and groundwater recharge rates was also evaluated using regression analysis.

The analysis of variance (ANOVA) test was performed to compare spatial variability of surface soil hydrophobicity *within* and *between* the 10 measured vegetation

plots as well as *within* and *between* the pine plots with similar plantation density. The null hypothesis condition was set to be that the average measured times of the water drop penetration times (WDPT) pertaining to the plots are equal and belong to the same statistical distribution. The sources of variability, termed as sum of squares (SS) of measured times for the *between* and *within* (designated by the subscripts *b* and *w*) plot statistics, were used to calculate the mean squares (MS_b and MS_w):

$$MS_b = \frac{SS_b}{df_b} \tag{8a}$$

$$MS_w = \frac{SS_w}{df_w} \tag{8b}$$

where df_b and df_w denote the degrees of freedom of *between* and *within* plots, respectively. The ANOVA test compares the two MS-types through the *F*-test:

$$F = \frac{MS_b}{MS_w} \tag{9}$$

The resulting probability value (*p*-value) obtained from the *F*-distribution was compared to the critical value set to be 0.05. Large *F*-values resulting from greater differences between the two variance-types (equation 9) will correspond to relatively small *p*-values in the analysis. The null hypothesis will either be accepted if the *p*-value was greater than 0.05 or rejected if the *p*-value was less than 0.05.

Results

Field moisture content and soil organic carbon

The field condition soil moisture content and soil organic carbon results of samples used in the WDPT laboratory experiment data are presented in Table 3.5. In linear regression analyses, the near surface depth-weighted sample moisture contents varied between vegetation plots and depth intervals with no trends. The moisture content values are very low for all land uses spanning from 2.83% up to 16.03%. Very low water content values in a sandy soil imply very low or even negligible water fluxes. However, the grasslands had the highest percentage of total moisture content over the entire 0 – 50 cm depth by a factor of 1.25 to 2 across plots. Based on the observed moisture values, it can be inferred that field condition soil moisture contents may not account for differences in the soil hydrophobicity characteristics between the grassland and plantations plots. Observations of different hydrological responses in the top layer between grassland and plantation sites under dry conditions may not be significantly impacted by instantaneous soil moisture content of this magnitude.

The soil organic carbon content of samples also varied between plots. Soil organic carbon content linearly decreased with vertical depth in all soil samples across all vegetation plots. The highest soil organic carbon content (2.64%) for the top layer samples was observed at the thinned pine (TP2) plot. Conversely, the lowest percentage of soil organic carbon content for the top layer was observed at DP2 (0.43%). The average surface soil sediment sample organic carbon content of the grassland plots (0.68%) was lower than the average value observed for the surface soils beneath the pine plots (1.17%).

WDPT and EPT analysis

The WDPT and EPT data are presented in Table 3.2. The field moist samples of the grasslands (G1 and G2), dense pines (DP1 and DP2), and dense cedar (DC) soils did not exhibit any soil hydrophobicity on field moist sediment samples at any of the depth intervals up to 50 cm. In the surface layer (0 to 12.5 cm depth interval) sediment samples, strong hydrophobicity was observed for the pine savannah (PS2) and thinned pine (TP2) where median drop penetration times were approximately 612 s and 607 s, respectively.

Table 3.5. Soil moisture content and organic carbon content results for soils samples from vegetation plots at Halsey NNF used in the WDPT and EPT laboratory tests.

	Moisture content (%)				Soil organic carbon (%)			
	Depth intervals (cm)				Depth interval (cm)			
Plot	0 - 12	12 - 25	25 - 37	37 - 50	0 - 12	12 - 25	25 - 37	37 - 50
G1	5.86	6.89	6.95	6.12	0.67	0.57	0.39	0.15
G2	11.17	12.03	11.23	11.70	0.69	0.39	0.28	0.23
SV	4.29	5.64	5.32	6.12	0.68	0.35	0.24	0.17
PS1	4.56	4.62	3.48	4.27	1.42	0.45	0.31	0.22
PS2	3.58	4.63	5.83	6.19	0.86	0.82	0.52	0.43
TP1	4.68	4.27	3.89	2.83	0.52	0.46	0.38	0.25
TP2	8.58	4.28	7.39	11.1	2.64	0.75	0.49	0.33
DP1	16.03	5.10	5.81	5.88	1.13	0.31	0.24	0.16
DP2	9.04	4.94	5.31	5.42	0.43	0.23	0.16	0.12
DC	5.60	5.30	4.90	4.33	0.61	0.34	0.31	0.22

The potential for soil hydrophobicity can be observed in the WDPT test on the oven-dried samples. In the oven-dried samples, the native and forest grasslands (G1 and G2) as well as the dense cedar (DC) vegetation plots did not exhibit any soil hydrophobicity. In contrast, all of the plots that contained pine vegetation regardless of plantation density showed strong soil hydrophobicity in the top 12.5 cm depth where median drop penetration times ranged from 612 s to 657 s. Similar to the WDPT results, the EPT data did not indicate any presence of soil hydrophobicity in the grasslands (G1

and G2) and the dense cedar (DC) vegetation plots at any depth. Meanwhile, all of the pine plots showed some degree of soil hydrophobicity near the surface.

The variability of the measured water drop penetration times in all vegetation plots are presented as boxplots in Fig. 3.2. The grassland (G1 and G2) and dense cedar (DC) plot water drop surface soil penetration times occurred in less than 3 seconds in each of the 5 trials while the sparse vegetation plot penetration times ranged from 15 s and 207 s. The pine savannah plots (PS1 and PS2) drop penetration time results ranged from 8 s to 740 s and 35 s to 812 s, respectively. In the more densely planted pine plots, the thinned pine (TP1 and TP2) penetration times ranged from 170 s to 682 s and 11 s to 827 s while the dense pine (DP1 and DP2) ranged from 26 s to 960 s and 337 s to 807 s, respectively.

Table 3.6. ANOVA test terms reported for all 10 plots and for the 6 pine plots (namely PS1, PS2, TP1, TP2, DP1, DP2)

	SS	df	MS	F	p
Between all plots	2911017.0	9	323352.6	5.32	0.0001†
Within all types	2428990.0	40	60724.7		
Between pine plots	176410.6	5	35282.1	0.35	0.875‡
Within pine types	2399150.8	24	99964.6		

†$p < 0.05$ null hypothesis rejected; ‡$p > 0.05$ null hypothesis accepted

The variability statistics in surface soil hydrophobicity (represented by WDPT) *between* all plots and *within* the pine vegetation plots is presented in Table 3.6. The grasslands (G1 and G2) as well as the dense cedar (DC) plot results did not suggest the presence of any surface soil hydrophobicity. In addition, these plots did not indicate any variability in the surface soil hydrophobicity assessment as each of the 5 WDPT trials resulted in surface soil penetration in less than 3 seconds. The pine tree plots, excluding

the sparse vegetation (SV), were characterized by similar distributions of soil hydrophobicity as represented by water drop penetration times. As anticipated, the ANOVA test performed on all 10 of the vegetation plots established that the water drop penetration time measurements were not equivalent and did not satisfy the null hypothesis (p = 0.001) that the distribution will be similar (p > 0.05). A second ANOVA test was performed by only grouping the plots containing pine trees (PS, TP, and DP) suggested that the means of the WDPT measured times are equivalent by satisfying the null hypothesis (p = 0.875).

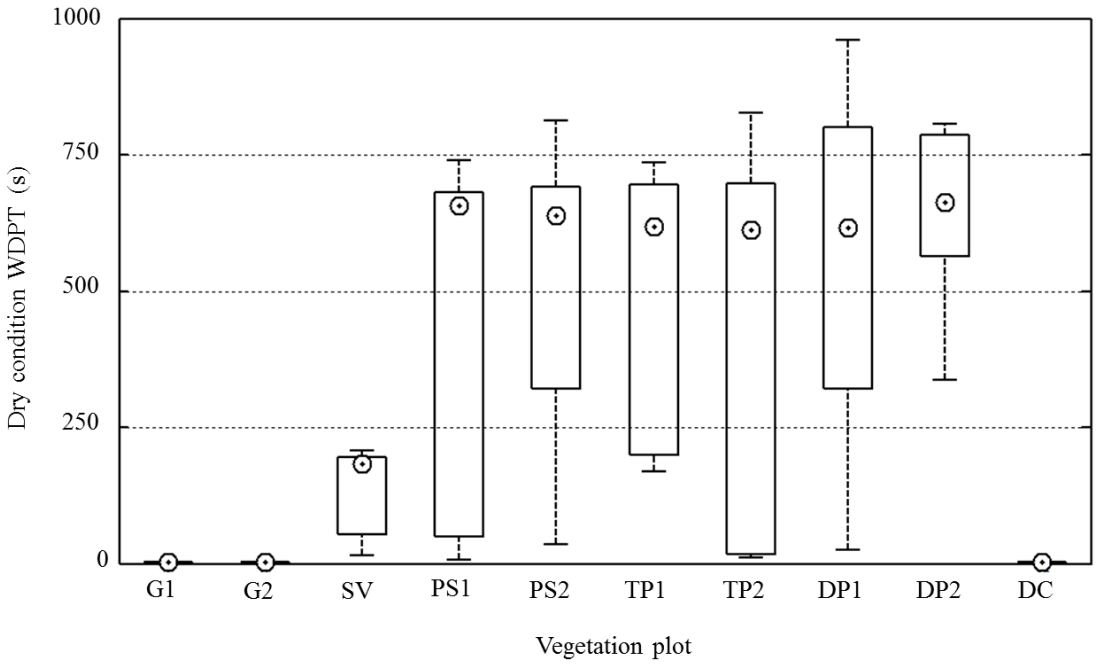

Fig. 3.2. Variability in surface soil hydrophobicity between different plots and within the same vegetation types as determined by the water drop penetration time (WDPT)

^{1}H NMR analysis

The results of the ^{1}H NMR spectral regions for the top layer soil samples are presented in Table 3.7. The integrated area for each of the regions varied between different plots. In the aliphatic region (3.2 – 0.5 ppm) the results did not indicate any particular trend. The 8.5 – 6.5 ppm spectrum region is characterized by the presence of aromatic compounds and the results varied by up to a factor of 2 across plots. Compounds containing halogens, alcohols, and esters are reflected in the 6.5 – 3.2 ppm region (Silverstein et al. 2014).

Table 3.7.^{1}H NMR spectral chemical shift signal area under the curve for the top 12 cm sediments

Vegetation Plot	^{1}H NMR spectrum regions (ppm) – integrated area			
	8.5 – 6.5	6.5 – 3.2	3.2 – 0.5	Hydrophobic ratio (%)
G1	3.5	2.7	93.8	2.8
G2	4.7	2.3	92.9	2.4
SV	3.4	4.1	92.5	4.3
PS1	2.5	4.3	94.2	4.4
PS2	4.5	3.6	88.6	3.7
TP1	2.7	5.0	92.3	5.3
TP2	2.6	8.7	88.6	9.6
DP1	2.9	9.0	88.1	9.9
DP2	3.5	3.4	93.3	3.6
DC	3.1	4.2	94.1	4.4

The averaged ^{1}H NMR integrated area of the 6.5 – 3.2 ppm region was lowest in the grassland (2.5%) and dense cedar (4.2%) plots where no soil hydrophobicity was detected (2.5%) and greatest in the dense pines plots where the presence of soil hydrophobicity was repeatedly observed (6.5%).

The analysis of major peak ratios of hydrophobic to non-hydrophobic regions suggests that the grasslands (G1 and G2) had the lowest average ratio of 2.6% in the top

12.5 cm and the dense cedar plot had a value of 4.4 while the average ratio was substantially greater in the pine plots (6.1%).

Field infiltration test

In-situ field water and ethanol infiltration tests were performed to obtain hydrological characteristics (equations 2 and 3) and soil hydrophobicity factor (equation 4). The soil moisture contents at the time of the infiltration tests indicate that G2, SV, and DC were the wettest while PS2, TP1, and TP2 had the driest surface soils. The water sorptivity (S_w) results were greatest at the grassland plots (G1 and G2) with 2.12×10^{-4} and 1.87×10^{-4} $ms^{-1/2}$, an order of magnitude higher than the treed plots. The ethanol sorptivity (S_e), which represents infiltration that is unimpeded by hydrophobicity, was greatest in the thinned pine plots ($4.4 \times 10^{-4} – 4.8 \times 10^{-4}$ $ms^{-1/2}$) and least in the dense pine plots (2.3×10^{-4} to 2.4×10^{-4}). The unsaturated hydraulic conductivity (K_u) values of the 10 plots varied from slowest in the dense pine (DP2) plot (1.2×10^{-6} ms^{-1}) to fastest at sparse vegetation and native grassland (~4.6×10^{-6} ms^{-1}). The hydrophobicity factor calculation results indicate that the grasslands had the lowest soil hydrophobicity with hydrophobicity index (H) value of 3.7. The index suggests that on average the pine plantation plots were 3 to 13 times more hydrophobic than the grassland plot (Table 3.7). The grassland plots, (G1 and G2), treed plots with low plantation density (SV, PS1, and PS2) and, the dense cedar plot (DC) were within the same order of magnitude ranging between 1.0×10^{-5} m s^{-1} and 9.1×10^{-5} ms^{-1}.

Recharge rate estimates

Recharge rate estimates based on chloride mass balance indicated a recharge rate of 36.7 mm yr^{-1} for the profile beneath the native grassland (G1). The dense pine (DP1) and dense cedar (DC) profiles had the lowest recharge rates of approximately 7.2 mm yr^{-1} and 4.0 mm yr^{-1}, respectively (Table 3.8). The recharge rate estimate results for all plots are described and thoroughly discussed in Adane and Gates (2015).

Table 3.8. Summary of water content, sorptivities, repellency factor, hydraulic conductivity, and recharge

Plot	θ (%)	S_w ($ms^{-1/2}$)	S_e ($ms^{-1/2}$)	H (-)	K_u (ms^{-1})	Recharge ($mmyr^{-1}$)
G1	3.8	2.1E-04	3.8E-04	3.5	4.6E-05	36.7
G2	5.4	1.9E-04	3.7E-04	3.9	1.0E-05	16.5
SV	6.1	6.1E-05	3.3E-04	10.5	4.9E-05	32.3
PS1	4.4	2.5E-05	3.2E-04	24.6	1.7E-05	21.4
PS2	3.1	1.3E-05	3.0E-04	44.2	1.2E-05	15.1
TP1	3.9	2.8E-05	4.4E-04	29.9	2.3E-06	8.1
TP2	2.8	3.6E-05	4.8E-04	25.4	1.7E-06	11.8
DP1	4.6	1.3E-05	2.3E-04	35.6	4.1E-06	7.2
DP2	4.9	2.7E-05	2.4E-04	17.1	1.2E-06	10.2
DC	5.9	5.1E-05	3.7E-04	14.3	9.1E-05	4.1

Numerical modeling with HYDRUS 1-D

The three synthetic numerical modeling scenarios indicate that the cumulative groundwater recharge generated beneath the grassland profile was substantially greater compared to the pine vegetation simulations over the 12 year period. The non-hydrophobic pine uniform (single-layer) profile simulation, which consisted of the same soil hydraulic properties as the grassland (no repellent uniform single-layer) but with a longer rooting depth, produced only 75% of the cumulative groundwater recharge of the baseline grassland scenario over the same time period. The simulated cumulative groundwater

recharge of the hydrophobic pine heterogeneous double-layered soil profile with the most severe hydrophobic surface soil layer was approximately 68% of the baseline grassland scenario at the end of the simulation (Fig 3.3). In the meantime, the cumulative surface soil evaporation increased by 17% in the repellent pine condition scenario (scenario 3) compared to the non-hydrophobic simulation (scenario 2) in response to the severely hydrophobic surface layer. On the other hand, the cumulative transpiration rate of the repellent pine scenario was reduced by approximately 7% relative to the non-repellent pine model run.

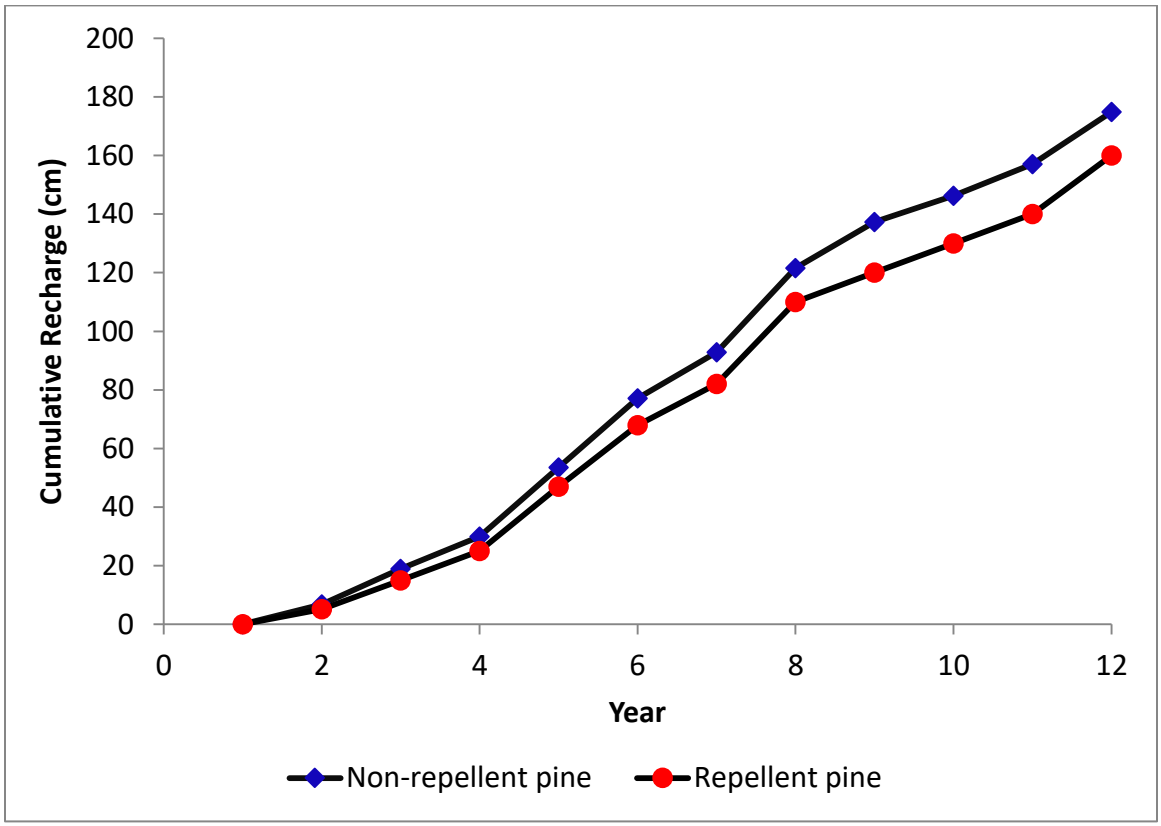

Fig. 3.3. Cumulative groundwater recharge differences between repellent and non-repellent pine forest condition simulations.

Discussion

Soil hydrophobicity in sediment samples

The WDPT and EPT for the surface layer under the pine plantations were substantially greater than the grasslands, mixed vegetation, and the dense cedar plots. This result is consistent with the findings of Flores-Mangual (2013) and Richardson and Hole (1978) who reported greater soil hydrophobicity in pine plantations. In a simple linear regression analysis, there was no relationship observed (R^2 = 0.12) between soil moisture content and soil hydrophobicity for the field condition soils. The results are in line with several studies that observed either ambiguous (Buczko et al. 2005) or weak correlation (Dekker and Ritsema 1994). However, stronger relationships between soil water content and soil hydrophobicity are common and have been reported (King 1981, de Jonge et al. 1999, Cerdà and Doerr 2005). Soil hydrophobicity is typically known to decrease with increasing soil moisture content until it reaches a critical soil water content, at which the repellent compound degrades and the soils becomes hydrophilic (Doerr et al. 2000). As a result, soils can be hydrophobic at high water contents and may not exhibit hydrophobic behavior at soil moisture contents as low as 2% (Dekker and Ritsema 1994). Hydrophobicity is thus often evaluated on the dry condition samples for potential hydrophobicity in addition to wet samples representing instantaneous field conditions.

The grassland and dense cedar plots were hydrophilic and did not indicate any variability in the water drop penetration time assessment, where drop penetration of surface soil occurred in less than 3 seconds. The analysis of variance results suggested that the variability in surface soil hydrophobicity between all 10 vegetation plots was statistically significant (p = 0.875). Meanwhile, the variability in surface soil hydrophobicity between the pine plots was not statistically significant (p = 0.001) (Table 3.6). The results imply

that the presence of soil hydrophobicity was primarily due to the presence of pine trees and agree with the conclusions of Lichner et al. (2010). However, a detailed study specifically designed to tackle the issue of spatial variability of hydrophobicity in pine forest settings will provide valuable information.

The data suggest that on average soil organic carbon in the surface layer is greater under the pine plantations than the grassland, and dense cedar plots. Greater soil hydrophobicity was also observed in all of the pine plots including the sparse mixed vegetation which also contains pine trees. The strongest hydrophobicity was observed in the plot with the greatest soil carbon content (TP2). However, the relationship was not strong (R^2 = 0.13) suggesting that soil organic carbon quantity is not the sole component that triggers soil hydrophobicity in the pine plots. The results are in agreement with other studies (Dekker and Ritsema 1994, Buczko et al. 2005) that also reported weak positive relationships between soil organic carbon content and hydrophobicity. Despite general trends of positive correlation (McKissock et al. 1998, Buczko et al. 2005) or negative correlation (Wallis et al. 1993), severity of soil hydrophobicity may not be proportional to the amount of organic carbon in soils. The organic carbon content is very low in most of the plots and depth intervals and as such the quantity of organic carbon may not be a factor in the severity of hydrophobicity. Therefore, identifying the quality of organic carbon or the type of carbon (hydrophobic or not) that make up the soil organic matter may prove a better tool to characterize hydrophobicity. The use of the ^{1}H NMR tool stems from this understanding of the limitations of soil organic carbon analysis for hydrophobicity studies. An explanation for this discrepancy may be the small quantity of water repellent compounds necessary to cause hydrophobicity regardless of the amount of organic carbon

present in soils (Doerr 1998). Further, an evaluation of organic matter components (i.e. quality) rather than organic carbon content may provide valuable information as to what drives hydrophobicity in soils.

An assessment of the combined effect of soil moisture and organic carbon content on hydrophobicity was performed. A qualitative observation of the results suggests that the soil samples with greater amounts of organic carbon and drier soil conditions (e.g. PS2, TP2) exhibited soil hydrophobicity even in the field condition (wet) soil samples. The elevated soil organic carbon content (2.6%) in TP2 and the subsequently high soil hydrophobicity in the water drop penetration test scale provide further evidence to this assessment. However, a multivariate linear regression analysis also suggests that the combined impact of soil moisture and organic carbon content on the surface soil hydrophobicity as measured by the median water drop penetration time is not significant ($R^2 = 0.07$).

^{1}H NMR spectral ratios of soil organics

An evaluation of data obtained from the ^{1}H NMR suggests that the increase in hydrophobicity in pines could be related to the quality of soil organic carbon. The analysis of major peak ratios of hydrophobic to non-hydrophobic regions suggests that the ratio was least under the grasslands with a range of 2.4% to 2.8% (Table 3.7). The results of the plantations with low density of pines (sparse vegetation and pine savannah) and the dense cedar plots also show relatively lower ratios ranging between 3.7% and 4.4%. While ponderosa pine and many pine species are considered highly hydrophobic (Doerr et al. 2000), soil hydrophobicity beneath the eastern cedar are known to be low and mostly

visible only under fire conditions (Madsen et al. 2011, Robinson et al. 2009). This is likely due to the differences in organic carbon type and litter compound composition that degrades on the soil surface. The ratios observed for the pine plots with greater planting density was much greater with ranges from 3.6% to 9.9% and 5.3% to 9.6% for the dense and thinned pine plots, respectively compared to the grasslands (2.4% to 2.8%). However, it is also important to note that variations in surface soil organic carbon content and composition, even within the same plot type, may have resulted in differences in the hydrophobic ratios. Similar results of soil organic carbon quality analysis in pines showed increased hydrophobicity in Flores-Mangual (2013) and were associated to pine root and shoot growth and subsequent decay of pines. The slight increase in hydrophobic to non-hydrophobic average ratios in thinned pines compared to the dense pines may be in response to an additional decaying biomass from the thinning management where pine needles and litter from natural fall and thinning activities are left on the soil surface to decompose. The results also signal that the quantity of soil organic carbon plays an important role in the spectral ratios. For instance, in the denser pine plots (TP and DP), the sediment with the greater soil organic carbon content (2.6% and 1.1% for TP2 and DP1, respectively) yielded greater hydrophobic to non-hydrophobic ratios compared to its replicate plot (TP1 and DP2) of similar density. Typically, samples showed greater ratio in the replicate plot with the greater soil organic carbon content. While a simple linear regression analysis between soil organic carbon content and hydrophobic ratios for the surface soils indicated a positive relationship it was not robust (R^2 = 0.48). Several species of pines including ponderosa pine are known to cause soil hydrophobicity. The soils beneath these pine-dominated vegetation exhibit hydrophobic behavior in response to pine

needle deposition and decomposition that release significant amount of resins, waxy substances, and oily organic compounds (Doerr et al. 2000). This hydrophobic trait may have evolved in higher order plants such as pines and eucalypts to increase their competitive advantage in capturing water in arid conditions by funneling water deep into the root zone, restraining the growth of understory plants, and limiting evaporative losses (Robinson et al. 2009). A detailed study specifically designed to tackle these prospects might provide a better understanding of the role of organic carbon content in inducing or enhancing soil hydrophobicity. Beneath 12.5 cm depths, the hydrophobicity ratios (not shown here) were much lower. Further, the samples showed no specific trend likely due to a combination of reduced hydrophobicity and low soil organic carbon contents. Soil clay content in the study site is minimal and uniform across the grass, pine, and cedar plots (in the order of 1%); nevertheless, clays are known to drastically enhance soil hydrophobicity of sandy soils that are already repellent (Dlapa et al. 2004, Leelamanie and Karube 2007, McKissock et al. 2002).

Soil hydraulic properties and hydrological processes under soil repellent conditions

Field infiltration tests performed to observe on site hydraulic conditions suggest that grassland conversions to pine plantations can significantly alter hydraulic processes in the surface layer. The hydrophobicity factor calculation results indicate that the grasslands had the lowest soil hydrophobicity value with hydrophobicity index (H) of 3.7, which is approximately 8 times lower than the average for the pine plots (Table 3.8). The results are in agreement with Lichner et al. (2010) that reported forest soils were significantly more hydrophobic than glades and grasses. The hydrophobicity factor observed had a reasonable negative relationship with water sorptivity (R^2 = 0.66). The unsaturated hydraulic

conductivity K_u is also greatest at the grassland and less densely planted treed plots (1×10^{-5} to 4.9×10^{-5} ms^{-1}) and least at the densely treed pine plots where the hydrophobicity factors were relatively higher (1.2×10^{-6} to 4.1×10^{-6} ms^{-1}). The dense cedar (DC) plot was an exception in that despite the density of tree plantation, the K_u value was relatively fast (9.1×10^{-5} ms^{-1}) providing further evidence that hydrophobicity was induced by pine vegetation. Changes in sorptivity properties may have resulted from altered capillary forces in response to pine plant induced hydrophobic substances covering soil surfaces. These changes in hydraulic properties may also be associated with preferential flow paths and the field condition moisture content differences at the time of infiltration tests; however there was no clear evidence to support this as several of the samples had similar moisture contents but exhibited significant differences in hydrophobicity factor in addition to sorptivity and K_u values. It should also be noted that the small diameter of the mini-disc infiltrometer may not capture existing macropores and preferential flow paths and as a result tests may not provide spatially averaged values. A paired (mini-disc and double-ring) infiltration assessment may point to differences in infiltration rates and severity of hydrophobicity directly associated to variability in spatial distribution.

Groundwater recharge in water repellent soil conditions

The relationship between soil hydrophobicity represented by the ^{1}H NMR hydrophobic spectral ratio and K_u and R values in the pine plantations relative to the baseline native grassland plot is depicted in Fig. 3.4. The native grassland (G1) is the best approximation of the natural conditions and its triangle values in Fig. 3.4 (i.e. ^{1}H NMR hydrophobic spectral ratio, K_u, and R) are at 100% to serve as a point of reference. All of

the pine plot surface soils (PS1, TP1, and DP1) have greater hydrophobic spectral ratio than the surface soils beneath the native grassland by approximately 150% to 350%.

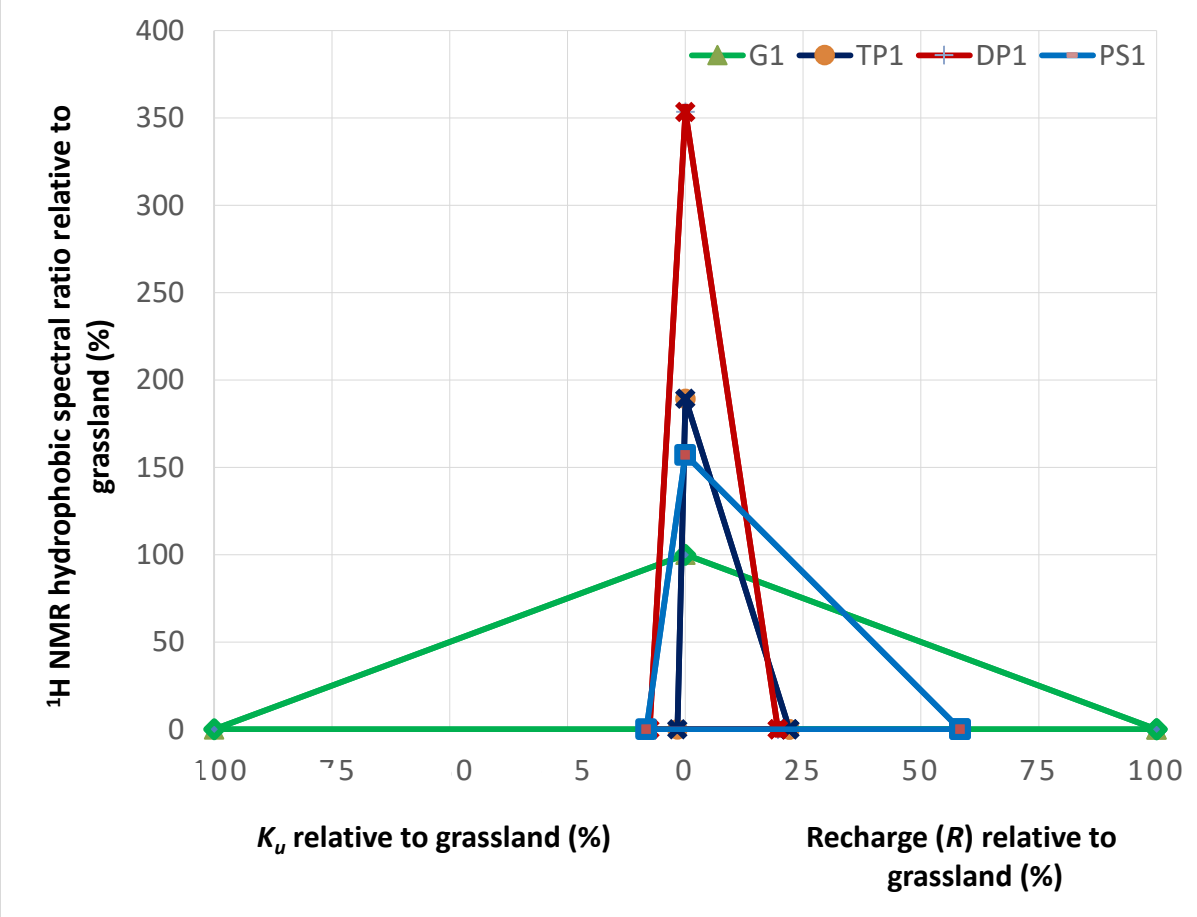

Fig. 3.4. 1H NMR, unsaturated hydraulic conductivity Ku, and Recharge rates (R) of pine profiles compared to the baseline native grassland profile

Further, as pine tree plantation density increases from pine savannah to dense pine, the hydrophobic spectral ratio also increases more than twofold likely due to greater pine needle production, needle deposition, and subsequent decomposition of litter which yields greater amounts of hydrophobic compounds to the surface soils beneath the vegetation. The results suggest that greater pine plantation density also corresponds to reduced

groundwater recharge due to a possible combination of increases in water extraction from roots and leaf interception but also as a consequence of reduced infiltration rate partially attributable to the hydrophobic surface layer as demonstrated by lower unsaturated hydraulic conductivity (K_u) and infiltration rates relative to the baseline native grassland.

The unsaturated hydraulic conductivity K_u, which controls early stage infiltration rates through capillary processes, shows a strong relationship in a linear regression analysis (R^2 = 0.94) with groundwater recharge; when the outlier dense cedar plot is omitted from the evaluation (Fig. 3.5).

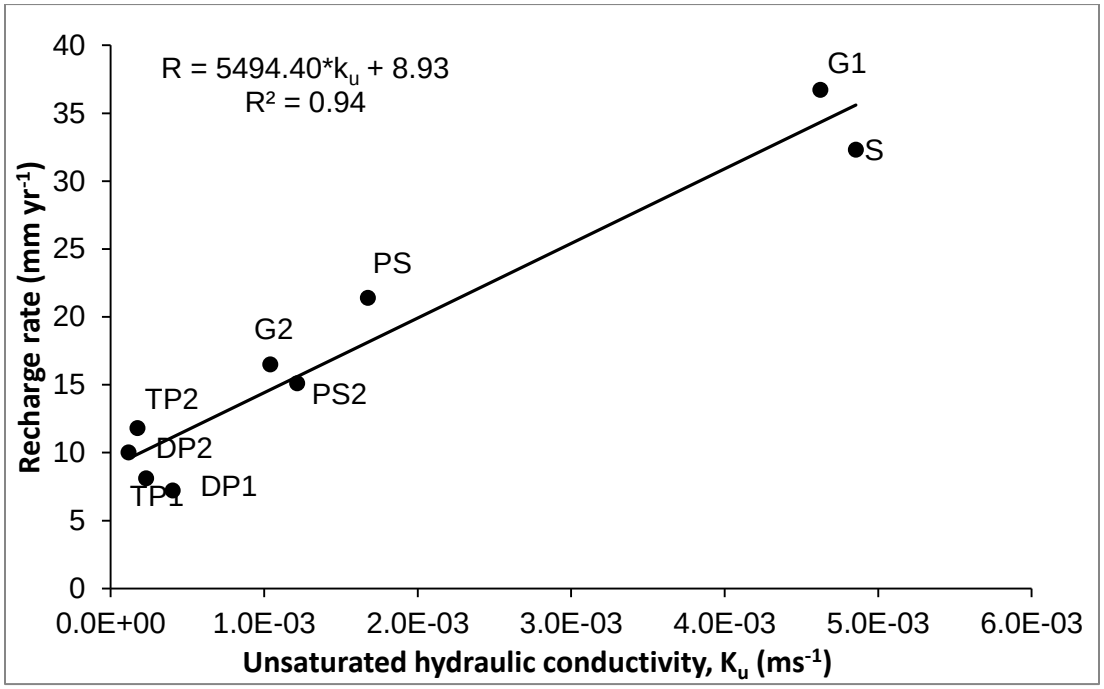

Fig. 3.5. Linear relationship between groundwater recharge rates and unsaturated hydraulic conductivity, Ku. Data for groundwater recharge from Adane and Gates (2015).

The soil hydraulic conductivity of the dense cedar (DC) plot is less than the grassland but greater than the pine plots. Wine et al. 2011 have also documented an order

of magnitude reduction in hydraulic conductivity and sorptivity in eastern red cedars compared to grasses. Despite the greater hydraulic conductivity rate, the dense cedar plot groundwater recharge rate (~4 mm yr^{-1}) is considerably less than the dense pines (~9 mm yr^{-1}). This severe reduction in groundwater recharge rates compared to the pines is likely due to the plantation density of the dense cedars which stands at 1800 to 2000 trees ha^{-1} compared to 700-1000 trees ha^{-1} pines for dense pines and 100-300 trees ha^{-1} pines for less dense pine plots (Table 3.1). While the leaf area index (LAI) of the cedars (1.87) is slightly less than the dense pines (2.2), the associated rainfall interception also contributes to the reduction in recharge. When infiltration rates are substantially reduced in response to intense soil hydrophobicity, moisture particularly from light rain events is exposed to atmospheric demand for a longer period and may not infiltrate the surface soil and percolate down the profile, which can explain reduction in groundwater recharge (Robinson et al. 2009).

The native grassland (G1) used as the baseline in the analysis exhibits low surface soil hydrophobicity and relatively high recharge rates. The forest grassland plot (G2) also indicates low soil hydrophobicity, however, the recharge rates were less than half (16 mm yr^{-1}) of the native grassland suggesting that either the recharge rate was underestimated or the previous assertion that recharge rates have not had sufficient time to recover since land use conversion from forestation back to grassland (Adane and Gates 2015). While the soils beneath the pine plots were more hydrophobic and the associated recharge rates were lower than grasslands, the dense cedar plot contained low hydrophobicity but also very low recharge rates. The recharge rates beneath the dense cedar profile were the lowest (4 mm yr^{-1}) suggesting that the reduced groundwater recharge may be primarily due to plantation-

induced increase in transpiration and rainfall interception and may not be significantly influenced by surface soil hydrophobicity.

The HYDRUS 1-D synthetic modeling results suggest that the 12 year cumulative groundwater recharge beneath the native grassland uniform soil profile (scenario 1) was substantially greater than the one pertaining to the pine plot with the uniform layer (scenario 2) and heterogeneous (double-layer) profile (scenario 3). The non-hydrophobic pine uniform soil profile (scenario 2) simulation indicates a cumulative groundwater recharge reduction of 25% compared to the grassland plots in the baseline scenario. Such reduction is primarily associated with an increase in transpiration. Similarly, the repellent pine with the heterogeneous profile simulation representing absolute maximum hydrophobicity suggests that cumulative groundwater recharge was reduced by 31.4% compared to the baseline scenario of the grassland profile (Fig. 3.3). The further decrease in cumulative groundwater recharge suggests that while transpiration rate increase associated with the pine vegetation accounts for the majority of the reduction in groundwater recharge (25%), surface water hydrophobic conditions caused by pine vegetation can also contribute to recharge losses of a further 7.4%. The chloride mass balance recharge estimates also indicate a 27.2% annual recharge rate reduction in the pine plot profile compared to the baseline native grassland plot (Fig. 3.5), however this long term recharge estimate may reflect all land use associated changes including retention and preferential flow.

Further, the hydrophobic soil conditions resulted in a 15% more cumulative evapotranspiration over the 12 year period in response to the decreased infiltration rate induced by the lower α and K_s used to represent hydrophobicity. Interestingly, the

hydrophobic pine soil condition also produced a 7% reduction in cumulative transpiration possibly because greater surface soil evaporation and reduced water infiltration resulted in less water availability within the soil profile for plant extraction. It should be noted that the HYDRUS 1-D simulation was designed to express the impact of maximum severity of hydrophobicity on the water budget, which may not occur in response to the variability in spatial and temporal distribution of hydrophobicity. Further, the substantial increase in evaporation between the hydrophobic and non-hydrophobic simulations is likely due to the limitation of the HYDRUS1-D model to consider soil moisture retention by the pine litter cover of the surface soil. The artificial reduction in saturated hydraulic conductivity (K_s) is causing the surface soil to resemble a relatively impermeable surface which as a result may increase evaporation considerably given the Sand Hills semi-arid climate with high potential ET (Potential ET > Precipitation). In addition, due to the low precipitation of the Nebraska Sand Hills; the runoff component of the soils is essentially zero (Szilagyi et al. 2011) even though hydrophobic soils are well known to enhance runoff, decrease infiltration, and indirectly reduce subsurface flow (Clothier et al. 2000).

Owing to the non-uniform nature of hydrophobicity in surface soil, preferential and bypass flows can increase water flow down soil profiles and subsequently recharge. The recharge rates beneath the 6 meter depths obtained in a solute mass balance study of the same forest area (Adane and Gates 2015) and the HYDRUS 1-D simulation do not indicate that the hydrophobic pine plots, which would exhibit greater preferential flow, have in fact greater groundwater recharge rates. The numerical simulations actually suggest that hydrophobicity reduces both transpiration and groundwater water recharge. However, studies have also suggested that soil hydrophobic layers perform some ecological function

such as funneling water deeper into the soil profile, inhibiting the growth of understory vegetation, and reducing evaporative losses from the subsurface soil to the atmosphere (Robinson et al. 2009). Simulating interception and preferential flow were beyond the scope of this study. However, a research study specifically designed to assess the impact of soil hydrophobicity on preferential flow in forest settings may provide valuable information that can also be used to infer the impact on groundwater recharge.

Conclusion

The outcome of this study suggests a weak link between soil hydrophobicity and reduced recharge beneath pine plantations. Results from multiple methods including WDPT and the ^{1}H NMR spectral analysis indicate near-surface soils beneath the pine plots were substantially more hydrophobic than the surrounding grasslands. The variability of surface soil hydrophobicity represented by WDPT between the ten vegetation plots was statistically significant but not the variability within the pine plots. The ^{1}H NMR analysis appears to show promise in identifying compounds that are hydrophobic and appears to be the better tool to show slight differences between plots whereas the WDPT method simply indicates the presence or absence of hydrophobicity. Field infiltration experiments also suggest that surface soil K_u values in the treed plots were up to an order of magnitude lower compared to the grasslands. Recharge rates beneath the dense plantations represent a substantial reduction relative to the grassland profile. Soil hydrophobicity was mainly observed in the pine plots thus lower recharge rates beneath the dense cedar profile are likely associated with increased transpiration and leaf rainfall interception given that the dense cedar plot is planted at more than twice the density of the dense pine plots. HYDRUS 1-D numerical simulations indicated that surface layer repellent conditions can affect the

water budget by altering surface soil evaporation and reducing groundwater recharge rates. The overall effect of grassland forestation is a significant change in the water budget including a decrease in groundwater recharge partially attributable to greater soil hydrophobicity in the near-surface soils. However, studies specifically designed to isolate the impact of hydrophobicity on the water budget, particularly recharge, would provide valuable information. Further research is also needed in identifying hydrophobic and non-hydrophobic organic compounds and how they differ between plant species. Forests provide numerous ecological benefits ranging from providing wildlife habitat and recreation to promoting soil conservation and carbon sequestration; however, impacts on water resources in general and groundwater in particular should be properly assessed prior to plantation and forest expansion efforts.

Acknowledgments

This material is partially based upon work supported by the National Science Foundation under award no. IIA-1415035. The authors would also like to thank Dr. Dave Wedin, Dr. Tala Awada, and Jeremy Hiller for providing data, site access, and logistical support and Dr. Martha Morton for laboratory access

References

Adane, Z.A. and J.B. Gates. 2015. Determining the impacts of experimental forest plantation on groundwater recharge in the Nebraska Sand Hills (USA) using chloride and sulfate. *Hydrogeol. J.* 23:81–94. doi: 10.1007/s10040-014-1181-6.

Allen, R.G., L.S. Pereira, D. Raes, and M. Smith. 1998. Crop Evapotranspiration: *Guidelines for Computing Crop Water Requirements. Irrigation and Drainage Paper No 56.* Food and Agriculture Organization of the United Nations (FAO), Rome, Italy. 24 p.

Bachmann, J., and R. R. Van Der Ploeg. 2002. A review on recent developments in soil water retention theory: Interfacial tension and temperature effects. P. 468–478 in *J. of Plant Nutr. and Soil Sci.* 165:4.

Bodí, M.B., I. Muñoz-Santa, C. Armero, S.H. Doerr, J. Mataix-Solera, A. Cerdà. 2013. Spatial andtemporal variations of water repellency and probability of its occurrence in calcareous Mediterranean rangeland soils affected by fires. *Catena*. 108:14-24. http://dx.doi.org/10.1016/j.catena.2012.04.002

Bosch, J. M. and J. D. Hewlett. 1982. A review of catchment experiments to determine the effect of vegetation changes on water yield and evapotranspiration. *J. Hydrol.* 55:3–23.

Brooks, T.M., R.A. Mittermeier, C.G. Mittermeier, G.A Da Fonseca, A.B Rylands, W.R. Konstant, P. Flick, J. Pilgrim, S. Oldfield, G. Magin, and C. Hilton-Taylor. 2002. Habitat loss and extinction in the hotspots of biodiversity. *Conserv. Biol*. 16:909–923.

Bruun, T.B., B. Elberling, A. de Neergaard, J. Magid. 2015. Organic carbon dynamics in different soil types after conversion of forest to agriculture. *Land Degradation and Development.* 3:272–283. DOI: 10.1002/ldr.2205

Buczko, U., O. Bens, H. Fischer, and R. F. Hüttl. 2002. Water repellency in sandy

luvisols under different forest transformation stages in northeast Germany. *Geoderma*. 109:1–18.

Buczko, U., O. Bens, and R. F. Hüttl. 2005. Variability of soil water repellency in sandy forest soils with different stand structure under Scots pine (Pinus sylvestris) and beech (Fagus sylvatica). *Geoderma*. 126:317–336.

Calder, I. R., K. T. Prasanna, and R. L. Hall. 1993. Hydrological impact of Eucalyptus plantation in India. *J. Hydrol.* 150:635–648.

Cerdà, A.and S.H. Doerr. 2005. Influence of vegetation recovery on soil hydrology and erodibility following fire: An 11-year investigation. *International J. of Wildland Fire*. 14, 4:423–437. DOI: 10.1071/WF05044

Clothier, B. E., I. Vogeler, and G. N. Magesan. 2000. The breakdown of water repellency and solute transport through a hydrophobic soil. *J. Hydrol*. 231:255–264.

Coe, M. T., M. H. Costa, and B. S. Soares-Filho. 2009. The influence of historical and potential future deforestation on the stream flow of the Amazon River–Land surface processes and atmospheric feedbacks. *J. Hydrol*. 369:165–174.

Dekker, L. W. and C. J. Ritsema. 1994. How water moves in a water repellent sandy soil: 1. Potential and actual water repellency. *Water Resour. Res.* 30: 2507–2517 .

Diamantopoulos E., W. Durner, A. Reszkowska, and J. Bachmann. 2013. Effect of soil water repellency on soil hydraulic properties estimated under dynamic conditions. *J. Hydrol*. 486:175–186.

Dlapa, P., S. H. Doerr, L. Lichner, M. Šír, and M. Tesař. 2004. Effect of kaolinite and Ca-montmorillonite on the alleviation of soil water repellency. *Plant, Soil Environ.*

50:358–363.

Doerr, S. H. 1998. On standardizing the “water drop penetration time” and the “molarity of an ethanol droplet” techniques to classify soil hydrophobicity: a case study using medium textured soils. *Earth Surf. Process. Landforms*. 23:663–668.

Doerr, S. H., R. A. Shakesby, and R. P. D. Walsh. 2000. Soil water repellency: Its causes, characteristics and hydro-geomorphological significance. *Earth Sci. Rev.* 51:33–65.

Doerr, S. H., and A. D. Thomas. 2000. The role of soil moisture in controlling water repellency: New evidence from forest soils in Portugal. *J. Hydrol.* 231:134–147.

Dohnal, M.J., J. Dusek, and T. Vogel. 2010. Improving hydraulic conductivity estimates from Minidisk infiltrometer measurements for soils with wide pore-size distributions. *Soil Sci. Am. J.* 74:804–811.

Eggemeyer, K. D., T. Awada, F. E. Harvey, D. A. Wedin, X. Zhou, and C. W. Zanner. 2009. Seasonal changes in depth of water uptake for encroaching trees Juniperus virginiana and Pinus ponderosa and two dominant C4 grasses in a semiarid grassland. *Tree Physiol.* 29:157–169.

FAO 2012. The state of the World's Forests 2012. Rome, Italy. 14 p.

Flores-Mangual, M. L., B. Lowery, J. G. Bockheim, P. H. Pagliari, and B. Scharenbroch. 2013. Hydrophobicity of Sparta Sand under Different Vegetation Types in the Lower Wisconsin River Valley. *Soil Sci. Soc. Am. J.* 77:1506–1516.

Gates, J. B., B. R. Scanlon, X. Mu, and L. Zhang. 2011. Impacts of soil conservation on groundwater recharge in the semi-arid Loess Plateau, China. *Hydrogeol. J.*

19:865–875 Available online at: http://link.springer.com/10.1007/s10040-011-0716-3.

Gosselin, D. C., V. Sridhar, F. E. Harvey, and J. W. Goeke. 2006. Hydrological effects and groundwater fluctuations in interdunal environments in the Nebraska Sandhills. *Gt. Plains Res.* 16:17–28.

Hallett, P. D. 2008. A brief overview of the causes, impacts and amelioration of soil water repellency – a review. *Soil Water Res.* 3:21–29. http://journals.uzpi.cz/uniqueFiles/01654.pdf.

Hallett, P. D., T. Baumgartl, and I. M. Young. 2001. Subcritical water repellency of aggregates from a range of soil management practices. *Soil Sci. Soc. Am. J.* 65:184–190.

Hellerich, J.A. 2006. *Influence of afforestation and hillslope position on soil carbon dynamics in the Nebraska Sand Hills*. M.Sc. Thesis, Univ of Nebraska-Lincoln, USA. 23–35 p.

Horn, D., Z. Kranz, and J. Lamberton. 1964. The composition of Eucalyptus and some other leaf waxes . *Aust. J. Chem.* 17:464.

Huang, M., and J. Gallichand. 2006. Use of the SHAW model to assess soil water recovery after apple trees in the gully region of the Loess Plateau, China. *Agric. Water Manag.* 85:67–76.

Huang, T., and Z. Pang. 2011. Estimating groundwater recharge following land-use change using chloride mass balance of soil profiles: a case study at Guyuan and Xifeng in the Loess Plateau of China. *Hydrogeol. J.* 19:177–186.

Ivanova, G. I., and E. W. Randall. 2003. 13C NMR and Mass Spectrometry of Soil Organic Matter. *Cent. Eur. J. Chem.* 1:10–27.

Janssens, I. A., W. Dieleman, S. Luyssaert, J. Subke, M. Reichstein, R. Ceulemans, P. Ciais et al. 2010. Reduction of forest soil respiration in response to nitrogen deposition. *Nature Geoscience* 5:315–322.

Jaramillo, D. F., L. W. Dekker, C. J. Ritsema, and J. M. H. Hendrickx. 2003. Soil water repellency in arid and humid climates. *Soil Water Repellency Occur. Consequences, Amelior.* 93–98.

Jobbágy, E. G., and R. B. Jackson. 2004. Groundwater use and salinization with grassland afforestation. *Glob. Chang. Biol.* 10:1299–1312.

de Jonge, L. W., O. H. Jacobsen, and P. Moldrup. 1999. Soil Water Repellency: Effects of Water Content, Temperature, and Particle Size. *Soil Sci. Soc. Am. J.* 63:437–442.

de Jonge, L. W., P. Moldrup, and O. H. Jacobsen. 2007. Soil-Wate Content Tendency of Water Repellency in Soils. *Soil Sci.* 172:577–588.

Kajiura, M., Y. Etori, and T. Tange. 2012. Water condition control of in situ soil water repellency: An observational study from a hillslope in a Japanese humid-temperate forest. *Hydrol. Process.* 26:3070–3078.

Keesstra S, L. Wittenberg, J. Maroulis, F. Sambalino, D. Malkinson, A. Cerdà, P. Pereira. 2016. The influence of fire history, plant species and post-fire management on soil water repellency in a Mediterranean catchment: The Mount Carmel range, Israel. *Catena*. DOI: 10.1016/j.catena.2016.04.006

Kettler, T. A., W. John, W. Doran, and T. L. Gilbert. 2001. Simplified method for soil particle-size determination to accompany soil-quality analyses. *Soil Sci. Soc. Am. J.* 65:849–852.

King, P. 1981. Comparison of methods for measuring severity of water repellence of sandy soils and assessment of some factors that affect its measurement. *Aust. J. Soil Res.* 19:275–285.

Leelamanie, D. A. L., and J. Karube. 2007. Effects of organic compounds, water content and clay on the water repellency of a model sandy soil. *Soil Sci. Plant Nutr.* 53:711–719.

Lesch, W., and D. F. Scott. 1997. The response in water yield to the thinning of Pinus radiata, Pinus patula and Eucalyptus grandis plantations. *For. Ecol. Manage.* 99:295–307.

Letey, J., M. L. K. Carrillo, and X. P. Pang. 2000. Approaches to characterize the degree of water repellency. *J. Hydrol.* 231-232:61–65.

Lichner, L., P. D. Hallett, D. S. Feeney, O. Ďugová, M. Šír, and M. Tesař. 2007. Field measurement of soil water repellency and its impact on water flow under different vegetation. *Biologia (Bratisl).* 62:537–541.

Lichner, L., P. D. Hallett, T. Orfánus, H. Czachor, K. Rajkai, M. Šír, and M. Tesař. 2010. Vegetation impact on the hydrology of an aeolian sandy soil in a continental climate. *Ecohydrology.* 3:413–420.

Lima, W. de P., M. J. B. Zakia, P. L. Libardi, and A. P. de S. Filho. 1990. Comparative evapotranspiration of Eucalyptus, Pine and natural “Cerrado” vegetation measure

by the soil water balance method. *IPEF Int.* 1:5–11.

Madsen, M.D., and D.G. Chandler. 2007 Automation and use of mini disk infiltrometers. *Soil Sci. Soc. Am. J. 71:1469–1472*.

Madsen, M.D., D. L. Zvirzdin, S. L. Petersen, B. G. Hopkins, B. A. Roundy, and D. G. Chandler. 2011. Soil water repellency within a burned piñon–juniper woodland: spatial distribution, severity, and ecohydrologic implications. *Soil Sci. Am. J*. 75:1543–1553.

Malhi, Y., J. T. Roberts, R. A. Betts, T. J. Killeen, W. Li, and C. A. Nobre. 2008. Climate change, deforestation, and the fate of the Amazon. *Science*. 5860:169–172.

McCleery, D.W. 1992. *American forests: a history of resiliency and recovery*. Durham, USA, USDA Forest Service and Forest History Society. 27–31 p.

McKissock, I., R. J. Gilkes, R. J. Harper, and D. J. Carter. 1998. Relationships of water repellency to soil properties for different spatial scales of study. *Aust. J. Soil Res.* 36:495–508.

McKissock, I., R. J. Gilkes, and E. L. Walker. 2002. The reduction of water repellency by added clay is influenced by clay and soil properties. *Appl. Clay Sci.* 20:225–241.

McVicar, T. R., L. Li, T. G. Van Niel, L. Zhang, R. Li, Q. Yang, X. Zhang, et al. 2007. Developing a decision support tool for China's re-vegetation program: Simulating regional impacts of afforestation on average annual streamflow in the Loess Plateau. *For. Ecol. Manage.* 251:65–81.

Moody, J. A., D. A. Kinner, and X. Úbeda. 2009. Linking hydraulic properties of fire-affected soils to infiltration and water repellency. *J. Hydrol.* 379:291–303.

Nadav, I., J. Tarchitzky, A. Lowengart-Aycicegi, and Y. Chen. 2011. Soil surface water repellency induced by treated wastewater irrigation: physico-chemical characterization and quantification. *Irrig. Sci.* 31:49–58.

Nasta, P., and J. B. Gates. 2013. Plot-scale modelling of soil water dynamics beneath rainfed maize druing seasonal rainfall extremes in Eastern Nebraska. *Agric. Water Manag.*128:120–130.

Novák, V., L. Lichner, B. Zhang, K. Kňava. 2009. The impact of heating on the hydraulic properties of soils sampled under different plant cover. *Biologia* 64:483–486.

Owens, M. K., R. K. Lyons, and C. L. Alejandro. 2006. Rainfall partitioning within semiarid juniper communities: Effects of event size and canopy cover. *Hydrol. Process.* 20:3179–3189.

Ozalp, M., Erdogan Yuksel, E., Yuksek, T. 2015. Soil Property Changes After Conversion from Forest to Pasture in Mount Sacinka, Artvin, Turkey. *Land Degradation and Development* 4: 1007–1017. DOI: 10.1002/ldr.2353.

Pereira P., X. Úbeda, J. Mataix-Solera, M. Oliva, A. Novara. 2014. Short-term changes in soil Munsell colour value, organic matter content and soil water repellency after a spring grassland fire in Lithuania. *Solid Earth*. 5:209-225. DOI: 10. 5194/se-5-209-2014

Philip, J. R. 1957. The theory of infiltration: 1. The infiltration equation and its solution. *Soil Sci*. 83:345–357.

Richardson, J. L. and F. D. Hole. 1978. Influence of vegetation on water repellency in selected western Wisconsin soils. *Soil Sci. Soc. Am. J*. 42:465–467.

Ritchie, J.T. 1972. Model for predicting evaporation from a row crop with incomplete cover. *Water Resour. Res.* 8:1204–1213.

Ritsema, C. J., J. L. Nieber, L. W. Dekker, and T. S. Steenhuis. 1998. Stable or unstable wetting fronts in water repellent soils - Effect of antecedent soil moisture content. *Soil Tillage Res.* 47:111–123.

Roberts, J. 2000. The influence of physical and physiological characteristics of vegetation on their hydrological response. *Hydrol. Process.* 14:2885–2901.

Robichaud, P. R., and R. D. Hungerford. 2000. Water repellency by laboratory burning of four northern Rocky Mountain forest soils. *J. Hydrol.* 231:207–219.

Robichaud, P. R., S. A. Lewis, R. E. Brown, and L. E. Ashmun. 2009. Emergency post-fire rehabilitation treatment effects on burned area ecology and long-term restoration. *Fire Ecol.* 5:115–128.

Robinson, D.A, I. Lebron, R.J. Ryel, and S.B. Jones. 2009. Soil Water Repellency: A Method of Soil Moisture Sequestration in Pinyon–Juniper Woodland. *Soil Sci. Soc. Am. J.* 74:624–634

Rye, C. F., and K. R. J. Smettem. 2015. Seasonal and Interannual Variability of the Effective Flow Cross-Sectional Area in a Water-Repellent Soil. *Vadose Zone J.* 14. doi:10.2136/vzj2014.10.0141

Scanlon, B.R., D. A. Stonestrom, R. C. Reedy, F. W. Leaney, Gates, J., and R. G. Cresswell. 2009. Inventories and mobilization of unsaturated zone sulfate, fluoride, and chloride related to land use change in semiarid regions, southwestern United States and Australia. *Water Resour. Res.* 45:1–17.

Schaap, M.G., F.J. Leij, and M. T. van Genuchten. 2001. ROSETTA: a computer program for estimating soil hydraulic parameters with hierarchical pedotransfer functions. *J. Hydrol.* 251:163–176.

Sheridan, G.J., P. Lane, P. Noske. 2007. Quantification of hillslope runoff and erosion processes before and after wildfire in a wet Eucalyptus forest. *J. Hydrol.* 343:12–28.

Silverstein R., F. Webster, D. J. Kiemle, and D. L., Bryce. 2014. *Spectrometric identification of organic compounds*. P 126 - 132 in *Proton (^1H) Magnetic Resonance Spectroscopy*. John Wiley & sons.

Šimůnek, J., M. Šejna, H. Saito,M. Sakai, and M.T. van Genuchten. 2008. *The HYDRUS-1D software package for simulating the one-dimensional movement of water, heat, and multiple solutes in variably-saturated media.* Version 4.0, HYDRUS Software Series 4. Department of Environmental Sciences, University of California Riverside, Riverside, CA, USA.

Szilagyi, J., V. A. Zlotnik, J. B. Gates, and J. Jozsa. 2011. Mapping mean annual groundwater recharge in the Nebraska Sand Hills, {USA}. *Hydrogeol. J.* 19:1503–1513.

Tarchitzky, J., O. Lerner, U. Shani, G. Arye, A. Lowengart-Aycicegi, A. Brener, and Y. Chen. 2007. Water distribution pattern in treated wastewater irrigated soils: Hydrophobicity effect. *Eur. J. Soil Sci.* 58:573–588.

Urbanek, E., P. Hallett, D. Feeney, and R. Horn. 2007. Water repellency and distribution of hydrophilic and hydrophobic compounds in soil aggregates from different

tillage systems. *Geoderma*. 140:147–155.

Wahl, N.A., O. Bens, B. schäfer, R.F. Hüttl. 2003. Impact of changes in land-use management on soil hydraulic properties: hydraulic conductivity, water repellency and water retention, *Phys. and Chem. of the Earth*. 28:1377–1387.

Wallis, M. G., D. J. Horne, and A. S. Palmer. 1993. Water Repellency in a New-Zealand Development Sequence of Yellow-Brown Sands. *Aust. J. Soil Res.* 31:641–654.

Wallis, M., D. Scotter, and D. Horne. 1991. An evaluation of the intrinsic sorptivity water repellency index on a range of New Zealand soils. *Aust. J. Soil Res.* 29:353.

Wang, T., D. Wedin, and V. A. Zlotnik. 2009. Field evidence of a negative correlation between saturated hydraulic conductivity and soil carbon in a sandy soil. *Water Resour. Res*. 45. W07503.

Wang, T., T. E. Franz, W. Yue, J. Szilagyi, V.A. Zlotnik, J. You, X. Chen, M.D Shulski, A. Young. 2015. Feasibility analysis of using inverse modeling for estimating natural groundwater recharge from a large scale soil moisture monitoring network. *J. Hydrol*. doi: http://dx.doi.org/10.1016/j.jhydrol.2015.12.019

Wang, T., V.A Zlotnik, D. Wedin, and K. D. Wally. 2008. Spatial trends in saturated hydraulic conductivity of vegetated dunes in the Nebraska Sand Hills: Effects of depth and topography. *J. Hydrol.* 349:88–97.

Wang, Z., Q. J. Wu, L. Wu, C. J. Ritsema, L. W. Dekker, and J. Feyen. 2003. Effects of water repellency on infiltration rate and flow instability. *Soil Water Repellency Occur. Consequences, Amelior.* 235–244.

Wine, M.L., T.E. Ochsner, A. Sutradhar, and R. Pepin. 2011. Effects of eastern redcedar encroachment on soil hydrualic properties along Oklahoma's grassland-forest ecotone. *Hydrol. Process*. 26:1720–1728.

Van Dam, J.C., J.M.H. Hendrickx, H.C. van Ommen, M.H. Bannink, M.T. van Genuchten, and L.W. Dekker. 1990. Water and solute movement in a coarse-textured water-repellent field soil. *J. Hydrol*. 120: 359-379.

van Genucten, M.T. 1980. A closed form equation for predicting the hydraulic conductivity of unsaturated soils. *Soil Sci. Am. J*. 144:892–898.

York, C. A., and P. M. Canaway. 2003. Water repellent soils on UK golf greens. *Soil Water Repellency Occur. Consequences, Amelior.* 113–119.

CHAPTER 4

IMPACT OF GRASSLAND CONVERSION TO FOREST ON GROUNDWATER RECHARGE IN THE NEBRASKA SAND HILLS

Zablon A. Adane · Paolo Nasta · Vitaly A. Zlotnik · David Wedin

Z.A. Adane · V.A. Zlotnik

Department of Earth and Atmospheric Sciences, University of Nebraska-Lincoln, Lincoln, NE 68588, USA, zablon@huskers.unl.edu; vzlotnik1@unl.edu

P. Nasta

University of Naples Federico II. Via Università, n. 100 – 80055 Portici (Napoli), Italy, paolo.nasta@unina.it

D. Wedin

School of Natural Resources, University of Nebraska-Lincoln, Lincoln, NE 68583, USA, dwedin1@unl.edu

To be submitted to Journal of Hydrology as: Adane, Z.A., Nasta, P., Zlotnik, V.A., Wedin. D. 2017. Impact of grassland conversion to forest on groundwater recharge in the Nebraska Sand Hills.

Abstract

The Nebraska Sand Hills grasslands have the greatest groundwater recharge rates in the High Plains Aquifer. However, the grasslands and the ecological services they provide are vulnerable to land use change and degradation. This study investigates the effects of grassland conversions to forest on recharge rates in a century-old experimental forest in the Nebraska Sand Hills. The DiffeRential Evolution Adaptive Metropolis ($DREAM_{ZS}$) global optimization algorithm was coupled with Markov-Chain Monte-

Carlo sampling scheme to estimate the effective soil hydraulic parameters from observed monthly soil moisture contents at 10 different depths for 220 cm deep uniform soil profiles. The historical recharge rates were then estimated by applying the numerical model HYDRUS 1-D for simulation of plots representing grasslands and dense pine forest conditions. The results indicate that conversion from grasslands to dense pine forests resulted in vegetation induced changes in soil hydraulic properties, increased rooting depth, and greater leaf area index, which together altered the water budget considerably. The impacts of land use change were a 7% increase in interception associated with an increase in leaf area index, 14% increase in actual evapotranspiration, and an overall reduction of groundwater recharge by nearly 100%. These outcomes highlight the significance of the grassland ecology for water resources, particularly groundwater recharge, in the Nebraska Sand Hills and the overall sustainability and vitality of the High Plains Aquifer.

Keywords: land-use change, afforestation, High Plains Aquifer, groundwater recharge rate; numerical model; soil hydraulic properties

Introduction

Over time, the ever-increasing alteration of landscapes and the exploitation of plants have provided various ecosystem services but also caused ill effects to the environment. For example, while the increase in agricultural lands and productivity in the last two centuries has increased the capacity to sustain unprecedented population growth,

it has also caused extensive deforestation, soil erosion and degradation, desertification, loss of biodiversity, and depletion of groundwater resources.

Concerns over the magnitude of deforestation and its associated impact on global climate change has made it imperative to maintain current forest coverage and reduce net loss of forest area through reforestation and afforestation programs. Afforestation, reforestation, and natural forest expansion have reduced net loss of forest area from approximately 9 million hectares per year in the 1990s to 7.3 million hectares per year by 2005 (FAO 2005). Most afforestation programs, however, have not been undertaken through conversion of agricultural lands but at the expense of natural vegetation, particularly grasslands. In fact, vast areas of grasslands worldwide were found suitable for future forest restoration programs to offset anthropogenic CO_2 emissions (Bond 2016).

In the last 100 years, natural regeneration and afforestation programs on various land uses have increased forest coverage (McCLeery 1992). Although forests provide several well documented ecological services (Nasi et al., 2002), a number of studies have also documented circumstances where conversions to forests have reduced streamflow (Brown et al., 2013), altered soil hydraulic properties (Kajiura et al., 2012), reduced soil moisture (James et al., 2003), and reduced recharge rates (Adane et al., 2015). The loss of soil moisture and groundwater recharge reductions have been attributed to the relatively higher evapotranspiration rates of the planted woody vegetation (Gates et al., 2011; Huang and Pang, 2011). Other studies have also partially associated these reductions in soil moisture and recharge rates to vegetation-induced soil water repellency (Adane et al., 2017) and greater rainfall interception of the introduced plantations (Allen and Chapman 2001; Owens et al., 2006; Simic et al. 2014; Starks et al. 2014).

In the early-20th century, over 75% (215 million hectares) of the grassland coverage in the western United States was reported to be experiencing widespread degradation (USDA, 2004). In the Great Plains, most counties have lost at least part of their natural grassland vegetation (Klopatek et al., 1979). For instance, 85% to 95 % of the native bluestem prairie vegetation in some areas had been converted to cropland (Sieg et al., 1999). The loss of grasslands has subsequently led to changes in the composition of vegetation, a loss of species diversity, and reductions in wildlife, such as the buffalo and prairie dogs in the Great Plains. While the Sand Hills grasslands are considered relatively intact at 85% of historical coverage, the region has experienced degradation related to conversion to cropland, habitat fragmentation, and overgrazing (FAO, 2005). Changes in soils associated with grassland deterioration include a reduction in soil porosity, decrease in organic matter, and decrease in nutrient contents, as well as reductions in water-retention capacity (Burke et al., 1989). Such large-scale and rapid land use change has been known to cause significant changes to the environment including changes in hydrological regimes (Schilling et al., 2008; Spracklen and Garcia-Carreras, 2015), land degradation (Bruun et al., 2013; Ozalp et al., 2016), loss of habitat and wild life (Ochoa-Quintero et al., 2015), and contributing to climate change (Longobardi et al., 2016).

There is also a growing interest in the consequences of land use change on water resources at global, continental, and local scales (Elmhagen et al., 2015) with particular emphasis on groundwater recharge rates (recharge rates, for brevity) that feed shallow aquifers. Groundwater levels of many aquifers around the world have been decreasing over the last few decades due to excessive groundwater extraction for irrigation that surpasses groundwater recharge and replenishing rates (Scanlon et al., 2012a; Terrell et al., 2002).

The vulnerability of groundwater resources emphasizes the need to know reliable relationships between land use change and recharge rates, particularly in semi-arid regions where water scarcity is a critical concern. While the effect of natural vegetation conversion to agricultural land with respect to water resources has been well documented (Scanlon et al., 2007), studies on water resources impacts of other land use changes not associated with cropland are less common. In particular, the effect of grassland conversions to forests on water resources need further consideration due to the recent expansion of afforestation efforts and future forest restoration plans all over the world including in the United States (Adane and Gates 2015; Eggemeyer et al., 2009; Huxman et al., 2005; Scanlon et al., 2009), China (Gates et al., 2011; Huang and Pang 2011; Yang et al., 2012), and India (Calder et al., 1997; Kallarackal and Somen 1997) where drastic population growth (in the latter two) and water resources sustainability are serious issues.

This study evaluated the impact of land use change from grassland to forest on historical recharge rates and overall water balance in a century-old natural laboratory setting in the semi-arid Great Plains. The objectives of this study are: 1) to obtain effective soil hydraulic properties for the grass and dense pine profiles through inverse modeling using monthly TDR soil moisture content measurements, and 2) to evaluate the impact of grassland conversions to forests on recharge and the overall water budget.

Site description

The Nebraska National Forest (NNF) (Bessey Ranger District) is located in the south-central part of the Nebraska Sand Hills (NSH) and within the northern part of the High Plains Aquifer (Fig. 4.1; 41°51’45” N and 100°22’06” W; near Halsey, Nebraska,

USA). The High Plains Aquifer covers an area of 450,000 km^2 and is ranked first in groundwater withdrawal for irrigation in the United States (Maupin and Barber, 2005; Scanlon et al., 2012b). The NSH landscape is comprised mainly of eolian sand dunes that were deposited as recently as a few thousand years ago (Miao et al. 2007). The soil is approximately 92-97% sand (Wang et al. 2009) and that contributes to the greatest recharge rates in the High Plains Aquifer (Scanlon et al., 2012b). The native vegetation of the NSH region consists of mixed-prairie grassland including little bluestem (*Schizachyrium scoparium*), switchgrass (*Panicum virgatum*), sand dropseed (*Sporobolus cryptandrus*), and Kentucky bluegrass (*Poa pratensis*) and is suitable to the historical land uses of ranching and cattle grazing (Eggemeyer et al., 2009). The climate is semi-arid continental with mean annual precipitation ranging between 40 and 70 $cm \cdot yr^{-1}$ and potential evapotranspiration ranging between 30 to 136 $cm \cdot yr^{-1}$ (Szilagyi et al. 2011).

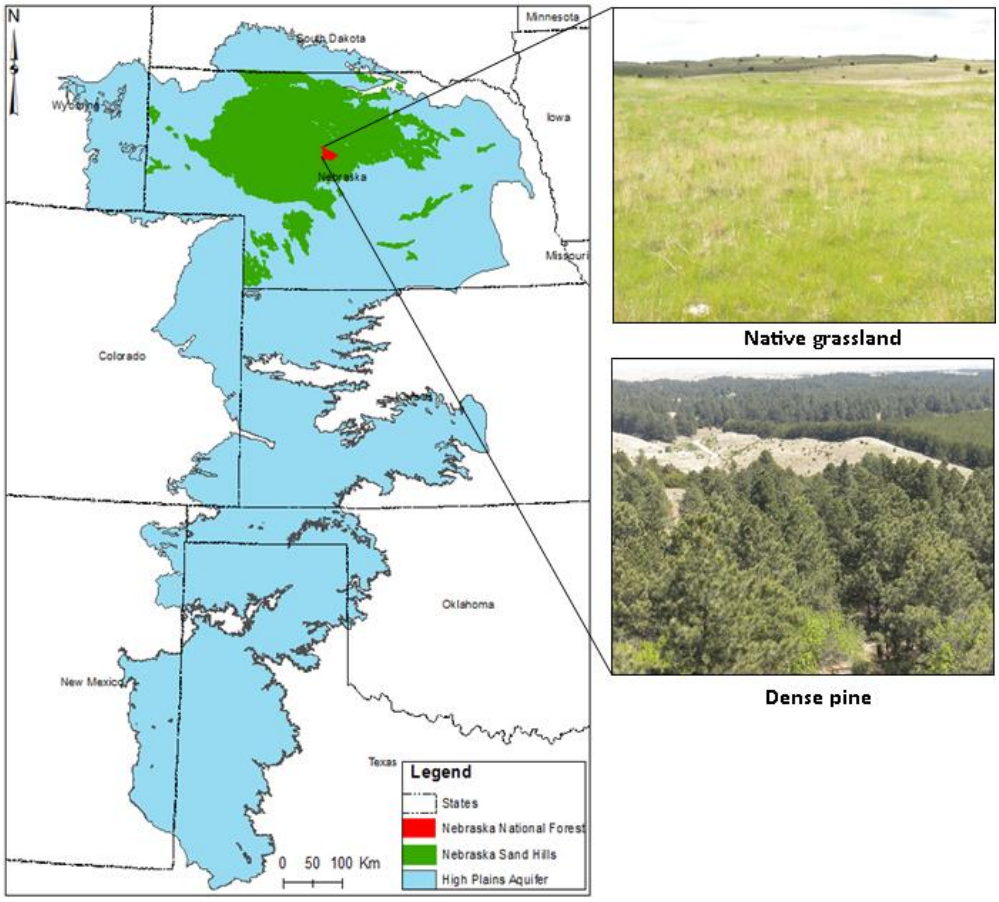

Figure 4.1. Location map of the Nebraska National Forest, the Nebraska Sand Hills, and the High Plains Aquifer and images of the native grassland and dense pine forest land uses

The Nebraska National Forest is the largest man-made forest in the United States covering over 10,000 ha and it contains various coniferous tree species, which were planted as early as the 1930s (Hellerich, 2006). The forest is predominantly planted with ponderosa pine (*Pinus ponderosa*) and is surrounded by the native grassland ecosystem. The grass (G) plot with 10 m × 10 m dimensions is considered to be the best approximation of the natural grassland conditions of the NSH within the forest (Fig.4.1). The dense pine (DP) plot contains ponderosa pine trees at density rate of 700–1000 trees·ha^{-1} and represents the change in land use from grassland. The selected dense pine plot contains the greatest pine

tree plantation density of the entire forest. The forest also contains pine savannah and thinned pines patches with much less tree density that are thoroughly covered in Adane and Gates (2015).

Table 4.1. Plot locations, vegetation type, elevations, tree density, and average Leaf Area Index (LAI)

Plot	Vegetation type	Longitude	Latitude	Elevation (m)	Tree density (trees·ha^{-1})	Average LAI (-)
G	Native grassland	100°21’16’’	41°50’41’’	860	-	0.77*
DP	Dense pine	100°19’71’’	41°51’69’’	854	700-1000	1.87

*Grass Average LAI for non-zero LAI days

Field data

Leaf area index

The Leaf Area Index (LAI) was measured for both the grassland and the dense pine plots. The LAI for the evergreen dense pine plot was determined to be 1.87 using hemispheric camera 360^{o} images with Ellipsoid-Campbell calculation method (Hellerich, 2006). The forest was planted in areas where the dense pine forests exist in non-contiguous patches in a grassland setting. The forest also contain parts that are pine savannah, thinned pine, and mixed vegetation patches with sporadic pine trees with much lower average LAI values ranging from 0.6 to 1.87 (Adane et al. 2017). Monthly LAI of the grasslands was obtained through a destructive method where the collected grass leaves were later scanned in the laboratory. The dataset included 66 separate data points spanning over 11 years of collection (2005–2015). Interpolations of the grassland LAI values were given by a second-order polynomial function that varies in time (day of year, DOY) during the growing season similar to the approach proposed by Nasta and Gates (2013):

$$LAI = \begin{cases} 319 \\ 100 \end{cases} - 8.877 \times 10^{-5}\, DOY + 0.0368\, DOY - 2.77 \qquad (1)$$

The observed and interpolated (Eq. 1) LAI values for the Sand Hills grasses as a function of time are depicted in Fig 4.2. The Leaf Area Index was approximately 0 in the cold winter and early spring (~0 to 100 and 319 to 365 days). The LAI steadily increased in the spring until it peaked at approximately 1.25 in the summer and early fall months of June to September (~150 to 270 days) and subsequently declines to 0 in late October.

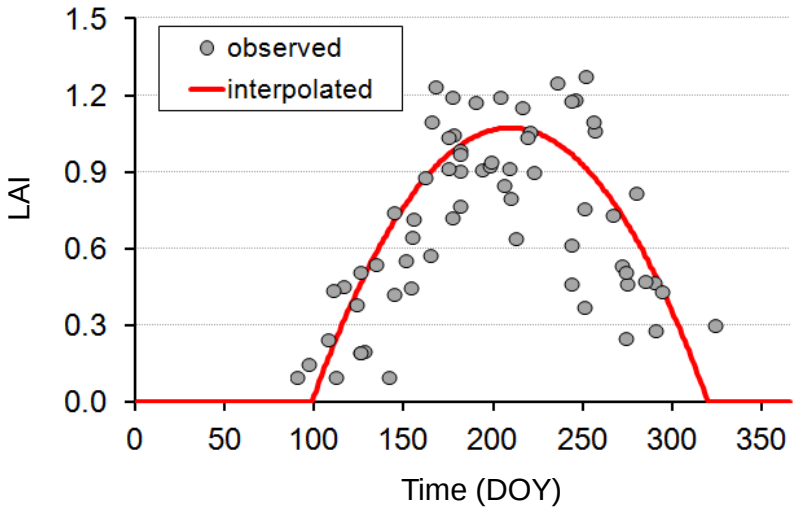

Figure 4.2. Observed and interpolated LAI values as a function of time (DOY) for the Sand Hills grasses.

Soil moisture data

The Time Domain Reflectometry (TDR) soil moisture measurements were collected monthly in both the grassland and dense pine plots. The plot profiles extended to 220 cm depth at approximately 20–30 cm intervals and data collected from March 2005 to January 2012 were used in this study. Quality control of the dataset removed abnormally high (> 30%) moisture contents associated with maintenance issues. This resulted in a total of 66 monthly readings over the span of 7 years that was used in model calibration and validation.

The soil moisture content was generally greater in the grassland plot soil profile

than in the dense pine plot. The total average moisture content for the grassland plot profile was approximately 13% and the average for each depth intervals ranged from 11.3% to 17.2% in the 2005 to 2012 dataset. The dense pine plot soil profile was drier compared with the grassland plot with the soil moisture content averaging approximately 9% and the average for each depth interval ranging from 8.3% to 12.7% over the 7-year dataset. The grassland plot profile had greater overall average soil moisture content for each of the depth intervals by approximately 48% to 84%. Instantaneous gravimetric data taken from soil profile cores in 2012 suggest that the average soil moisture contents were 8.4% for the grass and 4.5% for the dense pine profiles (Adane and Gates 2015), however, the low moisture values may also be partially attributed to the fact that 2012 was one of the driest years on record.

Historical climate data

Climate data output from the ensemble CMIP5 ESM was obtained from the CMIP5 Modeling Groups for the historical period 1950 – 2000. The dataset included daily precipitation and minimum and maximum daily temperatures at $1/8^{th}$ degree downscaled resolution (12 km × 12 km area) for the (41° 45' 0" N, 41° 52' 30" N) latitude and (100° 30' 0" W, 100° 22' 30" W) longitude bounds encompassing the NNF. The climate data were obtained from the ensemble for uniformity and continuousness of data throughout the study time period as well as to maintain continuity for a future study with climate projections. The CMIP5 historical climate data were reasonably consistent with the data obtained from High Plains Regional Climate Center (http://www.hprcc.unl.edu) for Halsey, Nebraska. The historical reference evapotranspiration (ET_0) was calculated using the Hargreaves equation (Hargreaves and Allen, 2003):

$$ET_0 = 0.0023\left(\frac{T_{max}+T_{min}}{2} + 17.8\right) \cdot \sqrt{T_{max} - T_{min}} \cdot R_a \qquad (2)$$

where T_{max} (°C) is the maximum daily temperature, T_{min} (°C) is the minimum daily temperature, R_a is extra-terrestrial solar radiation. ET_0 and R_a are expressed in the same units of equivalent water evaporation (L T^{-1}).

Figure 4.3 depicts the historical trends in annual averages of precipitation and reference evapotranspiration between 1950 and 2000.

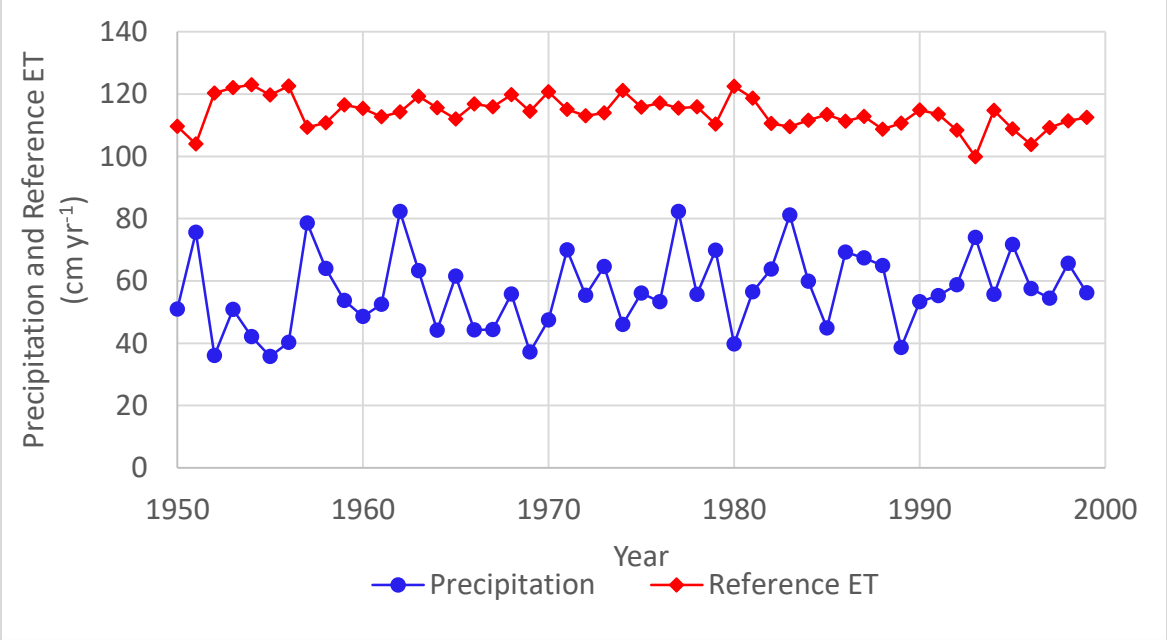

Figure 4.3. Historical trends in annual averages of precipitation *(P)* and reference evapotranspiration *(ET_0)*

The average historical precipitation for the 1950 to 2000 time period was approximately 57.0 cm·yr^{-1}, with the minimum of 35.8 cm·yr^{-1} and the maximum of 82.3 cm·yr^{-1} occurring in 1955 and 1966, respectively. The annual historical precipitation data also deviated from the mean by approximately 12.5 cm·yr^{-1}. The decadal averages of the historical precipitation data suggest an increase in precipitation from approximately 53

cm·yr^{-1} in the 1950s to 60 cm·yr^{-1} in the 1990s. The reference evapotranspiration rate estimates were substantially greater than the annual precipitation with an average of 114.0 cm·yr^{-1} and standard deviation of 5.0 cm·yr^{-1}.

Model and inversion approach

The water fluxes in the soil-plant-atmosphere system are simulated using the HYDRUS1-D software package (Šimůnek et al., 2008), which numerically solves the one-dimensional Richards equation for variably-saturated soil moisture flow:

$$\frac{\partial \theta}{\partial t} = \frac{\partial}{\partial z}\left\{K\left[\left[\frac{\partial h}{\partial z} + 1\right]\right]\right\} - \zeta \quad (3)$$

where t [T] is time, z [L] is the vertical coordinate (taken positive downward), h [L] is the water pressure head, θ [L^3 L^{-3}] is the soil volumetric water content, K [L T^{-1}] is the hydraulic conductivity and ζ [L^3 L^{-3} T^{-1}] is the sink term function that describes volumetric macroscopic root water uptake. The soil water retention function $\theta(h)$ is described by van Genuchten's equation (van Genuchten, 1980):

$$h = \theta_r + \frac{\theta_s - \theta_r}{[1+(\alpha h)^n]^m} \quad (4)$$

with Mualem's condition (Mualem, 1976):

$$m = 1 - \frac{1}{n} \quad (5)$$

where α (cm^{-1}), m (-) and n (-) are shape parameters, θ_r (cm^3 cm^{-3}) and θ_s (cm^3 cm^{-3}) are residual and saturated water contents, respectively. Using degree of soil saturation, S_e, which varies from 0 at ($\theta = \theta_r$) to 1 at ($\theta = \theta_s$), an expression for the unsaturated hydraulic conductivity function $K(S_e)$ is given by:

$$K(S_e) = K_s S_e^{\tau}\left[1 - \left\{1 - s_e^{1/m}\right\}^m\right]^2 \; ; S_e = (\theta-\theta_r)/(\theta_s-\theta_r) \quad (6)$$

where K_s (cm·d^{-1}) is saturated hydraulic conductivity, τ (-) is the tortuosity parameter,

assumed to be τ = 0.5 (Mualem, 1976). The potential evapotranspiration ET_p referred to the specific vegetation type is calculated by multiplying ET_0 by the specific crop coefficient, K_c. Subsequently ET_p is partitioned into potential evaporation, E_p (cm·d^{-1}) and potential transpiration, T_p (cm·d^{-1}) according to the following empirical equation:

$$E_p = ET_p \cdot e^{-k \cdot LAI} \quad (7)$$

where κ (-) is the dimensionless extinction coefficient for global solar radiation inside the canopy and is assumed to be equal to 0.463 (Ritchie, 1972), whereas LAI is the leaf area index that varies by day of year (DOY). The rainfall interception I (cm d^{-1}) is calculated according to Braden (1985) and Schwärzel et al. (2006):

$$I = a \cdot LAI \left(1 - \frac{1}{1 + bP/c \cdot LAI}\right) \quad (8)$$

where a (cm·d^{-1}) is an empirical coefficient, assumed to be 0.025 cm·d^{-1} and b (-) denotes the soil cover fraction given by:

$$b = 1 - e^{-k \cdot LAI} \quad (9)$$

Interception is subtracted from the gross precipitation (P_{gross}) in order to obtain the net precipitation (P_{net}) that falls to the soil surface. The soil profile which extends to 220 cm depth, is considered homogeneous over a single uniform layer with a set of "effective" soil hydraulic properties (e.g., Nasta and Romano, 2016). Net precipitation and potential evaporation represent the system-dependent atmospheric upper boundary conditions, whereas free drainage is assumed at and below the lower boundary of the soil profile and is considered potential groundwater recharge (R) in this study. The term T_p determines the potential root water uptake, $\zeta(h)$, which is reduced through the Feddes condition (Feddes et al., 2001). Two simulations are set up in HYDRUS 1-D: a) grass

with K_c=0.95 and 50 cm root depth; and b) pine with K_c=1.0 and 200 cm root depth. The Feddes parameters were retrieved from the database available within in HYDRUS 1-D.

Model calibration and validation

For each of the two simulations, the effective soil hydraulic parameters featuring in van Genuchten's relations (Eq. 5) and (Eq. 6) need to be estimated by inverse modeling. The robustness of any optimization algorithm used for inverse modeling often determines its suitability for specific parameter estimation. The first optimization routines were the local-search algorithms, such as the least-square estimators like the one embedded in HYDRUS1-D. The results in these algorithms strongly depend on the initial guesses of each parameter value, thus facing a high risk of early termination and failure in multiple-local minima (Vrugt et al., 2003).

As a measure to mitigate the dependence on the parameter initial guesses, there have been a series of robust global search algorithms to optimize soil hydraulic parameters. One of the most popular techniques proposed in the literature, the DiffeRential Evolution Adaptive Metropolis algorithm ($DREAM_{ZS}$) coupled to the efficient Markov-chain Monte-Carlo sampling scheme (Laloy and Vrugt, 2012; Vrugt, 2016; Vrugt et al., 2008) is adopted in this work because a Bayesian interpretation is more appropriate in order to infer "the most probable" set of parameters and their corresponding uncertainties (Moradkhani et al., 2005). The Bayesian statistical inference combines the data likelihood with a priori distribution to derive the posterior probability density functions of the model parameters. The objective function $\Phi(\boldsymbol{P})$ to be minimized in the optimization routine is defined as the root mean squared deviation (RMSD):

$$\min_P \Phi(\boldsymbol{P}, z) = \sqrt{\frac{\sum_{t=1}^{t_{TOT}} \sum_{z=1}^{z_{TOT}} [\theta_{TDR}(z,t) - \theta_{SIM}(z,t,\boldsymbol{P})]^2}{t_{TOT} + z_{TOT} - 1}} \quad (10)$$

where the vector $\boldsymbol{P}$ = (θ_r, θ_s, α, n, and K_s) contains the optimization parameters, and the subscripts *TDR* and *SIM* denote the observed and simulated soil water content values corresponding to depth *z* at observation time *t* for 66 days between 2005 up to 2012 at approximately one record per month. Maintenance months, where data were not collected and data points that are unrealistically high, were not considered.

For optimization, the HYDRUS 1-D model was implemented in DREAM$_{ZS}$ using the MATLAB environment. The minimum and maximum bounds for the grass profile soil hydraulic parameters were selected based on field data for Valentine sand (unpublished), pedotransfer function (Kettler et al. 2001) and global sand textures reported by Carsel and Parish (1988). The soil hydraulic property bounds for the pine profile were further broadened in order to account for the impact of soil hydrophobicity (Adane et al., 2017). Results are shown in Table 4.2. The main MATLAB text file (SELECTOR.IN) is automatically updated within the program with a new set of the five hydraulic parameters (θ_r, θ_s,α, n, and K_s) that have to be optimized, whereas the simulated water content values for each observation *z*-depth and each time step *t* are retrieved from the text file (Obs_Node.Out).

Table 4.2. Minimum and maximum bounds used for soil hydraulic property optimization

Parameter	Units	Grass		Pine	
		Min	Max	Min	Max
θr	$cm^3 \cdot cm^{-3}$	0.03	0.045	0.02	0.045

θs	$cm^3 \cdot cm^{-3}$	0.35	0.43	0.30	0.43
α	cm^{-1}	0.03	0.145	0.01	0.145
n	[-]	1.65	3.0	1.0	3.0
K_s	$cm \cdot d^{-1}$	200	750	100	750

The number of observed water contents were 660 in total and were recorded at 10 different depths and in 66 days (distributed over 7 years). A vector of 370 observed water content values (10 depths in 37 days collected over 4 years) for calibration (2005–2008) and the remaining 290 (10 depths in 29 days collected over 3 years) were used for model validation (2009–2011). The performance diagnostic is quantified through the root mean squared deviation (RMSD):

$$RMSD = \sqrt{\left[\frac{\sum_{i=1}^{N}(\theta_{TDR} - \theta_{SIM})^2}{N}\right]} \quad (11)$$

where N was the total number of θ-observations; N =370 and N =290 for model calibration and validation, respectively, and θ_{TDR} and θ_{SIM} were observed and simulated water content values.

Results

Model calibration and validation results

The target of the calibration and model setup for the grassland and the dense pine plots was to facilitate a reasonable simulation of recharge rate estimates for the grass and pine soil profiles under the historical climate conditions. The performance of the model was measured through the root mean squared deviation (RMSD) as specified in Eq. 11.

The calibration results comparing the observed and simulated soil moisture data subjected to observed precipitation (P) and potential evapotranspiration (ET_p) daily values

are depicted in Fig 4.4.

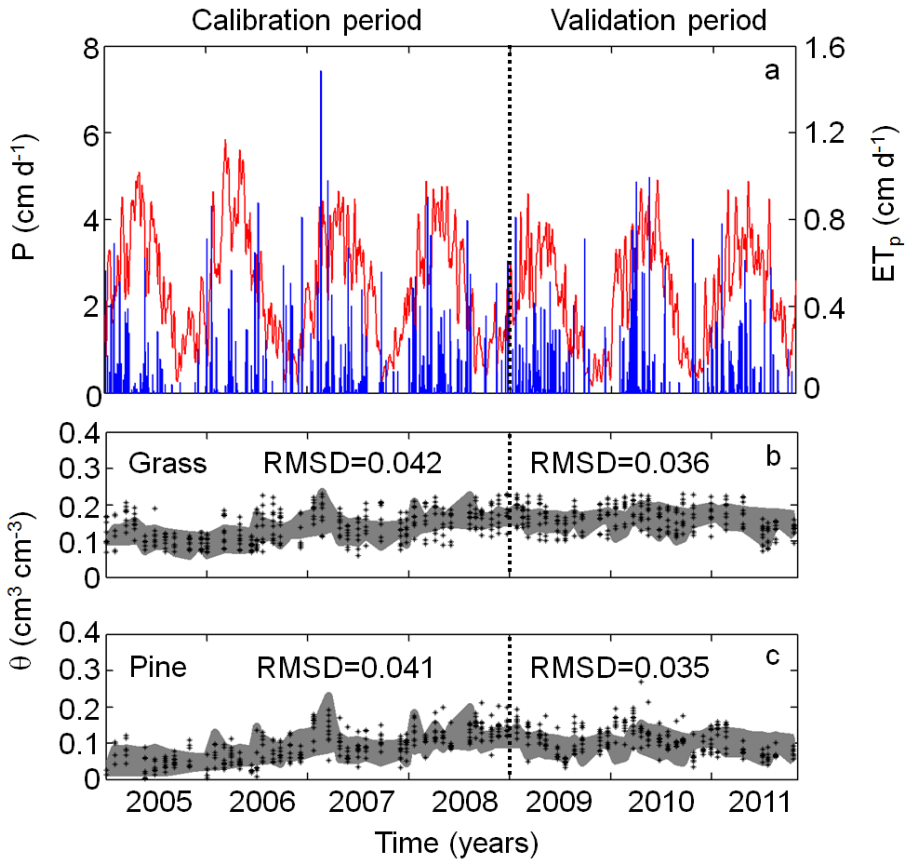

Figure 4.4. Calibration (2005-2008) and validation (2009-2011) results comparing the observed and simulated soil moisture data: (a) precipitation (blue) and potential evapotranspiration (red) in $cm \cdot d^{-1}$ for 2005-2011; (b) observed (black stars) and simulated (gray uncertainty bands) soil moisture content for the grass plot, and (c) observed (black stars) and simulated (gray uncertainty bands) soil moisture content for the dense pine plot

Ten observed (black stars) θ-values corresponding to each soil depth are reported in each time step while the gray bands signify the modeled θ-values of the uniform soil profile corresponding to posterior probability density functions of the effective soil hydraulic parameters. The calibration results comparing the observed and simulated soil

moisture data for all of depth intervals are depicted in Fig 4.4.

The model simulations were essentially able to reproduce the hydrological dynamics and trends of the observed soil moisture contents in both vegetation plots reasonably well. The RMSD values were relatively low (4.2% and 3.6% in the calibration and validation periods, respectively) for the grassland plot. Similarly, the dense pine plot soil moisture content calibration and validation processes resulted in low RMSD of 4.1% and 3.5%, respectively. Considering the calibrations were done based on a set of limited data, the optimization was reasonably robust, even though previous investigations have reported more robust performances (Wöhling and Vrugt, 2011).

The most probable values of the three estimated effective soil hydraulic parameters correspond to the median-values of their posterior frequency distributions and are reported in Table 4.3. The θ_r and θ_s parameter estimates for the grass and dense pine profiles were 0.041 and 0.021 and 0.43 and 0.32, respectively. The α parameter results were 0.077 cm^{-1} and 0.011 cm^{-1}, while the *n* parameter results were 1.65 and 1.36 for the grassland and dense pine plot soil profiles, respectively. One of the most uncertain parameters in this optimization for both grassland and dense pine soil profiles was K_s with values of 218 $cm \cdot d^{-1}$ and 185 $cm \cdot d^{-1}$ respectively. Since the study site generally consists of homogenous Valentine sands, the optimized K_s values are reasonable and are consistent with unpublished field data (K_s=240 $cm \cdot d^{-1}$), despite being much lower than the K_s = 713 $cm \cdot d^{-1}$ reported for a global sand texture in Carsel and Parish (1988). While the coefficients of variance indicate greater confidence in the θ_r, θ_s, and n parameter (6.7%, 1.9%, and 1.3%) estimates, uncertainties were greater for α (CV = 36.1%) and K_s (31.9%) parameters (Table 4.3). The coefficients of variance were also notably greater

for the pine profile and suggest that while the overall calibration is robust, it could be improved by refining individual parameter estimates. It is important to note that approximations applied in the model, such as uniform soil profile, estimated root depth and root distribution coupled with a coarse (monthly and at times non-contiguous) temporal resolution of observed soil moisture content data can generate "epistemic" errors and uncertainties (Nasta and Romano, 2016).

Table 4.3. The most probable values of the three optimized parameters *

Parameter	Units	Grass	Pine
θr	$cm^3 \cdot cm^{-3}$	0.041 (6.7%)	0.021 (42.8%)
θs	$cm^3 \cdot cm^{-3}$	0.43 (1.9%)	0.32 (6.9%)
α	cm^{-1}	0.077 (36.1%)	0.011 (14.2%)
n	[-]	1.65 (1.3%)	1.36 (3.4%)
K_s	$cm \cdot d^{-1}$	214.1 (31.9%)	186.7 (28.9%)

*associated coefficients of variance, CV are reported in parentheses

Simulated historical recharge rate and water budget results

Gross precipitation and evapotranspiration are fundamental factors in groundwater recharge and the overall soil water balance. The average historical gross precipitation (P_{gross}) for the 1950 to 2000 time period was 57.0 $cm \cdot yr^{-1}$ for the area. The estimated vegetation canopy interception of precipitation were approximately 1.3 $cm \cdot yr^{-1}$ in the grassland and 5.4 $cm \cdot yr^{-1}$ in the dense pine plots and accounted for approximately 2.3% and 9.5% of gross precipitation, respectively. The average historical annual actual evapotranspiration estimates were 43.6 $cm \cdot yr^{-1}$ in the grass to 52.2 $cm \cdot yr^{-1}$ for the dense pine plots. The averages of total actual evapotranspiration rates ($I+E_A+T_A$) represented 78.8% and 101.4% of the precipitation in the grass and dense pine profiles, respectively. These estimates are consistent with the results of Szilagyi et al. (2011) that reported the

ponderosa pine plantations in the NNF evaporated 5% to 10% more than the average annual precipitation. The average recharge rate estimates were 11.4 cm·yr^{-1} for the grass and 0.08 cm·yr^{-1} for the dense pine plots, which represent 20.0% and 0.17% of gross precipitation, respectively.

Table 4.4. Summary of historical average of climate and simulated water balance data

Profile	P_{gross} (cm·yr^{-1})	P_{net} (cm·yr^{-1})	ET_P (cm·yr^{-1})	I (cm·yr^{-1})	E_A (cm·yr^{-1})	T_A (cm·yr^{-1})	ET_A (cm·yr^{-1})	R (cm·yr^{-1})	R (% of P_{gross})
Grass	57.0	55.8	78.7	1.3	25.3	18.3	43.6	11.4	20.0%
Pine	57.0	52.8	114.0	5.4	29.4	21.8	52.2	0.08	0.14%

Discussion

Comparison with recharge studies in the Sand Hills

The historical recharge rate estimates were generally consistent with other field and modeled studies in the Nebraska Sand Hills. The average historical recharge rate estimated for the grasslands in this study was approximately 11.4 cm·yr^{-1} and 20% of precipitation and agreed with the results of Crosbie et al. (2013), which estimated 10 to 15 cm·yr^{-1} and 20 to 30% of annual precipitation. The recharge estimates for the grasslands were also consistent with Scanlon et al. (2012) that reported a range of 2.5 cm·yr^{-1} to 21.0 cm·yr^{-1} for an average of 9.2 cm·yr^{-1} for the Sand Hills in the Northern High Plains. While Szilagyi et al. (2003) estimated recharge rates to range between 3.7 and 4.9 cm·yr^{-1}, an improved model in Szilagyi et al. (2011) estimated an average rate of 7.3 cm·yr^{-1}. Billesbach and Arkebauer (2012) also reported 11.5±2.0 cm·yr^{-1} for a grazed grassland site with no plantations, located approximately 110 km from the present study site. A chloride mass balance study used to corroborate the remote sensing results estimated 10.3 cm·yr^{-1} for a sampling location closest to this study area near Halsey, NE (Szilagyi et al. 2011). A study

using soil moisture network data inverse modeling at Halsey estimated an annual recharge rate of 5.0 $cm \cdot yr^{-1}$ and 7.1% of precipitation (Wang et al., 2016). A chloride mass balance and sulfate mass balance recharge study for the same plot used in this study also estimated 3.7 $cm \cdot yr^{-1}$ and 10.0 $cm \cdot yr^{-1}$, respectively for the grasslands (Adane and Gates, 2015). However, the study conducted in the middle of a severe drought in 2012 contained considerably lower soil moisture contents compared to the long term soil moisture data obtained from TDR measurements and can potentially affect the final estimates of recharge. A study that used chemical tracers, (McMahon et al., 2006) estimated that recharge rates for the Sand Hills grassland can exhibit a broad range between 0.02 cm yr^{-1} to 7.0 $cm \cdot yr^{-1}$. While there have been a number of recharge studies in the Sand Hills, the range of estimates can still vary drastically because of spatial differences in precipitation and temperature gradient. As such, careful considerations of averaged values and thoughtful geographical partitioning of the NSH will provide more valuable information on recharge rates and the water balance.

Whereas few recharge estimates were available for the grasslands, estimates for the dense pine plantations have been even rarer. This study estimated almost negligible (0.08 $cm \cdot yr^{-1}$) average historical recharge rates for the dense pine plot. This result is consistent with the chloride mass balance method where Adane and Gates (2015) estimated the average recharge rate beneath the dense pine plot at approximately 0.7 to 1.0 $cm \cdot yr^{-1}$. In reference to the dense ponderosa pine plantation in the NNF, Szilagyi et al. (2011) reported that the plantations may evaporate more than annual precipitation suggesting that the recharge rate beneath the dense pine plantations may likely be negligible. In a temperate climate in south Western Australia, Farrington and Bartle (1991) estimated recharge

beneath pines (*Pinus pinaster*) was 114 mm (15% of precipitation) but still 35% less than the adjacent woodlands. In the semi-arid Mediterranean climate of Alicante, Spain, Bellot et al. (1999) also estimated recharge beneath pine trees to be negligible. Sharma et al. (1983) in Australia reported that conversion from grassland to pines (*Pinus radiata*) resulted in negligible recharge rates. Similarly, Holmes and Colville (1970a and 1970b) documented that conversion recharge rates beneath grasslands (6.3 $cm \cdot yr^{-1}$) were reduced to 0 $cm \cdot yr^{-1}$ beneath 24-year-old pines.

The severity of reduction in recharge is influenced by the plantation density of the pine trees. Adane and Gates (2015) reported that, compared to the native grassland, recharge beneath the sparse pine trees (LAI = 0.31) was only reduced by 14%. In the meantime, recharge beneath the pine savannah (LAI = 1.68) and dense pine trees (LAI = 2.20) were reduced by 51% and 73%, respectively. Comparing thinned and unthinned loblolly pine stands, Stogsdili et al. (1992) found that increased moisture in the soil profile is more a function of reduced leaf interception loss and increased throughfall rather than reduced water use from the tree stands. In addition to tree water use, understory vegetation, climate, and soil type play important roles on the severity of recharge reduction.

The impact of land use change on recharge and the soil water balance

The annual recharge rates for the grassland and dense pine profiles from 1950 to 2000 are shown in Fig 4.5. The impact of land use change on recharge rates and water balance was assessed through the difference between the native grassland and the dense pine plots, indicating the change in the historical land use. This change included an increased root depth from 50 cm in the grassland to 200 cm in the pine vegetation, as well

as increased canopy cover where the LAI ranged from 0 to 1.2 in the grasses and 1.87 for the evergreen dense ponderosa pines.

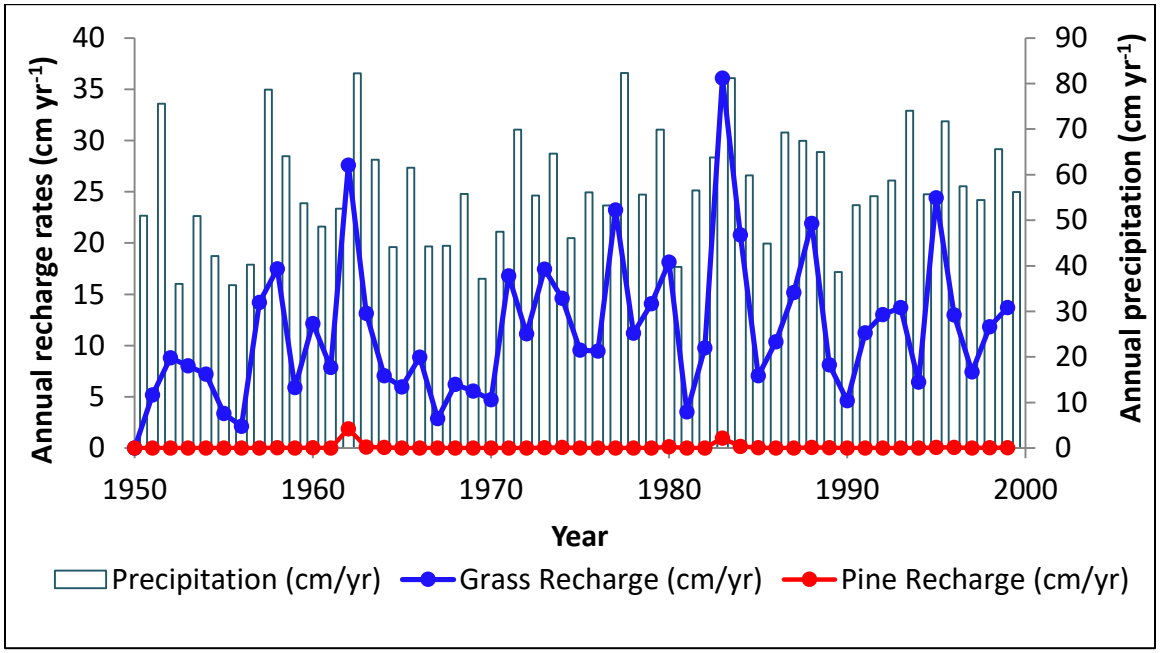

Figure 4.5. Annual recharge rates for the grass and dense pine plots under historical conditions.

These changes to the land use have increased average interception more than fourfold from 1.3 cm·yr^{-1} to 5.4 cm·yr^{-1}, which are equivalent to 2.3% and 9.0% of gross precipitation. Such increase in canopy interception in trees is consistent with what has been reported by (Bosch and Hewlett 1982), who found that canopy interception of 10% to 40%, which was considerably less than the 25-40% reported for coniferous trees in the UK (Calder, 2003), 19.4% for pines in Nepal (Ghimire et al., 2012), and 17% in semi-arid pine forest in Portugal (Valante et al., 1997). The conversion from grassland to dense pine vegetation also increased actual evapotranspiration from 43.6 cm·yr^{-1} to 52.4 cm·yr^{-1}, which agrees with the conclusions of Zhang et al. (2001), who reported that greater evapotranspiration in forests than pasture for semi-arid regions with less than 600 cm·yr^{-1}

precipitation. The average annual actual evapotranspiration including interception losses accounted for approximately 77.7% of the average gross precipitation in the grass plot and 101.3% in the dense pines profiles, which are consistent with studies that estimated 90% in semi-arid climates (Huxman et al., 2005). Szilagyi et al. (2011) also estimated that evapotranspiration rates may exceed annual precipitation by up to 10% in the dense ponderosa pine of the NNF. The average transpiration rates were 16.1% greater in the dense pine plot (21.8 $cm \cdot yr^{-1}$) than in the grasses (18.3 $cm \cdot yr^{-1}$), which is a conclusion consistent with other studies (Zhang et al. 2001; Harding et al. 1992; Bosch and Hewitt 1982) The actual evaporation estimate was also 13.4% greater in the dense pine (29.4 $cm \cdot yr^{-1}$) than in the grassland (25.3 $cm \cdot yr^{-1}$) profile, possibly in response to a 15% reduction experienced in soil hydraulic conductivity of the dense pine plot. The results are consistent with Allen and Chapman (2010) and Calder and Newson (1980) who reported the rate of extra water loss by evaporation in forests is much more efficient than grasslands due to turbulent winds generated by trees. Greater evaporation losses in the dense pine plot may also likely be due to longer exposure to radiation and the atmosphere compared to the grassland with the faster soil hydraulic property (K_s). Conversely, evaporation rates in grasses than trees have also been reported in Kelliher et al. (1993), where annual average evaporation rates were 168 $cm \cdot yr^{-1}$ compared to 146 $cm \cdot yr^{-1}$ in the coniferous trees likely due to the greater canopy cover of forests. Subsequently, land use change through grassland afforestation has reduced the average historical recharge rate by approximately 100% from 11.4 $cm \cdot yr^{-1}$ to 0.08 $cm \cdot yr^{-1}$ and was in agreement with the results of Adane and Gates (2015), who reported reductions up to 90% for the same study site. The recharge rate has also been reduced from 20.0% of precipitation in grasslands to 0.14% in the dense pine. The cumulative historical

recharge rate estimates suggest that land use conversion to dense pine vegetation has reduced recharge rate by 568 cm over 50 years (Fig 4.6).

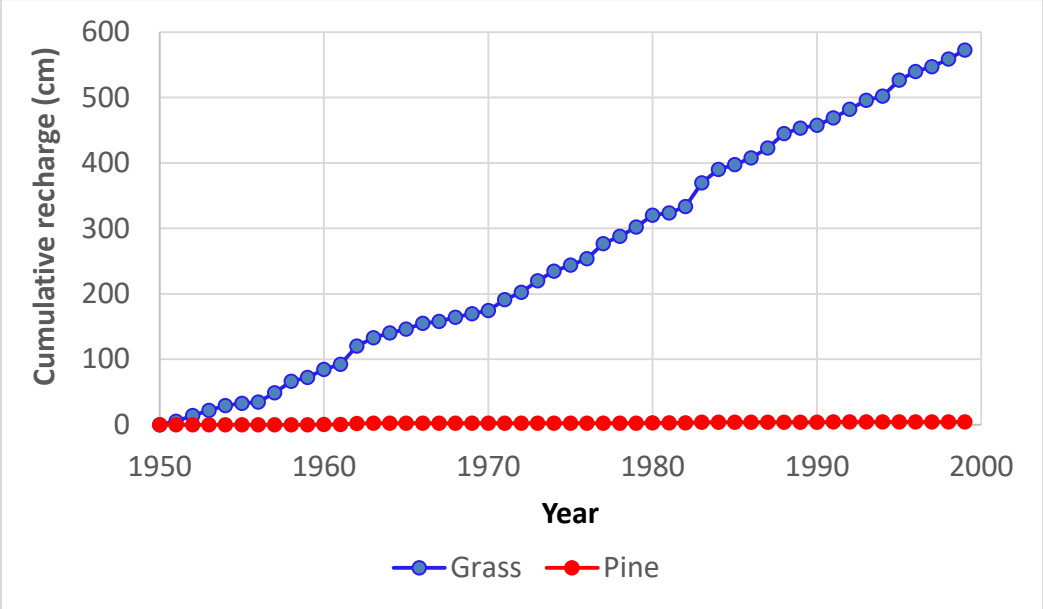

Figure 4.6. Cumulative groundwater recharge for the grass and dense pine plots under the historical time period.

The analysis also suggested that variation in annual precipitation alone did not explain the change in recharge rates. The analysis performed by Aich et al. (2014) on the impact of precipitation change on streamflow showed linear and exponential relationships between precipitation and change in streamflow in four African basins, because the changes that occurred were predominantly in the upper boundary conditions. This analysis, however, was not as clear in terms of groundwater recharge due to the non-linearity of the unsaturated zone flow in the lower boundary conditions. The relationship between annual precipitation and recharge was stronger in the grassland (R^2 = 0.41) than the pine profile (R^2 = 0.12) but was not robust (Fig 4.7). Although not considered in this analysis, the intensity and the timing of precipitation events have also been documented to be major

contributors to the amount of groundwater recharge (Mileham et al., 2008).

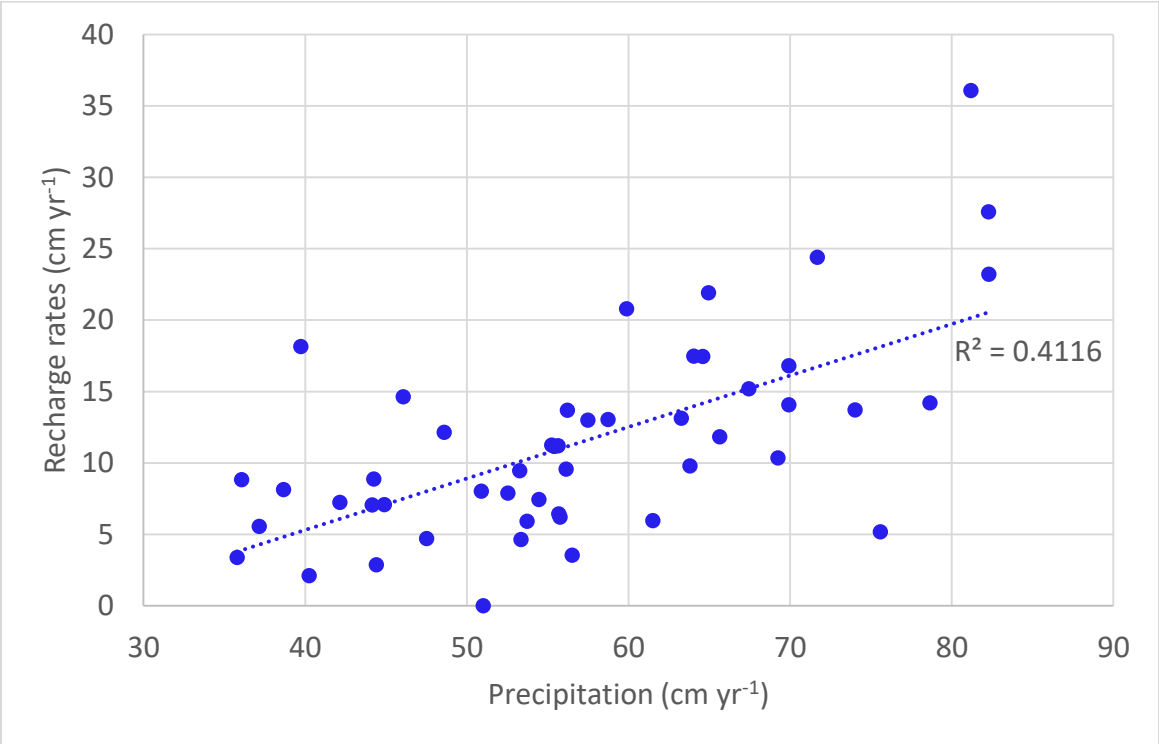

Figure 4.7. The relationship between annual precipitation and grassland profile recharge rates.

Groundwater recharge is not solely driven by precipitation but also is influenced by ambient temperature and evaporative demands. The ratio of precipitation to evapotranspiration rates is an important factor in the water budget of grasslands in semi-arid climates (Glen et al. 2015). Land use change or climate-induced variation in precipitation to evapotranspiration ratio could provide a better assessment of the impacts on recharge. The relationship between the ratio of precipitation and evapotranspiration and recharge was stronger, with R^2 = 0.64 for the grassland profile (Fig 4.8).

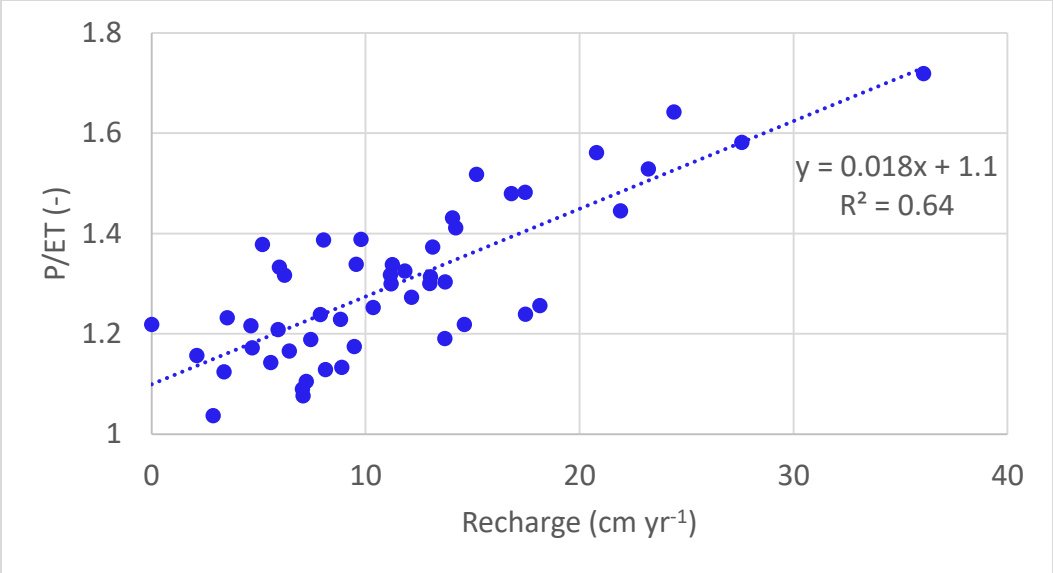

Figure 4.8. The relationship between the ratio of precipitation and evapotranspiration and groundwater recharge for the grassland soil profile.

Recharge often occurs when precipitation is greater than the evaporative demands. In the grassland soil profile, recharge rates events occur when precipitation is at least 3% greater than the annual evaporative demand. Recharge rates greater than the historical average occurred when annual precipitation exceeded 20%. In the observed period, nearly half of the years experienced precipitation exceeding this 20% threshold. In the dense pine profile, annual precipitation rarely exceeded the annual evapotranspiration requirement by more than 20%, keeping groundwater recharge at an almost negligible level. The analysis reinforces the importance of the grassland ecology to the water resources of the NSH.

Conclusion

This study was among a very few site-specific investigations that evaluated the impact of land use change on recharge rates in the Nebraska Sand Hills. This study quantified the considerable impact that land use change has on recharge rates and overall

water balance. The conversion from the historical native grassland to forested land reduced recharge rate by approximately 100%. The actual evapotranspiration rates of the dense forest profile were also substantially greater than the grassland in response to increased canopy cover and greater root extinction depth. Evaporation rate was also greater under the dense pine profile, partly due to lower saturated hydraulic conductivity value and longer exposure to ambient temperature and atmospheric demand. The potential for recharge rates to exceed historical averages exists when the ratio of precipitation to evapotranspiration exceeds 20%. This threshold can also be used to analyze the impact of climate variation on groundwater recharge rates in the grasslands.

Proper consideration needs to be given to the intrinsic uncertainties in the data, the simulations, and the parameter assumptions. The numerical model simulations did not consider the impact of preferential flow, discretized layer with different soil hydraulic properties, and hysteresis to mention a few. While the uncertainties in this analysis may have contributed to the drastic conclusion, the severe reduction in groundwater recharge as a result of land use change in the Sand Hills should attract the attentions of water resources managers, who will need to consider management actions, such as identifying tree species that are less water intensive, optimum plantation density, and adaptive forest management activities (e.g. clearing and thinning) directed at prolonging the vitality of the Nebraska Sand Hills and the long term sustainability of the High Plains Aquifer.

In the effort to combat CO_2 emissions and global climate change, many semi-arid grasslands have been identified as suitable for future forestation programs worldwide. This case study provides further evidence of the importance of grassland ecology to water

resources, particularly to groundwater systems. Thus, the impact of these plantation efforts on water sustainability, especially in the semi-arid climates must be thoroughly considered.

Acknowledgements

The authors would like to thank the Forestry lab at the School of Natural Resources, particularly Jeremy Hiller and Dr. Tala Awada for providing us with several sets of long term data and continuous access to the plots at the Nebraska National Forest near Halsey.

References

Adane, Z.A., Nasta, P., and Gates, J.B., 2017. Links between soil hydrophobicity and groundwater recharge under plantations in a sandy grassland setting, Nebraska Sand Hills, USA. Forest Science. doi:10.5849/FS-2016-137

Adane, Z.A. and Gates, J.B., 2015. Determining the impacts of experimental forest plantation on groundwater recharge in the Nebraska Sand Hills (USA) using chloride and sulfate. Hydrogeology Journal 23, 81–94, doi: 10.1007/s10040-014-1181-6.

Aich, V., Liersch, S., Vetter, T., Huang, S., Tecklenburg, J., Hoffmann, P., Koch, H., Fournet, S., Krysanova, V., Müller, E.N., Hattermann, F.F., 2014. Comparing impacts of climate change on streamflow in four large African river basins. Hydrol. Earth Syst. Sci. 18, 1305–1321. doi:10.5194/hess-18-1305-2014

Allen, A., Chapman, D. 2001. Impacts of afforestation on groundwater resources an quality. Hydrogeology Journal 9, 390-400. doil 10.1007/s100400100148

Bellot, J., Sanchez, J.R., Chirino, E., Hernandez, N., Abdelli, F., Martinez, J.M., 1999.

Effect of different vegetation type cover effects on the soil water balance in a semi-arid areas of south eastern Spain. Phys. Chem. Earth (B) 24, 24 353–357

Billesbach, D.P., Arkebauer, T.J., 2012. First long-term, direct measurements of evapotranspiration and surface water balance in the Nebraska Sand Hills. Agric For Meteorol 156, 104–110. doi:10.1016/j.agrformet.2012.01.001

Bond, W. J., 2016. Ancient grasslands at risk. Science. 351, 120–122.

Bosch, J.M., Hewlett, J.D., 1982. A review of catchment experiments to determine the effect of vegetation changes on water yield and evapotranspiration. J. Hydrol. 55, 3–23. doi:10.1016/0022-1694(82)90117-2

Brown, A.E., Western, A.W., McMahon, T.A., Zhang, L., 2013. Impact of forest cover changes on annual streamflow and flow duration curves. J. Hydrol. 483, 39–50. doi:10.1016/j.jhydrol.2012.12.031

Bruun, T.B., Elberling, B., de Neergaard, a, Magid, J., 2013. Organic Carbon Dynamics in Different Soil Types After Conversion of Forest To Agriculture. L. Degrad. Dev. 283, n/a-n/a. doi:10.1002/ldr.2205

Burke, I.C., Yonker, C.M., Parton, W.J., Cole, C. V., Schimel, D.S., Flach, K., 1989. Texture, Climate, and Cultivation Effects on Soil Organic Matter Content in U.S. Grassland Soils. Soil Sci. Soc. Am. J. 53, 800. doi:10.2136/sssaj1989.03615995005300030029x

Calder, I.R., 2003. Impact of lowland forests in England on water resources: Application of the Hydrological Land Use Change (HYLUC) model. Water Resour. Res. 39, 1–10. doi:10.1029/2003WR002042

Calder, I.R., Newson, M.D., 1980. The effects of afforestation on water resources in Scotland. In: Land Assessment in Scotland, Proc Symp Roy Geogr Soc Edinburgh, pp 51–62

Calder, I. R., Rosier, P. T. W., Prasanna, K. T., Parameswarappa, S., 1997. Eucalyptus water use

greater than rainfall input –a possible explanation from southern India. Hydrology and Earth

System Sciences 1, 249–256.

Crosbie, R.S., Scanlon, B.R., Mpelasoka, F.S., Reedy, R.C., Gates, J.B., Zhang, L., 2013. Potential climate change effects on groundwater recharge in the High Plains Aquifer, USA. Water Resour. Res. 49, 3936–3951. doi:10.1002/wrcr.20292

Eggemeyer, K.D., Awada, T., Harvey, F.E., Wedin, D.A., Zhou, X., Zanner, C.W., 2009. Seasonal changes in depth of water uptake for encroaching trees Juniperus virginiana and Pinus ponderosa and two dominant C4 grasses in a semiarid grassland. Tree Physiol. 29, 157–169. doi:10.1093/treephys/tpn019

Elmhagen, B., Eriksson, O., Lindborg, R., 2015. Implications of climate and land-use change for landscape processes, biodiversity, ecosystem services, and governance. Ambio 44. doi:10.1007/s13280-014-0596-6

Farrington, P and Bartle, G.A., 1991. Recharge beneath a Banksia woodland and a Pinus pinaster plantation on coastal deep sands in south Western Australia. Forest Ecol. and Manag. 40, 101–118. doi:10.1016/0378-1127(91)90096-E

Feddes, R.A., Hoff, H., Bruen, M., Dawson, T., De Rosnay, P., Dirmeyer, P., Jackson,

R.B., Kabat, P., Kleidon, A., Lilly, A., Pitman, A.J., 2001. Modeling root water uptake in hydrological and climate models. Bull. Am. Meteorol. Soc. 82, 2797–2809. doi:10.1175/1520-0477(2001)082<2797:MRWUIH>2.3.CO;2

Gates, J.B., Scanlon, B.R., Mu, X., Zhang, L., 2011. Impacts of soil conservation on groundwater recharge in the semi-arid Loess Plateau, China. Hydrogeol. J. 19, 865–875. doi:10.1007/s10040-011-0716-3

Ghimire, C.P., Bruijnzeel, L.A., Lubczynski, M.W., Bonell, M., 2012. Rainfall interception by natural and planted forests in the Middle Mountains of Central Nepal. J. Hydrol. 475, 270–280. doi:10.1016/j.jhydrol.2012.09.051

Glen, P.E., Scott, R.L., Nguyen, U., Nagler, P.L., 2015. Wide-area ratios of evapotranspiration to precipitation in monsoon-dependent semiarid vegetation communities. J. of Arid Environ.117, 84–89. doi:10.1016/j.jaridenv.2015.02.010

Gosselin, D.C., Sridhar, V., Harvey, F.E., Goeke, J.W., 2006. Hydrological effects and groundwater fluctuations in interdunal environments in the Nebraska Sandhills. Gt. Plains Res. 16, 17–28.

Hargreaves, G.H., Allen, R.G., 2003. History and evaluation of Hargreaves evapotranspiration equation. J. Irrig. Drain. Eng. 129, 53–63. doi:10.1061/(ASCE)0733-9437(2003)129:1(53)

Haverkamp, R., Leij, F.J., Fuentes, C., Zatarain, F., Ross, P.J., Sciortino, A., Leij, F.J., Fuentes, C., Sciortino, A., Ross, P.J., 2005. Soil Water Retention: I. Introduction of a Shape Index. Soil Sci. Soc. Am. J. 69, 1881. doi:10.2136/sssaj2004.0225

Holmes, J.W., and Colville, J.S., 1970a. Grassland hydrology in a karstic region in South

Australia. J. Hydrol. 10, 38–58

Holmes, J.W., and Colville, J.S., 1970b. Forest hydrology in a karstic region in South Australia. J. Hydrol. 10, 59–74

Huang, T. and Pang, Z., 2011. Estimating groundwater recharge following land-use change using chloride mass balance of soil profiles: A case study at Guyuan and Xifeng in the Loess Plateau of China. Hydrogeol. J. 19, 177–186. doi:10.1007/s10040-010-0643-8

Huxman, T.E., Wilcox, B.P., Breshears, D.D., Scott, R.L., Snyder, K.A., Small, E.E., Hultine, K., Pockman, W.T., Jackson, R.B., 2005. Ecohydrological implications of woody plant encroachment, in: Ecology. pp. 308–319. doi:10.1890/03-0583

James, S.E., Pärtel, M., Wilson, S.D., Peltzer, D.A., 2003. Temporal heterogeneity of soil moisture in grassland and forest. J. Ecol. 91, 234–239. doi:10.1046/j.1365-2745.2003.00758.x

Kajiura, M., Etori, Y., Tange, T., 2012. Water condition control of in situ soil water repellency: An observational study from a hillslope in a Japanese humid-temperate forest. Hydrol. Process. 26, 3070–3078. doi:10.1002/hyp.8310

Kelliher, F.M., Leuning, R., Schulze, E.D., 1993. Evaporation and canopy characteristics of coniferous forests and grasslands. Oecologia. doi:10.1007/BF00323485

Laloy, E., Vrugt, J. a., 2012. High-dimensional posterior exploration of hydrologic models using multiple-try DREAM(ZS) and high-performance computing. Water Resour. Res. 48, 1–18. doi:10.1029/2011WR010608

Longobardi, P., Montenegro, A., Beltrami, H., Eby, M., 2016. Deforestation induced

climate change: Effects of spatial scale. PLoS One 11. doi:10.1371/journal.pone.0153357

Maupin, M. a, Barber, N.L., 2005. Estimated withdrawals from principal aquifers in the United States, 2000, US Geological Survey Circular 1279.

McMahon, P.B., Dennehy, K.F., Bruce, B.W., Böhlke, J.K., Michel, R.L., Gurdak, J.J., Hurlbut, D.B., 2006. Storage and transit time of chemicals in thick unsaturated zones under rangeland and irrigated cropland, High Plains, United States. Water Resour. Res. 42. doi:10.1029/2005WR004417

Mileham, L., Taylor, R., Thompson, J., Todd, M., Tindimugaya, C., 2008. Impact of rainfall distribution on the parameterisation of a soil-moisture balance model of groundwater recharge in equatorial Africa. J. Hydrol. 359, 46–58. doi:10.1016/j.jhydrol.2008.06.007

Moradkhani, H., Sorooshian, S., Gupta, H. V., Houser, P.R., 2005. Dual state-parameter estimation of hydrological models using ensemble Kalman filter. Adv. Water Resour. 28, 135–147. doi:10.1016/j.advwatres.2004.09.002

Mualem, Y., 1976. A new model for predicting the hydraulic conductivity of unsaturated porous media. Water Resour. Res. 12, 513–522. doi:10.1029/WR012i003p00513

Nasi, R., Wunder, S., Campos, J.J.A., 2002. Forest ecosystem services: can they pay our way out of deforestation? Fondo Glob. para el Medio Ambient. 1–11.

Nasta, P., Gates, J.B., 2013. Plot-scale modeling of soil water dynamics and impacts of drought conditions beneath rainfed maize in Eastern Nebraska. Agric. Water Manag. 128, 120–130. doi:10.1016/j.agwat.2013.06.021

Nasta, P., Romano, N., 2016. Use of a flux-based field capacity criterion to identify effective hydraulic parameters of layered soil profiles subjected to synthetic drainage experiments. , Water Resour. Res., 52, 566–584, doi:10.1002/ 2015WR016979.

Ochoa-Quintero, J.M., Gardner, T.A., Rosa, I., de Barros Ferraz, S.F., Sutherland, W.J., 2015. Thresholds of species loss in Amazonian deforestation frontier landscapes. Conserv. Biol. 29, 440–451. doi:10.1111/cobi.12446

Owens, M.K., Lyons, R.K., Alejandro, C.L., 2006. Rainfall partitioning within semiarid juniper communities: Effects of event size and canopy cover. Hydrol. Process. 20, 3179–3189. doi:10.1002/hyp.6326

Ozalp, M., Erdogan Yuksel, E., Yuksek, T., 2016. Soil Property Changes After Conversion from Forest to Pasture in Mount Sacinka, Artvin, Turkey. L. Degrad. Dev. 27, 1007–1017. doi:10.1002/ldr.2353

Ritchie, J.T., 1972. Model for predicting evaporation from a row crop with incomplete cover. Water Resour. Res. 8, 1204–1213. doi:10.1029/WR008i005p01204

Scanlon, B.R., Faunt, C.C., Longuevergne, L., Reedy, R.C., Alley, W.M., McGuire, V.L., McMahon, P.B., 2012a. Groundwater depletion and sustainability of irrigation in the US High Plains and Central Valley. Proc. Natl. Acad. Sci. 109, 9320–9325. doi:10.1073/pnas.1200311109

Scanlon, B.R., Faunt, C.C., Longuevergne, L., Reedy, R.C., Alley, W.M., McGuire, V.L., McMahon, P.B., 2012b. Groundwater depletion and sustainability of irrigation in the US High Plains and Central Valley. Proc. Natl. Acad. Sci. 109, 9320–9325.

doi:10.1073/pnas.1200311109

Scanlon, B.R., Jolly I., Sophocleous, M., Zhang, L. 2007. Global impacts of conversions from natural to agricultural ecosystems on water resources: quantity versus quality. Water Resour Res. 43,1–18.

Schilling, K.E., Jha, M.K., Zhang, Y.-K., Gassman, P.W., Wolter, C.F., 2008. Impact of land use and land cover change on the water balance of a large agricultural watershed: Historical effects and future directions. Water Resour. Res. 44, 1–12. doi:10.1029/2007WR006644

Sharma, M.L., Farrington, P, FERNIE, M., 1983. Localised groundwater recharge on the "Gnangara Mound", Western Australia. Int. Conf. on Groundwater and Man, Sydney, 5-9 December . Conf.

Sieg, C.H., Flather, C.H., McCanny, S., 1999. Recent biodiversity patterns in the great plains: Implications for restoration and management. Gt. Plains Res. 9, 277–313.

Simic, A., Fernandes, R., Wang, S., 2014. Assessing the impact of leaf area index on evapotranspiration and groundwater recharge across a shallow water region for diverse land cover and soil properties. Journal of Water Resource and Hydraulic Engineering 3, 60–73.

Spracklen, D. V., Garcia-Carreras, L., 2015. The impact of Amazonian deforestation on Amazon basin rainfall. Geophys. Res. Lett. 42, 9546–9552. doi:10.1002/2015GL066063

Starks, P.J., Venuto, B.C., Dugas, W.A., Kiniry, J., 2014. Measurements of canopy interception and transpiration of eastern redcedar grown in open environments.

Environment and Natural Resources Research 4, 103–122. doi:10.5539/enrr.v4n3p103

Stogsdili Jr., W.R., Wittwer, R.F., Hennessey, T.C., Dougherty, P.M., 1992. Water use in thinned loblolly pine plantations. Forest Ecol. and Manag. 50, 233–245. Doi:10.1016/0378-1127(92)90338-A

Szilagyi, J., Zlotnik, V.A., Gates, J.B., Jozsa, J., 2011. Mapping mean annual groundwater recharge in the Nebraska Sand Hills, USA. Hydrogeol. J. 19, 1503–1513. doi:10.1007/s10040-011-0769-3

Terrell, B.L., Johnson, P.N., Segarra, E., 2002. Ogallala aquifer depletion: Economic impact on the Texas high plains. Water Policy 4, 33–46. doi:10.1016/S1366-7017(02)00009-0

Valante, F., David, J.S., Gash, J.H.C., 1997. Modelling interception loss for two sparse eucalypt and pine forests in central Portugal using reformulated Rutter and Gash analytical models. J. Hydrol. 190, 141–162. doi:10.1016/S0022-1694(96)03066-1

van Genuchten, M.T., 1980. A Closed-form Equation for Predicting the Hydraulic Conductivity of Unsaturated Soils1. Soil Sci. Soc. Am. J. doi:10.2136/sssaj1980.03615995004400050002x

Vrugt, J.A., 2016. Markov chain Monte Carlo simulation using the DREAM software package: Theory, concepts, and MATLAB implementation. Environ. Model. Softw. 75, 273–316. doi:10.1016/j.envsoft.2015.08.013

Vrugt, J.A., ter Braak, C.J.F., Clark, M.P., Hyman, J.M., Robinson, B.A., 2008. Treatment of input uncertainty in hydrologic modeling: Doing hydrology backwards

with Markov chain Monte Carlo simulation. Water Resour. Res. 44, W00B09. doi:10.1029/2007WR006720

Vrugt, J. a., Bouten, W., Gupta, H. V., Hopmans, J.W., 2003. Toward Improved Identifiability of Soil Hydraulic Parameters: On the Selection of a Suitable Parametric Model. Vadose Zo. J. 2, 98–113. doi:10.2113/2.1.98

Wang, T., Franz, T.E., Yue, W., Szilagyi, J., Zlotnik, V.A., You, J., Chen, X., Shulski, M.D., Young, A., 2016. Feasibility analysis of using inverse modeling for estimating natural groundwater recharge from a large-scale soil moisture monitoring network. J. Hydrol. 533, 250–265. doi:10.1016/j.jhydrol.2015.12.019

Wöhling, T. and J.A. Vrugt, J.A., 2011. Multi-response multi-layer vadose zone model calibration using Markov chain Monte Carlo simulation and field water retention data, Water Resour. Res. 47, W04510, doi:10.1029/2010WR009265.

Yang, L., Wei, W., Chen, L., Mob, B., 2012. Response of deep soil moisture to land use and afforestation in the semi-arid Loess Plateau, China. Journal of Hydrology 475, 111–122.

Zhang, L., Dawes, W.R., Walker, G.R., 2001. Response of mean annual evapotranspiration to vegetation changes at catchment scale. Water Resour. Res. 37, 701–708. doi:10.1029/2000WR900325

CHAPTER 5

CONCLUSIONS AND RECOMMENDATIONS

Conclusions

The impact of land use change on groundwater recharge in the semi-arid Nebraska Sand Hills was assessed with various field and laboratory methods. The evaluation of the impact of land use change suggested that grassland conversion to forests has produced substantial reduction in groundwater recharge rates. The decrease in moisture content, increase in solute concentration, and reduction in recharge from plantations varied considerably amongst different types of vegetation and plantation density. Estimates indicate that recharge was reduced the most in the dense ponderosa pine and eastern red cedar plots relative to grassland. The method of assessment particularly in the solute mass balance, also produced considerable differences in recharge rates. For example, the sulfate mass balance recharge estimates were approximately 40% greater than the chloride mass balance estimates, except in the thinned pine plots where the two solute mass balance estimates were equivalent.

Recharge rate reductions were observed in the pine and eastern red cedar tree soil profiles compared to the grassland. However, field and laboratory explorations revealed that near-surface soils beneath the pine plots were substantially more hydrophobic than the surrounding grasslands, whereas no soil hydrophobicity was observed in the eastern red cedar soils. Thus, while hydrophobicity may have an impact on recharge rates beneath pine profiles, lower recharge rates beneath the dense cedar profile are likely associated with increased transpiration and leaf rainfall interception. Among the methods used to characterize soil hydrophobicity, the ^{1}H NMR analysis showed promise in identifying compounds that are hydrophobic and appeared to be the better tool to show slight differences between plots, whereas the WDPT method simply indicated the presence or absence of hydrophobicity. HYDRUS 1-D numerical simulations under the

assumption of severe soil hydrophobicity indicated that surface layer repellent conditions can affect the water budget by altering surface soil evaporation and reducing groundwater recharge rates.

Grassland conversions to forests have been documented to alter the physical (Roberts 2000) and chemical (Doerr et al. 2000) properties of the soil profile. Numerical modeling of land use change needs to incorporate land use driven changes in soil hydraulic properties. The results of inverse modeling and optimization of observed soil moisture contents beneath the native grassland and the dense pine profiles suggest that land use change affected soil hydraulic properties. Numerical modeling using the optimized effective soil hydraulic properties also indicate that trees have severely reduced estimated historical recharge rates relative to the native grassland in response to increased canopy cover, greater root extinction depth, and possibly plantation-induced surface soil hydrophobicity.

While uncertainties in this analysis; stemming from data limitations and assumptions in soil water transport processes, may have contributed to the drastic conclusion, the overall impact of land use change for the Sand Hills indicates a severe reduction in groundwater recharge. The magnitude of reduction requires the attentions of foresters and water resources managers, who will need to consider management actions such as identifying tree species that do not induce soil hydrophobicity, are less water intensive, and have lower canopy cover. Further, such reforestation efforts need to establish optimum plantation density and institute appropriate adaptive forest management activities, such as tree clearing and forest thinning. Strong and regular cooperation between foresters, water managers, and other stakeholders should be

maintained to prolong the vitality of the Nebraska Sand Hills grasslands, the forest, and the long term sustainability of the High Plains Aquifer and other similar regions around the world.

Recommendations

Assessment of groundwater recharge rate estimates in the Sand Hills

Recharge estimates in the Sand Hills are variable, with estimates of ~40 $mm \cdot yr^{-1}$ (Adane and Gates 2015; Szilagyi et al. 2003, Wang et al. 2015), 73 $mm \cdot yr^{-1}$ (Szilagyi et al. 2011), 100 $mm \cdot yr^{-1}$ (Adane et al. 2015, Crosbie et al. 2013; McMahon et al. 2006; Billesbach and Arkebauer 2012), and even 221 $mm \cdot yr^{-1}$ (Scanlon et al. 2012a; Scanlon et al. 2012b). The variability in these estimates results from several factors including large size of the Sand Hills, which spans over 50,000 km^2 of land (Loope and Swinehart, 2000 across large gradients in precipitation and temperature. Therefore, recharge rates from a part of the Sand Hills that receives 700 $mm \cdot yr^{-1}$ of precipitation will likely be greater and a larger percent of precipitation than areas with 400 $mm \cdot yr^{-1}$ annual precipitation. Hence, studies have to report and emphasize their results and conclusions in reference to the specific region of the Sand Hills, rather than providing average values for the entire Sand Hills. The variation in estimates is also in part due to the methods used in the recharge evaluation. For instance, in this study (chapter 2), the sulfate mass balance results produced recharge estimates that were more comparable to other studies than the chloride mass balance method. Therefore, it is very important to consider appropriate techniques to evaluate recharge and apply several methods when possible to establish a range of estimates. Uncertainties in recharge estimation are also due to data limitation and the

deployment of several assumptions to fill in data gaps. Long-term soil moisture observations with high temporal resolution, installation of lysimeters, piezometers, well observations, and eddy covariance systems can help reduce some of the uncertainties and obtain recharge estimates that are more reliable. Proper considerations also need to be given to the intrinsic uncertainties of any data, model simulations, and parameter and soil-water-transport assumptions used in recharge assessments. Numerical model simulations need to account for the impact of preferential flow where soil hydrophobicity, desiccated roots, and faults and cracks are present within the soil profile. Simplification of soil profile layers can also introduce further uncertainty, thus studies should consider finer discretization with the appropriate soil hydraulic properties for each later and hysteretic behavior.

Considerations to tree species and planting density

Cost benefit analysis of restoration efforts is imperative prior to implementing these afforestation programs. In areas where the programs are deemed important, it is critical to plant trees that have minimal adverse impacts on the environment, particularly on water resources. In the Nebraska National Forest, the primary reasons for selecting the existing tree species (i.e. ponderosa pine and eastern red cedar) included seedling survival and regeneration capacity of these trees, whereas their adverse impacts were not properly studied. A compromise between maintaining native vegetation and reforestation efforts can include deliberation over the optimal plantation density to mitigate adverse impacts. In this study (chapter two), the recharge estimates beneath dense pine was only ~20%, whereas the sparse pine plot was ~87% of the recharge rate relative to the native grassland. Tree species types with low soil hydrophobicity and minimal canopy cover

would also allow greater throughfall and infiltration, which would mitigate reduction in groundwater recharge rates. Identifying an ideal plantation density to accomplish the intended objective of the afforestation program while minimizing its ill effects will help sustain the forest and the surrounding native grassland and its ecological services.

Investigation of surface soil hydrophobicity

Whereas surface soil hydrophobicity has been well documented in many environmental settings (DeBano, 2000), the impact on water resources, particularly groundwater recharge, needs to be thoroughly investigated. Surface soil hydrophobicity can reduce infiltration rate, enhance surface runoff, and increase evaporation rates due to longer exposure to ambient temperatures and atmospheric demand (Buckzo et al., 2005). These processes can indirectly impact groundwater recharge. In this study, the presence and severity of soil hydrophobicity in the pine vegetation profiles was well characterized and an indirect link to reduced recharge is apparent. However, the direct impact of surface soil hydrophobicity to recharge requires more scrutiny with regard to plot level soil heterogeneity and the temporal dynamics of water repellency. Several samples within a single plot need to be analyzed to estimate the percentage of hydrophobic coverage, as pockets of non-repellent soils can allow considerable preferential flow, greater infiltration, and recharge rates that may not be observed through traditional recharge estimation methods. In addition, moisture above the critical water content degrades soil hydrophobicity (Dekker and Ritsema 1994), thus water repellency may not manifest itself or have an impact in rainy seasons and under wet soil conditions. This process is particularly complex in the semi-arid continental climate of the Nebraska Sand Hills, where spring and summer precipitation occur simultaneously with high ambient

temperatures. The numerical modeling used in this study (chapter 3) to assess impact of hydrophobicity on recharge, for example, assumed that repellency persists throughout the year (due to lack of data) when in fact the seasonal dynamics are not that clear cut. The spatial and temporal dynamics have to be painstakingly assessed in order to isolate the impact of soil hydrophobicity on recharge reduction. Further research is also needed in identifying and quantifying hydrophobic organic compounds and how they differ between plant species. Studies specifically designed to isolate the impact of hydrophobicity on the water budget, particularly recharge, would provide valuable information.

Evaluation of future climate change impact

The historical average decadal precipitation for the Nebraska National Forest near Halsey, Nebraska has increased from 53 cm in the 1950–1960 to 57 cm in the 1990–2000. The amount of precipitation, its intensity, seasonality, and precipitation patterns are projected to change in the Northern High Plains region (Bathke et al. 2014). In this study, grassland recharge rates mostly exceeded historical averages when the ratio of precipitation to evapotranspiration was greater than 20%. This threshold can also be used to analyze the impact of future climate variation on groundwater recharge rates in the grasslands. It is also critical to investigate if climate change provides any competitive advantage to either the native or the afforested vegetation and how that impacts water resources. For instance, projected increases in temperatures would make some C3 and C4 plants activate stomatal closures, which may reduce transpiration and allow for greater water flux down the soil profile.

Consideration for water managers in the Great Plains and worldwide

In the effort to mitigate increasing CO_2 emissions and the associated global climate change, many semi-arid grasslands have been identified as suitable for future forestation programs worldwide (Bond 2016). In addition to carbon sequestration, many places have also established similar programs for soil conservation and stabilization, manage microclimate and windbreak, and logging. This dissertation contains studies that provide conclusive evidence of the importance of the native grassland to water resources, particularly to groundwater systems in shallow aquifers. Therefore, the impact of these tree plantation efforts on water sustainability, particularly in semi-arid climates facing water scarcity concerns, must be thoroughly evaluated prior to converting grassland ecosystems and other native vegetation in favor trees.

References

Adane, Z.A., Nasta, P., and Gates, J.B., 2017. Links between soil hydrophobicity and groundwater recharge under plantations in a sandy grassland setting, Nebraska Sand Hills, USA. Forest Science. doi:10.5849/FS-2016-137

Bathke, D.J., Oglesby, R.J., Rowe, C.M., Wilhite, D.A., 2014. Understanding and Assessing Climate Change: Implications for Nebraska. University of Nebraska-Lincoln. pp. 1–70.

Billesbach, D.P., Arkebauer, T.J., 2012. First long-term, direct measurements of evapotranspiration and surface water balance in the Nebraska Sand Hills. Agric For Meteorol 156, 104–110. doi:10.1016/j.agrformet.2012.01.001

Bond, W. J., 2016. Ancient grasslands at risk. Science. 351, 120–122.

Buczko, U., Bens, O., Hüttl, R.F., 2005. Variability of soil water repellency in sandy forest soils with different stand structure under Scots pine (Pinus sylvestris) and beech (Fagus sylvatica). Geoderma. 126, 317–336.

Crosbie, R.S., Scanlon, B.R., Mpelasoka, F.S., Reedy, R.C., Gates, J.B., Zhang, L., 2013. Potential climate change effects on groundwater recharge in the High Plains Aquifer, USA. Water Resour. Res. 49, 3936–3951. doi:10.1002/wrcr.20292

DeBano, L.F., 2000. The role of fire and soil heating on water repellency in wildland environments: a review. J. Hydrol. 231, 195–206.

Dekker, L. W., Ritsema, C. J., 1994. How water moves in a water repellent sandy soil: 1. Potential and actual water repellency. Water Resour. Res. 30, 2507–2517 .

Doerr, S. H., and Thomas, A. D., 2000. The role of soil moisture in controlling water repellency: New evidence from forest soils in Portugal. J. Hydrol. 231, 134–147.

Loope, D.B., Swinehart, J.B., 2000. Thinking like a dune field: Geological history in the Nebraska Sand Hills. Gt. Plains Res. 10, 5–35.

McMahon, P.B., Dennehy, K.F., Bruce, B.W., Böhlke, J.K., Michel, R.L., Gurdak, J.J., Hurlbut, D.B., 2006. Storage and transit time of chemicals in thick unsaturated zones under rangeland and irrigated cropland, High Plains, United States. Water Resour. Res. 42. doi:10.1029/2005WR004417

Roberts, J., 2000. The influence of physical and physiological characteristics of vegetation on their hydrological response. Hydrol. Process. 14, 2885–2901.

Scanlon, B.R., Faunt, C.C., Longuevergne, L., Reedy, R.C., Alley, W.M., McGuire, V.L., McMahon, P.B., 2012a. Groundwater depletion and sustainability of irrigation in the

US High Plains and Central Valley. Proc. Natl. Acad. Sci. 109, 9320–9325. doi:10.1073/pnas.1200311109

Scanlon, B.R., Faunt, C.C., Longuevergne, L., Reedy, R.C., Alley, W.M., McGuire, V.L., McMahon, P.B., 2012b. Groundwater depletion and sustainability of irrigation in the US High Plains and Central Valley. Proc. Natl. Acad. Sci. 109, 9320–9325. doi:10.1073/pnas.1200311109

Scanlon, B.R., Jolly I., Sophocleous, M., Zhang, L. 2007. Global impacts of conversions from natural to agricultural ecosystems on water resources: quantity versus quality. Water Resour Res. 43,1–18.

Szilagyi, J., Harve, F., Ayers, J.F., 2011. Regional estimation of total recharge to ground water in Nebraska. Groundwater. 43, 63–69.

Szilagyi, J., Zlotnik, V.A., Gates, J.B., Jozsa, J., 2011. Mapping mean annual groundwater recharge in the Nebraska Sand Hills, USA. Hydrogeol. J. 19, 1503–1513. doi:10.1007/s10040-011-0769-3

Wang, T., Franz, T.E., Yue, W., Szilagyi, J., Zlotnik, V.A., You, J., Chen, X., Shulski, M.D., Young, A., 2016. Feasibility analysis of using inverse modeling for estimating natural groundwater recharge from a large-scale soil moisture monitoring network. J. Hydrol. 533, 250–265. doi:10.1016/j.jhydrol.2015.12.019

APPENDICES

APPENDIX 1

SUPPORTING INFORMATION FOR CHAPTER 2

Appendix 1.1 and 1.2 contain information on how chloride and sulfate mass balances were calculated for each of the 10 plot core profiles. The data input include soil moisture contents for each depth interval, porewater chloride and sulfate concentrations, assumed bulk density, estimated average precipitation from High Plains Regional Climate Center (HPRCC) for the 1988 to 2012 time period, and average solute concentration in precipitation and dry deposition from National Atmospheric Deposition Program (NADP).

Appendix 1.1 Chloride mass balance analysis

Profile: **G1**				Bulk Density	1.5		Calculations						density, precipitation and Cl(P)			
				Precipitation	487								are user defined on "graphs" worksheet			
				Cl in Precip	0.14		Water = Depth * (MC / 100) * soil density * 1000									
							Average Cl = Total Cl / Total Water = 1.857265 mg/L						Recharge	36.7099	mm/year	
							Time = Σ Cl / (Precipitation * Cl(P))						Total Time	20.2775	years	
	Raw data			Replace blanks in data with												
	Depth	Moisture Content	Lab Cl		0	0	Water	Σ Water	Total W	Cl	Σ Cl	Total Cl	Time	Date	1/Cl	Cum Cl
	(m)	(%)	(mg/L)		MC	Cl	(Kg/m2)	(Kg/m2)	(Kg/m2)	(mg/m2)	(mg/m2)	(mg/m2)	(years)			(mg cm2)
	0.1	6.2	11.1		5.9	11.1	11.0	11.0	744.4	121.8	121.8	1382.5	1.8	-1.8	0.1	0.0
	0.3	6.9	9.2		6.9	9.2	12.9	23.9	744.4	119.3	241.1	1382.5	3.5	-3.5	0.1	0.0
	0.4	6.9	5.2		7.0	5.2	13.0	36.9	744.4	68.3	309.5	1382.5	4.5	-4.5	0.2	0.0
	0.5	5.9	4.2		6.1	4.2	11.5	48.4	744.4	48.7	358.1	1382.5	5.3	-5.3	0.2	0.0
	0.6	6.6	6.5		6.6	6.5	12.4	60.8	744.4	80.5	438.6	1382.5	6.4	-6.4	0.2	0.0
	0.8	7.7	4.1		8.4	4.1	15.7	76.5	744.4	64.4	503.0	1382.5	7.4	-7.4	0.2	0.1
	0.9	12.3	2.3		12.0	2.3	22.4	99.0	744.4	51.3	554.3	1382.5	8.1	-8.1	0.4	0.1
	1.0	12.5	2.5		12.7	2.5	23.7	122.7	744.4	58.6	612.9	1382.5	9.0	-9.0	0.4	0.1
	1.3	13.4	1.4		13.7	1.4	51.5	174.2	744.4	71.6	684.5	1382.5	10.0	-10.0	0.7	0.1
	1.5	8.4	1.3		8.4	1.3	31.4	205.6	744.4	40.2	724.7	1382.5	10.6	-10.6	0.8	0.1
	1.8	11.8	1.4		12.7	1.4	47.7	253.3	744.4	64.6	789.4	1382.5	11.6	-11.6	0.7	0.1
	2.0	12.8	0.7		12.0	0.7	45.0	298.3	744.4	32.5	821.9	1382.5	12.1	-12.1	1.4	0.1
	2.3	6.9	1.5		6.7	1.5	25.2	323.4	744.4	36.9	858.8	1382.5	12.6	-12.6	0.7	0.1
	2.5	6.0	1.3		6.1	1.3	22.7	346.2	744.4	29.4	888.2	1382.5	13.0	-13.0	0.8	0.1
	2.8	5.2	2.0		5.8	2.0	21.8	367.9	744.4	44.4	932.7	1382.5	13.7	-13.7	0.5	0.1
	3.0	6.4	0.9		6.8	0.9	25.6	393.5	744.4	24.0	956.7	1382.5	14.0	-14.0	1.1	0.1
	3.5	6.7	1.4		5.4	1.4	40.8	434.3	744.4	58.0	1014.7	1382.5	14.9	-14.9	0.7	0.1
	4.0	6.0	1.5		6.1	1.5	46.0	480.3	744.4	70.8	1085.5	1382.5	15.9	-15.9	0.6	0.1
	4.5	5.9	1.1		5.7	1.1	42.6	522.9	744.4	47.0	1132.5	1382.5	16.6	-16.6	0.9	0.1
	5.0	5.8	1.2		5.8	1.2	43.5	566.4	744.4	51.7	1184.2	1382.5	17.4	-17.4	0.8	0.1
	5.5	9.4	1.1		9.2	1.1	69.0	635.4	744.4	78.9	1263.1	1382.5	18.5	-18.5	0.9	0.1
	6.0	15.2	1.1		14.5	1.1	109.0	744.4	744.4	119.4	1382.5	1382.5	20.3	-20.3	0.9	0.1

Profile:	**G2**				Bulk Density	1.5			Calculations							density, precipitation and Cl(P)		
					Precipitation	487										are user defined on "graphs" worksheet		
					Cl in Precip	0.14			Water = Depth * (MC / 100) * soil density * 1000									
									Average Cl = Total Cl / Total Water = 4.132832 mg/L							Recharge	16.497163	mm/year
	Raw data				Replace blanks in data with											Time = Σ Cl / (Precipitation * Cl(P))		
					0	0										Total Time	56.148224	years
	Depth	Moisture Content	Lab Cl				Water	Σ Water	Total W	Cl	Σ Cl	Total Cl	Time					
	(m)	(%)	(mg/L)		MC	Cl	(Kg/m2)	(Kg/m2)	(Kg/m2)	(mg/m2)	(mg/m2)	(mg/m2)	(years)	Date	1/Cl	Cum Cl		
																(mg cm2)		
	0.1	11.2	1.0		11.2	1.0	20.9	20.9	926.3	21.1	21.1	3828.2	0.3	-0.3	1.0	0.0		
	0.3	12.0	2.2		12.0	2.2	22.6	43.5	926.3	48.6	69.7	3828.2	1.0	-1.0	0.5	0.0		
	0.4	11.2	1.4		11.2	1.4	21.1	64.6	926.3	28.4	98.1	3828.2	1.4	-1.4	0.7	0.0		
	0.5	11.7	2.4		11.7	2.4	21.9	86.5	926.3	53.0	151.2	3828.2	2.2	-2.2	0.4	0.0		
	0.6	14.1	1.3		14.1	1.3	26.5	113.0	926.3	34.9	186.0	3828.2	2.7	-2.7	0.8	0.0		
	0.8	15.6	3.0		15.6	3.0	29.2	142.1	926.3	86.2	272.2	3828.2	4.0	-4.0	0.3	0.0		
	0.9	14.7	0.3		14.7	0.3	27.6	169.7	926.3	8.5	280.8	3828.2	4.1	-4.1	3.2	0.0		
	1.0	16.1	4.2		16.1	4.2	30.3	200.0	926.3	128.1	408.8	3828.2	6.0	-6.0	0.2	0.0		
	1.3	14.6	0.3		14.6	0.3	54.7	254.7	926.3	17.1	426.0	3828.2	6.2	-6.2	3.2	0.0		
	1.5	14.3	5.1		14.3	5.1	53.5	308.2	926.3	273.2	699.1	3828.2	10.3	-10.3	0.2	0.1		
	1.8	8.6	6.6		8.6	6.6	32.3	340.4	926.3	213.2	912.3	3828.2	13.4	-13.4	0.2	0.1		
	2.0	7.0	11.5		7.0	11.5	26.1	366.5	926.3	301.3	1213.6	3828.2	17.8	-17.8	0.1	0.1		
	2.3	6.3	8.5		6.3	8.5	23.5	390.1	926.3	198.9	1412.5	3828.2	20.7	-20.7	0.1	0.1		
	2.5	7.3	5.9		7.3	5.9	27.5	417.5	926.3	162.5	1575.0	3828.2	23.1	-23.1	0.2	0.2		
	2.8	7.7	0.7		7.7	0.7	28.8	446.3	926.3	19.1	1594.1	3828.2	23.4	-23.4	1.5	0.2		
	3.0	9.8	3.1		9.8	3.1	36.6	483.0	926.3	113.6	1707.8	3828.2	25.0	-25.0	0.3	0.2		
	3.5	8.5	5.6		8.5	5.6	63.9	546.8	926.3	355.1	2062.9	3828.2	30.3	-30.3	0.2	0.2		
	4.0	13.0	3.2		13.0	3.2	97.2	644.0	926.3	308.6	2371.4	3828.2	34.8	-34.8	0.3	0.2		
	4.5	10.5	3.0		10.5	3.0	78.8	722.8	926.3	233.3	2604.7	3828.2	38.2	-38.2	0.3	0.3		
	5.0	10.1	4.4		10.1	4.4	75.5	798.3	926.3	331.8	2936.5	3828.2	43.1	-43.1	0.2	0.3		
	5.5	7.4	8.2		7.4	8.2	55.4	853.7	926.3	453.0	3389.5	3828.2	49.7	-49.7	0.1	0.3		
	6.0	9.7	6.0		9.7	6.0	72.6	926.3	926.3	438.6	3828.2	3828.2	56.1	-56.1	0.2	0.4		

Profile:	**PS1**			Bulk Density	1.5			Calculations							density, precipitation and Cl(P)			
				Precipitation	487										are user defined on "graphs" worksheet			
				Cl in Precip	0.14			Water = Depth * (MC / 100) * soil density * 1000										
								Average Cl = Total Cl / Total Water = 3.18458 mg/L							Recharge	21.40942	mm/year	
								Time = Σ Cl / (Precipitation * Cl(P))							Total Time	26.10582	years	
	Raw data				Replace blanks in data with													
	Depth	Moisture Content	Lab Cl		0	0		Water	Σ Water	Total W	Cl	Σ Cl	Total Cl		Time	Date	1/Cl	Cum Cl
	(m)	(%)	(mg/L)		MC	Cl		(Kg/m2)	(Kg/m2)	(Kg/m2)	(mg/m2)	(mg/m2)	(mg/m2)		(years)			(mg cm2)
	0.1	6.7			4.6	9.3		8.5	8.5	558.9	79.6	79.6	1779.9		1.2	-1.2	0.1	0.0
	0.3	4.4			4.6	10.2		8.7	17.2	558.9	88.2	167.9	1779.9		2.5	-2.5	0.1	0.0
	0.4	4.1			3.5	9.9		6.5	23.7	558.9	64.8	232.7	1779.9		3.4	-3.4	0.1	0.0
	0.5	3.8			4.3	7.4		8.0	31.8	558.9	59.6	292.3	1779.9		4.3	-4.3	0.1	0.0
	0.6	3.8			3.6	5.2		6.8	38.5	558.9	35.5	327.8	1779.9		4.8	-4.8	0.2	0.0
	0.8	4.0			3.0	7.5		5.7	44.2	558.9	42.2	369.9	1779.9		5.4	-5.4	0.1	0.0
	0.9	4.8			4.4	7.7		8.2	52.4	558.9	63.2	433.1	1779.9		6.4	-6.4	0.1	0.0
	1.0	6.4			6.3	3.1		11.8	64.2	558.9	36.6	469.7	1779.9		6.9	-6.9	0.3	0.0
	1.3	2.9			4.7	4.3		17.6	81.8	558.9	75.4	545.1	1779.9		8.0	-8.0	0.2	0.1
	1.5	4.7			5.9	3.7		21.9	103.7	558.9	82.3	627.4	1779.9		9.2	-9.2	0.3	0.1
	1.8	3.6			7.1	2.6		26.5	130.2	558.9	69.1	696.4	1779.9		10.2	-10.2	0.4	0.1
	2.0	7.7			9.6	3.4		36.1	166.3	558.9	124.3	820.8	1779.9		12.0	-12.0	0.3	0.1
	2.3	10.6			10.2	2.9		38.2	204.6	558.9	111.3	932.1	1779.9		13.7	-13.7	0.3	0.1
	2.5	1.8			14.2	3.0		53.4	257.9	558.9	158.3	1090.4	1779.9		16.0	-16.0	0.3	0.1
	2.8	3.2			4.9	2.3		18.5	276.5	558.9	43.0	1133.4	1779.9		16.6	-16.6	0.4	0.1
	3.0	2.9			3.5	4.3		13.3	289.8	558.9	56.5	1189.9	1779.9		17.5	-17.5	0.2	0.1
	3.5	3.6			4.4	2.7		32.8	322.6	558.9	88.3	1278.2	1779.9		18.7	-18.7	0.4	0.1
	4.0	4.0			3.8	3.1		28.7	351.3	558.9	88.0	1366.2	1779.9		20.0	-20.0	0.3	0.1
	4.5	4.7			9.2	1.4		68.7	419.9	558.9	98.2	1464.4	1779.9		21.5	-21.5	0.7	0.1
	5.0	3.7			6.1	2.5		45.8	465.7	558.9	113.5	1578.0	1779.9		23.1	-23.1	0.4	0.2
	5.5	3.5			5.7	2.1		43.0	508.7	558.9	92.0	1670.0	1779.9		24.5	-24.5	0.5	0.2
	6.0	6.3			6.7	2.2		50.2	558.9	558.9	109.9	1779.9	1779.9		26.1	-26.1	0.5	0.2

Profile:	**PS2**			Bulk Density	1.5		Calculations						density, precipitation and Cl(P)			
				Precipitation	487								are user defined on "graphs" worksheet			
				Cl in Precip	0.14		Water	= Depth * (MC / 100) * soil density * 1000								
							Average Cl	= Total Cl / Total Water =	4.512116	mg/L			Recharge	15.11043	mm/year	
							Time	= Σ Cl / (Precipitation * Cl(P))					Total Time	32.70051	years	
	Raw data			Replace blanks in data with												
	Depth	Moisture Content	Lab Cl		0	0	Water	Σ Water	Total W	Cl	Σ Cl	Total Cl	Time	Date	1/Cl	Cum Cl
	(m)	(%)	(mg/L)		MC	Cl	(Kg/m2)	(Kg/m2)	(Kg/m2)	(mg/m2)	(mg/m2)	(mg/m2)	(years)			(mg cm2)
	0.1	3.4	30.3		3.6	30.3	6.7	6.7	494.1	203.9	203.9	2229.5	3.0	-3.0	0.0	0.0
	0.3	4.4	3.9		4.6	3.9	8.7	15.4	494.1	34.0	237.8	2229.5	3.5	-3.5	0.3	0.0
	0.4	5.9	1.4		5.8	1.4	10.9	26.3	494.1	15.7	253.5	2229.5	3.7	-3.7	0.7	0.0
	0.5	6.8	2.3		6.2	2.3	11.6	37.9	494.1	26.8	280.4	2229.5	4.1	-4.1	0.4	0.0
	0.6	4.0	1.7		4.4	1.7	8.3	46.2	494.1	13.7	294.0	2229.5	4.3	-4.3	0.6	0.0
	0.8	5.3	0.8		5.2	0.8	9.7	55.9	494.1	7.6	301.6	2229.5	4.4	-4.4	1.3	0.0
	0.9	7.3	1.5		5.4	1.5	10.1	66.1	494.1	15.6	317.2	2229.5	4.7	-4.7	0.6	0.0
	1.0	5.0	4.4		6.5	4.4	12.2	78.3	494.1	53.8	371.0	2229.5	5.4	-5.4	0.2	0.0
	1.3	10.5	0.8		5.1	0.8	19.1	97.4	494.1	16.2	387.2	2229.5	5.7	-5.7	1.2	0.0
	1.5	6.2	1.4		6.1	1.4	22.8	120.1	494.1	32.2	419.4	2229.5	6.2	-6.2	0.7	0.0
	1.8	7.2	4.0		7.1	4.0	26.7	146.9	494.1	106.3	525.7	2229.5	7.7	-7.7	0.3	0.1
	2.0	7.3	3.7		6.7	3.7	25.2	172.1	494.1	92.9	618.6	2229.5	9.1	-9.1	0.3	0.1
	2.3	8.7	2.6		6.0	2.6	22.5	194.6	494.1	58.7	677.3	2229.5	9.9	-9.9	0.4	0.1
	2.5	7.7	5.2		7.3	5.2	27.4	221.9	494.1	142.6	820.0	2229.5	12.0	-12.0	0.2	0.1
	2.8	6.7	3.5		5.9	3.5	22.2	244.2	494.1	78.9	898.8	2229.5	13.2	-13.2	0.3	0.1
	3.0	6.3	3.3		6.2	3.3	23.2	267.3	494.1	75.7	974.6	2229.5	14.3	-14.3	0.3	0.1
	3.5	4.9	7.2		5.3	7.2	39.7	307.0	494.1	287.5	1262.1	2229.5	18.5	-18.5	0.1	0.1
	4.0	5.8	9.1		5.3	9.1	39.8	346.8	494.1	361.5	1623.6	2229.5	23.8	-23.8	0.1	0.2
	4.5	2.3	1.3		6.0	1.3	44.7	391.5	494.1	58.4	1682.0	2229.5	24.7	-24.7	0.8	0.2
	5.0	2.5	5.3		6.4	5.3	48.1	439.6	494.1	256.4	1938.4	2229.5	28.4	-28.4	0.2	0.2
	5.5	4.3	6.0		3.3	6.0	25.0	464.6	494.1	148.8	2087.3	2229.5	30.6	-30.6	0.2	0.2
	6.0	3.4	4.8		3.9	4.8	29.5	494.1	494.1	142.2	2229.5	2229.5	32.7	-32.7	0.2	0.2

Profile:	**TP1**			Bulk Density	1.5		Calculations						density, precipitation and Cl(P)			
				Precipitation	487								are user defined on "graphs" worksheet			
				Cl in Precip	0.14		Water = Depth * (MC / 100) * soil density * 1000									
							Average Cl = Total Cl / Total Water = 8.452789 mg/L						Recharge	8.065977	mm/year	
							Time = Σ Cl / (Precipitation * Cl(P))						Total Time	28.20555	years	
	Raw data			Replace blanks in data with												
	Depth	Moisture Content	Lab Cl		0	0	Water	Σ Water	Total W	Cl	Σ Cl	Total Cl	Time	Date	1/Cl	Cum Cl
	(m)	(%)	(mg/L)		MC	Cl	(Kg/m2)	(Kg/m2)	(Kg/m2)	(mg/m2)	(mg/m2)	(mg/m2)	(years)			(mg cm2)
	0.1	4.5	9.3		4.7	9.3	8.8	8.8	227.5	81.9	81.9	1923.1	1.2	-1.2	0.1	0.0
	0.3	4.1	15.0		4.3	15.0	8.0	16.8	227.5	120.6	202.4	1923.1	3.0	-3.0	0.1	0.0
	0.4	3.9	11.0		3.9	11.0	7.3	24.1	227.5	80.2	282.6	1923.1	4.1	-4.1	0.1	0.0
	0.5	2.6	19.8		2.8	19.8	5.3	29.4	227.5	104.8	387.4	1923.1	5.7	-5.7	0.1	0.0
	0.6	3.1	9.8		3.4	9.8	6.4	35.8	227.5	62.6	450.0	1923.1	6.6	-6.6	0.1	0.0
	0.8	3.3	18.0		2.7	18.0	5.1	41.0	227.5	92.2	542.2	1923.1	8.0	-8.0	0.1	0.1
	0.9	2.5	9.7		2.5	9.7	4.6	45.6	227.5	45.0	587.2	1923.1	8.6	-8.6	0.1	0.1
	1.0	2.0	18.3		1.3	18.3	2.5	48.0	227.5	45.0	632.2	1923.1	9.3	-9.3	0.1	0.1
	1.3	2.7	7.8		2.0	7.8	7.3	55.4	227.5	57.4	689.6	1923.1	10.1	-10.1	0.1	0.1
	1.5	2.2	7.2		2.0	7.2	7.3	62.7	227.5	53.1	742.7	1923.1	10.9	-10.9	0.1	0.1
	1.8	2.1	5.6		2.2	5.6	8.3	71.1	227.5	46.7	789.4	1923.1	11.6	-11.6	0.2	0.1
	2.0	1.6	9.0		1.2	9.0	4.6	75.7	227.5	41.3	830.7	1923.1	12.2	-12.2	0.1	0.1
	2.3	1.5	6.9		1.5	6.9	5.8	81.5	227.5	40.1	870.8	1923.1	12.8	-12.8	0.1	0.1
	2.5	1.6	8.1		2.0	8.1	7.3	88.8	227.5	59.0	929.8	1923.1	13.6	-13.6	0.1	0.1
	2.8	1.9	8.0		1.5	8.0	5.7	94.5	227.5	45.9	975.7	1923.1	14.3	-14.3	0.1	0.1
	3.0	2.7	8.2		3.1	8.2	11.8	106.3	227.5	97.1	1072.7	1923.1	15.7	-15.7	0.1	0.1
	3.5	2.5	11.0		2.6	11.0	19.2	125.4	227.5	210.6	1283.3	1923.1	18.8	-18.8	0.1	0.1
	4.0	2.6	5.7		2.5	5.7	18.7	144.2	227.5	107.5	1390.8	1923.1	20.4	-20.4	0.2	0.1
	4.5	3.0	4.8		2.9	4.8	22.1	166.3	227.5	105.4	1496.2	1923.1	21.9	-21.9	0.2	0.1
	5.0	2.0	3.9		2.5	3.9	19.0	185.2	227.5	73.4	1569.6	1923.1	23.0	-23.0	0.3	0.2
	5.5	1.7	11.3		1.8	11.3	13.3	198.5	227.5	150.8	1720.4	1923.1	25.2	-25.2	0.1	0.2
	6.0	2.9	7.0		3.9	7.0	29.0	227.5	227.5	202.6	1923.1	1923.1	28.2	-28.2	0.1	0.2

Profile:	**TP2**			Bulk Density	1.5		Calculations						density, precipitation and Cl(P)			
				Precipitation	487								are user defined on "graphs" worksheet			
				Cl in Precip	0.14		Water = Depth * (MC / 100) * soil density * 1000									
							Average Cl = Total Cl / Total Water = 5.791027 mg/L						Recharge	11.77339	mm/year	
							Time = Σ Cl / (Precipitation * Cl(P))						Total Time	34.69683	years	
	Raw data			Replace blanks in data with												
	Depth	Moisture Content	Lab Cl		0	0	Water	Σ Water	Total W	Cl	Σ Cl	Total Cl	Time	Date	1/Cl	Cum Cl
	(m)	(%)	(mg/L)		MC	Cl	(Kg/m2)	(Kg/m2)	(Kg/m2)	(mg/m2)	(mg/m2)	(mg/m2)	(years)			(mg cm2)
	0.1	11.1	26.8		8.6	26.8	16.1	16.1	408.5	432.1	432.1	2365.6	6.3	-6.3	0.0	0.0
	0.3	4.3	20.0		4.3	20.0	8.0	24.1	408.5	160.3	592.3	2365.6	8.7	-8.7	0.1	0.1
	0.4	3.1	16.0		7.4	16.0	13.9	38.0	408.5	221.4	813.7	2365.6	11.9	-11.9	0.1	0.1
	0.5	3.3	9.3		7.6	9.3	14.3	52.3	408.5	133.1	946.8	2365.6	13.9	-13.9	0.1	0.1
	0.6	4.0	0.8		4.7	0.8	8.7	61.0	408.5	6.6	953.4	2365.6	14.0	-14.0	1.3	0.1
	0.8	4.3	6.3		5.0	6.3	9.4	70.4	408.5	58.9	1012.3	2365.6	14.8	-14.8	0.2	0.1
	0.9	5.9	1.4		5.7	1.4	10.7	81.1	408.5	14.4	1026.7	2365.6	15.1	-15.1	0.7	0.1
	1.0	4.8	1.9		4.5	1.9	8.5	89.6	408.5	16.1	1042.8	2365.6	15.3	-15.3	0.5	0.1
	1.3	4.1	1.9		3.9	1.9	14.7	104.3	408.5	28.5	1071.3	2365.6	15.7	-15.7	0.5	0.1
	1.5	4.1	2.3		4.1	2.3	15.5	119.8	408.5	35.8	1107.2	2365.6	16.2	-16.2	0.4	0.1
	1.8	4.0	6.4		3.3	6.4	12.5	132.3	408.5	80.7	1187.8	2365.6	17.4	-17.4	0.2	0.1
	2.0	7.3	3.6		5.8	3.6	21.7	154.0	408.5	77.4	1265.3	2365.6	18.6	-18.6	0.3	0.1
	2.3	4.8	5.3		4.1	5.3	15.4	169.4	408.5	82.1	1347.4	2365.6	19.8	-19.8	0.2	0.1
	2.5	6.5	2.7		5.6	2.7	21.1	190.6	408.5	57.9	1405.2	2365.6	20.6	-20.6	0.4	0.1
	2.8	6.1	2.4		5.7	2.4	21.4	212.0	408.5	52.4	1457.6	2365.6	21.4	-21.4	0.4	0.1
	3.0	4.2	4.6		4.5	4.6	16.8	228.8	408.5	78.1	1535.8	2365.6	22.5	-22.5	0.2	0.2
	3.5	3.8	3.3		4.6	3.3	34.3	263.1	408.5	114.6	1650.3	2365.6	24.2	-24.2	0.3	0.2
	4.0	3.2	6.5		2.9	6.5	21.9	285.0	408.5	142.2	1792.5	2365.6	26.3	-26.3	0.2	0.2
	4.5	3.2	5.4		3.5	5.4	26.5	311.6	408.5	144.5	1937.1	2365.6	28.4	-28.4	0.2	0.2
	5.0	5.7	4.6		5.5	4.6	40.9	352.5	408.5	189.8	2126.9	2365.6	31.2	-31.2	0.2	0.2
	5.5	4.2	6.4		3.3	6.4	25.1	377.6	408.5	160.0	2286.9	2365.6	33.5	-33.5	0.2	0.2
	6.0	5.2	2.5		4.1	2.5	30.9	408.5	408.5	78.8	2365.6	2365.6	34.7	-34.7	0.4	0.2

Profile:	**DP1**			Bulk Density	1.5			Calculations						density, precipitation and Cl(P)			
				Precipitation	487									are user defined on "graphs" worksheet			
				Cl in Precip	0.14			Water = Depth * (MC / 100) * soil density * 1000									
								Average Cl = Total Cl / Total Water = 9.434218 mg/L						Recharge	7.226884	mm/year	
								Time = Σ Cl / (Precipitation * Cl(P))						Total Time	50.29064	years	
	Raw data			Replace blanks in data with													
	Depth	Moisture Content	Lab Cl		0	0		Water	Σ Water	Total W	Cl	Σ Cl	Total Cl	Time	Date	1/Cl	Cum Cl
	(m)	(%)	(mg/L)		MC	Cl		(Kg/m2)	(Kg/m2)	(Kg/m2)	(mg/m2)	(mg/m2)	(mg/m2)	(years)			(mg cm2)
	0.1	16.0	20.5		16.0	20.5		30.1	30.1	363.4	616.6	616.6	3428.8	9.0	-9.0	0.0	0.1
	0.3	5.1	12.6		5.1	12.6		9.6	39.6	363.4	120.0	736.7	3428.8	10.8	-10.8	0.1	0.1
	0.4	5.8	13.8		5.8	13.8		10.9	50.5	363.4	150.5	887.1	3428.8	13.0	-13.0	0.1	0.1
	0.5	5.9	16.7		5.9	16.7		11.0	61.5	363.4	184.1	1071.2	3428.8	15.7	-15.7	0.1	0.1
	0.6	5.7	4.4		5.7	4.4		10.7	72.3	363.4	47.0	1118.2	3428.8	16.4	-16.4	0.2	0.1
	0.8	5.3	6.4		5.3	6.4		9.9	82.2	363.4	63.0	1181.2	3428.8	17.3	-17.3	0.2	0.1
	0.9	4.7	8.2		4.7	8.2		8.9	91.0	363.4	72.9	1254.2	3428.8	18.4	-18.4	0.1	0.1
	1.0	4.7	9.3		4.7	9.3		8.8	99.8	363.4	81.8	1336.0	3428.8	19.6	-19.6	0.1	0.1
	1.3	3.2	14.6		3.2	14.6		12.1	111.9	363.4	177.1	1513.1	3428.8	22.2	-22.2	0.1	0.2
	1.5	1.5	20.5		1.5	20.5		5.6	117.5	363.4	114.6	1627.7	3428.8	23.9	-23.9	0.0	0.2
	1.8	5.4	2.3		5.4	2.3		20.4	137.9	363.4	47.6	1675.3	3428.8	24.6	-24.6	0.4	0.2
	2.0	1.9	24.0		1.9	24.0		6.9	144.9	363.4	166.6	1841.8	3428.8	27.0	-27.0	0.0	0.2
	2.3	1.6	7.3		1.6	7.3		6.0	150.8	363.4	43.7	1885.5	3428.8	27.7	-27.7	0.1	0.2
	2.5	3.1	2.3		3.1	2.3		11.6	162.4	363.4	26.9	1912.4	3428.8	28.0	-28.0	0.4	0.2
	2.8	2.8	2.6		2.8	2.6		10.4	172.8	363.4	26.8	1939.1	3428.8	28.4	-28.4	0.4	0.2
	3.0	2.7	3.6		2.7	3.6		10.0	182.8	363.4	35.6	1974.8	3428.8	29.0	-29.0	0.3	0.2
	3.5	4.4	1.8		4.4	1.8		33.1	215.9	363.4	58.9	2033.6	3428.8	29.8	-29.8	0.6	0.2
	4.0	2.2	4.6		2.2	4.6		16.4	232.3	363.4	75.8	2109.4	3428.8	30.9	-30.9	0.2	0.2
	4.5	3.8	13.8		3.8	13.8		28.4	260.7	363.4	392.6	2502.1	3428.8	36.7	-36.7	0.1	0.3
	5.0	4.1	13.5		4.1	13.5		30.8	291.6	363.4	416.2	2918.3	3428.8	42.8	-42.8	0.1	0.3
	5.5	4.4	7.9		4.4	7.9		33.2	324.7	363.4	261.2	3179.5	3428.8	46.6	-46.6	0.1	0.3
	6.0	5.2	6.4		5.2	6.4		38.7	363.4	363.4	249.3	3428.8	3428.8	50.3	-50.3	0.2	0.3

Profile:	**DP2**			Bulk Density	1.5		Calculations						density, precipitation and Cl(P)			
				Precipitation	487								are user defined on "graphs" worksheet			
				Cl in Precip	0.14		Water = Depth * (MC / 100) * soil density * 1000									
							Average Cl = Total Cl / Total Water = 6.789035 mg/L						Recharge	10.04266	mm/year	
							Time = Σ Cl / (Precipitation * Cl(P))						Total Time	47.91051	years	
	Raw data			Replace blanks in data with												
	Depth	Moisture Content	Lab Cl		0	0	Water	Σ Water	Total W	Cl	Σ Cl	Total Cl	Time	Date	1/Cl	Cum Cl
	(m)	(%)	(mg/L)		MC	Cl	(Kg/m2)	(Kg/m2)	(Kg/m2)	(mg/m2)	(mg/m2)	(mg/m2)	(years)			(mg cm2)
	0.1	5.8	3.2		9.0	3.2	17.0	17.0	481.1	54.6	54.6	3266.5	0.8	-0.8	0.3	0.0
	0.3	5.3	3.4		4.9	3.4	9.3	26.2	481.1	31.8	86.5	3266.5	1.3	-1.3	0.3	0.0
	0.4	5.0	14.7		5.3	14.7	10.0	36.2	481.1	146.9	233.3	3266.5	3.4	-3.4	0.1	0.0
	0.5	5.6	2.6		5.4	2.6	10.2	46.3	481.1	26.3	259.6	3266.5	3.8	-3.8	0.4	0.0
	0.6	6.6	3.1		7.6	3.1	14.2	60.5	481.1	44.1	303.7	3266.5	4.5	-4.5	0.3	0.0
	0.8	7.3	4.9		7.2	4.9	13.5	74.0	481.1	65.4	369.0	3266.5	5.4	-5.4	0.2	0.0
	0.9	9.0	3.7		12.0	3.7	22.5	96.5	481.1	83.5	452.5	3266.5	6.6	-6.6	0.3	0.0
	1.0	6.9	4.6		7.5	4.6	14.1	110.6	481.1	64.9	517.4	3266.5	7.6	-7.6	0.2	0.1
	1.3	7.6	2.0		8.2	2.0	30.6	141.3	481.1	60.7	578.1	3266.5	8.5	-8.5	0.5	0.1
	1.5	9.1	4.4		8.2	4.4	30.6	171.9	481.1	134.9	713.0	3266.5	10.5	-10.5	0.2	0.1
	1.8	7.2	2.9		7.5	2.9	28.0	199.9	481.1	81.3	794.3	3266.5	11.6	-11.6	0.3	0.1
	2.0	6.3	1.7		9.1	1.7	34.0	233.9	481.1	59.2	853.5	3266.5	12.5	-12.5	0.6	0.1
	2.3	7.2	3.3		8.4	3.3	31.6	265.5	481.1	104.2	957.8	3266.5	14.0	-14.0	0.3	0.1
	2.5	3.8	4.1		8.1	4.1	30.4	296.0	481.1	125.9	1083.6	3266.5	15.9	-15.9	0.2	0.1
	2.8	2.6	16.0		3.4	16.0	12.9	308.9	481.1	207.2	1290.8	3266.5	18.9	-18.9	0.1	0.1
	3.0	0.2	5.2		3.2	5.2	12.2	321.0	481.1	63.0	1353.8	3266.5	19.9	-19.9	0.2	0.1
	3.5	0.9	10.7		3.6	10.7	27.0	348.1	481.1	288.6	1642.4	3266.5	24.1	-24.1	0.1	0.2
	4.0	3.9	9.9		3.8	9.9	28.7	376.7	481.1	284.3	1926.7	3266.5	28.3	-28.3	0.1	0.2
	4.5	1.7	14.9		3.4	14.9	25.2	401.9	481.1	374.5	2301.1	3266.5	33.8	-33.8	0.1	0.2
	5.0	3.2	12.7		3.7	12.7	27.5	429.4	481.1	348.7	2649.8	3266.5	38.9	-38.9	0.1	0.3
	5.5	2.1	11.4		3.8	11.4	28.7	458.1	481.1	326.4	2976.2	3266.5	43.7	-43.7	0.1	0.3
	6.0	3.4	12.6		3.1	12.6	23.1	481.1	481.1	290.4	3266.5	3266.5	47.9	-47.9	0.1	0.3

Profile:	**SV**			Bulk Density	1.5		Calculations						density, precipitation and Cl(P)			
				Precipitation	487								are user defined on "graphs" worksheet			
				Cl in Precip	0.14		Water = Depth * (MC / 100) * soil density * 1000									
							Average Cl = Total Cl / Total Water = 2.1099 mg/L						Recharge	32.31433	mm/year	
							Time = Σ Cl / (Precipitation * Cl(P))						Total Time	27.88212	years	
	Raw data			Replace blanks in data with												
	Depth	Moisture Content	Lab Cl		0	0	Water	Σ Water	Total W	Cl	Σ Cl	Total Cl	Time	Date	1/Cl	Cum Cl
	(m)	(%)	(mg/L)		MC	Cl	(Kg/m2)	(Kg/m2)	(Kg/m2)	(mg/m2)	(mg/m2)	(mg/m2)	(years)			(mg cm2)
	0.1	4.3	10.3		4.3	10.3	8.0	8.0	901.0	82.5	82.5	1901.0	1.2	-1.2	0.1	0.0
	0.3	5.6	6.1		5.6	6.1	10.6	18.6	901.0	64.9	147.4	1901.0	2.2	-2.2	0.2	0.0
	0.4	5.3	0.8		5.3	0.8	10.0	28.6	901.0	8.0	155.4	1901.0	2.3	-2.3	1.3	0.0
	0.5	6.1	2.9		6.1	2.9	11.5	40.1	901.0	33.0	188.3	1901.0	2.8	-2.8	0.3	0.0
	0.6	6.7	0.7		6.7	0.7	12.5	52.6	901.0	8.9	197.2	1901.0	2.9	-2.9	1.4	0.0
	0.8	8.1	3.7		8.1	3.7	15.1	67.7	901.0	55.5	252.8	1901.0	3.7	-3.7	0.3	0.0
	0.9	3.6	5.5		3.6	5.5	6.8	74.4	901.0	37.4	290.2	1901.0	4.3	-4.3	0.2	0.0
	1.0	7.2	3.7		7.2	3.7	13.5	87.9	901.0	49.7	339.9	1901.0	5.0	-5.0	0.3	0.0
	1.3	5.4	3.0		5.4	3.0	20.4	108.3	901.0	62.1	401.9	1901.0	5.9	-5.9	0.3	0.0
	1.5	5.9	15.8		5.9	15.8	22.0	130.3	901.0	347.3	749.2	1901.0	11.0	-11.0	0.1	0.1
	1.8	8.1	2.4		8.1	2.4	30.2	160.6	901.0	71.3	820.5	1901.0	12.0	-12.0	0.4	0.1
	2.3	7.4	1.7		7.4	1.7	55.4	215.9	901.0	96.5	917.0	1901.0	13.4	-13.4	0.6	0.1
	2.5	6.8	2.2		6.8	2.2	25.5	241.5	901.0	54.9	971.9	1901.0	14.3	-14.3	0.5	0.1
	2.8	6.5	3.1		6.5	3.1	24.3	265.8	901.0	75.0	1046.9	1901.0	15.4	-15.4	0.3	0.1
	3.0	7.1	1.4		7.1	1.4	26.6	292.4	901.0	38.3	1085.2	1901.0	15.9	-15.9	0.7	0.1
	3.5	7.2	1.5		7.2	1.5	54.0	346.4	901.0	83.2	1168.4	1901.0	17.1	-17.1	0.6	0.1
	4.0	9.8	1.2		9.8	1.2	73.1	419.5	901.0	85.5	1253.9	1901.0	18.4	-18.4	0.9	0.1
	4.5	15.1	1.0		15.1	1.0	113.5	533.0	901.0	111.7	1365.6	1901.0	20.0	-20.0	1.0	0.1
	5.0	17.1	1.0		17.1	1.0	128.3	661.3	901.0	127.0	1492.5	1901.0	21.9	-21.9	1.0	0.1
	5.5	18.3	0.9		18.3	0.9	137.1	798.4	901.0	125.0	1617.5	1901.0	23.7	-23.7	1.1	0.2
	6.0	13.7	2.8		13.7	2.8	102.6	901.0	901.0	283.5	1901.0	1901.0	27.9	-27.9	0.4	0.2

Profile:	DC			Bulk Density	1.5		Calculations						density, precipitation and Cl(P)			
				Precipitation	487								are user defined on "graphs" worksheet			
				Cl in Precip	0.14		Water = Depth * (MC / 100) * soil density * 1000									
							Average Cl = Total Cl / Total Water = 16.85294 mg/L						Recharge	4.045586	mm/year	
							Time = Σ Cl / (Precipitation * Cl(P))						Total Time	45.72466	years	
	Raw data			Replace blanks in data with												
	Depth	Moisture Content	Lab Cl		0	0	Water	Σ Water	Total W	Cl	Σ Cl	Total Cl	Time	Date	1/Cl	Cum Cl
	(m)	(%)	(mg/L)		MC	Cl	(Kg/m2)	(Kg/m2)	(Kg/m2)	(mg/m2)	(mg/m2)	(mg/m2)	(years)			(mg cm2)
	0.1	5.6	26.9		5.6	26.9	10.5	10.5	185.0	282.7	282.7	3117.5	4.1	-4.1	0.0	0.0
	0.3	5.3	15.5		5.3	15.5	9.9	20.4	185.0	153.6	436.2	3117.5	6.4	-6.4	0.1	0.0
	0.4	4.9	46.7		4.9	46.7	9.2	29.6	185.0	429.0	865.3	3117.5	12.7	-12.7	0.0	0.1
	0.5	4.3	14.8		4.3	14.8	8.1	37.7	185.0	120.0	985.2	3117.5	14.5	-14.5	0.1	0.1
	0.6	3.1	19.6		3.1	19.6	5.9	43.6	185.0	114.7	1099.9	3117.5	16.1	-16.1	0.1	0.1
	0.8	4.5	10.5		4.5	10.5	8.4	51.9	185.0	87.8	1187.7	3117.5	17.4	-17.4	0.1	0.1
	0.9	1.9	17.1		1.9	17.1	3.6	55.6	185.0	62.0	1249.7	3117.5	18.3	-18.3	0.1	0.1
	1.0	1.5	12.5		1.5	12.5	2.8	58.3	185.0	34.5	1284.2	3117.5	18.8	-18.8	0.1	0.1
	1.3	2.1	19.0		2.1	19.0	7.9	66.2	185.0	149.1	1433.4	3117.5	21.0	-21.0	0.1	0.1
	1.5	1.6	15.6		1.6	15.6	5.9	72.1	185.0	92.5	1525.8	3117.5	22.4	-22.4	0.1	0.2
	1.8	2.9	7.9		2.9	7.9	10.9	83.0	185.0	86.0	1611.9	3117.5	23.6	-23.6	0.1	0.2
	2.0	3.3	7.4		3.3	7.4	12.4	95.4	185.0	91.0	1702.9	3117.5	25.0	-25.0	0.1	0.2
	2.3	1.8	10.3		1.8	10.3	6.6	102.0	185.0	68.3	1771.2	3117.5	26.0	-26.0	0.1	0.2
	2.5	1.4	4.9		1.4	4.9	5.2	107.3	185.0	25.6	1796.9	3117.5	26.4	-26.4	0.2	0.2
	2.8	1.9	10.6		1.9	10.6	7.0	114.2	185.0	73.9	1870.8	3117.5	27.4	-27.4	0.1	0.2
	3.0	1.1	13.4		1.1	13.4	4.1	118.3	185.0	54.4	1925.1	3117.5	28.2	-28.2	0.1	0.2
	3.5	1.1	21.9		1.1	21.9	8.6	126.9	185.0	188.7	2113.9	3117.5	31.0	-31.0	0.0	0.2
	4.0	1.0	22.7		1.0	22.7	7.8	134.7	185.0	177.6	2291.4	3117.5	33.6	-33.6	0.0	0.2
	4.5	1.8	24.1		1.8	24.1	13.6	148.3	185.0	327.6	2619.0	3117.5	38.4	-38.4	0.0	0.3
	5.0	1.5	14.9		1.5	14.9	11.0	159.3	185.0	163.6	2782.6	3117.5	40.8	-40.8	0.1	0.3
	5.5	1.3	18.0		1.3	18.0	9.6	169.0	185.0	173.7	2956.3	3117.5	43.4	-43.4	0.1	0.3
	6.0	2.1	10.1		2.1	10.1	16.0	185.0	185.0	161.2	3117.5	3117.5	45.7	-45.7	0.1	0.3

Appendix 1.2 Sulfate mass balance analysis

Profile:	**G1**			Bulk Density	1.5		Calculations						density, precipitation and SO4(P)			
				Precipitation	487								are user defined on "graphs" worksheet			
				SO4 in Precip	1.62		Water = Depth * (MC / 100) * soil density * 1000									
							Average S = Total SO4 / Total Water = 8.079427 mg/L						Recharge	97.64801	mm/year	
							Time = Σ SO4 / (Precipitation * SO4(P))						Total Time	7.731934	years	
	Raw data			Replace blanks in data with												
	Depth	Moisture Content	Lab SO4		0	0	Water	Σ Water	Total W	SO4	Σ SO4	Total SO4	Time	Date	1/SO4	Cum SO4
	(m)	(%)	(mg/L)		MC	SO4	(Kg/m2)	(Kg/m2)	(Kg/m2)	(mg/m2)	(mg/m2)	(mg/m2)	(years)			(mg cm2)
	0.125	6.18			6.1821974	26.997469	11.5916	11.592	755.008	312.9444006	312.9444	6100.032	0.396664	-0.39666	0.037041	0.031294
	0.25	6.90			6.8983983	67.971612	12.9345	24.526	755.008	879.1785909	1192.123	6100.032	1.511044	-1.51104	0.014712	0.119212
	0.375	6.87			6.8664639	28.782075	12.8746	37.401	755.008	370.5582776	1562.681	6100.032	1.980735	-1.98074	0.034744	0.156268
	0.5	5.88			5.8768761	18.593644	11.0191	48.42	755.008	204.886016	1767.567	6100.032	2.240433	-2.24043	0.053782	0.176757
	0.625	6.60			6.6040986	13.273938	12.3827	60.803	755.008	164.3669852	1931.934	6100.032	2.448772	-2.44877	0.075336	0.193193
	0.75	7.73			7.7267431	10.543653	14.4876	75.29	755.008	152.7526908	2084.687	6100.032	2.64239	-2.64239	0.094844	0.208469
	0.875	12.31			12.309884	13.022667	23.081	98.371	755.008	300.5766128	2385.264	6100.032	3.023378	-3.02338	0.076789	0.238526
	1	12.52			12.515952	10.539359	23.4674	121.84	755.008	247.331454	2632.595	6100.032	3.336876	-3.33688	0.094882	0.26326
	1.25	13.41			13.411573	4.5890554	50.2934	172.13	755.008	230.7991896	2863.394	6100.032	3.629419	-3.62942	0.21791	0.286339
	1.5	8.37			8.3679813	5.7612732	31.3799	203.51	755.008	180.7883488	3044.183	6100.032	3.858573	-3.85857	0.173573	0.304418
	1.75	11.81			11.807709	7.5841898	44.2789	247.79	755.008	335.819649	3380.002	6100.032	4.284232	-4.28423	0.131853	0.338
	2	12.79			12.786897	4.1148906	47.9509	295.74	755.008	197.3125598	3577.315	6100.032	4.534331	-4.53433	0.24302	0.357731
	2.25	6.89			6.8919168	6.822604	25.8447	321.59	755.008	176.3280712	3753.643	6100.032	4.757831	-4.75783	0.146572	0.375364
	2.5	5.99			5.9913307	6.3712666	22.4675	344.05	755.008	143.1463699	3896.789	6100.032	4.939272	-4.93927	0.156955	0.389679
	2.75	5.19			5.1930551	10.393676	19.474	363.53	755.008	202.4059931	4099.195	6100.032	5.195826	-5.19583	0.096212	0.40992
	3	6.37			6.3659482	4.3413854	23.8723	387.4	755.008	103.6388791	4202.834	6100.032	5.327191	-5.32719	0.230341	0.420283
	3.5	6.65			6.6506147	6.5339672	49.8796	437.28	755.008	325.91174	4528.746	6100.032	5.740292	-5.74029	0.153046	0.452875
	4	6.00			5.998265	7.7763322	44.987	482.27	755.008	349.8337575	4878.58	6100.032	6.183714	-6.18371	0.128595	0.487858
	4.5	5.94			5.9398054	5.8116494	44.5485	526.82	755.008	258.9004974	5137.48	6100.032	6.511877	-6.51188	0.172068	0.513748
	5	5.78			5.7827983	6.0690631	43.371	570.19	755.008	263.2212581	5400.701	6100.032	6.845516	-6.84552	0.16477	0.54007
	5.5	9.43			9.4307188	3.7815746	70.7304	640.92	755.008	267.4722511	5668.174	6100.032	7.184543	-7.18454	0.26444	0.566817
	6	15.21			15.212173	3.785201	114.091	755.01	755.008	431.8584857	6100.032	6100.032	7.731934	-7.73193	0.264187	0.610003

Profile:	**G2**			Bulk Density	1.5		Calculations							density, precipitation and SO4(P)			
				Precipitation	487									are user defined on "graphs" worksheet			
				SO4 in Precip	1.62		Water	= Depth * (MC / 100) * soil density * 1000									
							Average S	= Total SO4 / Total Water =	19.1616	mg/L				Recharge	41.17297	mm/year	
							Time	= Σ SO4 / (Precipitation * SO4(P))						Total Time	23.27734	years	
	Raw data			Replace blanks in data with													
	Depth	Moisture Content	Lab SO4		0	0	Water	Σ Water	Total W	SO4	Σ SO4	Total SO4	Time	Date	1/SO4	Cum SO4	
	(m)	(%)	(mg/L)		MC	SO4	(Kg/m2)	(Kg/m2)	(Kg/m2)	(mg/m2)	(mg/m2)	(mg/m2)	(years)			(mg cm2)	
	0.125	11.57			11.56699	27.92986	21.6881	21.6881	958.3973	605.7455	605.7455	18364.43	0.767797	-0.7678	0.035804	0.060575	
	0.25	11.05			11.04516	17.32538	20.70967	42.39777	958.3973	358.8028	964.5484	18364.43	1.222588	-1.22259	0.057719	0.096455	
	0.375	11.87			11.86726	17.41482	22.2511	64.64887	958.3973	387.499	1352.047	18364.43	1.713752	-1.71375	0.057422	0.135205	
	0.5	10.56			10.56352	16.96307	19.8066	84.45547	958.3973	335.9807	1688.028	18364.43	2.139615	-2.13962	0.058952	0.168803	
	0.625	10.03			10.03488	13.66839	18.8154	103.2709	958.3973	257.1763	1945.204	18364.43	2.465592	-2.46559	0.073162	0.19452	
	0.75	16.58			16.57819	13.69238	31.0841	134.355	958.3973	425.6153	2370.82	18364.43	3.00507	-3.00507	0.073033	0.237082	
	0.875	13.58			13.57836	17.21791	25.45943	159.8144	958.3973	438.3581	2809.178	18364.43	3.560699	-3.5607	0.058079	0.280918	
	1	16.63			16.62623	17.72883	31.17418	190.9886	958.3973	552.6816	3361.859	18364.43	4.261236	-4.26124	0.056405	0.336186	
	1.25	15.42			15.42337	13.81549	57.83763	248.8262	958.3973	799.0554	4160.915	18364.43	5.274057	-5.27406	0.072383	0.416091	
	1.5	14.03			14.02626	13.29291	52.59849	301.4247	958.3973	699.1872	4860.102	18364.43	6.160293	-6.16029	0.075228	0.48601	
	1.75	8.79			8.794653	18.33202	32.97995	334.4046	958.3973	604.589	5464.691	18364.43	6.926624	-6.92662	0.054549	0.546469	
	2	7.65			7.651617	27.73689	28.69357	363.0982	958.3973	795.8702	6260.561	18364.43	7.935408	-7.93541	0.036053	0.626056	
	2.25	7.04			7.037873	20.06242	26.39202	389.4902	958.3973	529.4878	6790.049	18364.43	8.606547	-8.60655	0.049844	0.679005	
	2.5	7.93			7.92844	16.3678	29.73165	419.2219	958.3973	486.6416	7276.69	18364.43	9.223376	-9.22338	0.061096	0.727669	
	2.75	7.97			7.972209	25.42356	29.89578	449.1177	958.3973	760.0573	8036.748	18364.43	10.18677	-10.1868	0.039334	0.803675	
	3	9.30			9.29672	14.1393	34.8627	483.9804	958.3973	492.9341	8529.682	18364.43	10.81157	-10.8116	0.070725	0.852968	
	3.5	8.87			8.868492	24.59671	66.51369	550.4941	958.3973	1636.018	10165.7	18364.43	12.88526	-12.8853	0.040656	1.01657	
	4	11.80			11.7962	20.30488	88.47153	638.9656	958.3973	1796.404	11962.1	18364.43	15.16225	-15.1622	0.049249	1.19621	
	4.5	10.54			10.53812	23.38751	79.0359	718.0015	958.3973	1848.453	13810.56	18364.43	17.50521	-17.5052	0.042758	1.381056	
	5	10.96			10.96172	25.38019	82.21288	800.2144	958.3973	2086.578	15897.14	18364.43	20.14999	-20.15	0.039401	1.589714	
	5.5	9.00			9.001281	11.40467	67.50961	867.724	958.3973	769.9247	16667.06	18364.43	21.12589	-21.1259	0.087683	1.666706	
	6	12.09			12.08978	18.71956	90.67335	958.3973	958.3973	1697.365	18364.43	18364.43	23.27734	-23.2773	0.05342	1.836443	

Profile:	**PS1**			Bulk Density	1.5		Calculations						density, precipitation and SO4(P)			
				Precipitation	487								are user defined on "graphs" worksheet			
				SO4 in Precip	1.62		Water	= Depth * (MC / 100) * soil density * 1000								
							Average SO	= Total SO4 / Total Water =	26.30462	mg/L			Recharge	29.99245	mm/year	
	Raw data				Replace blanks in data with		Time	= Σ SO4 / (Precipitation * SO4(P))					Total Time	13.49492	years	
	Depth	Moisture Content	Lab SO4		0	0	Water	Σ Water	Total W	SO4	Σ SO4	Total SO4	Time	Date	1/SO4	Cum SO4
	(m)	(%)	(mg/L)		MC	SO4	(Kg/m2)	(Kg/m2)	(Kg/m2)	(mg/m2)	(mg/m2)	(mg/m2)	(years)			(mg cm2)
	0.125	6.74			6.74023	79.36058	12.63793	12.63793	404.7456	1002.954	1002.954	10646.68	1.271267	-1.27127	0.012601	0.100295
	0.25	4.35			4.352596	37.06474	8.161117	20.79905	404.7456	302.4897	1305.443	10646.68	1.65468	-1.65468	0.02698	0.130544
	0.375	4.11			4.113533	43.35735	7.712874	28.51192	404.7456	334.4097	1639.853	10646.68	2.078552	-2.07855	0.023064	0.163985
	0.5	3.83			3.827275	30.59154	7.176141	35.68806	404.7456	219.5292	1859.382	10646.68	2.356811	-2.35681	0.032689	0.185938
	0.625	3.81			3.813009	34.65045	7.149391	42.83745	404.7456	247.7296	2107.112	10646.68	2.670814	-2.67081	0.02886	0.210711
	0.75	4.00			3.999808	40.66889	7.49964	50.33709	404.7456	305.0021	2412.114	10646.68	3.057411	-3.05741	0.024589	0.241211
	0.875	4.75			4.750644	28.56962	8.907458	59.24455	404.7456	254.4826	2666.597	10646.68	3.379974	-3.37997	0.035002	0.26666
	1	6.45			6.44607	23.28594	12.08638	71.33093	404.7456	281.4428	2948.039	10646.68	3.736709	-3.73671	0.042944	0.294804
	1.25	2.91			2.907261	30.34014	10.90223	82.23316	404.7456	330.7751	3278.814	10646.68	4.155974	-4.15597	0.03296	0.327881
	1.5	4.71			4.709212	26.81915	17.65955	99.89271	404.7456	473.614	3752.428	10646.68	4.756291	-4.75629	0.037287	0.375243
	1.75	3.60			3.601803	20.79344	13.50676	113.3995	404.7456	280.852	4033.28	10646.68	5.112278	-5.11228	0.048092	0.403328
	2	7.74			7.736356	27.01354	29.01134	142.4108	404.7456	783.699	4816.979	10646.68	6.105635	-6.10563	0.037018	0.481698
	2.25	10.64			10.63766	22.06061	39.89123	182.302	404.7456	880.0247	5697.004	10646.68	7.221087	-7.22109	0.04533	0.5697
	2.5	1.82			1.815235	22.4675	6.807131	189.1092	404.7456	152.9392	5849.943	10646.68	7.414941	-7.41494	0.044509	0.584994
	2.75	3.19			3.187276	22.19769	11.95229	201.0615	404.7456	265.3131	6115.257	10646.68	7.751231	-7.75123	0.04505	0.611526
	3	2.90			2.904023	38.59137	10.89009	211.9515	404.7456	420.2633	6535.52	10646.68	8.283925	-8.28393	0.025913	0.653552
	3.5	3.57			3.5718	22.67687	26.7885	238.74	404.7456	607.4793	7142.999	10646.68	9.05392	-9.05392	0.044098	0.7143
	4	3.96			3.960819	29.21405	29.70614	268.4462	404.7456	867.8367	8010.836	10646.68	10.15392	-10.1539	0.03423	0.801084
	4.5	4.66			4.664893	14.30281	34.9867	303.4329	404.7456	500.4082	8511.244	10646.68	10.7882	-10.7882	0.069916	0.851124
	5	3.73			3.728654	23.26361	27.9649	331.3978	404.7456	650.5645	9161.809	10646.68	11.61281	-11.6128	0.042986	0.916181
	5.5	3.51			3.506144	20.59501	26.29608	357.6939	404.7456	541.5679	9703.377	10646.68	12.29926	-12.2993	0.048555	0.970338
	6	6.27			6.273567	20.0482	47.05176	404.7456	404.7456	943.303	10646.68	10646.68	13.49492	-13.4949	0.04988	1.064668

Profile:	**PS2**			Bulk Density	1.5		Calculations						density, precipitation and SO4(P)			
				Precipitation	487								are user defined on "graphs" worksheet			
				SO4 in Precip	1.62		Water	= Depth * (MC / 100) * soil density * 1000								
							Average SO	= Total SO4 / Total Water =	29.22589	mg/L			Recharge	26.99456	mm/year	
	Raw data				Replace blanks in data with		Time	= Σ SO4 / (Precipitation * SO4(P))					Total Time	17.76612	years	
	Depth	Moisture Content	Lab SO4		0	0	Water	Σ Water	Total W	SO4	Σ SO4	Total SO4	Time	Date	1/SO4	Cum SO4
	(m)	(%)	(mg/L)		MC	SO4	(Kg/m2)	(Kg/m2)	(Kg/m2)	(mg/m2)	(mg/m2)	(mg/m2)	(years)			(mg cm2)
	0.125	3.39			3.385246	80.58208	6.347336	6.347336	479.5886	511.4815	511.4815	14016.4	0.648315	-0.64831	0.01241	0.051148
	0.25	4.35			4.354679	51.41138	8.165023	14.51236	479.5886	419.7751	931.2567	14016.4	1.18039	-1.18039	0.019451	0.093126
	0.375	5.93			5.926313	45.6853	11.11184	25.6242	479.5886	507.6476	1438.904	14016.4	1.823845	-1.82384	0.021889	0.14389
	0.5	6.81			6.810985	38.81732	12.7706	38.39479	479.5886	495.7204	1934.625	14016.4	2.452182	-2.45218	0.025762	0.193462
	0.625	3.98			3.977631	39.65208	7.458058	45.85285	479.5886	295.7275	2230.352	14016.4	2.827024	-2.82702	0.025219	0.223035
	0.75	5.30			5.303863	49.17075	9.944742	55.79759	479.5886	488.9904	2719.343	14016.4	3.446831	-3.44683	0.020337	0.271934
	0.875	7.29			7.294044	31.87757	13.67633	69.47393	479.5886	435.9682	3155.311	14016.4	3.999431	-3.99943	0.03137	0.315531
	1	5.02			5.020256	25.42711	9.412981	78.88691	479.5886	239.3449	3394.656	14016.4	4.302806	-4.30281	0.039328	0.339466
	1.25	10.45			10.45085	42.00681	39.19069	118.0776	479.5886	1646.276	5040.932	14016.4	6.389499	-6.3895	0.023806	0.504093
	1.5	6.22			6.222028	40.74689	23.33261	141.4102	479.5886	950.7311	5991.663	14016.4	7.594574	-7.59457	0.024542	0.599166
	1.75	7.16			7.161493	24.39567	26.8556	168.2658	479.5886	655.1603	6646.823	14016.4	8.425005	-8.425	0.040991	0.664682
	2	7.30			7.303543	21.31548	27.38828	195.6541	479.5886	583.7943	7230.617	14016.4	9.164978	-9.16498	0.046914	0.723062
	2.25	8.65			8.650767	25.0581	32.44038	228.0945	479.5886	812.8942	8043.512	14016.4	10.19534	-10.1953	0.039907	0.804351
	2.5	7.72			7.717457	24.67671	28.94046	257.0349	479.5886	714.1554	8757.667	14016.4	11.10055	-11.1005	0.040524	0.875767
	2.75	6.72			6.720016	24.13579	25.20006	282.235	479.5886	608.2234	9365.89	14016.4	11.87149	-11.8715	0.041432	0.936589
	3	6.32			6.320819	12.11804	23.70307	305.9381	479.5886	287.2348	9653.125	14016.4	12.23556	-12.2356	0.082522	0.965313
	3.5	4.92			4.91585	24.31203	36.86888	342.8069	479.5886	896.3572	10549.48	14016.4	13.37172	-13.3717	0.041132	1.054948
	4	5.80			5.799729	5.414885	43.49797	386.3049	479.5886	235.5365	10785.02	14016.4	13.67027	-13.6703	0.184676	1.078502
	4.5	2.27			2.265741	29.15951	16.99306	403.298	479.5886	495.5093	11280.53	14016.4	14.29833	-14.2983	0.034294	1.128053
	5	2.48			2.483964	20.2193	18.62973	421.9277	479.5886	376.6802	11657.21	14016.4	14.77579	-14.7758	0.049458	1.165721
	5.5	4.27			4.27233	40.22002	32.04248	453.9702	479.5886	1288.749	12945.96	14016.4	16.40931	-16.4093	0.024863	1.294596
	6	3.42			3.415794	41.78416	25.61846	479.5886	479.5886	1070.446	14016.4	14016.4	17.76612	-17.7661	0.023933	1.40164

Profile:	**TP1**			Bulk Density	1.5			Calculations							density, precipitation and SO4(P)			
				Precipitation	487										are user defined on "graphs" worksheet			
				SO4 in Precip	1.62			Water = Depth * (MC / 100) * soil density * 1000										
								Average SO = Total SO4 / Total Water = 98.45893 mg/L							Recharge	8.012884	mm/year	
								Time = Σ SO4 / (Precipitation * SO4(P))							Total Time	27.31705	years	
	Raw data			Replace blanks in data with														
	Depth	Moisture Content	Lab SO4		0	0		Water	Σ Water	Total W	SO4	Σ SO4	Total SO4		Time	Date	1/SO4	Cum SO4
	(m)	(%)	(mg/L)		MC	SO4		(Kg/m2)	(Kg/m2)	(Kg/m2)	(mg/m2)	(mg/m2)	(mg/m2)		(years)			(mg cm2)
	0.125	4.54			4.538346	44.97784		8.509398	8.509398	218.8883	382.7344	382.7344	21551.5099		0.485125	-0.48512	0.022233	0.038273
	0.25	4.05			4.054205	50.4516		7.601634	16.11103	218.8883	383.5146	766.249	21551.5099		0.971239	-0.97124	0.019821	0.076625
	0.375	3.88			3.882712	49.98912		7.280084	23.39112	218.8883	363.925	1130.174	21551.5099		1.432522	-1.43252	0.020004	0.113017
	0.5	2.55			2.550243	79.17329		4.781705	28.17282	218.8883	378.5833	1508.757	21551.5099		1.912385	-1.91239	0.012631	0.150876
	0.625	3.06			3.057769	67.24509		5.733317	33.90614	218.8883	385.5374	1894.295	21551.5099		2.401063	-2.40106	0.014871	0.189429
	0.75	3.30			3.302919	129.2588		6.192973	40.09911	218.8883	800.4965	2694.791	21551.5099		3.415711	-3.41571	0.007736	0.269479
	0.875	2.46			2.456192	66.51726		4.605361	44.70447	218.8883	306.336	3001.127	21551.5099		3.803999	-3.804	0.015034	0.300113
	1	1.96			1.963934	135.8707		3.682377	48.38685	218.8883	500.327	3501.454	21551.5099		4.438175	-4.43818	0.00736	0.350145
	1.25	2.70			2.699659	97.84311		10.12372	58.51057	218.8883	990.5365	4491.991	21551.5099		5.693704	-5.6937	0.01022	0.449199
	1.5	2.22			2.223992	97.1099		8.339969	66.85054	218.8883	809.8936	5301.884	21551.5099		6.720263	-6.72026	0.010298	0.530188
	1.75	2.07			2.068036	58.60945		7.755136	74.60568	218.8883	454.5243	5756.409	21551.5099		7.296383	-7.29638	0.017062	0.575641
	2	1.57			1.5701	262.7082		5.887876	80.49355	218.8883	1546.793	7303.202	21551.5099		9.25698	-9.25698	0.003807	0.73032
	2.25	1.53			1.534961	178.9598		5.756102	86.24965	218.8883	1030.111	8333.313	21551.5099		10.56267	-10.5627	0.005588	0.833331
	2.5	1.58			1.578829	179.4039		5.92061	92.17026	218.8883	1062.181	9395.493	21551.5099		11.90901	-11.909	0.005574	0.939549
	2.75	1.85			1.854699	233.53		6.955122	99.12539	218.8883	1624.23	11019.72	21551.5099		13.96776	-13.9678	0.004282	1.101972
	3	2.72			2.715158	58.32395		10.18184	109.3072	218.8883	593.8451	11613.57	21551.5099		14.72047	-14.7205	0.017146	1.161357
	3.5	2.46			2.462276	109.3381		18.46707	127.7743	218.8883	2019.153	13632.72	21551.5099		17.2798	-17.2798	0.009146	1.363272
	4	2.56			2.55855	181.2259		19.18912	146.9634	218.8883	3477.566	17110.29	21551.5099		21.68769	-21.6877	0.005518	1.711029
	4.5	3.04			3.038394	75.99369		22.78796	169.7514	218.8883	1731.741	18842.03	21551.5099		23.88271	-23.8827	0.013159	1.884203
	5	1.96			1.956849	56.22332		14.67636	184.4277	218.8883	825.1539	19667.18	21551.5099		24.92862	-24.9286	0.017786	1.966718
	5.5	1.66			1.662947	72.2548		12.4721	196.8998	218.8883	901.1694	20568.35	21551.5099		26.07087	-26.0709	0.01384	2.056835
	6	2.93			2.931797	44.71243		21.98847	218.8883	218.8883	983.1581	21551.51	21551.5099		27.31705	-27.317	0.022365	2.155151

Profile:	**TP2**			Bulk Density	1.5		Calculations						density, precipitation and SO4(P)			
				Precipitation	487								are user defined on "graphs" worksheet			
				SO4 in Precip	1.62		Water	= Depth * (MC / 100) * soil density * 1000								
							Average SO4	= Total SO4 / Total Water =		76.08814	mg/L		Recharge	10.36876	mm/year	
							Time	= Σ SO4 / (Precipitation * SO4(P))					Total Time	40.5707	years	
	Raw data				Replace blanks in data with											
	Depth	Moisture Content	Lab SO4		0	0	Water	Σ Water	Total W	SO4	Σ SO4	Total SO4	Time	Date	1/SO4	Cum SO4
	(m)	(%)	(mg/L)		MC	SO4	(Kg/m2)	(Kg/m2)	(Kg/m2)	(mg/m2)	(mg/m2)	(mg/m2)	(years)			(mg cm2)
	0.125	11.05			11.05447	60.40837417	20.72713	20.72713381	420.6680151	1252.092	1252.092	32007.85	1.587057	-1.58706	0.016554	0.125209
	0.25	4.35			4.348801	61.90006731	8.154002	28.88113566	420.6680151	504.7333	1756.826	32007.85	2.226818	-2.22682	0.016155	0.175683
	0.375	3.13			3.13101	37.94241263	5.870643	34.7517791	420.6680151	222.7464	1979.572	32007.85	2.509154	-2.50915	0.026356	0.197957
	0.5	3.35			3.345927	40.52899666	6.273612	41.02539148	420.6680151	254.2632	2233.835	32007.85	2.831439	-2.83144	0.024674	0.223384
	0.625	3.98			3.981394	34.94321336	7.465113	48.49050483	420.6680151	260.855	2494.69	32007.85	3.162079	-3.16208	0.028618	0.249469
	0.75	4.33			4.328206	38.84385996	8.115387	56.60589174	420.6680151	315.233	2809.923	32007.85	3.561644	-3.56164	0.025744	0.280992
	0.875	5.92			5.917328	32.92437725	11.09499	67.70088106	420.6680151	365.2956	3175.219	32007.85	4.024665	-4.02466	0.030373	0.317522
	1	4.77			4.771656	37.4809102	8.946856	76.64773688	420.6680151	335.3363	3510.555	32007.85	4.449711	-4.44971	0.02668	0.351056
	1.25	4.12			4.124225	238.3172216	15.46584	92.11358171	420.6680151	3685.777	7196.332	32007.85	9.121521	-9.12152	0.004196	0.719633
	1.5	4.13			4.127345	201.0287916	15.47754	107.5911247	420.6680151	3111.432	10307.76	32007.85	13.06533	-13.0653	0.004974	1.030776
	1.75	4.04			4.037324	55.00202429	15.13997	122.7310904	420.6680151	832.7288	11140.49	32007.85	14.12084	-14.1208	0.018181	1.114049
	2	7.30			7.295981	44.22636532	27.35993	150.0910204	420.6680151	1210.03	12350.52	32007.85	15.65458	-15.6546	0.022611	1.235052
	2.25	4.77			4.769933	39.11813065	17.88725	167.9782678	420.6680151	699.7157	13050.24	32007.85	16.54148	-16.5415	0.025564	1.305024
	2.5	6.48			6.48276	5.031030011	24.31035	192.2886168	420.6680151	122.3061	13172.54	32007.85	16.69651	-16.6965	0.198766	1.317254
	2.75	6.09			6.086234	34.75911793	22.82338	215.1119929	420.6680151	793.3204	13965.87	32007.85	17.70206	-17.7021	0.028769	1.396587
	3	4.22			4.220861	125.8377294	15.82823	230.9402215	420.6680151	1991.788	15957.65	32007.85	20.2267	-20.2267	0.007947	1.595765
	3.5	3.82			3.8244	87.27342544	28.683	259.6232215	420.6680151	2503.264	18460.92	32007.85	23.39965	-23.3996	0.011458	1.846092
	4	3.17			3.166436	185.5467862	23.74827	283.3714886	420.6680151	4406.415	22867.33	32007.85	28.98488	-28.9849	0.005389	2.286733
	4.5	3.19			3.185235	107.760883	23.88926	307.2607503	420.6680151	2574.328	25441.66	32007.85	32.2479	-32.2479	0.00928	2.544166
	5	5.73			5.731587	84.51312404	42.9869	350.2476553	420.6680151	3632.958	29074.62	32007.85	36.85276	-36.8528	0.011832	2.907462
	5.5	4.18			4.183587	48.01690088	31.3769	381.6245567	420.6680151	1506.622	30581.24	32007.85	38.76244	-38.7624	0.020826	3.058124
	6	5.21			5.205794	36.538963	39.04346	420.6680151	420.6680151	1426.607	32007.85	32007.85	40.5707	-40.5707	0.027368	3.200785

Profile:	**DP1**			Bulk Density	1.5		Calculations						density, precipitation and SO4(P)			
				Precipitation	487								are user defined on "graphs" worksheet			
				SO4 in Precip	1.62		Water	= Depth * (MC / 100) * soil density * 1000								
							Average S	= Total SO4 / Total Water =	46.69003	mg/L			Recharge	16.8974	mm/year	
	Raw data				Replace blanks in data		Time	= Σ SO4 / (Precipitation * SO4(P))					Total Time	17.87595	years	
	Depth	Moisture Content	Lab V		with	0										
	(m)	(%)	(mg/L)		MC	SO4	Water (Kg/m2)	Σ Water (Kg/m2)	Total W (Kg/m2)	SO4 (mg/m2)	Σ SO4 (mg/m2)	Total SO4 (mg/m2)	Time (years)	Date	1/SO4	Cum SO4 (mg cm2)
	0.125	14.82			14.8196	88.52562	27.78674	27.78674	302.057	2459.838	2459.838	14103.05	3.117903	-3.1179	0.011296	0.245984
	0.25	4.52			4.524594	19.46806	8.483613	36.27035	302.057	165.1594	2624.998	14103.05	3.327246	-3.32725	0.051366	0.2625
	0.375	5.76			5.756434	32.48118	10.79331	47.06367	302.057	350.5796	2975.577	14103.05	3.771614	-3.77161	0.030787	0.297558
	0.5	4.73			4.733415	49.12883	8.875154	55.93882	302.057	436.0259	3411.603	14103.05	4.324287	-4.32429	0.020355	0.34116
	0.625	5.75			5.751414	14.87965	10.7839	66.72272	302.057	160.4607	3572.064	14103.05	4.527675	-4.52768	0.067206	0.357206
	0.75	5.05			5.048316	14.0475	9.465592	76.18831	302.057	132.9679	3705.032	14103.05	4.696215	-4.69622	0.071187	0.370503
	0.875	4.42			4.422244	16.94755	8.291708	84.48002	302.057	140.5241	3845.556	14103.05	4.874333	-4.87433	0.059006	0.384556
	1	5.25			5.245875	19.46932	9.836016	94.31604	302.057	191.5006	4037.057	14103.05	5.117064	-5.11706	0.051363	0.403706
	1.25	2.23			2.233613	73.7983	8.376049	102.6921	302.057	618.1382	4655.195	14103.05	5.900569	-5.90057	0.01355	0.465519
	1.5	3.67			3.674462	150.1817	13.77923	116.4713	302.057	2069.388	6724.583	14103.05	8.523567	-8.52357	0.006659	0.672458
	1.75	1.34			1.342483	17.66986	5.034312	121.5056	302.057	88.9556	6813.538	14103.05	8.63632	-8.63632	0.056594	0.681354
	2	1.75			1.748685	64.93639	6.557571	128.0632	302.057	425.825	7239.363	14103.05	9.176063	-9.17606	0.0154	0.723936
	2.25	2.25			2.254502	33.41871	8.454384	136.5176	302.057	282.5346	7521.898	14103.05	9.534182	-9.53418	0.029923	0.75219
	2.5	2.35			2.353675	20.18697	8.82628	145.3439	302.057	178.1758	7700.074	14103.05	9.760025	-9.76002	0.049537	0.770007
	2.75	2.45			2.454205	26.61754	9.203268	154.5471	302.057	244.9684	7945.042	14103.05	10.07053	-10.0705	0.037569	0.794504
	3	2.44			2.439653	40.5503	9.148698	163.6958	302.057	370.9825	8316.025	14103.05	10.54076	-10.5408	0.024661	0.831602
	3.5	2.60			2.5952	31.84204	19.464	183.1598	302.057	619.7734	8935.798	14103.05	11.32633	-11.3263	0.031405	0.89358
	4	2.26			2.261225	42.89249	16.95919	200.119	302.057	727.4218	9663.22	14103.05	12.24836	-12.2484	0.023314	0.966322
	4.5	3.08			3.077507	85.98601	23.0813	223.2003	302.057	1984.669	11647.89	14103.05	14.76397	-14.764	0.01163	1.164789
	5	3.28			3.281267	33.89706	24.6095	247.8098	302.057	834.1898	12482.08	14103.05	15.82133	-15.8213	0.029501	1.248208
	5.5	3.10			3.096861	37.47251	23.22646	271.0363	302.057	870.3535	13352.43	14103.05	16.92452	-16.9245	0.026686	1.335243
	6	4.14			4.136092	24.19731	31.02069	302.057	302.057	750.6171	14103.05	14103.05	17.87595	-17.8759	0.041327	1.410305

Profile:	**DP2**			Bulk Density	1.5		Calculations							density, precipitation and SO4(P)			
				Precipitation	487									are user defined on "graphs" worksheet			
				SO4 in Precip	1.62		Water	= Depth * (MC / 100) * soil density * 1000									
							Average SO	= Total SO4 / Total Water =	34.38129	mg/L				Recharge	22.94678	mm/year	
							Time	= Σ SO4 / (Precipitation * SO4(P))						Total Time	16.37761	years	
	Raw data			Replace blanks in data with													
	Depth	Moisture Content	Lab SO4		0	0	Water	Σ Water	Total W	SO4	Σ SO4	Total SO4	Time	Date		1/SO4	Cum SO4
	(m)	(%)	(mg/L)		MC	SO4	(Kg/m2)	(Kg/m2)	(Kg/m2)	(mg/m2)	(mg/m2)	(mg/m2)	(years)				(mg cm2)
	0.125	5.77			5.771967	21.81606818	10.82244	10.82244	375.8134	236.1031	236.1031	12920.95	0.299266	-0.29927		0.045838	0.02361
	0.25	5.35			5.347703	30.27289295	10.02694	20.84938	375.8134	303.5446	539.6476	12920.95	0.684016	-0.68402		0.033033	0.053965
	0.375	5.04			5.044627	10.8645529	9.458675	30.30806	375.8134	102.7643	642.4119	12920.95	0.814272	-0.81427		0.092042	0.064241
	0.5	5.58			5.576871	30.87146251	10.45663	40.76469	375.8134	322.8115	965.2234	12920.95	1.223443	-1.22344		0.032392	0.096522
	0.625	6.63			6.62698	7.646941886	12.42559	53.19028	375.8134	95.01774	1060.241	12920.95	1.343881	-1.34388		0.130771	0.106024
	0.75	7.25			7.253115	24.71516407	13.59959	66.78987	375.8134	336.1161	1396.357	12920.95	1.769916	-1.76992		0.040461	0.139636
	0.875	8.97			8.965961	17.99679934	16.81118	83.60104	375.8134	302.5474	1698.905	12920.95	2.153402	-2.1534		0.055565	0.16989
	1	6.94			6.935089	7.784254271	13.00329	96.60434	375.8134	101.2209	1800.126	12920.95	2.281702	-2.2817		0.128464	0.180013
	1.25	7.65			7.647579	15.38683345	28.67842	125.2828	375.8134	441.2701	2241.396	12920.95	2.841022	-2.84102		0.064991	0.22414
	1.5	9.10			9.100979	5.439942412	34.12867	159.4114	375.8134	185.658	2427.054	12920.95	3.076348	-3.07635		0.183825	0.242705
	1.75	7.19			7.187394	18.7046166	26.95273	186.3642	375.8134	504.1404	2931.194	12920.95	3.715357	-3.71536		0.053463	0.293119
	2	6.33			6.330279	5.953904313	23.73855	210.1027	375.8134	141.337	3072.531	12920.95	3.894505	-3.89451		0.167957	0.307253
	2.25	7.17			7.166285	13.07508787	26.87357	236.9763	375.8134	351.3743	3423.905	12920.95	4.339881	-4.33988		0.076481	0.342391
	2.5	3.76			3.763546	19.40809051	14.1133	251.0896	375.8134	273.9122	3697.818	12920.95	4.687071	-4.68707		0.051525	0.369782
	2.75	2.65			2.648128	55.7016456	9.930479	261.02	375.8134	553.144	4250.962	12920.95	5.388194	-5.38819		0.017953	0.425096
	3	0.16			0.155509	135.2065679	0.583159	261.6032	375.8134	78.84697	4329.809	12920.95	5.488134	-5.48813		0.007396	0.432981
	3.5	0.89			0.894966	68.56663697	6.712246	268.3155	375.8134	460.2362	4790.045	12920.95	6.071494	-6.07149		0.014584	0.479004
	4	3.89			3.893607	58.44022	29.20205	297.5175	375.8134	1706.574	6496.619	12920.95	8.234618	-8.23462		0.017112	0.649662
	4.5	1.73			1.731238	69.16790185	12.98428	310.5018	375.8134	898.0957	7394.715	12920.95	9.372975	-9.37297		0.014458	0.739471
	5	3.24			3.242064	89.68274437	24.31548	334.8173	375.8134	2180.679	9575.394	12920.95	12.13704	-12.137		0.01115	0.957539
	5.5	2.10			2.096085	79.6341817	15.72064	350.5379	375.8134	1251.9	10827.29	12920.95	13.72385	-13.7238		0.012557	1.082729
	6	3.37			3.370064	82.83350746	25.27548	375.8134	375.8134	2093.656	12920.95	12920.95	16.37761	-16.3776		0.012072	1.292095

Profile:	**SV**			Bulk Density	1.5			Calculations							density, precipitation and SO4(P)			
				Precipitation	487										are user defined on "graphs" worksheet			
				SO4 in Precip	1.62			Water	= Depth * (MC / 100) * soil density * 1000									
								Average SO4	= Total SO4 / Total Water =			21.46024	mg/L		Recharge	36.76287	mm/year	
								Time	= Σ SO4 / (Precipitation * SO4(P))						Total Time	23.4557	years	
	Raw data				Replace blanks in data with													
	Depth	Moisture Content	Lab SO4		0	0		Water	Σ Water	Total W	SO4	Σ SO4	Total SO4	Time	Date	1/SO4	Cum SO4	
Sample Interval	(m)	(%)	(mg/L)		MC	SO4		(Kg/m2)	(Kg/m2)	(Kg/m2)	(mg/m2)	(mg/m2)	(mg/m2)	(years)			(mg cm2)	
H30_0-12.5	0.125	4.25			4.250977	94.7006		7.970582	7.970582	862.299	754.8189448	754.8189	18505.14	0.956751	-0.95675	0.01056	0.075482	
H30_12.5-25	0.25	4.45			4.445031	135.2912		8.334433	16.30502	862.299	1127.575176	1882.394	18505.14	2.385979	-2.38598	0.007391	0.188239	
H30_25-37.5	0.375	4.96			4.960354	74.69772		9.300664	25.60568	862.299	694.738365	2577.132	18505.14	3.266576	-3.26658	0.013387	0.257713	
H30_37.5-50	0.5	6.99			6.986161	46.56916		13.09905	38.70473	862.299	610.0118418	3187.144	18505.14	4.03978	-4.03978	0.021473	0.318714	
H30_50-62.5	0.625	6.21			6.207015	5.087279		11.63815	50.34289	862.299	59.20653777	3246.351	18505.14	4.114826	-4.11483	0.196569	0.324635	
H30_62.5-75	0.75	7.52			7.521269	7.561877		14.10238	64.44526	862.299	106.6404534	3352.991	18505.14	4.249995	-4.25	0.132242	0.335299	
H30_75-87.5	0.875	8.25			8.252631	116.4706		15.47368	79.91895	862.299	1802.229377	5155.221	18505.14	6.534363	-6.53436	0.008586	0.515522	
H30_87.5-100	1	7.33			7.331126	55.88692		13.74586	93.66481	862.299	768.2138179	5923.435	18505.14	7.508093	-7.50809	0.017893	0.592343	
H30_100-125	1.25	5.51			5.507203	3.446431		20.65201	114.3168	862.299	71.17573468	5994.61	18505.14	7.598309	-7.59831	0.290155	0.599461	
H30_125-150	1.5	4.67			4.672568	9.194198		17.52213	131.839	862.299	161.1019448	6155.712	18505.14	7.80251	-7.80251	0.108764	0.615571	
H30_150-175	1.75	8.14			8.144697	14.85461		30.54262	162.3816	862.299	453.6987174	6609.411	18505.14	8.377584	-8.37758	0.067319	0.660941	
H30_175-225	2.25	6.93			6.928582	20.01974		51.96436	214.3459	862.299	1040.313205	7649.724	18505.14	9.696205	-9.69621	0.049951	0.764972	
H30_225-250	2.5	7.28			7.276889	22.61071		27.28834	241.6343	862.299	617.0086209	8266.733	18505.14	10.47828	-10.4783	0.044227	0.826673	
H30_250-275	2.75	6.91			6.914487	10.63585		25.92932	267.5636	862.299	275.7804489	8542.513	18505.14	10.82784	-10.8278	0.094022	0.854251	
H30_275-300	3	6.93			6.928867	22.40568		25.98325	293.5468	862.299	582.1723308	9124.686	18505.14	11.56575	-11.5658	0.044632	0.912469	
H30_300-350	3.5	7.23			7.226427	19.05102		54.1982	347.745	862.299	1032.530843	10157.22	18505.14	12.87451	-12.8745	0.052491	1.015722	
H30_350-400	4	10.17			10.16714	14.10895		76.25358	423.9986	862.299	1075.858319	11233.07	18505.14	14.23819	-14.2382	0.070877	1.123307	
H30_400-450	4.5	14.84			14.84438	24.60627		111.3328	535.3314	862.299	2739.485735	13972.56	18505.14	17.71055	-17.7105	0.04064	1.397256	
H30_450-500	5	17.51			17.51269	17.75158		131.3452	666.6766	862.299	2331.584504	16304.14	18505.14	20.66589	-20.6659	0.056333	1.630414	
H30_500-550	5.5	17.69			17.68592	13.14475		132.6444	799.321	862.299	1743.577443	18047.72	18505.14	22.87591	-22.8759	0.076076	1.804772	
H30_550-600	6	8.40			8.397066	7.263166		62.97799	862.299	862.299	457.4196082	18505.14	18505.14	23.4557	-23.4557	0.137681	1.850514	

Profile:	**DC**			Bulk Density	1.5		Calculations							density, precipitation and SO4(P)			
				Precipitation	487									are user defined on "graphs" worksheet			
				SO4 in Precip	1.62		Water	= Depth * (MC / 100) * soil density * 1000									
							Average SO	= Total SO4 / Total Water =	57.71628	mg/L				Recharge	13.66928	mm/year	
							Time	= Σ SO4 / (Precipitation * SO4(P))						Total Time	13.53276	years	
	Raw data			Replace blanks in data with													
	Depth	Moisture Content	Lab SO4	0	0		Water	Σ Water	Total W	SO4	Σ SO4	Total SO4	Time	Date	1/SO4	Cum SO4	
	(m)	(%)	(mg/L)	MC	SO4		(Kg/m2)	(Kg/m2)	(Kg/m2)	(mg/m2)	(mg/m2)	(mg/m2)	(years)			(mg cm2)	
	0.125	5.60		5.59525	17.05642891		10.49109	10.49109	184.983	178.9406	178.9406	10676.53	0.226811	-0.22681	0.058629	0.017894	
	0.25	5.30		5.300858	19.56879782		9.93911	20.4302	184.983	194.4964	373.437	10676.53	0.47334	-0.47334	0.051102	0.037344	
	0.375	4.90		4.896899	32.53448212		9.181686	29.61189	184.983	298.7214	672.1584	10676.53	0.851977	-0.85198	0.030737	0.067216	
	0.5	4.33		4.326823	23.05765235		8.112792	37.72468	184.983	187.0619	859.2203	10676.53	1.089082	-1.08908	0.04337	0.085922	
	0.625	3.12		3.120185	17.46946504		5.850347	43.57503	184.983	102.2024	961.4228	10676.53	1.218626	-1.21863	0.057243	0.096142	
	0.75	4.46		4.460293	16.99659876		8.363049	51.93808	184.983	142.1434	1103.566	10676.53	1.398796	-1.3988	0.058835	0.110357	
	0.875	1.93		1.933948	32.72269321		3.626152	55.56423	184.983	118.6575	1222.224	10676.53	1.549197	-1.5492	0.03056	0.122222	
	1	1.47		1.473289	115.0846037		2.762417	58.32665	184.983	317.9117	1540.135	10676.53	1.952158	-1.95216	0.008689	0.154014	
	1.25	2.09		2.094568	108.2549726		7.854631	66.18128	184.983	850.3029	2390.438	10676.53	3.029937	-3.02994	0.009237	0.239044	
	1.5	1.58		1.580022	50.99196051		5.925081	72.10636	184.983	302.1315	2692.57	10676.53	3.412895	-3.4129	0.019611	0.269257	
	1.75	2.92		2.916021	30.4121906		10.93508	83.04144	184.983	332.5597	3025.129	10676.53	3.834423	-3.83442	0.032882	0.302513	
	2	3.30		3.301446	21.65942353		12.38042	95.42186	184.983	268.1528	3293.282	10676.53	4.174313	-4.17431	0.046169	0.329328	
	2.25	1.76		1.762983	55.60089583		6.611186	102.033	184.983	367.5879	3660.87	10676.53	4.640239	-4.64024	0.017985	0.366087	
	2.5	1.39		1.394189	73.54828194		5.228207	107.2613	184.983	384.5257	4045.396	10676.53	5.127634	-5.12763	0.013597	0.40454	
	2.75	1.86		1.857732	231.091832		6.966497	114.2277	184.983	1609.901	5655.296	10676.53	7.168221	-7.16822	0.004327	0.56553	
	3	1.08		1.083729	123.979497		4.063982	118.2917	184.983	503.8504	6159.147	10676.53	7.806863	-7.80686	0.008066	0.615915	
	3.5	1.15		1.149743	65.40670355		8.623074	126.9148	184.983	564.0069	6723.154	10676.53	8.521755	-8.52176	0.015289	0.672315	
	4	1.04		1.043333	61.12402034		7.824994	134.7398	184.983	478.2951	7201.449	10676.53	9.128005	-9.12801	0.01636	0.720145	
	4.5	1.81		1.811471	138.9340273		13.58603	148.3258	184.983	1887.562	9089.01	10676.53	11.52053	-11.5205	0.007198	0.908901	
	5	1.47		1.468714	56.54545984		11.01536	159.3412	184.983	622.8684	9711.879	10676.53	12.31003	-12.31	0.017685	0.971188	
	5.5	1.29		1.286475	43.81374141		9.648566	168.9898	184.983	422.7398	10134.62	10676.53	12.84587	-12.8459	0.022824	1.013462	
	6	2.13		2.132437	33.88381178		15.99328	184.983	184.983	541.9133	10676.53	10676.53	13.53276	-13.5328	0.029513	1.067653	

APPENDIX 2

SUPPORTING INFORMATION FOR CHAPTER 3

Appendix 2.1 contains a summary of the Water Drop Penetration Time (WDPT) and the Ethanol Percentage Test (EPT) collected in the laboratory for each of the vegetation plots up to the 50 cm depths. These tests were performed to observe the presence and severity of surface soil hydrophobicity where drop penetration below 3 seconds is considered hydrophilic (not water repellent). Samples below the 50 cm depths were not included because hydrophobicity did not manifest in any of the samples and drop penetrations were less than 3 seconds. Appendix 2.2 shows the summary of the soil organic carbon data obtained from 20 mg of sediment samples through the combustion method. Appendix 2.3 displays ^{1}H NMR data provided by Dr. Martha Morton used to evaluate the presence of aliphatic and other hydrophobic compounds in the surface soil sediments samples of each vegetation type. Appendix 2.4 contains mini-disk field water infiltration data used to determine surface layer unsaturated hydraulic conductivity, sorptivity, and hydrophobicity index in conjunction with ethanol infiltration data, which is not included in the appendices.

Appendix 2.1 Water Drop Penetration (WDPT) data

		G1							G2							PS1							PS2						
Depth (cm)	Trial	WDPT (s)	EPT (ethanol %)						WDPT(s)	EPT (ethanol %)						WDPT(s)	EPT (ethanol %)						WDPT(s)	EPT (ethanol %)					
0-12.5		0	3	5	8.5	13	24	36	0	3	5	8.5	13	24	36	0	3	5	8.5	13	24	36	0	3	5	8.5	13	24	36
	1	3	3	3	3	3	3	3	3	3	3	3	3	3	3	740	20	5	3	3	3	3	652	20	10	5	3	3	3
	2	3	3	3	3	3	3	3	3	3	3	3	3	3	3	63	20	5	3	3	3	3	417	19	10	5	3	3	3
	3	3	3	3	3	3	3	3	3	3	3	3	3	3	3	657	20	5	3	3	3	3	35	17	10	9	3	3	3
	4	3	3	3	3	3	3	3	3	3	3	3	3	3	3	662	20	5	3	3	3	3	812	16	10	3	3	3	3
	5	3	3	3	3	3	3	3	3	3	3	3	3	3	3	8	20	5	3	3	3	3	638	13	10	5	3	3	3
12.5-25	1	3	3	3	3	3	3	3	3	3	3	3	3	3	3	3	3	3	3	3	3	3	3	6	6	5	3	3	3
	2	3	3	3	3	3	3	3	3	3	3	3	3	3	3	3	3	3	3	3	3	3	190	5	5	5	3	3	3
	3	3	3	3	3	3	3	3	3	3	3	3	3	3	3	3	3	3	3	3	3	3	203	3	6	5	3	3	3
	4	3	3	3	3	3	3	3	3	3	3	3	3	3	3	3	3	3	3	3	3	3	238	3	5	5	3	3	3
	5	3	3	3	3	3	3	3	3	3	3	3	3	3	3	3	3	3	3	3	3	3	3	7	3	5	3	3	3
25-37.5	1	3	3	3	3	3	3	3	3	3	3	3	3	3	3	3	3	3	3	3	3	3	3	3	3	3	3	3	3
	2	3	3	3	3	3	3	3	3	3	3	3	3	3	3	3	3	3	3	3	3	3	3	3	3	3	3	3	3
	3	3	3	3	3	3	3	3	3	3	3	3	3	3	3	3	3	3	3	3	3	3	3	3	3	3	3	3	3
	4	3	3	3	3	3	3	3	3	3	3	3	3	3	3	3	3	3	3	3	3	3	3	3	3	3	3	3	3
	5	3	3	3	3	3	3	3	3	3	3	3	3	3	3	3	3	3	3	3	3	3	3	3	3	3	3	3	3
37.5-50	1	3	3	3	3	3	3	3	3	3	3	3	3	3	3	3	3	3	3	3	3	3	3	3	3	3	3	3	3
	2	3	3	3	3	3	3	3	3	3	3	3	3	3	3	3	3	3	3	3	3	3	3	3	3	3	3	3	3
	3	3	3	3	3	3	3	3	3	3	3	3	3	3	3	3	3	3	3	3	3	3	3	3	3	3	3	3	3
	4	3	3	3	3	3	3	3	3	3	3	3	3	3	3	3	3	3	3	3	3	3	3	3	3	3	3	3	3
	5	3	3	3	3	3	3	3	3	3	3	3	3	3	3	3	3	3	3	3	3	3	3	3	3	3	3	3	3

		TP1								TP2							DP1							DP2						
Depth (cm)	Trial	WDPT(s)	EPT (ethanol %)						WDPT(s)	EPT (ethanol %)						WDPT(s)	EPT (ethanol %)						WDPT(s)	EPT (ethanol %)					
0-12.5		0	3	5	8.5	13	24	36	0	3	5	8.5	13	24	36	0	3	5	8.5	13	24	36	0	3	5	8.5	13	24	36
	1	210	110	3	3	3	3	3	827	86	131	5	5	3	3	617	8	3	5	3	3	3	640	5	5	4	3	3	3
	2	682	335	51	3	3	3	3	654	74	89	5	5	3	3	419	3	20	5	3	3	3	807	5	5	4	3	3	3
	3	618	335	3	3	3	3	3	11	21	65	5	5	3	3	960	6	110	5	3	3	3	662	5	5	4	3	3	3
	4	170	212	5	3	3	3	3	18	14	29	5	5	3	3	748	5	67	5	3	3	3	337	6	5	4	3	3	3
	5	735	110	5	3	3	3	3	612	112	12	5	5	3	3	26	5	49	5	3	3	3	780	5	5	4	3	3	3
12.5-25	1	148	3	7	3	3	3	3	67	5	5	3	3	3	3	3	5	3	3	3	3	3	3	3	3	3	3	3	3
	2	120	3	5	3	3	3	3	15	5	5	3	3	3	3	34	3	3	3	3	3	3	3	3	3	3	3	3	3
	3	40	47	5	3	3	3	3	25	3	5	3	3	3	3	3	3	3	3	3	3	3	3	3	3	3	3	3	3
	4	190	21	3	3	3	3	3	10	3	5	3	3	3	3	3	5	3	3	3	3	3	3	3	3	3	3	3	3
	5	25	60	9	3	3	3	3	3	5	5	3	3	3	3	5	5	3	3	3	3	3	3	3	3	3	3	3	3
25-37.5	1	12	3	3	3	3	3	3	3	3	3	3	3	3	3	3	3	3	3	3	3	3	3	3	3	3	3	3	3
	2	9	3	3	3	3	3	3	3	3	3	3	3	3	3	3	3	3	3	3	3	3	3	3	3	3	3	3	3
	3	3	3	3	3	3	3	3	3	3	3	3	3	3	3	3	3	3	3	3	3	3	3	3	3	3	3	3	3
	4	23	3	3	3	3	3	3	3	3	3	3	3	3	3	3	3	3	3	3	3	3	3	3	3	3	3	3	3
	5	3	3	3	3	3	3	3	3	3	3	3	3	3	3	3	3	3	3	3	3	3	3	3	3	3	3	3	3
37.5-50	1	7	3	3	3	3	3	3	3	3	3	3	3	3	3	3	3	3	3	3	3	3	3	3	3	3	3	3	3
	2	5	3	3	3	3	3	3	3	3	3	3	3	3	3	3	3	3	3	3	3	3	3	3	3	3	3	3	3
	3	3	3	3	3	3	3	3	3	3	3	3	3	3	3	3	3	3	3	3	3	3	3	3	3	3	3	3	3
	4	9	3	3	3	3	3	3	3	3	3	3	3	3	3	3	3	3	3	3	3	3	3	3	3	3	3	3	3
	5	3	3	3	3	3	3	3	3	3	3	3	3	3	3	3	3	3	3	3	3	3	3	3	3	3	3	3	3

		SV							DC						
Depth (cm)	Trial	WDPT(s)	EPT (ethanol %)						WDPT(s)	EPT (ethanol %)					
0-12.5		0	3	5	8.5	13	24	36	0	3	5	8.5	13	24	36
	1	184	5	6	3	3	3	3	3	3	3	3	3	3	3
	2	207	7	5	3	3	3	3	3	3	3	3	3	3	3
	3	67	5	5	3	3	3	3	3	3	3	3	3	3	3
	4	192	5	3	3	3	3	3	3	3	3	3	3	3	3
	5	15	5	5	3	3	3	3	3	3	3	3	3	3	3
12.5-25	1	3	3	3	3	3	3	3	3	3	3	3	3	3	3
	2	3	3	3	3	3	3	3	3	3	3	3	3	3	3
	3	3	3	3	3	3	3	3	3	3	3	3	3	3	3
	4	3	3	3	3	3	3	3	3	3	3	3	3	3	3
	5	3	3	3	3	3	3	3	3	3	3	3	3	3	3
25-37.5	1	3	3	3	3	3	3	3	3	3	3	3	3	3	3
	2	3	3	3	3	3	3	3	3	3	3	3	3	3	3
	3	3	3	3	3	3	3	3	3	3	3	3	3	3	3
	4	3	3	3	3	3	3	3	3	3	3	3	3	3	3
	5	3	3	3	3	3	3	3	3	3	3	3	3	3	3
37.5-50	1	3	3	3	3	3	3	3	3	3	3	3	3	3	3
	2	3	3	3	3	3	3	3	3	3	3	3	3	3	3
	3	3	3	3	3	3	3	3	3	3	3	3	3	3	3
	4	3	3	3	3	3	3	3	3	3	3	3	3	3	3
	5	3	3	3	3	3	3	3	3	3	3	3	3	3	3

Appendix 2.2 Soil organic carbon laboratory data

Investigator:	Zablon Adane
Description:	Organic Carbon
Instrument:	Costech ECS 4010

	Organic carbon (%)									
Depth (cm)	**G1**	**G2**	**PS1**	**PS2**	**TP1**	**TP2**	**DP1**	**DP2**	**SV**	**DC**
12	0.667	0.685	1.416	0.820	0.517	2.640	1.129	0.429	0.676	0.609
25	0.571	0.391	0.450	0.857	0.456	0.752	0.307	0.228	0.351	0.339
37	0.393	0.281	0.310	0.523	0.381	0.488	0.241	0.161	0.241	0.312
50	0.154	0.229	0.215	0.431	0.254	0.328	0.160	0.162	0.173	0.220
62	0.117	0.147	0.147	0.194	0.217	0.239	0.124	0.124	0.133	0.164
75	0.111	0.171	0.144	0.143	0.156	0.181	0.097	0.108	0.108	0.122
87	0.114	0.173	0.118	0.171	0.109	0.133	0.110	0.071	0.116	0.093
100	0.071	0.167	0.097	0.109	0.162	0.123	0.093	0.082	0.089	0.116
125	0.073	0.145	0.082	0.099	0.091	0.108	0.076	0.067	0.104	0.092
150	0.039	0.205	0.094	0.112	0.094	0.177	0.069	0.048	0.064	0.084
175	0.051	0.250	0.042	0.079	0.080	0.084	0.061	0.072	0.075	0.071
200	0.053	0.186	0.066	0.050	0.063	0.087	0.066	0.069	0.057	0.066

Appendix 2.3 ^{1}H NMR laboratory data

		1H NMR Area under the curve					
Plot	Depth(cm)	10-8.5	8.5-6.5	6.5-3.2	3.2-0.5	sum_8.5-6.5_3.2-0.5	Ratio
G1	12	0.02	3.46	2.68	93.83	97.29	2.75
	25	0.00	4.49	2.58	92.93	97.42	2.65
	37	0.00	4.05	2.31	89.66	93.71	2.47
	50	0.06	2.94	4.35	92.64	95.58	4.55
TP1	12	0.00	2.70	5.04	92.25	94.95	5.31
	25	0.06	3.19	4.60	93.15	96.34	4.77
	37	0.02	3.60	2.80	93.58	97.18	2.88
	50	0.02	3.71	2.95	93.31	97.02	3.04
PS1	12	0.03	2.52	4.30	94.17	96.69	4.45
	25	0.00	4.02	2.30	93.68	97.70	2.35
	37	0.00	6.68	1.95	91.37	98.05	1.99
	50	0.00	5.98	1.99	92.02	98.00	2.03
PS2	12	0.03	4.53	3.59	91.86	96.39	3.72
	25	0.05	4.46	7.66	87.83	92.29	8.30
	37	0.00	5.69	3.23	91.09	96.78	3.34
	50	0.00	4.49	2.87	92.65	97.14	2.95
TP2	12	0.04	2.64	8.74	88.58	91.22	9.58
	25	0.03	3.12	4.22	92.68	95.80	4.41
	37	0.04	4.85	3.20	91.92	96.77	3.31
	50	0.02	5.24	2.61	92.14	97.38	2.68
G2	12	0.01	4.73	2.34	92.93	97.66	2.40
	25	0.00	0.07	0.02	1.00	1.07	1.87
	37	0.00	5.23	1.96	92.80	98.03	2.00
	50	0.00	6.51	1.96	91.52	98.03	2.00
DP1	12	0.05	2.92	8.97	88.06	90.98	9.86
	25	0.00	0.05	0.02	1.00	1.05	1.90
	37	0.00	5.66	2.86	91.47	97.13	2.94
	50	0.00	7.04	1.74	91.22	98.26	1.77
DP2	12	0.03	3.46	3.44	93.28	96.74	3.56
	25	0.04	4.74	2.59	92.62	97.36	2.66
	37	0.01	4.06	2.02	93.91	97.97	2.06
	50	0.00	5.32	2.25	92.43	97.75	2.30
SV	12	0.05	3.35	4.08	92.52	95.87	4.26
	25	0.00	4.04	2.33	93.62	97.66	2.39
	37	0.01	3.62	2.44	93.94	97.56	2.50
	50	0.01	4.60	3.14	92.25	96.85	3.24
DC	12	0.05	3.11	4.24	94.06	97.17	4.36
	25	0.03	3.32	3.21	93.45	96.77	3.32
	37	0.00	4.10	1.99	93.91	98.01	2.03
	50	*	*	*	*	*	*

Appendix 2.4 Mini-disk filed infiltration data

G1				G2				PS1				PS2			
Time (s)	sqrt (t)	Volume (mL)	Infilt (cm)	Time (s)	sqrt (t)	Volume (mL)	Infilt (cm)	Time (s)	sqrt (t)	Volume (mL)	Infilt (cm)	Time (s)	sqrt (t)	Volume (mL)	Infilt (cm)
0	0	62	0	0	0	58	0	0	0	62	0	0	0	62	0
5	2.236068	61	0.062893	5	2.236068	57	0.062893	5	2.236068	62	0	5	2.236068	62	0
10	3.162278	60	0.125786	10	3.162278	56	0.125786	10	3.162278	62	0	10	3.162278	62	0
15	3.872983	58	0.251572	15	3.872983	56	0.125786	15	3.872983	62	0	15	3.872983	62	0
20	4.472136	57	0.314465	20	4.472136	55	0.188679	20	4.472136	62	0	20	4.472136	62	0
25	5	56	0.377358	25	5	55	0.188679	25	5	60	0.125786	25	5	62	0
30	5.477226	55	0.440252	30	5.477226	54	0.251572	30	5.477226	60	0.125786	30	5.477226	62	0
35	5.91608	54	0.503145	35	5.91608	54	0.251572	35	5.91608	60	0.125786	35	5.91608	62	0
40	6.324555	54	0.503145	40	6.324555	53	0.314465	40	6.324555	60	0.125786	40	6.324555	60	0.125786
45	6.708204	53	0.566038	45	6.708204	53	0.314465	45	6.708204	60	0.125786	45	6.708204	60	0.125786
50	7.071068	52	0.628931	50	7.071068	53	0.314465	50	7.071068	59	0.188679	50	7.071068	60	0.125786
55	7.416198	51	0.691824	55	7.416198	52	0.377358	55	7.416198	59	0.188679	55	7.416198	60	0.125786
60	7.745967	50	0.754717	60	7.745967	52	0.377358	60	7.745967	59	0.188679	60	7.745967	60	0.125786
65	8.062258	49	0.81761	65	8.062258	52	0.377358	65	8.062258	59	0.188679	65	8.062258	60	0.125786
70	8.3666	48	0.880503	70	8.3666	52	0.377358	70	8.3666	59	0.188679	70	8.3666	60	0.125786
75	8.660254	47	0.943396	75	8.660254	51	0.440252	75	8.660254	57	0.314465	75	8.660254	60	0.125786
80	8.944272	47	0.943396	80	8.944272	51	0.440252	80	8.944272	57	0.314465	80	8.944272	59	0.188679
85	9.219544	46	1.006289	85	9.219544	51	0.440252	85	9.219544	57	0.314465	85	9.219544	59	0.188679
90	9.486833	45	1.069182	90	9.486833	50	0.503145	90	9.486833	57	0.314465	90	9.486833	59	0.188679
95	9.746794	44	1.132075	95	9.746794	50	0.503145	95	9.746794	57	0.314465	95	9.746794	59	0.188679
100	10	44	1.132075	100	10	50	0.503145	100	10	56	0.377358	100	10	59	0.188679
105	10.24695	43	1.194969	105	10.24695	50	0.503145	105	10.24695	56	0.377358	105	10.24695	59	0.188679
110	10.48809	42	1.257862	110	10.48809	49	0.566038	110	10.48809	56	0.377358	110	10.48809	59	0.188679
115	10.72381	41	1.320755	115	10.72381	49	0.566038	115	10.72381	56	0.377358	115	10.72381	59	0.188679
120	10.95445	40	1.383648	120	10.95445	49	0.566038	120	10.95445	55	0.440252	120	10.95445	58	0.251572
125	11.18034	40	1.383648	125	11.18034	49	0.566038	125	11.18034	55	0.440252	125	11.18034	58	0.251572
130	11.40175	39	1.446541	130	11.40175	48	0.628931	130	11.40175	55	0.440252	130	11.40175	58	0.251572
135	11.61895	38	1.509434	135	11.61895	48	0.628931	135	11.61895	55	0.440252	135	11.61895	58	0.251572
140	11.83216	37	1.572327	140	11.83216	48	0.628931	140	11.83216	55	0.440252	140	11.83216	58	0.251572
145	12.04159	36	1.63522	145	12.04159	48	0.628931	145	12.04159	55	0.440252	145	12.04159	58	0.251572
150	12.24745	36	1.63522	150	12.24745	47	0.691824	150	12.24745	54	0.503145	150	12.24745	57	0.314465
155	12.4499	35	1.698113	155	12.4499	47	0.691824	155	12.4499	54	0.503145	155	12.4499	57	0.314465
160	12.64911	34	1.761006	160	12.64911	47	0.691824	160	12.64911	54	0.503145	160	12.64911	57	0.314465
165	12.84523	33	1.823899	165	12.84523	47	0.691824	165	12.84523	54	0.503145	165	12.84523	57	0.314465
170	13.0384	32	1.886792	170	13.0384	47	0.691824	170	13.0384	54	0.503145	170	13.0384	57	0.314465
175	13.22876	32	1.886792	175	13.22876	46	0.754717	175	13.22876	54	0.503145	175	13.22876	57	0.314465
180	13.41641	31	1.949686	180	13.41641	46	0.754717	180	13.41641	53	0.566038	180	13.41641	56	0.377358
185	13.60147	30	2.012579	185	13.60147	46	0.754717	185	13.60147	53	0.566038	185	13.60147	56	0.377358
190	13.78405	29	2.075472	190	13.78405	46	0.754717	190	13.78405	53	0.566038	190	13.78405	56	0.377358
195	13.96424	28	2.138365	195	13.96424	45	0.81761	195	13.96424	53	0.566038	195	13.96424	56	0.377358
200	14.14214	28	2.138365	200	14.14214	45	0.81761	200	14.14214	52	0.628931	200	14.14214	56	0.377358
205	14.31782	27	2.201258	205	14.31782	45	0.81761	205	14.31782	52	0.628931	205	14.31782	56	0.377358
210	14.49138	27	2.201258	210	14.49138	45	0.81761	210	14.49138	52	0.628931	210	14.49138	55	0.440252
215	14.66288	26	2.264151	215	14.66288	45	0.81761	215	14.66288	52	0.628931	215	14.66288	55	0.440252
220	14.8324	25	2.327044	220	14.8324	44	0.880503	220	14.8324	52	0.628931	220	14.8324	55	0.440252
225	15	24	2.389937	225	15	44	0.880503	225	15	52	0.628931	225	15	55	0.440252
230	15.16575	23	2.45283	230	15.16575	44	0.880503	230	15.16575	52	0.628931	230	15.16575	55	0.440252
235	15.32971	22	2.515723	235	15.32971	44	0.880503	235	15.32971	51	0.691824	235	15.32971	55	0.440252
240	15.49193	21	2.578616	240	15.49193	44	0.880503	240	15.49193	51	0.691824	240	15.49193	55	0.440252
245	15.65248	21	2.578616	245	15.65248	44	0.880503	245	15.65248	51	0.691824	245	15.65248	55	0.440252
250	15.81139	20	2.641509	250	15.81139	43	0.943396	250	15.81139	51	0.691824	250	15.81139	55	0.440252
255	15.96872	20	2.641509	255	15.96872	43	0.943396	255	15.96872	51	0.691824	255	15.96872	55	0.440252
260	16.12452	19	2.704403	260	16.12452	43	0.943396	260	16.12452	51	0.691824	260	16.12452	55	0.440252
265	16.27882	19	2.704403	265	16.27882	42	1.006289	265	16.27882	51	0.691824	265	16.27882	55	0.440252
270	16.43168	18	2.767296	270	16.43168	42	1.006289	270	16.43168	50	0.754717	270	16.43168	54	0.503145
275	16.58312	17	2.830189	275	16.58312	42	1.006289	275	16.58312	50	0.754717	275	16.58312	54	0.503145
280	16.7332	17	2.830189	280	16.7332	41	1.069182	280	16.7332	50	0.754717	280	16.7332	54	0.503145
285	16.88194	16	2.893082	285	16.88194	41	1.069182	285	16.88194	50	0.754717	285	16.88194	54	0.503145
290	17.02939	15	2.955975	290	17.02939	41	1.069182	290	17.02939	50	0.754717	290	17.02939	54	0.503145
295	17.17556	15	2.955975	295	17.17556	41	1.069182	295	17.17556	50	0.754717	295	17.17556	54	0.503145
300	17.32051	14	3.018868	300	17.32051	41	1.069182	300	17.32051	49	0.81761	300	17.32051	53	0.566038
305	17.46425	13	3.081761	305	17.46425	41	1.069182	305	17.46425	49	0.81761	305	17.46425	53	0.566038
310	17.60682	13	3.081761	310	17.60682	40	1.132075	310	17.60682	49	0.81761	310	17.60682	53	0.566038
315	17.74824	12	3.144654	315	17.74824	40	1.132075	315	17.74824	49	0.81761	315	17.74824	53	0.566038
320	17.88854	11	3.207547	320	17.88854	40	1.132075	320	17.88854	49	0.81761	320	17.88854	53	0.566038
325	18.02776	11	3.207547	325	18.02776	40	1.132075	325	18.02776	49	0.81761	325	18.02776	53	0.566038
330	18.1659	10	3.27044	330	18.1659	39	1.194969	330	18.1659	49	0.81761	330	18.1659	52	0.628931

TP1				TP2				DP1				DP2			
Time (s)	sqrt (t)	Volume (mL)	Infilt (cm)	Time (s)	sqrt (t)	Volume (mL)	Infilt (cm)	Time (s)	sqrt (t)	Volume (mL)	Infilt (cm)	Time (s)	sqrt (t)	Volume (mL)	Infilt (cm)
0	0	72	0	0	0	63	0	0	0	61	0	0	0	60	0
5	2.236068	72	0	5	2.236068	62	0.062893	5	2.236068	61	0	5	2.236068	60	0
10	3.162278	72	0	10	3.162278	62	0.062893	10	3.162278	61	0	10	3.162278	60	0
15	3.872983	72	0	15	3.872983	62	0.062893	15	3.872983	61	0	15	3.872983	60	0
20	4.472136	72	0	20	4.472136	62	0.062893	20	4.472136	61	0	20	4.472136	60	0
25	5	72	0	25	5	62	0.062893	25	5	61	0	25	5	60	0
30	5.477226	72	0	30	5.477226	62	0.062893	30	5.477226	61	0	30	5.477226	60	0
35	5.91608	72	0	35	5.91608	61	0.125786	35	5.91608	61	0	35	5.91608	60	0
40	6.324555	72	0	40	6.324555	61	0.125786	40	6.324555	61	0	40	6.324555	60	0
45	6.708204	72	0	45	6.708204	61	0.125786	45	6.708204	61	0	45	6.708204	60	0
50	7.071068	72	0	50	7.071068	61	0.125786	50	7.071068	61	0	50	7.071068	60	0
55	7.416198	72	0	55	7.416198	61	0.125786	55	7.416198	61	0	55	7.416198	60	0
60	7.745967	72	0	60	7.745967	61	0.125786	60	7.745967	60	0.062893	60	7.745967	60	0
65	8.062258	72	0	65	8.062258	61	0.125786	65	8.062258	60	0.062893	65	8.062258	60	0
70	8.3666	72	0	70	8.3666	61	0.125786	70	8.3666	60	0.062893	70	8.3666	60	0
75	8.660254	72	0	75	8.660254	61	0.125786	75	8.660254	60	0.062893	75	8.660254	60	0
80	8.944272	72	0	80	8.944272	61	0.125786	80	8.944272	60	0.062893	80	8.944272	60	0
85	9.219544	72	0	85	9.219544	61	0.125786	85	9.219544	60	0.062893	85	9.219544	60	0
90	9.486833	72	0	90	9.486833	61	0.125786	90	9.486833	60	0.062893	90	9.486833	59	0.062893
95	9.746794	72	0	95	9.746794	61	0.125786	95	9.746794	60	0.062893	95	9.746794	59	0.062893
100	10	72	0	100	10	61	0.125786	100	10	60	0.062893	100	10	59	0.062893
105	10.24695	72	0	105	10.24695	61	0.125786	105	10.24695	60	0.062893	105	10.24695	59	0.062893
110	10.48809	72	0	110	10.48809	61	0.125786	110	10.48809	60	0.062893	110	10.48809	59	0.062893
115	10.72381	72	0	115	10.72381	61	0.125786	115	10.72381	60	0.062893	115	10.72381	59	0.062893
120	10.95445	72	0	120	10.95445	61	0.125786	120	10.95445	59	0.125786	120	10.95445	59	0.062893
125	11.18034	72	0	125	11.18034	61	0.125786	125	11.18034	59	0.125786	125	11.18034	59	0.062893
130	11.40175	72	0	130	11.40175	61	0.125786	130	11.40175	59	0.125786	130	11.40175	59	0.062893
135	11.61895	72	0	135	11.61895	61	0.125786	135	11.61895	59	0.125786	135	11.61895	59	0.062893
140	11.83216	72	0	140	11.83216	61	0.125786	140	11.83216	59	0.125786	140	11.83216	59	0.062893
145	12.04159	72	0	145	12.04159	61	0.125786	145	12.04159	59	0.125786	145	12.04159	59	0.062893
150	12.24745	72	0	150	12.24745	61	0.125786	150	12.24745	59	0.125786	150	12.24745	58	0.125786
155	12.4499	72	0	155	12.4499	61	0.125786	155	12.4499	59	0.125786	155	12.4499	58	0.125786
160	12.64911	72	0	160	12.64911	61	0.125786	160	12.64911	59	0.125786	160	12.64911	58	0.125786
165	12.84523	72	0	165	12.84523	61	0.125786	165	12.84523	59	0.125786	165	12.84523	58	0.125786
170	13.0384	72	0	170	13.0384	61	0.125786	170	13.0384	59	0.125786	170	13.0384	58	0.125786
175	13.22876	72	0	175	13.22876	61	0.125786	175	13.22876	59	0.125786	175	13.22876	58	0.125786
180	13.41641	72	0	180	13.41641	61	0.125786	180	13.41641	59	0.125786	180	13.41641	58	0.125786
185	13.60147	72	0	185	13.60147	60	0.188679	185	13.60147	59	0.125786	185	13.60147	58	0.125786
190	13.78405	72	0	190	13.78405	60	0.188679	190	13.78405	59	0.125786	190	13.78405	58	0.125786
195	13.96424	72	0	195	13.96424	60	0.188679	195	13.96424	59	0.125786	195	13.96424	58	0.125786
200	14.14214	72	0	200	14.14214	60	0.188679	200	14.14214	59	0.125786	200	14.14214	58	0.125786
205	14.31782	72	0	205	14.31782	60	0.188679	205	14.31782	59	0.125786	205	14.31782	58	0.125786
210	14.49138	71	0.062893	210	14.49138	60	0.188679	210	14.49138	59	0.125786	210	14.49138	58	0.125786
215	14.66288	71	0.062893	215	14.66288	60	0.188679	215	14.66288	59	0.125786	215	14.66288	58	0.125786
220	14.8324	71	0.062893	220	14.8324	60	0.188679	220	14.8324	59	0.125786	220	14.8324	58	0.125786
225	15	71	0.062893	225	15	60	0.188679	225	15	59	0.125786	225	15	58	0.125786
230	15.16575	71	0.062893	230	15.16575	60	0.188679	230	15.16575	59	0.125786	230	15.16575	58	0.125786
235	15.32971	71	0.062893	235	15.32971	60	0.188679	235	15.32971	59	0.125786	235	15.32971	58	0.125786
240	15.49193	71	0.062893	240	15.49193	60	0.188679	240	15.49193	58	0.188679	240	15.49193	58	0.125786
245	15.65248	71	0.062893	245	15.65248	60	0.188679	245	15.65248	58	0.188679	245	15.65248	58	0.125786
250	15.81139	71	0.062893	250	15.81139	60	0.188679	250	15.81139	58	0.188679	250	15.81139	58	0.125786
255	15.96872	71	0.062893	255	15.96872	60	0.188679	255	15.96872	58	0.188679	255	15.96872	58	0.125786
260	16.12452	71	0.062893	260	16.12452	60	0.188679	260	16.12452	58	0.188679	260	16.12452	58	0.125786
265	16.27882	71	0.062893	265	16.27882	60	0.188679	265	16.27882	58	0.188679	265	16.27882	58	0.125786
270	16.43168	71	0.062893	270	16.43168	60	0.188679	270	16.43168	58	0.188679	270	16.43168	57	0.188679
275	16.58312	71	0.062893	275	16.58312	60	0.188679	275	16.58312	58	0.188679	275	16.58312	57	0.188679
280	16.7332	71	0.062893	280	16.7332	60	0.188679	280	16.7332	58	0.188679	280	16.7332	57	0.188679
285	16.88194	71	0.062893	285	16.88194	60	0.188679	285	16.88194	58	0.188679	285	16.88194	57	0.188679
290	17.02939	71	0.062893	290	17.02939	60	0.188679	290	17.02939	58	0.188679	290	17.02939	57	0.188679
295	17.17556	71	0.062893	295	17.17556	60	0.188679	295	17.17556	58	0.188679	295	17.17556	57	0.188679
300	17.32051	71	0.062893	300	17.32051	60	0.188679	300	17.32051	58	0.188679	300	17.32051	57	0.188679
305	17.46425	71	0.062893	305	17.46425	59	0.251572	305	17.46425	58	0.188679	305	17.46425	57	0.188679
310	17.60682	71	0.062893	310	17.60682	59	0.251572	310	17.60682	58	0.188679	310	17.60682	57	0.188679
315	17.74824	71	0.062893	315	17.74824	59	0.251572	315	17.74824	58	0.188679	315	17.74824	57	0.188679
320	17.88854	71	0.062893	320	17.88854	59	0.251572	320	17.88854	58	0.188679	320	17.88854	57	0.188679
325	18.02776	71	0.062893	325	18.02776	59	0.251572	325	18.02776	58	0.188679	325	18.02776	57	0.188679
330	18.1659	71	0.062893	330	18.1659	59	0.251572	330	18.1659	58	0.188679	330	18.1659	57	0.188679

TP1				TP2				DP1				DP2			
Time (s)	sqrt (t)	Volume (mL)	Infilt (cm)	Time (s)	sqrt (t)	Volume (mL)	Infilt (cm)	Time (s)	sqrt (t)	Volume (mL)	Infilt (cm)	Time (s)	sqrt (t)	Volume (mL)	Infilt (cm)
345	18.57418	71	0.062893	345	18.57418	59	0.251572	345	18.57418	58	0.188679	345	18.57418	57	0.188679
350	18.70829	71	0.062893	350	18.70829	59	0.251572	350	18.70829	58	0.188679	350	18.70829	57	0.188679
355	18.84144	71	0.062893	355	18.84144	59	0.251572	355	18.84144	58	0.188679	355	18.84144	57	0.188679
360	18.97367	71	0.062893	360	18.97367	59	0.251572	360	18.97367	57	0.251572	360	18.97367	57	0.188679
365	19.10497	71	0.062893	365	19.10497	59	0.251572	365	19.10497	57	0.251572	365	19.10497	57	0.188679
370	19.23538	71	0.062893	370	19.23538	59	0.251572	370	19.23538	57	0.251572	370	19.23538	57	0.188679
375	19.36492	70	0.125786	375	19.36492	59	0.251572	375	19.36492	57	0.251572	375	19.36492	57	0.188679
380	19.49359	70	0.125786	380	19.49359	59	0.251572	380	19.49359	57	0.251572	380	19.49359	57	0.188679
385	19.62142	70	0.125786	385	19.62142	59	0.251572	385	19.62142	57	0.251572	385	19.62142	57	0.188679
390	19.74842	70	0.125786	390	19.74842	59	0.251572	390	19.74842	57	0.251572	390	19.74842	57	0.188679
395	19.87461	70	0.125786	395	19.87461	59	0.251572	395	19.87461	57	0.251572	395	19.87461	57	0.188679
400	20	70	0.125786	400	20	59	0.251572	400	20	57	0.251572	400	20	57	0.188679
405	20.12461	70	0.125786	405	20.12461	59	0.251572	405	20.12461	57	0.251572	405	20.12461	57	0.188679
410	20.24846	70	0.125786	410	20.24846	59	0.251572	410	20.24846	57	0.251572	410	20.24846	57	0.188679
415	20.37155	70	0.125786	415	20.37155	59	0.251572	415	20.37155	57	0.251572	415	20.37155	57	0.188679
420	20.4939	70	0.125786	420	20.4939	59	0.251572	420	20.4939	57	0.251572	420	20.4939	56	0.251572
425	20.61553	70	0.125786	425	20.61553	58	0.314465	425	20.61553	57	0.251572	425	20.61553	56	0.251572
430	20.73644	70	0.125786	430	20.73644	58	0.314465	430	20.73644	57	0.251572	430	20.73644	56	0.251572
435	20.85665	70	0.125786	435	20.85665	58	0.314465	435	20.85665	57	0.251572	435	20.85665	56	0.251572
440	20.97618	70	0.125786	440	20.97618	58	0.314465	440	20.97618	57	0.251572	440	20.97618	56	0.251572
445	21.09502	70	0.125786	445	21.09502	58	0.314465	445	21.09502	57	0.251572	445	21.09502	56	0.251572
450	21.2132	70	0.125786	450	21.2132	58	0.314465	450	21.2132	57	0.251572	450	21.2132	56	0.251572
455	21.33073	70	0.125786	455	21.33073	58	0.314465	455	21.33073	57	0.251572	455	21.33073	56	0.251572
460	21.44761	70	0.125786	460	21.44761	58	0.314465	460	21.44761	57	0.251572	460	21.44761	56	0.251572
465	21.56386	70	0.125786	465	21.56386	58	0.314465	465	21.56386	57	0.251572	465	21.56386	56	0.251572
470	21.67948	70	0.125786	470	21.67948	58	0.314465	470	21.67948	57	0.251572	470	21.67948	56	0.251572
475	21.79449	70	0.125786	475	21.79449	58	0.314465	475	21.79449	57	0.251572	475	21.79449	56	0.251572
480	21.9089	70	0.125786	480	21.9089	58	0.314465	480	21.9089	57	0.251572	480	21.9089	56	0.251572
485	22.02272	70	0.125786	485	22.02272	58	0.314465	485	22.02272	57	0.251572	485	22.02272	56	0.251572
490	22.13594	70	0.125786	490	22.13594	58	0.314465	490	22.13594	57	0.251572	490	22.13594	56	0.251572
495	22.2486	70	0.125786	495	22.2486	58	0.314465	495	22.2486	57	0.251572	495	22.2486	56	0.251572
500	22.36068	70	0.125786	500	22.36068	58	0.314465	500	22.36068	57	0.251572	500	22.36068	56	0.251572
505	22.47221	70	0.125786	505	22.47221	58	0.314465	505	22.47221	57	0.251572	505	22.47221	56	0.251572
510	22.58318	70	0.125786	510	22.58318	58	0.314465	510	22.58318	56	0.314465	510	22.58318	56	0.251572
515	22.69361	70	0.125786	515	22.69361	58	0.314465	515	22.69361	56	0.314465	515	22.69361	56	0.251572
520	22.80351	70	0.125786	520	22.80351	58	0.314465	520	22.80351	56	0.314465	520	22.80351	56	0.251572
525	22.91288	70	0.125786	525	22.91288	58	0.314465	525	22.91288	56	0.314465	525	22.91288	56	0.251572
530	23.02173	70	0.125786	530	23.02173	58	0.314465	530	23.02173	56	0.314465	530	23.02173	56	0.251572
535	23.13007	70	0.125786	535	23.13007	58	0.314465	535	23.13007	56	0.314465	535	23.13007	56	0.251572
540	23.2379	70	0.125786	540	23.2379	58	0.314465	540	23.2379	56	0.314465	540	23.2379	56	0.251572
545	23.34524	70	0.125786	545	23.34524	58	0.314465	545	23.34524	56	0.314465	545	23.34524	56	0.251572
550	23.45208	70	0.125786	550	23.45208	58	0.314465	550	23.45208	56	0.314465	550	23.45208	56	0.251572
555	23.55844	70	0.125786	555	23.55844	58	0.314465	555	23.55844	56	0.314465	555	23.55844	56	0.251572
560	23.66432	70	0.125786	560	23.66432	58	0.314465	560	23.66432	56	0.314465	560	23.66432	56	0.251572
565	23.76973	70	0.125786	565	23.76973	58	0.314465	565	23.76973	56	0.314465	565	23.76973	56	0.251572
570	23.87467	70	0.125786	570	23.87467	58	0.314465	570	23.87467	56	0.314465	570	23.87467	56	0.251572
575	23.97916	70	0.125786	575	23.97916	58	0.314465	575	23.97916	56	0.314465	575	23.97916	56	0.251572
580	24.08319	70	0.125786	580	24.08319	58	0.314465	580	24.08319	56	0.314465	580	24.08319	56	0.251572
585	24.18677	70	0.125786	585	24.18677	58	0.314465	585	24.18677	56	0.314465	585	24.18677	56	0.251572
590	24.28992	70	0.125786	590	24.28992	58	0.314465	590	24.28992	56	0.314465	590	24.28992	56	0.251572
595	24.39262	70	0.125786	595	24.39262	58	0.314465	595	24.39262	56	0.314465	595	24.39262	56	0.251572
600	24.4949	69	0.188679	600	24.4949	58	0.314465	600	24.4949	55	0.377358	600	24.4949	56	0.251572
605	24.59675	69	0.188679	605	24.59675	58	0.314465	605	24.59675	55	0.377358	605	24.59675	56	0.251572
610	24.69818	69	0.188679	610	24.69818	58	0.314465	610	24.69818	55	0.377358	610	24.69818	56	0.251572
615	24.79919	69	0.188679	615	24.79919	58	0.314465	615	24.79919	55	0.377358	615	24.79919	56	0.251572
620	24.8998	69	0.188679	620	24.8998	58	0.314465	620	24.8998	55	0.377358	620	24.8998	56	0.251572
625	25	69	0.188679	625	25	58	0.314465	625	25	55	0.377358	625	25	56	0.251572
630	25.0998	69	0.188679	630	25.0998	58	0.314465	630	25.0998	55	0.377358	630	25.0998	56	0.251572
635	25.19921	69	0.188679	635	25.19921	58	0.314465	635	25.19921	55	0.377358	635	25.19921	56	0.251572
640	25.29822	69	0.188679	640	25.29822	58	0.314465	640	25.29822	55	0.377358	640	25.29822	56	0.251572
645	25.39685	69	0.188679	645	25.39685	58	0.314465	645	25.39685	55	0.377358	645	25.39685	56	0.251572
650	25.4951	69	0.188679	650	25.4951	58	0.314465	650	25.4951	55	0.377358	650	25.4951	56	0.251572
655	25.59297	69	0.188679	655	25.59297	58	0.314465	655	25.59297	55	0.377358	655	25.59297	56	0.251572
660	25.69047	69	0.188679	660	25.69047	58	0.314465	660	25.69047	55	0.377358	660	25.69047	55	0.314465

TP1				TP2				DP1				DP2			
Time (s)	sqrt (t)	Volume (mL)	Infilt (cm)	Time (s)	sqrt (t)	Volume (mL)	Infilt (cm)	Time (s)	sqrt (t)	Volume (mL)	Infilt (cm)	Time (s)	sqrt (t)	Volume (mL)	Infilt (cm)
670	25.88436	69	0.188679	670	25.88436	57	0.377358	670	25.88436	55	0.377358	670	25.88436	55	0.314465
675	25.98076	69	0.188679	675	25.98076	57	0.377358	675	25.98076	55	0.377358	675	25.98076	55	0.314465
680	26.07681	69	0.188679	680	26.07681	57	0.377358	680	26.07681	55	0.377358	680	26.07681	55	0.314465
685	26.1725	69	0.188679	685	26.1725	57	0.377358	685	26.1725	55	0.377358	685	26.1725	55	0.314465
690	26.26785	69	0.188679	690	26.26785	57	0.377358	690	26.26785	55	0.377358	690	26.26785	55	0.314465
695	26.36285	69	0.188679	695	26.36285	57	0.377358	695	26.36285	55	0.377358	695	26.36285	55	0.314465
700	26.45751	69	0.188679	700	26.45751	57	0.377358	700	26.45751	55	0.377358	700	26.45751	55	0.314465
705	26.55184	69	0.188679	705	26.55184	57	0.377358	705	26.55184	55	0.377358	705	26.55184	55	0.314465
710	26.64583	69	0.188679	710	26.64583	57	0.377358	710	26.64583	55	0.377358	710	26.64583	55	0.314465
715	26.73948	69	0.188679	715	26.73948	57	0.377358	715	26.73948	55	0.377358	715	26.73948	55	0.314465
720	26.83282	69	0.188679	720	26.83282	57	0.377358	720	26.83282	55	0.377358	720	26.83282	55	0.314465
725	26.92582	69	0.188679	725	26.92582	57	0.377358	725	26.92582	55	0.377358	725	26.92582	55	0.314465
730	27.01851	69	0.188679	730	27.01851	57	0.377358	730	27.01851	55	0.377358	730	27.01851	55	0.314465
735	27.11088	69	0.188679	735	27.11088	57	0.377358	735	27.11088	55	0.377358	735	27.11088	55	0.314465
740	27.20294	69	0.188679	740	27.20294	57	0.377358	740	27.20294	55	0.377358	740	27.20294	55	0.314465
745	27.29469	69	0.188679	745	27.29469	57	0.377358	745	27.29469	55	0.377358	745	27.29469	55	0.314465
750	27.38613	69	0.188679	750	27.38613	57	0.377358	750	27.38613	54	0.440252	750	27.38613	55	0.314465
755	27.47726	69	0.188679	755	27.47726	57	0.377358	755	27.47726	54	0.440252	755	27.47726	55	0.314465
760	27.5681	69	0.188679	760	27.5681	57	0.377358	760	27.5681	54	0.440252	760	27.5681	55	0.314465
765	27.65863	69	0.188679	765	27.65863	57	0.377358	765	27.65863	54	0.440252	765	27.65863	55	0.314465
770	27.74887	69	0.188679	770	27.74887	57	0.377358	770	27.74887	54	0.440252	770	27.74887	55	0.314465
775	27.83882	69	0.188679	775	27.83882	57	0.377358	775	27.83882	54	0.440252	775	27.83882	55	0.314465
780	27.92848	69	0.188679	780	27.92848	57	0.377358	780	27.92848	54	0.440252	780	27.92848	55	0.314465
785	28.01785	69	0.188679	785	28.01785	57	0.377358	785	28.01785	54	0.440252	785	28.01785	55	0.314465
790	28.10694	69	0.188679	790	28.10694	57	0.377358	790	28.10694	54	0.440252	790	28.10694	55	0.314465
795	28.19574	69	0.188679	795	28.19574	57	0.377358	795	28.19574	54	0.440252	795	28.19574	55	0.314465
800	28.28427	69	0.188679	800	28.28427	57	0.377358	800	28.28427	54	0.440252	800	28.28427	55	0.314465
805	28.37252	69	0.188679	805	28.37252	57	0.377358	805	28.37252	54	0.440252	805	28.37252	55	0.314465
810	28.4605	69	0.188679	810	28.4605	57	0.377358	810	28.4605	54	0.440252	810	28.4605	55	0.314465
815	28.5482	69	0.188679	815	28.5482	57	0.377358	815	28.5482	54	0.440252	815	28.5482	55	0.314465
820	28.63564	69	0.188679	820	28.63564	57	0.377358	820	28.63564	54	0.440252	820	28.63564	55	0.314465
825	28.72281	69	0.188679	825	28.72281	57	0.377358	825	28.72281	54	0.440252	825	28.72281	55	0.314465
830	28.80972	69	0.188679	830	28.80972	57	0.377358	830	28.80972	54	0.440252	830	28.80972	55	0.314465
835	28.89637	69	0.188679	835	28.89637	57	0.377358	835	28.89637	54	0.440252	835	28.89637	55	0.314465
840	28.98275	68	0.251572	840	28.98275	57	0.377358	840	28.98275	53	0.503145	840	28.98275	55	0.314465
845	29.06888	68	0.251572	845	29.06888	57	0.377358	845	29.06888	53	0.503145	845	29.06888	55	0.314465
850	29.15476	68	0.251572	850	29.15476	57	0.377358	850	29.15476	53	0.503145	850	29.15476	55	0.314465
855	29.24038	68	0.251572	855	29.24038	57	0.377358	855	29.24038	53	0.503145	855	29.24038	55	0.314465
860	29.32576	68	0.251572	860	29.32576	57	0.377358	860	29.32576	53	0.503145	860	29.32576	55	0.314465
865	29.41088	68	0.251572	865	29.41088	57	0.377358	865	29.41088	53	0.503145	865	29.41088	55	0.314465
870	29.49576	68	0.251572	870	29.49576	57	0.377358	870	29.49576	53	0.503145	870	29.49576	55	0.314465
875	29.5804	68	0.251572	875	29.5804	57	0.377358	875	29.5804	53	0.503145	875	29.5804	55	0.314465
880	29.66479	68	0.251572	880	29.66479	57	0.377358	880	29.66479	53	0.503145	880	29.66479	55	0.314465
885	29.74895	68	0.251572	885	29.74895	57	0.377358	885	29.74895	53	0.503145	885	29.74895	55	0.314465
890	29.83287	68	0.251572	890	29.83287	57	0.377358	890	29.83287	53	0.503145	890	29.83287	55	0.314465
895	29.91655	68	0.251572	895	29.91655	57	0.377358	895	29.91655	53	0.503145	895	29.91655	55	0.314465
900	30	68	0.251572	900	30	57	0.377358	900	30	53	0.503145	900	30	55	0.314465
905	30.08322	68	0.251572	905	30.08322	56	0.440252	905	30.08322	53	0.503145	905	30.08322	55	0.314465
910	30.16621	68	0.251572	910	30.16621	56	0.440252	910	30.16621	53	0.503145	910	30.16621	55	0.314465
915	30.24897	68	0.251572	915	30.24897	56	0.440252	915	30.24897	53	0.503145	915	30.24897	55	0.314465
920	30.3315	68	0.251572	920	30.3315	56	0.440252	920	30.3315	53	0.503145	920	30.3315	55	0.314465
925	30.41381	68	0.251572	925	30.41381	56	0.440252	925	30.41381	53	0.503145	925	30.41381	55	0.314465
930	30.4959	68	0.251572	930	30.4959	56	0.440252	930	30.4959	52	0.566038	930	30.4959	55	0.314465
935	30.57777	68	0.251572	935	30.57777	56	0.440252	935	30.57777	52	0.566038	935	30.57777	55	0.314465
940	30.65942	68	0.251572	940	30.65942	56	0.440252	940	30.65942	52	0.566038	940	30.65942	55	0.314465
945	30.74085	68	0.251572	945	30.74085	56	0.440252	945	30.74085	52	0.566038	945	30.74085	55	0.314465
950	30.82207	68	0.251572	950	30.82207	56	0.440252	950	30.82207	52	0.566038	950	30.82207	55	0.314465
955	30.90307	68	0.251572	955	30.90307	56	0.440252	955	30.90307	52	0.566038	955	30.90307	55	0.314465
960	30.98387	67	0.314465	960	30.98387	56	0.440252	960	30.98387	52	0.566038	960	30.98387	55	0.314465
965	31.06445	67	0.314465	965	31.06445	56	0.440252	965	31.06445	52	0.566038	965	31.06445	55	0.314465
970	31.14482	67	0.314465	970	31.14482	56	0.440252	970	31.14482	52	0.566038	970	31.14482	55	0.314465
975	31.22499	67	0.314465	975	31.22499	56	0.440252	975	31.22499	52	0.566038	975	31.22499	55	0.314465
980	31.30495	67	0.314465	980	31.30495	56	0.440252	980	31.30495	52	0.566038	980	31.30495	55	0.314465
985	31.38471	67	0.314465	985	31.38471	56	0.440252	985	31.38471	52	0.566038	985	31.38471	55	0.314465
990	31.46427	67	0.314465	990	31.46427	56	0.440252	990	31.46427	52	0.566038	990	31.46427	55	0.314465

TP1				TP2				DP1				DP2			
Time (s)	sqrt (t)	Volume (mL)	Infilt (cm)	Time (s)	sqrt (t)	Volume (mL)	Infilt (cm)	Time (s)	sqrt (t)	Volume (mL)	Infilt (cm)	Time (s)	sqrt (t)	Volume (mL)	Infilt (cm)
1005	31.70173	67	0.314465	1005	31.70173	56	0.440252	1005	31.70173	52	0.566038	1005	31.70173	55	0.314465
1010	31.7805	67	0.314465	1010	31.7805	56	0.440252	1010	31.7805	52	0.566038	1010	31.7805	55	0.314465
1015	31.85906	67	0.314465	1015	31.85906	56	0.440252	1015	31.85906	52	0.566038	1015	31.85906	55	0.314465
1020	31.93744	67	0.314465	1020	31.93744	56	0.440252	1020	31.93744	51	0.628931	1020	31.93744	55	0.314465
1025	32.01562	67	0.314465	1025	32.01562	56	0.440252	1025	32.01562	51	0.628931	1025	32.01562	55	0.314465
1030	32.09361	67	0.314465	1030	32.09361	56	0.440252	1030	32.09361	51	0.628931	1030	32.09361	55	0.314465
1035	32.17142	67	0.314465	1035	32.17142	56	0.440252	1035	32.17142	51	0.628931	1035	32.17142	55	0.314465
1040	32.24903	67	0.314465	1040	32.24903	56	0.440252	1040	32.24903	51	0.628931	1040	32.24903	55	0.314465
1045	32.32646	67	0.314465	1045	32.32646	56	0.440252	1045	32.32646	51	0.628931	1045	32.32646	55	0.314465
1050	32.4037	67	0.314465	1050	32.4037	56	0.440252	1050	32.4037	51	0.628931	1050	32.4037	55	0.314465
1055	32.48076	67	0.314465	1055	32.48076	56	0.440252	1055	32.48076	51	0.628931	1055	32.48076	55	0.314465
1060	32.55764	67	0.314465	1060	32.55764	56	0.440252	1060	32.55764	51	0.628931	1060	32.55764	55	0.314465
1065	32.63434	67	0.314465	1065	32.63434	56	0.440252	1065	32.63434	51	0.628931	1065	32.63434	55	0.314465
1070	32.71085	67	0.314465	1070	32.71085	56	0.440252	1070	32.71085	51	0.628931	1070	32.71085	55	0.314465
1075	32.78719	67	0.314465	1075	32.78719	56	0.440252	1075	32.78719	51	0.628931	1075	32.78719	55	0.314465
1080	32.86335	67	0.314465	1080	32.86335	56	0.440252	1080	32.86335	51	0.628931	1080	32.86335	54	0.377358
1085	32.93934	67	0.314465	1085	32.93934	55	0.503145	1085	32.93934	51	0.628931	1085	32.93934	54	0.377358
1090	33.01515	67	0.314465	1090	33.01515	55	0.503145	1090	33.01515	51	0.628931	1090	33.01515	54	0.377358
1095	33.09078	67	0.314465	1095	33.09078	55	0.503145	1095	33.09078	51	0.628931	1095	33.09078	54	0.377358
1100	33.16625	67	0.314465	1100	33.16625	55	0.503145	1100	33.16625	51	0.628931	1100	33.16625	54	0.377358
1105	33.24154	67	0.314465	1105	33.24154	55	0.503145	1105	33.24154	51	0.628931	1105	33.24154	54	0.377358
1110	33.31666	67	0.314465	1110	33.31666	55	0.503145	1110	33.31666	51	0.628931	1110	33.31666	54	0.377358
1115	33.39162	67	0.314465	1115	33.39162	55	0.503145	1115	33.39162	51	0.628931	1115	33.39162	54	0.377358
1120	33.4664	67	0.314465	1120	33.4664	55	0.503145	1120	33.4664	51	0.628931	1120	33.4664	54	0.377358
1125	33.54102	67	0.314465	1125	33.54102	55	0.503145	1125	33.54102	51	0.628931	1125	33.54102	54	0.377358
1130	33.61547	67	0.314465	1130	33.61547	55	0.503145	1130	33.61547	51	0.628931	1130	33.61547	54	0.377358
1135	33.68976	67	0.314465	1135	33.68976	55	0.503145	1135	33.68976	51	0.628931	1135	33.68976	54	0.377358
1140	33.76389	67	0.314465	1140	33.76389	55	0.503145	1140	33.76389	50	0.691824	1140	33.76389	54	0.377358
1145	33.83785	67	0.314465	1145	33.83785	55	0.503145	1145	33.83785	50	0.691824	1145	33.83785	54	0.377358
1150	33.91165	67	0.314465	1150	33.91165	55	0.503145	1150	33.91165	50	0.691824	1150	33.91165	54	0.377358
1155	33.98529	67	0.314465	1155	33.98529	55	0.503145	1155	33.98529	50	0.691824	1155	33.98529	54	0.377358
1160	34.05877	67	0.314465	1160	34.05877	55	0.503145	1160	34.05877	50	0.691824	1160	34.05877	54	0.377358
1165	34.1321	67	0.314465	1165	34.1321	55	0.503145	1165	34.1321	50	0.691824	1165	34.1321	54	0.377358
1170	34.20526	67	0.314465	1170	34.20526	55	0.503145	1170	34.20526	50	0.691824	1170	34.20526	54	0.377358
1175	34.27827	67	0.314465	1175	34.27827	55	0.503145	1175	34.27827	50	0.691824	1175	34.27827	54	0.377358
1180	34.35113	67	0.314465	1180	34.35113	55	0.503145	1180	34.35113	50	0.691824	1180	34.35113	54	0.377358
1185	34.42383	67	0.314465	1185	34.42383	55	0.503145	1185	34.42383	50	0.691824	1185	34.42383	54	0.377358
1190	34.49638	67	0.314465	1190	34.49638	55	0.503145	1190	34.49638	50	0.691824	1190	34.49638	54	0.377358
1195	34.56877	67	0.314465	1195	34.56877	55	0.503145	1195	34.56877	50	0.691824	1195	34.56877	54	0.377358
1200	34.64102	66	0.377358	1200	34.64102	55	0.503145	1200	34.64102	49	0.754717	1200	34.64102	54	0.377358
1205	34.71311	66	0.377358	1205	34.71311	55	0.503145	1205	34.71311	49	0.754717	1205	34.71311	54	0.377358
1210	34.78505	66	0.377358	1210	34.78505	55	0.503145	1210	34.78505	49	0.754717	1210	34.78505	54	0.377358
1215	34.85685	66	0.377358	1215	34.85685	55	0.503145	1215	34.85685	49	0.754717	1215	34.85685	54	0.377358
1220	34.9285	66	0.377358	1220	34.9285	55	0.503145	1220	34.9285	49	0.754717	1220	34.9285	54	0.377358
1225	35	66	0.377358	1225	35	55	0.503145	1225	35	49	0.754717	1225	35	54	0.377358
1230	35.07136	66	0.377358	1230	35.07136	55	0.503145	1230	35.07136	49	0.754717	1230	35.07136	54	0.377358
1235	35.14257	66	0.377358	1235	35.14257	55	0.503145	1235	35.14257	49	0.754717	1235	35.14257	54	0.377358
1240	35.21363	66	0.377358	1240	35.21363	55	0.503145	1240	35.21363	49	0.754717	1240	35.21363	54	0.377358
1245	35.28456	66	0.377358	1245	35.28456	55	0.503145	1245	35.28456	49	0.754717	1245	35.28456	54	0.377358
1250	35.35534	66	0.377358	1250	35.35534	55	0.503145	1250	35.35534	49	0.754717	1250	35.35534	54	0.377358
1255	35.42598	66	0.377358	1255	35.42598	55	0.503145	1255	35.42598	49	0.754717	1255	35.42598	54	0.377358
1260	35.49648	66	0.377358	1260	35.49648	55	0.503145	1260	35.49648	49	0.754717	1260	35.49648	54	0.377358
1265	35.56684	66	0.377358	1265	35.56684	54	0.566038	1265	35.56684	49	0.754717	1265	35.56684	54	0.377358
1270	35.63706	66	0.377358	1270	35.63706	54	0.566038	1270	35.63706	49	0.754717	1270	35.63706	54	0.377358
1275	35.70714	66	0.377358	1275	35.70714	54	0.566038	1275	35.70714	49	0.754717	1275	35.70714	54	0.377358
1280	35.77709	66	0.377358	1280	35.77709	54	0.566038	1280	35.77709	49	0.754717	1280	35.77709	54	0.377358
1285	35.8469	66	0.377358	1285	35.8469	54	0.566038	1285	35.8469	49	0.754717	1285	35.8469	54	0.377358
1290	35.91657	66	0.377358	1290	35.91657	54	0.566038	1290	35.91657	49	0.754717	1290	35.91657	54	0.377358
1295	35.98611	66	0.377358	1295	35.98611	54	0.566038	1295	35.98611	49	0.754717	1295	35.98611	54	0.377358
1300	36.05551	66	0.377358	1300	36.05551	54	0.566038	1300	36.05551	49	0.754717	1300	36.05551	54	0.377358
1305	36.12478	66	0.377358	1305	36.12478	54	0.566038	1305	36.12478	49	0.754717	1305	36.12478	54	0.377358
1310	36.19392	66	0.377358	1310	36.19392	54	0.566038	1310	36.19392	49	0.754717	1310	36.19392	54	0.377358
1315	36.26293	66	0.377358	1315	36.26293	54	0.566038	1315	36.26293	49	0.754717	1315	36.26293	54	0.377358
1320	36.3318	66	0.377358	1320	36.3318	54	0.566038	1320	36.3318	48	0.81761	1320	36.3318	53	0.440252

SV				DC			
Time (s)	sqrt (t)	Volume (mL)	Infilt (cm)	Time (s)	sqrt (t)	Volume (mL)	Infilt (cm)
0	0	60	0	0	0	61	0
5	2.236068	59	0.062893	5	2.236068	60	0.062893
10	3.162278	58	0.125786	10	3.162278	59	0.125786
15	3.872983	58	0.125786	15	3.872983	58	0.188679
20	4.472136	57	0.188679	20	4.472136	57	0.251572
25	5	56	0.251572	25	5	55	0.377358
30	5.477226	56	0.251572	30	5.477226	54	0.440252
35	5.91608	55	0.314465	35	5.91608	53	0.503145
40	6.324555	55	0.314465	40	6.324555	52	0.566038
45	6.708204	54	0.377358	45	6.708204	51	0.628931
50	7.071068	54	0.377358	50	7.071068	50	0.691824
55	7.416198	53	0.440252	55	7.416198	49	0.754717
60	7.745967	53	0.440252	60	7.745967	47	0.880503
65	8.062258	52	0.503145	65	8.062258	46	0.943396
70	8.3666	52	0.503145	70	8.3666	45	1.006289
75	8.660254	51	0.566038	75	8.660254	43	1.132075
80	8.944272	51	0.566038	80	8.944272	42	1.194969
85	9.219544	50	0.628931	85	9.219544	41	1.257862
90	9.486833	50	0.628931	90	9.486833	40	1.320755
95	9.746794	49	0.691824	95	9.746794	39	1.383648
100	10	48	0.754717	100	10	37	1.509434
105	10.24695	48	0.754717	105	10.24695	36	1.572327
110	10.48809	47	0.81761	110	10.48809	35	1.63522
115	10.72381	47	0.81761	115	10.72381	34	1.698113
120	10.95445	46	0.880503	120	10.95445	32	1.823899
125	11.18034	45	0.943396	125	11.18034	31	1.886792
130	11.40175	45	0.943396	130	11.40175	30	1.949686
135	11.61895	44	1.006289	135	11.61895	29	2.012579
140	11.83216	44	1.006289	140	11.83216	28	2.075472
145	12.04159	43	1.069182	145	12.04159	27	2.138365
150	12.24745	43	1.069182	150	12.24745	25	2.264151
155	12.4499	42	1.132075	155	12.4499	24	2.327044
160	12.64911	42	1.132075	160	12.64911	23	2.389937
165	12.84523	41	1.194969	165	12.84523	22	2.45283
170	13.0384	41	1.194969	170	13.0384	21	2.515723
175	13.22876	40	1.257862	175	13.22876	19	2.641509
180	13.41641	40	1.257862	180	13.41641	18	2.704403
185	13.60147	39	1.320755	185	13.60147	17	2.767296
190	13.78405	39	1.320755	190	13.78405	16	2.830189
195	13.96424	38	1.383648	195	13.96424	15	2.893082
200	14.14214	36	1.509434	200	14.14214	13	3.018868
205	14.31782	36	1.509434	205	14.31782	12	3.081761
210	14.49138	35	1.572327	210	14.49138	11	3.144654
215	14.66288	34	1.63522	215	14.66288	10	3.207547
220	14.8324	33	1.698113	220	14.8324	8	3.333333
225	15	33	1.698113	225	15	7	3.396226
230	15.16575	32	1.761006	230	15.16575	6	3.459119
235	15.32971	31	1.823899	235	15.32971	5	3.522013
240	15.49193	31	1.823899	240	15.49193	4	3.584906
245	15.65248	30	1.886792	245	15.65248	2	3.710692
250	15.81139	29	1.949686	250	15.81139	1	3.773585
255	15.96872	29	1.949686	255	15.96872	0	3.836478

APPENDIX 3

SUPPORTING INFORMATION FOR CHAPTER 4

Appendix 3.1 include data provided by Dr. Dave Wedin from Forestry Lab at School of Natural Resources and contains grassland Leaf Area Index (LAI) in the Nebraska Sand Hills near Halsey. These data were used in the estimation of rainfall interception and evapotranspiration rates. Leaf Area Index of approximately 1.87 estimated by Dr. Wedin's group was used to represent canopy cover for the ever-green dense ponderosa pine tree plots. Appendix 3.2 contains long term (2005-2012) monthly TDR soil moisture data for the grass and dense pine plots also provided by Dr. Wedin's group at the Forestry Lab. Appendix 3.2 shows the scripts used for the DREAMzs global optimizer for the inverse modelling to estimate effective soil hydraulic properties and for the forward run using HYDRUS 1-D numerical simulation with the MATLAB environment. This global optimizer algorithm is developed by Jasper A. Vrugt and Cajo ter Braak at the University of California, Irvine and is publically available. Appendix 3.4 contains the HYDRUS 1-D output summary of the forward numerical simulations using the effective soil hydraulic properties obtained from inverse modelling, climate input, and root depth distribution. Modelling output values that were not directly relevant to the discussion were not included in this appendix.

The authors would be glad to share information or data used in these studies with any scientist with a request sent to zablon@huskers.unl.edu at any time. Requests for raw data obtained from other scientists, particularly Dr. Dave Wedin, will be duly forwarded as some data have yet to be published.

Appendix 3.1 Grass Leaf Area Index (LAI) data

Date	DOY	Live grass LAI (m2/m2)		Date	DOY	Live grass LAI (m2/m2)
4/1/2005	91	0.10		7/1/2009	182	1.79
4/18/2005	108	0.25		7/23/2009	204	1.64
5/6/2005	126	0.51		9/3/2009	246	1.46
6/17/2005	168	1.24		10/2/2009	275	0.47
7/13/2005	194	0.91		5/6/2010	126	0.20
8/11/2005	223	0.90		9/24/2010	267	0.74
9/8/2005	251	0.76		5/25/2011	145	0.43
10/18/2005	291	0.28		6/24/2011	175	0.92
11/20/2005	324	0.30		7/18/2011	199	0.94
4/7/2006	97	0.15		8/24/2011	236	1.25
5/4/2006	124	0.39		10/7/2011	280	0.82
5/31/2006	151	0.56		4/20/2012	111	0.44
6/14/2006	165	0.58		5/24/2012	145	0.75
6/26/2006	177	0.73		6/26/2012	178	1.05
7/17/2006	198	0.93		7/31/2012	213	0.65
8/9/2006	221	1.06		9/7/2012	251	0.38
9/14/2006	257	1.07		5/22/2013	142	0.10
10/17/2006	290	0.47		6/24/2013	175	1.04
5/15/2007	135	0.54		7/25/2013	206	0.85
6/11/2007	162	0.88		9/1/2013	244	0.62
6/26/2007	177	1.40		9/29/2013	272	0.54
7/9/2007	190	1.38		5/8/2014	128	0.20
8/7/2007	219	1.04		6/4/2014	155	0.65
9/13/2007	256	1.40		7/1/2014	182	0.77
10/12/2007	285	0.48		7/28/2014	209	0.92
4/21/2008	112	0.10		9/1/2014	244	0.47
6/4/2008	156	0.72		10/1/2014	274	0.25
6/30/2008	182	0.91		5/6/2015	126	0.20
7/28/2008	210	1.81		6/3/2015	154	0.45
9/8/2008	252	1.58		7/1/2015	182	0.98
10/20/2008	294	0.44		8/4/2015	216	1.16
4/27/2009	117	0.46		9/1/2015	244	1.18
6/15/2009	166	1.50		10/1/2015	274	0.51

Appendix 3.2 TDR Monthly soil moisture content for grass and dense pine plots

	TDR soil moisture contents (%) for Grass (G1) 2005 - 2012									
DOY	0-20 cm	20-40 cm	40-60 cm	60-80 cm	80-100 cm	100-120 cm	130-150 cm	150-170 cm	180-200 cm	210-230 cm
1	0.1	0.126	0.168	0.167	0.153		0.094		0.07	0.098
32	0.114	0.128	0.174	0.171	0.173		0.072		0.072	0.075
71	0.187	0.143	0.196	0.183	0.206		0.123		0.181	0.158
102	0.134	0.191	0.147	0.155	0.176		0.102		0.161	0.145
140		0.076	0.088	0.088	0.099		0.077		0.115	0.1
176	0.115	0.19	0.128	0.118	0.086		0.103		0.098	0.09
213	0.112	0.111	0.081	0.119	0.094	0.122	0.071	0.113	0.12	0.104
247	0.113	0.071	0.088	0.091	0.113	0.083	0.121	0.113	0.109	
302	0.092	0.077	0.081	0.075	0.097	0.108	0.081	0.109	0.115	0.105
343	0.072	0.079	0.075	0.076	0.095	0.111	0.077	0.107	0.123	0.106
365	0.079	0.083	0.07	0.119	0.087	0.106	0.072	0.108	0.116	0.095
427	0.08	0.129	0.171	0.172	0.175	0.184	0.078	0.103	0.123	0.098
483	0.074	0.076	0.116	0.131	0.166	0.146	0.076	0.107	0.102	0.093
526	0.087	0.11	0.074	0.07	0.091	0.092	0.103	0.089	0.073	0.114
545	0.189	0.142	0.177	0.087	0.081	0.091	0.102	0.083	0.074	0.103
567	0.199	0.144	0.2	0.176	0.162	0.105	0.071	0.098	0.096	0.227
603	0.102	0.142	0.202	0.18	0.173	0.156	0.118	0.094	0.108	0.22
630	0.17	0.153	0.189	0.166	0.164	0.145	0.112	0.089	0.094	0.178
703	0.097	0.082	0.096	0.138	0.175	0.179	0.086	0.089	0.092	0.175
751	0.147	0.188	0.207	0.162	0.194	0.191	0.168	0.214	0.22	
782	0.112	0.157	0.229	0.201	0.204	0.222	0.114	0.167	0.191	
845	0.155	0.19	0.117	0.136	0.159	0.177	0.11	0.153	0.168	
874	0.076	0.105	0.117	0.077	0.116	0.141	0.084	0.13	0.143	0.124
911	0.061	0.103	0.165	0.161	0.153	0.152	0.079	0.117	0.135	
939	0.087	0.14	0.204	0.186	0.168	0.162	0.088	0.122	0.129	
994	0.1	0.16	0.208	0.199	0.204	0.206	0.111	0.146	0.147	
1064	0.076	0.115	0.087	0.15	0.179	0.159	0.092	0.132	0.13	
1085	0.114	0.12	0.137	0.157	0.18	0.162	0.096	0.137	0.133	
1114	0.152	0.168	0.166	0.21	0.195	0.194	0.106	0.144	0.149	
1155	0.093	0.146	0.206	0.195	0.204	0.204	0.103	0.155	0.17	
1189	0.102	0.13	0.196	0.193	0.209	0.22	0.122	0.175	0.194	
1218	0.116	0.19	0.19	0.173	0.177	0.089	0.137	0.146		
1247	0.099	0.136	0.186	0.173	0.176	0.171	0.09	0.139	0.151	
1315	0.146	0.2	0.165	0.178	0.178	0.167	0.135	0.179		
1337	0.138	0.176	0.165	0.221	0.166	0.212	0.132	0.189		
1358	0.117	0.181	0.177	0.163	0.172	0.187	0.136	0.183		
1392	0.145	0.112	0.209	0.205	0.161	0.2	0.132	0.18		
1420	0.151	0.138	0.214	0.202	0.227	0.227	0.122	0.172		
1449	0.188	0.177	0.227	0.229	0.228	0.168	0.119	0.171		
1485	0.142	0.199	0.215	0.201	0.228	0.22	0.136	0.192		
1506	0.146	0.186	0.185	0.164	0.191	0.166	0.137	0.195		
1526	0.15	0.141	0.209	0.204	0.162	0.225	0.11	0.169	0.187	0.204
1567	0.104	0.147	0.205	0.202	0.225	0.216	0.119	0.176		
1589	0.176	0.101	0.151	0.163	0.196	0.181	0.115	0.169	0.179	
1631	0.168	0.105	0.126	0.128	0.156	0.149	0.102	0.155	0.157	
1660	0.116	0.128	0.108	0.123	0.147	0.157	0.102	0.15	0.164	

	TDR soil moisture contents (%) for Dense Pine (DP1) 2005 - 2012									
DOY	0-20 cm	20-40 cm	40-60 cm	60-80 cm	80-100 cm	100-120 cm	130-150 cm	150-170 cm	180-200 cm	210-230 cm
1	0.013	0.026								
32	0.067	0.042		0.103	0.1					
71	0.08	0.068		0.114	0.121	0.083	0.044			
140	0.004		0.003	0.023	0.017	0.061	0.058	0.067	0.09	
176	0.03	0.051	0.057	0.024	0.026	0.056	0.034	0.012	0.014	
213	0.058	0.054	0.041	0.033	0.035	0.048	0.064	0.029	0.021	
247	0.065	0.046	0.043	0.04	0.047	0.033	0.056	0.088	0.079	0.055
302	0.109	0.087	0.041	0.037	0.036	0.051	0.051	0.073	0.095	0.051
365	0.07			0.004		0.004	0.012	0.026	0.026	0.03
393	0.061	0.097	0.098	0.068	0.074			0.002	0.031	
427	0.046	0.042	0.054	0.09	0.097	0.09	0.028	0.034	0.034	0.045
453	0.087	0.112	0.073	0.069	0.065	0.047	0.062	0.052	0.081	0.041
483	0.04	0.057	0.053	0.047	0.045	0.03	0.049	0.056	0.075	0.043
526	0.04			0.019	0.019	0.022	0.024	0.027	0.026	0.027
545	0.136	0.074	0.008	0.026	0.031	0.026	0.034	0.039	0.034	0.033
567	0.119	0.13	0.111	0.06	0.052	0.047	0.061	0.073	0.096	0.06
603	0.108	0.08	0.071	0.11	0.056	0.05	0.048	0.051	0.05	0.049
630	0.087	0.108	0.103	0.068	0.06	0.051	0.078	0.08	0.103	0.066
664	0.128	0.124	0.096	0.061	0.05	0.044	0.073	0.071	0.095	0.061
703	0.069	0.068	0.06	0.062	0.052	0.048	0.074	0.071	0.093	0.058
751	0.171	0.18	0.163	0.174	0.156	0.143	0.164	0.098	0.106	0.081
805	0.192	0.177	0.147	0.126	0.109	0.112	0.135	0.137	0.162	0.054
845	0.065	0.085	0.093	0.115	0.104	0.093	0.123	0.133	0.17	0.106
874	0.06	0.049	0.059	0.065	0.058	0.057	0.079	0.108	0.145	0.087
911	0.035	0.088	0.094	0.078	0.092	0.062	0.084	0.099	0.133	0.082
939	0.091	0.136	0.112	0.079	0.086	0.059	0.085	0.098	0.135	0.089
994	0.096	0.125	0.121	0.111	0.1	0.076	0.102	0.107	0.151	0.1
1064	0.033	0.061	0.105	0.112	0.098	0.056	0.084	0.086	0.12	0.078
1085	0.109	0.102	0.104	0.108	0.096	0.052	0.085	0.09	0.125	0.076
1114	0.171	0.175	0.134	0.146	0.13	0.108	0.111	0.113	0.147	0.095
1155	0.104	0.117	0.116	0.124	0.111	0.104	0.119	0.086	0.105	0.061
1189	0.105	0.13	0.131	0.134	0.114	0.11	0.157	0.161	0.185	0.117
1218	0.131	0.131	0.122	0.13	0.117	0.102	0.132	0.147	0.2	0.115
1247	0.095	0.09	0.085	0.1	0.09	0.084	0.091	0.11	0.157	0.092
1315	0.151	0.152	0.137	0.117	0.131	0.104	0.13	0.109	0.156	0.098
1337	0.155	0.162	0.158	0.161	0.148	0.146	0.182	0.153	0.173	0.115
1358	0.109	0.156	0.145	0.157	0.14	0.128	0.157	0.15	0.211	0.106
1392	0.067	0.135	0.137	0.144	0.125	0.118	0.143	0.136	0.177	0.107
1420	0.12	0.146	0.139	0.151	0.133	0.121	0.152	0.148	0.203	0.118
1449	0.136	0.163	0.148	0.159	0.145	0.122	0.135	0.142	0.199	0.119
1485	0.167	0.173	0.159	0.163	0.143	0.128	0.146	0.135	0.194	0.112
1526	0.118	0.097	0.05	0.128	0.157	0.153	0.147	0.138	0.145	0.127
1567	0.102	0.098	0.123	0.118	0.152	0.125	0.135	0.115	0.114	0.121
1589	0.086	0.095	0.098	0.107	0.099	0.092	0.123	0.129	0.176	0.111
1631	0.064	0.07	0.064	0.069	0.062	0.057	0.085	0.114	0.144	0.091
1660	0.059	0.058	0.049	0.056	0.046	0.048	0.06	0.041	0.033	0.056
1694	0.133	0.173	0.14	0.079	0.07	0.071	0.083	0.108	0.155	0.092
1722	0.117	0.156	0.143	0.109	0.111	0.077	0.083	0.109	0.148	0.098
1785	0.069	0.108	0.132	0.127	0.116	0.079	0.08	0.099	0.138	0.094
1813	0.091	0.097	0.122	0.134	0.129	0.096	0.086	0.114	0.142	0.102
1842	0.16	0.195	0.172	0.17	0.16	0.148	0.145	0.119	0.153	0.102
1876	0.141	0.159	0.149	0.157	0.148	0.134	0.149	0.123	0.165	0.096
1905	0.19	0.198	0.183	0.172	0.163	0.147	0.135	0.127	0.17	0.085
1934	0.087	0.13	0.135	0.147	0.131	0.118	0.142	0.17	0.269	0.139
1959	0.095	0.121	0.132	0.127	0.11	0.108	0.125	0.15	0.214	0.128
2001	0.053	0.095	0.106	0.121	0.115	0.113	0.11	0.125	0.156	0.104
2030	0.097	0.123	0.119	0.096	0.088	0.083	0.093	0.106	0.132	0.082
2061	0.105	0.103	0.105	0.099	0.091	0.092	0.102	0.122	0.162	0.105
2086	0.1	0.109	0.111	0.11	0.108	0.103	0.106	0.132	0.176	0.113
2122	0.036	0.067	0.062	0.06	0.05	0.054	0.064	0.09	0.125	0.074
2158	0.069	0.105	0.081	0.083	0.08	0.077	0.082	0.097	0.119	0.083
2186	0.11	0.149	0.14	0.077	0.073	0.07	0.083	0.098	0.138	0.09
2211	0.139	0.159	0.153	0.151	0.141	0.074	0.063	0.089	0.124	0.077
2241	0.144	0.152	0.152	0.158	0.15	0.118	0.071	0.095	0.133	0.086
2302	0.084	0.108	0.082	0.082	0.075	0.077	0.073	0.08	0.108	0.056
2373	0.047	0.066	0.067	0.072	0.065	0.062	0.067	0.078	0.084	0.062
2393	0.041	0.07	0.063	0.062	0.056	0.052	0.062	0.067	0.09	0.051
2422	0.067	0.101	0.101	0.07	0.062	0.063	0.066	0.081	0.101	0.064
2485	0.057	0.083	0.078	0.072	0.067	0.067	0.068	0.078	0.092	0.156

Appendix 3.3 Optimization ($DREAM_{ZS}$) inverse and forward model run scripts

DREAM OPTIMIZATION INVERSE MODELING RUN

```
% The DREAM(ZS) algorithm is developed by Jasper A. Vrugt and Cajo ter
Braak and has been described in:
%
% Vrugt, J.A., C.J.F. ter Braak, C.G.H. Diks, D. Higdon, B.A. Robinson,
and J.M. Hyman,
%
% Accelerating Markov chain Monte Carlo simulation by differential
evolution with self-adaptive randomized subspace sampling,
International Journal of Nonlinear Sciences and Numerical Simulation},
10(3), 273-290, 2009.                                                  %

% Copyright (C) 2011-2012 the authors
%
% This program is free software: you can modify it under the terms of
the GNU General
%
% Public License as published by the Free Software Foundation, either
version 3 of the License, or (at your option) any later version.
%
% This program is distributed in the hope that it will be useful, but
WITHOUT ANY WARRANTY; without even the implied warranty of
MERCHANTABILITY or FITNESS FOR A PARTICULAR PURPOSE.
%
%%%%%%%%%%%%%%%%%%%%%%%%%%%%%%%%%%%%%%%%%%%%%%%%%%%%%%%%%%%%%%%%%%%%%%%
%%%%%%
%
%
% Written by Jasper A. Vrugt: jasper@uci.edu
%
%
% Version 1.4: January 2013       Simplification of metrop.m and
dream_zs.m
%
% --------------------------------------------------------------------

% Clear memory
clear all; clc;close all; clear;

% Which example to run?
example = 18;

global DREAM_dir EXAMPLE_dir MEAS_DATA

% Store working directory and subdirectory containing the files needed
to run this example
DREAM_dir = pwd; EXAMPLE_dir = [pwd '\example_' num2str(example)];

% Add subdirectory to search path
addpath(EXAMPLE_dir);

% Recommended parameter settings
```

```
MCMCPar.seq = 3;
% Number of Markov chains / sequences (for high dimensional and highly
nonlinear problems, larger values work beter!!)
MCMCPar.DEpairs = 1;
% Number of chain pairs to generate candidate points
MCMCPar.nCR = 3;
% Number of crossover values used
MCMCPar.k = 10;
% Thinning parameter for appending X to Z
MCMCPar.parallelUpdate = 0.9;
% Fraction of parallel direction updates
MCMCPar.eps = 5e-2;
% Perturbation for ergodicity
MCMCPar.steps = inline('MCMCPar.ndraw/(20 * MCMCPar.seq)'); % Number of
steps before calculating convergence diagnostics
MCMCPar.m0 = inline('10 * MCMCPar.n');
% Initial size of matrix Z
MCMCPar.pJumpRate_one = 0.20;
% Probability of selecting a jumprate of 1 --> jump between modes
MCMCPar.pCR = 'Yes';
% Adaptive tuning of crossover values (Yes or No)
MCMCPar.Restart = 'No';
% Restart run (Yes or No)
MCMCPar.modout = 'Yes';
% Return model (function) simulations of samples Yes or No)?
MCMCPar.save = 'No';
% Save output during the run (Yes or No)
MCMCPar.ABC = 'No';
% Approximate Bayesian Computation or Not?

% ------------------------------------------------------------------------
% If MCMCPar.modout = 'Yes' --> the simulations of the model are
stored.
% But this only happens if calibration data vector exists!!
% ------------------------------------------------------------------------

if example == 18

    % Problem specific parameter settings
    MCMCPar.n = 5;
% Dimension of the problem (number of parameters to be estimated)
    MCMCPar.ndraw = 5000;
% Maximum number of function evaluations
    MCMCPar.T = 1;
% Each Tth sample is collected in the chains
    MCMCPar.prior = 'LHS';
% Latin Hypercube sampling (options, "LHS", "COV" and "PRIOR")
    MCMCPar.BoundHandling = 'Reflect';
% Boundary handling (options, "Reflect", "Bound", "Fold", and "None");
    MCMCPar.lik = 3;
% Define likelihood function -- Sum of Squared Error
    MCMCPar.modout = 'Yes';
% Return model (function) simulations of samples Yes or No)?

% Define modelName
    ModelName = 'FORWARD';
```

```
% Give the parameter ranges (minimum and maximum values)
% theta_res=0 by assumption!
    ParRange.minn = [0.03      1.65      200     0.030     0.35];
%alpha n Ks thetar thetas
    ParRange.maxn = [0.1451    2.0       750     0.045     0.43];
%

load('Time_POS.txt')
MeasTime=Time_POS(1:350,1);
MeasTH=Time_POS(1:350,2);
POS=Time_POS(1:350,3);
%MeasTime(632:end)=2484;

% Define measurement data as one vector
    MEAS_DATA=MeasTH;
    SD=std(MEAS_DATA);
% Define std of measurement error (prior knowledge)
    Measurement.Sigma = [SD.*ones(length(MEAS_DATA),1)];

% Define the measured data (to be used in likelihood function)
    Measurement.MeasData = MEAS_DATA;

% Since all the model inputs are defined in the model, we don't specify
the "Extra" variable
    Extra = [];

% We need to specify the Measurement error of the data in
Measurement.Sigma
% With option 3, Measurement.Sigma is integrated out the likelihood
function
% With any other option, Sigma needs to be defined

% We can estimate the measurement error directly if we use temporal
differencing
% The function MeasError provides an estimate of error versus flow
level
% out = MeasError(Measurement.MeasData;
% For the Leaf River watershed this results in a heteroscedastic error
% that is about 10% of the actual measured discharge value, thus
% You can check this by plotting out(:,1) versus out(:,2)
% Measurement.Sigma = 0.1*Measurement.MeasData; % --> option 2

% Run the DREAM_ZS algorithm
    [Sequences,X,Z,output,fx] =
dream_zs(MCMCPar,ModelName,Extra,ParRange,Measurement);

end;

% Create a single matrix with values sampled by chains
ParSet = GenParSet(Sequences,MCMCPar);

%%% Verify parametric convergence. The line has to be lower than 1.2!
figure(1)
subplot(1,5,1);plot(output.R_stat(:,1),output.R_stat(:,2))
```

```
%%%%% parameter 2
subplot(1,5,2);plot(output.R_stat(:,1),output.R_stat(:,3))
%%%%% parameter 3
subplot(1,5,3);plot(output.R_stat(:,1),output.R_stat(:,4))
%%%% parameter 4
subplot(1,5,4);plot(output.R_stat(:,1),output.R_stat(:,5))
%%%%% parameter 5
subplot(1,5,5);plot(output.R_stat(:,1),output.R_stat(:,6))

thetar=ParSet(0.8*end:end,4);
thetas=ParSet(0.8*end:end,5);
alpha=ParSet(0.8*end:end,1);
n=ParSet(0.8*end:end,2);
Ks=ParSet(0.8*end:end,3);

thetar_BEST=median(ParSet(.8*end:end,4));
thetas_BEST=median(ParSet(.8*end:end,5));
alpha_BEST=median(ParSet(.8*end:end,1));
n_BEST=median(ParSet(.8*end:end,2));
Ks_BEST=median(ParSet(.8*end:end,3));

MTX=[thetar thetas alpha n Ks];
save MTX_VG.txt MTX -ascii

MTX_BEST=[thetar_BEST thetas_BEST alpha_BEST n_BEST Ks_BEST];
save MTX_VG_BEST.txt MTX_BEST -ascii

figure(2)
subplot(2,3,1);hist(thetar)
xlabel('thetar','fontsize',20);
%set(gca,'xLim',[0.2 0.6]);

subplot(2,3,2);hist(thetas)
xlabel('thetas','fontsize',20);
%set(gca,'xLim',[0 50]);

subplot(2,3,3);hist(log10(alpha))
xlabel('alpha','fontsize',20);
%set(gca,'xLim',[0 1]);

subplot(2,3,4);hist(n)
xlabel('n','fontsize',20);
%set(gca,'xLim',[0 1000]);

subplot(2,3,5);hist(log10(Ks))
xlabel('Ks','fontsize',20);
%set(gca,'xLim',[0 1000]);
```

DREAM OPTIMIZATION FORWARD MODELING RUN WITH HYDRUS 1-D

```
%% This function optimizes the parameters in the vector pars in order
to minimize the sum of squared difference between meas vs simul data
%%%%%%%%%%%%
function [SIM_DATA]=FORWARD(Pars, Extra);

load('Time_POS.txt')
MeasTime=Time_POS(:,1);
MeasTH=Time_POS(:,2);
POS=Time_POS(:,3);
%MeasTime(632:end)=2484;

%%%%%%%%%%%%%%%%%%%%%%%%%%%%%%%%%%%%%%%%%%%%%%%%%%%%%%%%%%%%%%%%%%%%%%%%%%%%
%RUN HYDRUS in DREAMzs
%%%%%%%%%%%%%%%%%%%%%%%%%%%%%%%%%%%%%%%%%%%%%%%%%%%%%%%%%%%%%%%%%%%%%%%%%%%%

% In order to run Hydrus in DOS, follow these two steps:
% 1) generate the LEVEL_01.DIR file with the directory path
% 2) copy the batch file H1D_CALC.EXE from HYDRUS folder and paste it
in your directory

% %  STEP 1 ------------LEVEL_01.DIR-------------
% lFile = fopen('LEVEL_01.DIR','w'); % set automatically the directory
% fprintf(lFile, '%s', pwd);
% fclose(lFile);
%


VG_PARS=[Pars(4) Pars(5) Pars(1) Pars(2) Pars(3) 0.5];
% VG-parameters to optimize: theta_res - theta_sat - alpha - n - Ks - l
a=fopen('original_SELECTOR.IN','r');
%Read the original file of SELECTOR.IN
b=fopen('SELECTOR.IN','w');
i=1;
while 1;
    s= fgetl(a);
    if ~ischar(s), break,end

    if (i==27)
        fprintf(b,'  %1.2f     %1.2f    %1.4f    %1.2f   %3.4f
%1.1f\r\n',VG_PARS);

    else
        fprintf(b,'%s\r\n',s);
    end
    i=i+1;
end
fclose (a);
fclose (b);

%%%%%%%%%%%%%%%%%%%%%%%%%%%%%%%%%%%%%%%%%%%%%%%%%%%%%%%%%%%%%%%%%%%%%%%%%%%%
```

```
% ------------------------ Ready to run HYDRUS 1D --------------
%
2) Run HYDRUS automatically
%
! H1D_CALC.EXE
%
% --------------------------------------------------------------------

%dos('H2d_calc.exe < input.txt') % in "input.txt" for example, write
the
%code 50.34 for the command ENTER
%%%%%%%%%%%%%%%%%%%%%%%%%%%%%%%%%%%%%%%%%%%%%%%%%%%%%%%%%%%%%%%%%%%%%%%
%%%%%
% OUTPUT
%%%%%%%%%%%%%%%%%%%%%%%%%%%%%%%%%%%%%%%%%%%%%%%%%%%%%%%%%%%%%%%%%%%%%%%
%%

Output = textread('Obs_Node.out','%s','headerlines',11);

S=size(Output);

if S(1)<2078
    SIMtheta=ones(length(POS),1).*999;
else
    time=char(Output{1:31:2047});

    h1=char(Output{2:31:2048});
    t1=char(Output{3:31:2049});
    q1=char(Output{4:31:2050});

    h2=char(Output{5:31:2051});
    t2=char(Output{6:31:2052});
    q2=char(Output{7:31:2053});

    h3=char(Output{8:31:2054});
    t3=char(Output{9:31:2055});
    q3=char(Output{10:31:2056});

    h4=char(Output{11:31:2057});
    t4=char(Output{12:31:2058});
    q4=char(Output{13:31:2059});

    h5=char(Output{14:31:2060});
    t5=char(Output{15:31:2061});
    q5=char(Output{16:31:2062});

    h6=char(Output{17:31:2063});
    t6=char(Output{18:31:2064});
    q6=char(Output{19:31:2065});

    h7=char(Output{20:31:2066});
    t7=char(Output{21:31:2067});
    q7=char(Output{22:31:2068});
```

```
h8=char(Output{23:31:2069});
t8=char(Output{24:31:2070});
q8=char(Output{25:31:2071});

h9=char(Output{26:31:2072});
t9=char(Output{27:31:2073});
q9=char(Output{28:31:2074});

h10=char(Output{29:31:2075});
t10=char(Output{30:31:2076});
q10=char(Output{31:31:2077});

Time=str2num(time);
T1=str2num(t1);
H1=str2num(h1);
Q1=str2num(q1);

T2=str2num(t2);
H2=str2num(h2);
Q2=str2num(q2);

T3=str2num(t3);
H3=str2num(h3);
Q3=str2num(q3);

T4=str2num(t4);
H4=str2num(h4);
Q4=str2num(q4);

T5=str2num(t5);
H5=str2num(h5);
Q5=str2num(q5);

T6=str2num(t6);
H6=str2num(h6);
Q6=str2num(q6);

T7=str2num(t7);
H7=str2num(h7);
Q7=str2num(q7);

T8=str2num(t8);
H8=str2num(h8);
Q8=str2num(q8);

T9=str2num(t9);
H9=str2num(h9);
Q9=str2num(q9);

T10=str2num(t10);
H10=str2num(h10);
Q10=str2num(q10);

MTX=[Time,T1,T2,T3,T4,T5,T6,T7,T8,T9,T10];
```

```
    %%%%%%%%%%%%%%%%%%%%%%%%%%%%%%%%%

    for i=1:length(POS)

        ind=find(MTX(:,1)==MeasTime(i));
        SIMtheta(i,1)=MTX(ind,POS(i)+1);

    end

    if isempty(SIMtheta)==1  || length(SIMtheta)~=length(POS)
        SIMtheta=ones(length(POS),1).*999;
    end

    ind1=find(POS==1);
    ind2=find(POS==2);
    ind3=find(POS==3);
    ind4=find(POS==4);
    ind5=find(POS==5);
    ind6=find(POS==6);
    ind7=find(POS==7);
    ind8=find(POS==8);
    ind9=find(POS==9);
    ind10=find(POS==10);

    MTX=[Time,T1,T2,T3,T4,T5,T6,T7,T8,T9,T10];
    %%%%%%%%%%%%%%%%%%%%%%%%%%%%%%%%%

    for i=1:length(POS)

        ind=find(MTX(:,1)==MeasTime(i));
        SIMtheta(i,1)=MTX(ind,POS(i)+1);

    end


    if isempty(SIMtheta)==1  || length(SIMtheta)~=length(POS)
        SIMtheta=ones(length(POS),1).*999;
    end
end


SIM_DATA=SIMtheta(1:350);
```

Appendix 3.4 HYDRUS-1D numerical model run outputs for grass and pine

Plot G1	Cum Act Evap	Annual Evap	Cum Act Transp	Annual Transp	Cum Recharge	Annual Recharge
Year	cm	cm	cm	cm	cm	cm
1950	25.0	25.0	16.8	16.8	0.0	0.0
1951	58.1	33.0	38.6	21.8	5.2	5.2
1952	76.2	18.1	49.9	11.2	14.0	8.8
1953	99.2	23.1	63.5	13.6	22.0	8.0
1954	122.1	22.8	78.8	15.3	29.3	7.2
1955	141.2	19.2	91.5	12.7	32.7	3.4
1956	161.6	20.4	105.9	14.4	34.8	2.1
1957	194.2	32.6	129.0	23.1	49.0	14.2
1958	223.4	29.2	151.5	22.5	66.5	17.5
1959	249.6	26.3	169.7	18.2	72.4	5.9
1960	22.8	22.8	15.3	15.3	12.1	12.1
1961	47.8	24.9	32.8	17.5	20.0	7.9
1962	76.6	28.8	56.0	23.2	47.6	27.6
1963	102.3	25.7	76.4	20.3	60.8	13.1
1964	126.8	24.5	92.4	16.1	67.8	7.1
1965	153.3	26.6	112.0	19.6	73.8	6.0
1966	174.4	21.1	130.0	18.0	82.7	8.9
1967	199.7	25.3	147.5	17.5	85.5	2.9
1968	224.8	25.1	164.7	17.2	91.7	6.2
1969	244.4	19.6	177.6	13.0	97.3	5.6
1970	23.4	23.4	17.1	17.1	4.7	4.7
1971	53.7	30.3	34.1	16.9	21.5	16.8
1972	78.1	24.3	51.8	17.7	32.7	11.2
1973	103.4	25.3	70.0	18.3	50.1	17.5
1974	125.3	21.9	86.0	15.9	64.8	14.6
1975	148.1	22.8	105.1	19.2	74.3	9.6
1976	172.1	24.0	126.5	21.3	83.8	9.5
1977	203.7	31.6	148.7	22.2	107.0	23.2
1978	229.8	26.1	165.4	16.7	118.2	11.2
1979	256.3	26.5	187.8	22.3	132.3	14.1
1980	16.5	16.5	15.1	15.1	18.1	18.1
1981	42.6	26.0	35.0	19.9	21.7	3.5
1982	70.7	28.1	52.8	17.8	31.5	9.8
1983	96.5	25.8	74.2	21.4	67.5	36.1
1984	122.9	26.4	86.1	11.9	88.3	20.8
1985	146.1	23.1	104.7	18.6	95.4	7.1
1986	178.3	32.2	127.8	23.1	105.8	10.4
1987	203.5	25.2	147.0	19.2	121.0	15.2
1988	228.1	24.6	167.3	20.3	142.9	21.9
1989	245.7	17.6	184.0	16.6	151.0	8.1
1990	26.3	26.3	17.6	17.6	4.6	4.6
1991	51.1	24.8	34.1	16.5	15.9	11.3
1992	75.3	24.2	54.6	20.5	28.9	13.0
1993	107.9	32.7	78.7	24.1	42.6	13.7
1994	135.9	28.0	98.5	19.8	49.1	6.4
1995	162.2	26.2	115.9	17.4	73.5	24.4
1996	188.0	25.8	134.3	18.4	86.5	13.0
1997	214.9	26.9	153.2	18.9	93.9	7.4
1998	242.4	27.5	175.3	22.0	105.8	11.8
1999	268.3	25.9	196.6	21.3	119.5	13.7

Plot DP1	Cum Act Evap	Annual Evap	Cum Act Transp	Annual Transp	Cum Recharge	Annual Recharge
Year	cm	cm	cm	CM	cm	cm
1950	31.9	31.9	10.2	10.2	0.000	0.000
1951	68.0	36.1	38.1	28.0	0.001	0.001
1952	93.2	25.1	46.5	8.4	0.008	0.008
1953	125.8	32.7	57.2	10.6	0.019	0.011
1954	154.3	28.5	69.7	12.5	0.035	0.016
1955	179.0	24.7	77.1	7.4	0.047	0.012
1956	205.0	26.0	86.5	9.5	0.059	0.011
1957	244.7	39.7	117.7	31.2	0.084	0.025
1958	282.9	38.3	142.9	25.2	0.122	0.038
1959	315.8	32.9	156.8	13.9	0.136	0.014
1960	31.0	31.0	16.0	16.0	0.028	0.028
1961	62.4	31.5	32.8	16.8	0.042	0.014
1962	97.7	35.3	70.3	37.4	1.923	1.881
1963	132.3	34.6	94.2	23.9	2.026	0.103
1964	162.6	30.2	107.6	13.4	2.091	0.065
1965	195.9	33.3	128.5	20.9	2.105	0.014
1966	223.3	27.4	143.5	15.0	2.127	0.022
1967	251.6	28.3	156.2	12.7	2.139	0.013
1968	282.1	30.5	174.9	18.7	2.152	0.012
1969	307.2	25.1	184.0	9.1	2.166	0.014
1970	28.9	28.9	15.1	15.1	0.015	0.015
1971	67.1	38.2	40.2	25.1	0.040	0.024
1972	97.0	29.9	60.5	20.3	0.062	0.023
1973	133.4	36.5	83.1	22.6	0.089	0.027
1974	163.3	29.8	100.1	17.1	0.149	0.060
1975	196.8	33.5	117.1	17.0	0.164	0.015
1976	227.3	30.5	138.4	21.3	0.178	0.014
1977	269.6	42.3	171.7	33.3	0.199	0.021
1978	302.8	33.3	187.1	15.4	0.216	0.018
1979	341.1	38.2	211.3	24.2	0.242	0.025
1980	26.8	26.8	16.8	16.8	0.150	0.150
1981	59.8	33.0	33.1	16.3	0.165	0.015
1982	94.5	34.7	53.1	20.0	0.179	0.014
1983	133.9	39.4	90.8	37.7	0.648	0.469
1984	171.8	37.9	109.4	18.6	0.798	0.151
1985	200.3	28.5	125.9	16.5	0.837	0.039
1986	239.7	39.3	150.2	24.3	0.851	0.014
1987	276.6	36.9	171.9	21.7	0.871	0.020
1988	311.5	34.9	201.2	29.3	0.953	0.082
1989	335.4	23.9	214.3	13.1	0.979	0.026
1990	32.2	32.2	15.3	15.3	0.013	0.013
1991	61.8	29.6	36.3	21.0	0.029	0.016
1992	97.8	36.1	55.4	19.1	0.048	0.019
1993	137.5	39.7	83.3	27.9	0.069	0.021
1994	170.8	33.3	100.6	17.3	0.089	0.020
1995	205.3	34.5	131.0	30.4	0.174	0.086
1996	237.9	32.6	153.5	22.5	0.260	0.085
1997	271.1	33.2	169.0	15.5	0.282	0.022
1998	306.6	35.5	193.3	24.3	0.316	0.034
1999	340.2	33.7	215.7	22.4	0.358	0.042